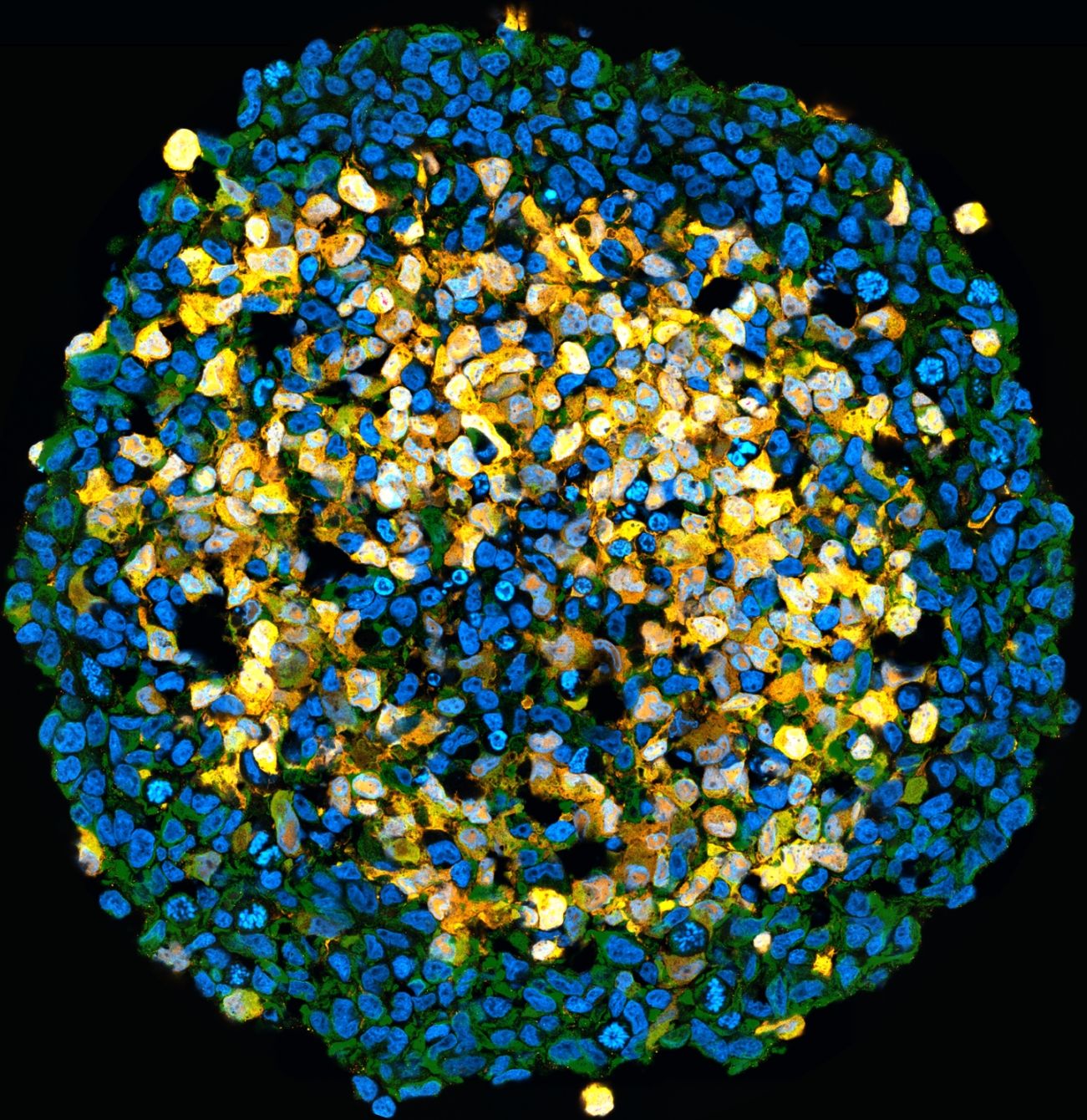


University of Liege
Faculty of Sciences

Design and characterization of a CXCR4-retargeted and sTRAIL-armed oncolytic HSV-1 to attack Glioblastoma stem-like cells (GSCs)



Judit Sánchez Gil

Laboratory of Virology and Immunology

Promotors: Professor Catherine SADZOT
Professor Bernard ROGISTER

Thesis submitted for the degree of
Doctor of Science

Academic year 2021-2022

Cover Image

Immunofluorescences of infected T013 with oHSV/Nb-gD

Infection: 10^7 pfu/ml 48h pi

Taken by Alexandre Hego at confocal Microscope Zeiss HR LSM 880

“The scientific vocation is not born, it is made”

-Margarita Salas-

ACKNOWLEDGEMENTS

Je voudrais à présent remercier toutes les personnes qui ont participé d'une façon ou d'une autre à la réalisation de cette thèse.

Je commencerais par ma promotrice, la Professeur Catherine Sadzot, chef du Laboratoire de Virologie et d'Immunologie. Merci pour son soutien durant ces 5 années de recherche, son engagement et son aide tout au long de la rédaction de cette thèse.

Je tiens aussi à remercier mon co-promoteur, le Professeur Bernard Rogister pour son engagement, ses conseils et sa précieuse collaboration.

Merci aux membres de mon comité de thèse pour leurs conseils tout au long de ce travail ainsi qu'au président Franck Dequiedt et aux membres du jury de thèse pour leurs disponibilités. « Specially I would like to thanks the external members of the jury to accept the invitation and participate in my thesis ».

Je voudrais ensuite remercier l'ensemble de l'équipe de neurosciences et, plus particulièrement, Virginie, member aussi du jury. En effet, elle m'a non seulement guidée au début de ma carrière scientifique en 2015, mais m'a également aidée en cette fin de thèse lorsque nos chemins se sont à nouveau croisés.

Un grand merci à Damla, de m'avoir aidée en tant que mémorante et, ensuite, en tant que PhD. Merci pour ton infinie motivation, ton soutien et ta bonne humeur tout au long de ces années ! Merci aussi à Thérèse pour son aide pendant les expériences in vivo. Sans elle, cela n'aurait pas été possible. (Prépare-toi d'ailleurs à recevoir un appel des US ... hahaha). Merci encore à Arnaud Lombard qui a su trouver du temps afin de nous aider tout au long des expériences in vivo. Merci à Benoit pour sa disponibilité et son expérience technique. Merci finalement au reste de l'équipe de Neuro, Odile, Laetitia et Marc-Antoine.

Je tiens aussi à remercier ceux qui ont été ma famille tout au long de ma thèse. Merci à Marielle pour ses conseils judicieux et sa motivation pendant toutes ces années ! Elle a été pour moi LE modèle à suivre et m'a aidée à garder le rythme pendant ce parcours.

Merci à Cédric pour son aide technique et sa bonne humeur pendant tous ces années. Merci à Julien pour son enthousiasme et pour ses cours d'expressions liégeoises : « on va bientôt se claquer des petites binouzes ensemble ! » Thanks also to Paolo for all the help and advice during my PhD.

Merci à Margaud pour ce chemin de doctorat ensemble, pour ses nombreuses corrections de mails en français ainsi que pour ses traductions espagnol-français au labo lorsque personne ne me comprenait ! Ton soutien pendant ces 4 ans m'a permis de ne pas devenir folle ! Bonne chance pour ta rédaction, tu vas gérer !

Merci à Zahra pour son soutien et son parfait équilibre entre ses merveilleux conseils et ses blagues horribles... hahaha. Beaucoup de courage pour ta rédaction, je suis sûre que tu trouveras le « postdoc » de tes rêves, tu le mérites plus que personne. Même si la vie nous sépare, je sais qu'on se retrouvera bientôt quelque part dans le monde.

Merci à Maxime qui, après s'être perdu dans les couloirs du GIGA 1233465 fois, a trouvé le chemin et a pu m'aider à la fin de la rédaction. Merci aussi à Mégane pour sa bonne humeur et pour trouver toujours un moment pour descendre au + 2. Merci à Chloé pour son aide avec FlowJo en échange de quelque cours d'espagnol hahaha (elle est parfaitement bilingue maintenant !).

Merci à toute l'équipe de PSI : Bart, Loïc, Florence, Margaux, Jeremy, Steph, Olivia, Greg et John ainsi qu'à l'équipe de PSI/DM : Giulia, Céline, Sarah, Sanaa, Clara ... pour la bonne ambiance qui a existé durant ces années. Une équipe toujours partante pour une Beer hour. Je remercie aussi Émeline et Alice pour tous les soupers qui ont fini en soirées. Merci d'avoir toujours été là !

Merci à la Plateforme de Viral Vectors : Manu, Alex et plus particulièrement François (qui est d'ailleurs devenu un ami) pour leurs conseils ainsi que leur aide. Merci aussi à Vinciane et Audrey pour avoir été à mes côtés depuis le master où elles m'ont bien appris à faire la fête à la liégeoise. Je suis heureuse d'avoir vécu autant

de bons moments en leur compagnie et d'avoir su maintenir cette amitié. J'espère la garder pour toujours !

Il est temps de remercier quelqu'un de très spécial dans ma vie, mi Nico. Qui aurait dit à la Judit de 22 ans qui venait de débarquer en Belgique pour un Erasmus, qu'elle allait se marier avec un Belge... Merci d'avoir été à mes côtés pendant toute cette épreuve et surtout d'y rester. Sans toi, cette thèse n'aurait pas été possible. Je me réjouis de continuer cette aventure aux USA avec toi. Merci aussi à ma belle-famille qui m'a accueillie et aimée comme une fille pendant toutes ces années.

Bueno, es momento de cambiar al español. Empiezo por David que si no se enfada, jajaja. Muchas gracias por haber estado a mi lado estos años, quien hubiera dicho que Bélgica me regalaría uno de mis mejores amigos. ¡Gracias por ser como eres y por apoyarme en los momentos buenos y malos! Nunca pensé que a los 25 años se podía seguir creando amistades como la tuya. No cambies nunca y sobre todo ¡ven a verme pronto a Boston! Gracias a todo el clan español (David, Ale, Carlos, Jose y Silvia), por crear un pedacito de hogar en Bélgica. Gracias a Ale por siempre estar a mi lado desde 2015 y haber mantenido la amistad durante tantos años, a Carlos que, aunque nos hayamos conocido más tarde de lo que hubiéramos querido has conseguido ser uno mas en esta familia de expatriados. Gracias a Carmen por haber creado esta amistad desde que nos conocimos en esa clase de Francés en 2016.

Finalmente, no podría faltar dar gracias a mis mejores amigas que, aunque hayan pasado ya 6 años desde que me fui de Barcelona hemos seguido queriéndonos a distancia. Gracias a Lau, Vic y Andrea por ser las mejores, sé que, aunque mamasuel se vaya a Harvard y me vaya aún mas lejos, no cambiara nada en nuestra amistad. Gracias a Laia y Isa por ser mis amigas desde que tengo memoria y por quererme a pesar de la distancia entre nosotras.

No podrían faltar los mas importantes, mi familia. Gracias Papá y Mamá por vuestro amor y apoyo incondicional. Gracias por la educación y los valores que nos habéis dado a Eva y a mi. Gracias por creer en nuestros sueños y poner todo vuestro esfuerzo en ello, sin vuestra confianza y apoyo esto no hubiera sido posible. Gracias a mi hermana Eva quien siempre ha sido y será mi modelo a seguir y a Patrick que forma

ya parte de nuestra familia. No será complicado ser la tía más guay de la familia, ya que sere la única, jajaja. Finalmente, gracias a mis abuelos, yaya Puri, yaya Herminia y yayo Emilio que, aunque la ciencia les queda un poco lejos nunca se cansaron de preguntar por el avance del proyecto.

“Gracias de corazón a todos y a cada uno de vosotros, a los nombrados y a los que he olvidado de nombrar. Sin todo el apoyo y el amor recibido durante todos estos años, esta tesis no hubiera sido posible”

“Merci de tout mon cœur à toutes les personnes nommées ainsi qu’à celles que j’ai oublié de nommer. Sans votre soutien et votre amour pendant toutes ces années cette thèse n’aurait pas été possible.”

SUMMARY

Virotherapy is one of the techniques that has been highlighted as a promising new therapeutic approach against cancer. Oncolytic Herpes simplex virus (oHSV) has been shown to have potent oncolytic effects against tumour cells and tumour microenvironment.

Glioblastoma (GBM) is the most aggressive primary brain tumour in adults, and patients have a poor prognosis mainly due to recurrences. It has been shown that GBM cells can escape the tumour mass and invade healthy parenchyma. This migration is mediated by a CXCL12/CXCR4 pathway. These CXCR4+ cells share characteristics with stem cells and are considered as GBM stem-like cells (GSC) partly responsible of the recurrences. They appear therefore, as a target for oncolytic virus therapy.

We have created a retargeted and armed oHSV. The glycoprotein D has been modified by inserting a nanobody specific to human CXCR4 to selectively target GSCs, and the virus has been armed with a soluble form of TRAIL to induce the extrinsic apoptosis pathway under the control of nestin promoter. Infection of U87MG or U87MG CXCR4+ with the retargeted oHSV showed a viral replication only in cells over-expressing CXCR4, indicating an efficient retargeting. The analysis of the arming in U87MG CXCR4+ infected cells showed more apoptosis with the sTRAIL-armed virus. Further evaluation on human patient-derived glioblastoma cells cultured as tumourspheres was done, showing a correlation between CXCR4 expression and viral infection. Finally, an *in vivo* orthotopic xenograft model with U87MG CXCR4+ cells demonstrates the ability of this retargeted and armed virus to significantly reduce the tumour volume and increase survival. In the future, improving the arming strategy and the validation of the retargeting safety by the creation of a nanobody that recognise human and murine CXCR4 will be addressed.

INDEX

I. INTRODUCTION	1
1. Glioblastoma (GBM)	1
1.1 General Features.....	1
1.1.1 Epidemiology context	1
1.1.2 Histological aspects	2
1.1.3 Genetic and Molecular alterations.....	3
1.1.4 Classification	5
1.1.5 Risk Factors.....	7
1.1.6 Diagnosis and current markers.....	8
1.2 Surgery and current treatments	9
1.2.1 Surgical resection.....	9
1.2.2 Radiotherapy and Chemotherapy.....	10
1.3 Glioblastoma Stem-like Cells (GSCs).....	11
1.3.1 GSC tumour niches.....	12
1.3.2 Models of GSC development.....	16
1.3.3 CXCR4/CXCL12 axis	18
1.4 Importance of the Microenvironment and the Immune system.....	21
1.4.1 Tumour Associated Macrophages (TAMs) and Microglia.....	22
1.4.2 Regulatory T cells (Tregs)	23
1.4.3 Tumour-Infiltrating Lymphocytes (TILs).....	23
1.4.4 Dendritic cells (DC)	24
1.4.5 Myeloid-Derived Suppressor Cells (MDSCs)	24
1.5 Current Immunotherapies	24
2. Oncolytic virus therapy	30
2.1 Oncolytic virus types and characteristics.....	30
2.2 Herpes Simplex Virus 1 (HSV-1)	34
2.2.1 Structure and Genome organisation.....	34
2.2.2 Infectious cycle.....	35
2.2.3 Gene expression and protein synthesis.....	37
2.2.4 DNA replication, capsid assembly and egress	38
2.3 HSV as oncolytic virus	41
2.3.1 Attenuations of oHSV for GBM treatment	41

2.3.2	<i>oHSV Re-targeting oHSV for GBM therapy</i>	45
2.3.3	<i>Armed oHSV for GBM</i>	47
2.4	<i>oHSV in combination with other treatments</i>	53
2.4.1	<i>oHSV and standard therapies</i>	53
2.4.2	<i>oHSV and immune checkpoints inhibitors</i>	53
2.5	<i>Impact of viral infection on GBM immune system</i>	55
2.5.1	<i>Innate immune response activation and impact</i>	56
2.5.2	<i>Adaptive immune response activation and impact</i>	56
2.6	<i>Clinical evolution of oHSV for glioblastoma</i>	57
II. AIM OF WORK		62
III. MATERIALS AND METHODS		63
1.	Cell lines	63
2.	Construction of a recombinant oHSV by Two-steps recombination technique	63
3.	Viral growth assay.....	64
4.	Entry assay.....	65
5.	RT-qPCR	65
6.	Flow cytometry	66
7.	Annexin V/DAPI apoptosis test.....	66
8.	Viability assay.....	67
9.	Cryosection and Immunofluorescence of patient-derived tumourspheres.....	67
10.	Western Blot assay	67
11.	<i>In vivo</i> experiments	68
12.	Bioluminescence assay in vivo experiments.....	68
13.	Intracardiac perfusion of PFA 4% in mice	69
14.	Brain tissue processing and tumour volume measurement.....	69
15.	Statistical analysis	70
IV. RESULTS		71
1.	Construction of a retargeted oncolytic herpesvirus	71
2.	In vitro efficacy of the CXCR4-retargeting	72

3.	Construction of an armed oncolytic herpesvirus.....	75
4.	<i>In vitro</i> viability upon sTRAIL treatment or oHSV infection.....	76
5.	<i>In vitro</i> efficacy of sTRAIL-arming.....	78
6.	Therapeutic efficacy of oHSV/Nb-gD and oHSV/Nb-gD:sTRAIL using and orthotopic xenograft U87MG CXCR4+ GBM model.....	80
7.	Infection of patient derived Glioblastoma stem-like cells.....	87
8.	<i>In vitro</i> sensitivity to oHSV infection and sTRAIL apoptotic effect in tumourospheres.....	89
9.	Therapeutic efficacy of oHSV/Nb-gD and oHSV/Nb-gD:sTRAIL using and orthotopic xenograft GSC-like GBM model.....	93
V.	<i>DISCUSSION</i>	95
1.	Creation of an oHSV CXCR4 retargeted and armed with sTRAIL.....	95
1.1	Retargeting strategy.....	96
1.2	Arming strategy.....	97
2.	Efficacy of oHSV/Nb-gD and oHSV/Nb-gD:sTRAIL in tumourospheres.....	100
3.	What about the immune system and TME role?.....	105
VI.	<i>CONCLUSION AND PERSPECTIVES</i>	108
VII.	<i>BIBLIOGRAPHY</i>	110
VIII.	<i>APPENDICES</i>	145

ABBREVIATIONS

5-ALA	5-Aminolevulinic Acid
AAAIR	average annual age-adjusted incidence rate
Akt	Ak strain transforming
ALL	Acute lymphocytic leukemia
ALT	Alanine transaminase
APC	Antigen presenting cells
ATRX	Alpha-thalassemia/mental retardation syndrome X-linked
BAC	Bacterial artificial chromosome
BBB	Blood brain barrier
c-FLIP	cellular FADD-like interleukin-1b-coverting enzyme-inhibitory protein
CARs	Chimeric antigen receptor
CC	Corpus callosum
CDK	Cyclin-dependent Kinases
CHEK2	Checkpoint Kinase 2
CNS	Central Nervous System
CPA	Cyclophosphamide
CRT	Calreticulin
CSC	Cancer Stem Cells
CSF-1R	Colony stimulating factor 1 receptor
CT	Computed tomography
CTL	Cytotoxic T-lymphocyte
CTLA-4	Cytotoxic T-lymphocyte antigen 4
DAMPs	Damage-associated molecular patterns
DC	Dendritic cells
DLBCL	Diffuse large B cell lymphoma
DLT	Dose-limiting toxicity
DNA	Deoxyribonucleic acid
DR	Death receptor
E	Early
ECM	Extracellular matrix
EGF	Epidermal growth factor

EGFR	Epidermal growth factor receptor
EMT	Epithelio-mesenchymal transition
EOR	Extended of resection
FDA	Food and drug administration
FGF	Fibroblast growth factor
FLAIR	Fluid attenuated inversion recovery
Flt3L	FMS-like tyrosine kinase 3 ligand
GBM	Glioblastoma Multiforme
GBO	Glioblastoma organoids
GEMM	Genetically engineered mouse models
GF	Growth Factors
GFP	Green fluorescent protein
GM-CSF	Granulocyte-macrophage colony-stimulating factor
GPCR	G-protein coupled receptors
GSC	Glioblastoma Stem Cells
HCMV	Human Cytomegalovirus
HER2	Human epidermal growth factor receptor 2
HGG	High-grade glioma
HIF-1/2	Hypoxia-inducible factor
HIV-1	Human immunodeficient virus -1
HLA	Human leukocyte antigen
HMGB1	High mobility group box 1 protein
HOX	Homeobox gene
HPV	Human papillomavirus
HSPG	Heparan sulfate proteoglycans
HSV-1	Herpes simplex virus -1
HVEM	Herpes virus entry mediator
ICD	Immunogenic cell death
ICI	Immune checkpoint inhibitor
ICOS	Inducible T-cell Costimulator
IDH1/2	Isocitrate Dehydrogenase 1/2
IE	Immediate-early
IFN- γ	Interferon gamma
INM	Inner nuclear membrane

iNOS	Inducible nitric oxide synthase
ISG	Interferon-stimulated genes
L	Late
LGG	Low-Grade Glioma
LV	Left ventricle
MAPK	Mitogen-activated protein kinase
MDMs	Monocyte-derived Macrophages
MDSC	Myeloid-derived suppressor cells
MFI	Median fluorescent intensity
MG	Microglia
MG1	Mucin glycoprotein 1
MGMT	O[6]-methylguanine-DNA methyltransferase
MHC	Major histocompatibility complex
MMP	Matrix metalloproteinases
MOI	Multiplicity of infection
MRI	Magnetic resonance imaging
MTOC	Microtubule organizing centre
MV	Measles virus
MVD	Micro-vessel density
MYXV	Myxoma virus
NADPH	Nicotinamide adenine dinucleotide phosphate
NDV	Newcastle disease vaccine
NK	Natural killer
NSC	Neuronal stem cells
NSCLC	Non-small cell lung cancer
oHSV	Oncolytic Herpesvirus
ONM	Outer nuclear membrane
OPC	Oligodendrocytes precursor cell
ORF	Open reading frame
OV	Oncolytic virus
PAMPs	Pathogen-associated molecular patterns
PBMC	Peripheral blood mononuclear cells
PD-1	Programmed cell death protein 1
PDGF	Platelet-derived growth factor

PIP3K	Phosphoinositide 3-kinase
PKR	Protein kinase RNA-activated
PRRs	Pattern recognition receptors
PTEN	Phosphatase and TENsin homolog deleted on chromosome 10
PVN	Perivascular niche
RAS-GTP	Rat Sarcoma Virus-GTP
RB	Retinoblastoma
RNA	Ribonucleic acid
RR	Ribonucleotide reductase
RT	Radiotherapy
RTK	Receptor Tyrosine Kinase
SBV	Schmallenberg virus
SCC	Squamous cell carcinoma
SCCHN	Squamous Cell Carcinoma of the Head and Neck
SNP	single-nucleotide polymorphisms
SOC	Standard of care
SRS	Stereotactic radiosurgery
SRT	Stereotactic radiotherapy
STING	Stimulator interferon gene signalling pathway
SVV	Seneca valley virus
SVZ	Subventricular zone
T-VEC	Talimogene Laherparepvec
TAM	Tumour associated macrophages
TAP	Transporter associated with antigen processing
TCGA	The cancer genomic atlas
TERT	Telomerase reverse transcriptase
TGN	Trans-golgi network
TI	Therapeutic index
TILs	Tumour-Infiltrating Lymphocytes
TIM-3	T-cell immunoglobulin and mucin domain 3
TK	Thymidine Kinase
TL	True-late
TLR	Toll-like receptor
TM	Tumour mass

TME	Tumour microenvironment
TMZ	Temozolomide
TP53	Tumour protein 53
TRAIL	TNF-related apoptosis-inducing ligand
VEGF	Vascular Endothelial Growth Factors
VSV	Vesicular stomatitis virus
VV	Vaccinia virus
VZV	Varicella-Zoster Virus
WHO	World Health Organisation

I. INTRODUCTION

1. Glioblastoma (GBM)

1.1 General Features

Glioblastoma (IDH-wildtype, astrocytoma) is one of the most common aggressive primary brain tumours. In 2021, the fifth WHO classification of Tumours of the central nervous system (WHO CNS5) classified Glioblastoma as an adult-type diffuse IDH-wildtype glioma, of grade 4, representing 55% of the gliomas¹. Although classification has long been based on histological observations, molecular biological techniques have allowed to characterise better markers that recently became important to improve the classification of tumours and diagnosis¹.

Glioblastoma heterogeneity presents a major problem to diagnosis and treatment. Genetic, epigenetic and microenvironment modifications play a role in this heterogeneity². The study of molecular expression profiles of 401 diagnosed GBM specimens from the “The Cancer Genome Atlas Network” (TCGA) and single-cell RNA-sequencing of 28 tumours demonstrate the presence of genetic intra-tumour diversity. Based on gene bulk expression profiles, it is suggested that there are, at least, three subtypes of GBM: the proneural, the classical and the mesenchymal subtypes³. The same tumour specimen can present different subtypes at different regions and these subtypes can change over time and during treatment³.

1.1.1 *Epidemiology context*

The rate of incidence of GBM is higher in men than women, and GBM is more common among people of 75-years old and older⁴. The average annual age-adjusted incidence rate (AAAIR) ranges from 0.50/100.000 to 3.69/100.000 and is the highest among malignant primary brain tumours⁵. The rate of incidence analysed between different regions of the world with similar economic situations shows that Northern Europe’s rate is almost twice higher than in Japan⁶. Regarding the rate between ethnicities, European Americans have a 2.5 higher GBM rate than African Americans, while Hispanics have a lower rate than non-Hispanics⁷.

1.1.2 *Histological aspects*

Glioblastoma neoplasm is characterised by small polygonal and spindle-shaped cells with acidophilic cytoplasm and oval nuclei with clumped hyperchromatic chromatin. Moreover, they present an increased nuclear/cytoplasmic ratio with nuclear pleomorphism with binuclear or polynuclear cells^{8,9}. Occasionally, adipocytes-like cells derived from astrocytic tumour cells can be observed. When observed, they characterised what is called “glioblastomas with adipocyte-like tumour differentiation” or “lipid-rich glioblastomas”¹⁰. The presence of microglia and tumour associated macrophages (TAMs) is quantitatively important in glioblastoma. Representing up to 50% of the tumour mass, they play a crucial role in the tumour microenvironment (TME)¹¹. Further characterisation of the immune microenvironment in GBM is explained in section 1.4.

One of the hallmarks of GBM diagnosis is the presence of endothelial cells forming small blood vessels within the tumour mass, followed by a discontinuous layer of pericytes¹². The morphology of these endothelial cells is different from the normal blood vessels. They show hyperplasia and focal distensions between inter-endothelial junctions that may participate in the blood brain barrier (BBB) defect, increasing thus its permeability¹³.

Necrosis is another hallmark to differentiate glioblastoma from lower-grade astrocytoma. Two main types of necrosis have been described in GBM: (1) large necrosis from thrombotic origin, usually located in the centre of the tumour, mainly caused by an insufficient blood supply (Figure 1A)¹⁴ and (2) pseudopalisading necrosis, composed by several small necrotic foci with surrounding tumour cells (Figure 1B)¹⁵. The second necrotic type is detected in both primary (the GBM appears without any pre-existing lower grade glioma) and secondary GBM¹⁶ (the GBM appears after a previous resected lower grade glioma). Hypoxia which leads to stabilising and activating the two subunits of Hypoxia-Inducible factor HIF-1/2 factor is a key element for necrosis development¹⁷.

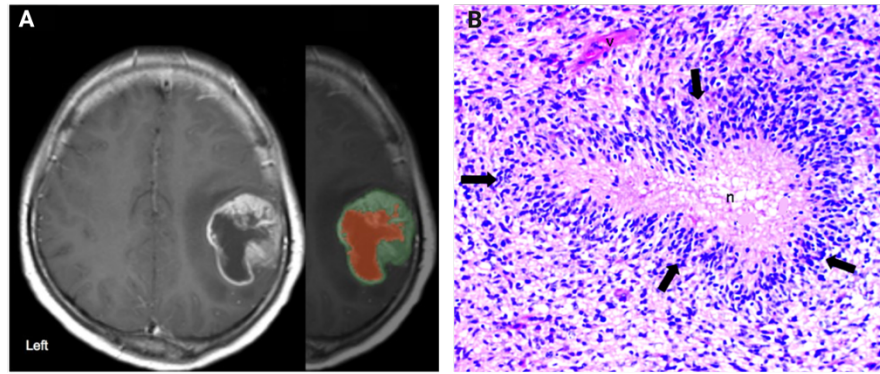


Figure 1: Representation of the two main types of necrosis in glioblastoma patients. (A) MRI of a glioblastoma patient with a representative necrotic tumour mass. Segmentation of the tumour (green area) and necrotic area (red) (Adapted from Shuai Liu, et al., 2017). **(B)** Histological image of a representative pseudopalisading necrosis characterised by an arrangement of hypercellular tumour nuclei (arrows) around a tumour necrotic focus (n). (Image from F.J. Wippold II et al., 2006).

1.1.3 Genetic and Molecular alterations

In contrast to other cancers, which result from a very well-defined sequence of events leading to their development, glioblastoma formation occurs in a complex network of different genetic and molecular alterations driving important modifications in important signalling pathways¹⁸. Although GBM commonly carries isocitrate dehydrogenase (IDH)-wildtype sequence, TERT promoter mutation and copy number changes for chromosomes 7 and 10, they are highly heterogeneous. This heterogeneity comes from the presence of diverse sub-populations of cells carrying supplementary genetic mutations in addition to the main genetic alterations¹⁹. IDH-mutations are one of the first alterations during gliomagenesis, and they are more likely to be present in low-grade gliomas (LGG) and secondary gliomas than in primary GBM. These mutations induce a change in enzyme functions, causing the production of 2-hydroxyglutarate and do not produce NADPH²⁰. Indeed, the metabolic consequences of IDH mutations allow a better sensitivity to therapeutic treatments, leading patients with mutated IDH gliomas with a better prognosis²¹.

The most commonly mutated pathways in GBM will be described in this paragraph and we will make an overview of the molecular diversity and compare primary and secondary GBM.

- **Oncogenic pathways**

Three pathways are commonly altered in GBM (Figure 2). However, any of these pathways or combination of them can contribute to GBM formation and this complexity leads to a high variability between different tumours and within the same tumour¹⁸.

One of the alterations is related to the receptor tyrosine kinases (RTKs), which can bind growth factors (GFs) or cytokines and activate the downstream activating cascades. In GBM, EGF receptor (EGFR) or its ligand are frequently overexpressed²². Moreover, aside from this overexpression, EGFR deletions and point mutations are frequent in GBM. The most common corresponds to the loss of the exons 2-7, leading to the expression of the so-called EGFRvIII mutated receptor. This mutation accounts for 60 to 70% of EGFR mutations in primary GBM, leading to constitutive activation of the receptor due to the deletion of its extracellular domain²³. In turn, the increased activation of EGFR activates the RAS pathway, which is increased in nearly all GBM. Activation of Ras guanosine binding protein (RAS-GTP) promotes cell cycle, survival and migration by activating PIP3K/PTEN/Akt pathway²⁴ (Figure 2A).

Another modified pathway regulating the cell cycle is the retinoblastoma (RB) pathway²⁵. In non-proliferating cells, RB binds the E2F transcription factor and subsequently blocks the transcription of genes necessary for mitosis and cell cycle. In proliferating cells, the CDK/cyclin complex is activated and phosphorylates RB allowing the release of E2F and the transcription of genes necessary for proliferation. In some GBM, RB promoter is methylated, leading to a gene silencing and a constitute release of E2F (Figure 2B)²⁶.

Finally, the third and more frequently altered pathway in GBM is the TP53 pathway, which is important in DNA damage responses, cell death and differentiation. In glioblastoma, TP53 mutations target exons essential for DNA binding. Moreover, in

this pathway GBMs can present MDM2 and MDM4 amplification and CDKN2A-p14^{ARF} deletion²⁷ (Figure 2C).

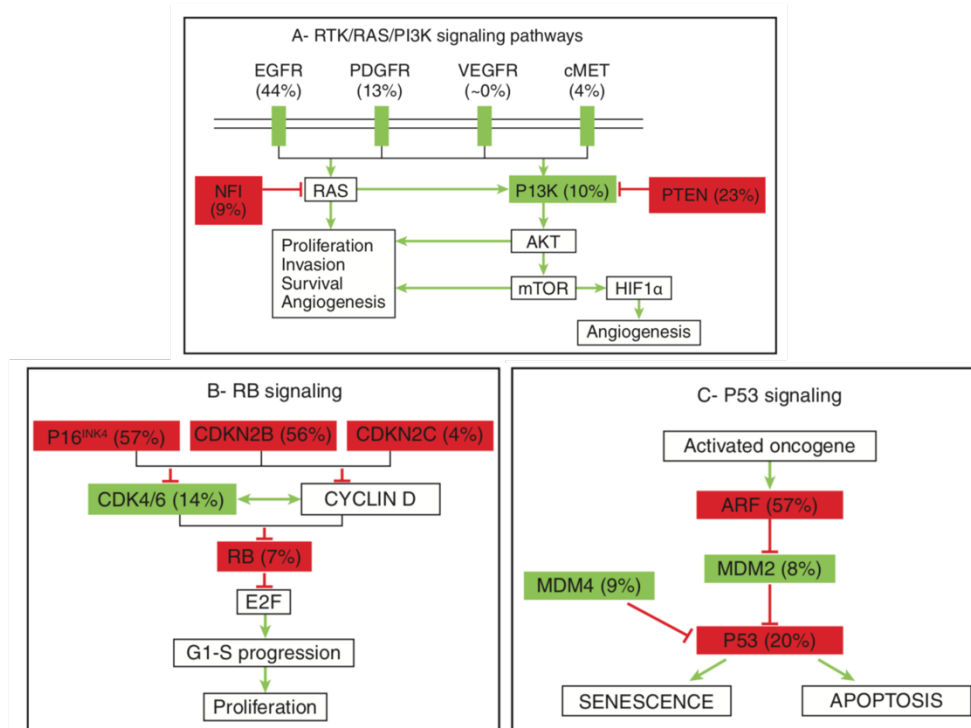


Figure 2: Three main altered pathway in GBM. Mutations related to deletions and amplifications in the RTK/RAS/PI3K pathway (A) the RB pathway (B) and the p53 signalling (C). Green boxes indicate activations or genes amplification and red boxes indicates inactivation or gene deletions. The percentage of alterations are indicated in each box (Adapted from Lombardi M.et al., 2017).

1.1.4 Classification

Classification of tumours of the central nervous system has been modified in 2021. The revised fifth edition of the WHO (WHO CNS5) adds some new recognised tumour types and introduce several important changes related to nomenclature, grading and classification¹. Specifically, the 2021 classification has changed the nomenclature from Roman (I, II, III, IV) to Arabic numbers (1, 2, 3, 4). Tumour entities are now defined as tumour types and variants as subtypes. Moreover, in this new classification an entity can be assigned to multiple tumour grades, like astrocytoma, IDH-mutant which can now be classified either grade 2, 3 or 4. Classification of glioblastoma has vastly changed from the 2016 WHO (Figure 3)²⁸.

Now only IDH-wildtype astrocytoma's are considered glioblastomas and primary or secondary glioblastoma classification is no longer used. It considers that, even without high-grade histopathologic features, the patient is diagnosed of glioblastoma if it presents at least one of the following molecular alteration: loss of chromosome 10 (+7/-10), EGFR amplification or TERT promoter mutation²⁹ (Figure 4).

Astrocytomas are characterised as IDH-mutant diffuse gliomas. IDH-mutant gliomas originate low-grade tumours that develops by the progressive accumulation of additional genetic alterations. Indeed, IDH-mutation is associated with mutations on tumour protein TP53 and ATRX which is mutually exclusive with 1p/19p codeletion³⁰. Finally, it has been shown that the presence of homozygous deletion of CDKN2A/B is related to a negative prognosis³¹. Thus, astrocytomas IDH-mutants that present CDKN2A/B deletion are classified as a grade 4, the highest grade of an IDH-mutant²⁹ (Figure 4).

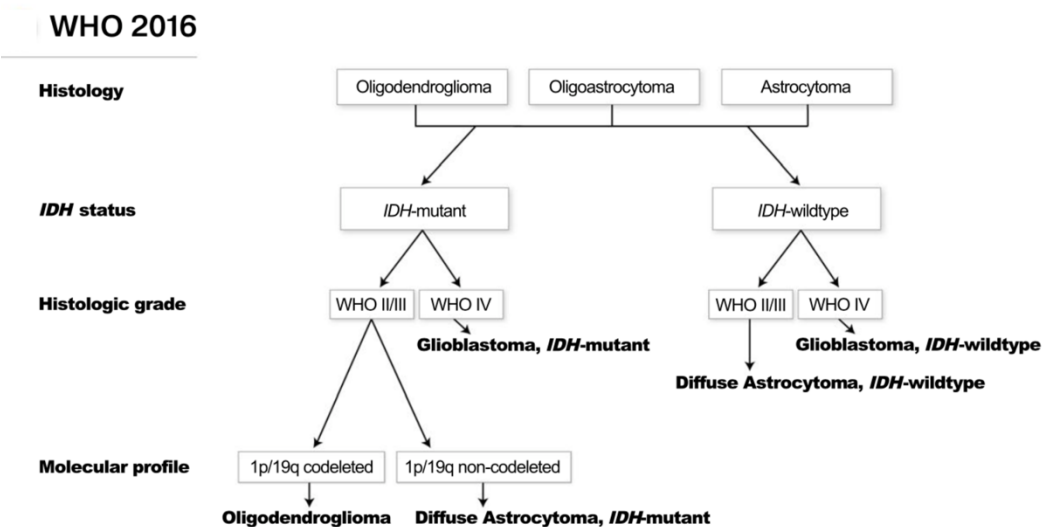


Figure 3: Simplified classification based on the 2016 edition of the World Health Organisation (WHO) classification of central nervous (CNS) tumours. In 2016 classification, glioblastomas were classified as primary GBM (IDH-wildtype) and secondary GBM (IDH-mutants) derived from the progression of low-grade astrocytoma. (Adapted from Gritsch, S. et al.,2021)

WHO 2021

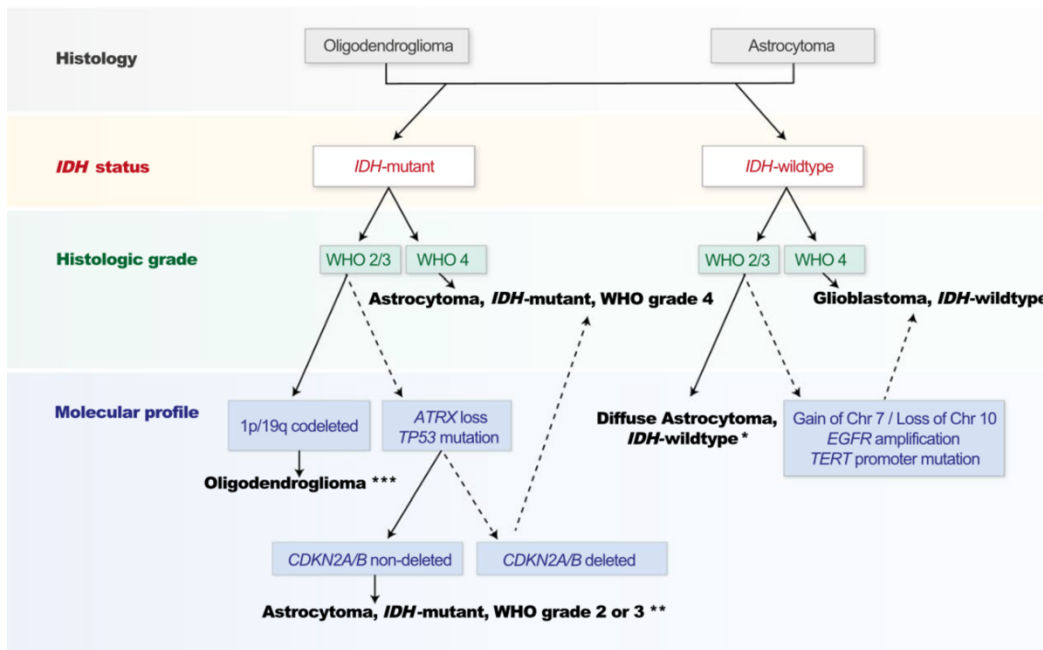


Figure 4: Actual classification of diffuse gliomas based on the 2021 WHO classification of the CNS tumours. Dashed lines show the changes compared to the 2016 classification. * Diffuse astrocytoma with an IDH-wildtype is considered rare. To exclude glioblastoma diagnosis, (+7/-10) mutations, EGFR amplification and TERT mutation are required to be tested. ** Astrocytoma, IDH-mutant can be classified as grade 2,3 or 4 depending on the CDKN2A/B status. *** Oligodendrogliomas, IDH-mutant with 1p/9p co-deletion can be diagnose as grade 2 or grade 3 based on histological analysis. (Adapted from Gritsch, S. et al.,2021)

1.1.5 Risk Factors

One of the major risk factors that can cause glioblastoma is the exposure to therapeutic high-dose radiation. Even though the presence of high-dose chemotherapy outside the brain has also been related as a risk. Moreover, some immune factors and some nucleotides polymorphism have demonstrated an impact on the GBM risk⁷. It is interesting to highlight that single-nucleotide polymorphism (SNPs) in genes that are linked to asthma are also linked to GBM, confirming an inverse association between asthma and GBM. This correlation demonstrates that genotypes increasing asthma, eczema and psoriasis are associated with a decrease in GBM risk³². In the same line, viral infections such as Varicella-Zoster Virus (VZV) infection and the presence of anti-VZV IgG show an inverse association to adult GBM risk. Other viruses and parasitic infections have been related to gliomagenesis,

although their possible role in glioblastoma initiation or progression remain fully elusive³³.

Concerning genetic risk factors, brain tumours are associated with some familial predisposition syndromes such as Li-Fraumeni syndrome, neurofibromatosis, tuberous sclerosis and Turcot's syndrome. As previously mentioned, the accumulation of several mutations in cells is required for tumourigenesis. Thus, these patients have an increased risk because all cells already carry a mutation. In the case of Li-Fraumeni syndrome, individuals carry the mutations of the *TP53* checkpoint gene and *CHEK2*. Turcot's syndrome carries DNA repair mutations while neurofibromatosis and tuberous sclerosis have mutations in tumour suppressor genes. Consequently, in this case, GBM risk increases due to an excessive growth allowing the accumulation of additional mutations³⁴.

1.1.6 Diagnosis and current markers

Clinical manifestations depend on the tumour location and the size of the oedema at the time of diagnosis. In the case of a large tumour, the most common symptoms are the presence of headache and/or nausea. Intracranial hypertension syndrome represents 30% of clinical cases, followed by a motor deficit (20%), loss of body weight (17%), confusion (15%) and visual or speech deficit (13%). In some cases, epilepsy is observed (15-20%) and is correlated with a better outcome due to the cortical location of the GBM³⁵. Glioblastomas are commonly located in the supratentorial space (85%), explaining the symptoms mentioned above. In adult brains, they are less frequent in the brainstem and spinal cord (less than 5% each) or in the cerebellum (3%). Up to 25% occur in the frontal lobe being responsible for mood and executive disabilities in 15% of the patients³⁶.

Magnetic resonance imaging (MRI) and Computed tomography (CT) are frequently performed after the first clinical symptoms to confirm the initial diagnosis. MRI images of GBM reveal infiltrative, heterogeneous intraparenchymal lesions which arise from the white matter. T1-weighted MRI images show dark colouration in the centre of the lesion due to the necrosis surrounded by oedema, which appears lighter³⁷. MR spectroscopy, which is a non-invasive technique allowing to determine the biomedical composition of imaged tissue, complements MRI observation. It reveals that GBM is characterised by an increase of choline/N-acetylaspartate and

choline/creatine ratios. This data, supplemented by a peak of lactate and lipids and a decrease of myoinositol are sufficient for diagnosis of glioblastoma^{38,39}. Another important marker to be considered not only for GBM diagnosis and its treatment is the methylation of MGMT (O⁶-methylguanine-DNA methyltransferase). Indeed, several studies have shown that methylation of MGMT can be beneficial for treating alkylating products such as temozolomide (TMZ) which is a good treatment for these patients⁴⁰.

1.2 Surgery and current treatments

1.2.1 *Surgical resection*

As explained before, after the first symptoms, patients go through CT and MRI analyses. T1-weighted MRI images allow the detection of vascularised tumours and possible disruption of the BBB. T2-weighted MRI and fluid-attenuated inversion recovery (FLAIR) images show as correlate oedema or non-contrast-enhancing tumour⁴¹. After imaging results, MR spectroscopy can be done to help to the diagnosis but due to the lack of time the patient is very quickly placed to surgery.

Directly after diagnosis by medical imaging, the standard of care (SOC) treatment imposes the maximal resection of tumour tissue by surgery. Most of the time, surgical resection is performed during general anaesthesia. However, some teams are now putting forward awake craniotomy (asleep-awake anaesthesia) that sometimes may help to decrease postoperative neurologic deficits and allow the resection of a bigger area given the localization of the initial lesion. Moreover, the patient's verbal can help to detect potential problems in the sensory motor, language, or visual domains during surgery⁴². However, although not novel, this approach is not yet normally used for routine glioma surgery. Only in critical areas, this technique is mandatory to ensure the patient's safety.

If critical tissues are correctly determined, supra-maxima GBM resection can be done⁴³. However, the achievement of supra-maxima resection is very challenging by using only classical white light microsurgical techniques. The pro-drug 5-aminolevulinic acid (5-ALA) used as a proof-of-concept for improving the tumour visualization was convincingly demonstrated. After oral administration of the pro-drug, the fluorescent molecule protoporphyrin IX (PpIX) accumulates in high-grade

gliomas allowing thereby a better larger and safer resection of the tumour (Figure 5). Using this technique, total resection was possible in 65% of the cases compared to 36% of the cases when conventional techniques were used^{44,45}. Upon surgery, tumour's samples are saved for further histopathological and genetical analyses to better understand the nature of the cancer⁴⁴.

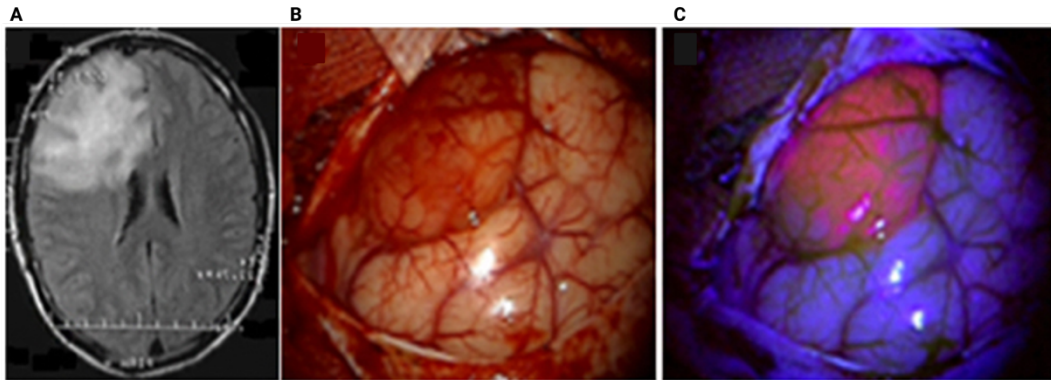


Figure 5: Improvement of tumour visualization with 5-ALA in diffuse oligodendroglioma WHO grade II. (A) pre-operative FLAIR image showing a hyperintense lesion. (B) White light microscopy shows abnormalities in the cortex. (C) 5-ALA-injection prior to surgery reveals moderate fluorescence with violet-blue excitation light and allows a better identification of tumour tissues (Adapted from Goryaynov, S. et al., 2019)

1.2.2 Radiotherapy and Chemotherapy

Surgery is rarely complete due to the nature of the tumour, which usually infiltrate the healthy brain tissue, thus is always followed by radiotherapy and/or chemotherapy to kill cancerous cells that are left behind⁴⁶. The current treatment following surgery is a combination of chemotherapy with temozolomide (TMZ) (75mg/m²/day for a duration of 6 weeks) and/or radiotherapy (RT) (60 Gy in 30 fractions). Finally, six cycles of TMZ for maintenance (150-200 mg/m²/day) are done after 4 weeks of break⁴⁷. The outcome of this heavy treatment generally depends on the age of the patient, its neurological status, the extend of resection (EOR) capacity, the presence of IDH mutations and methylation of MGMT are the prognostic factors established in GBM patients.

Despite this heavy treatment, recurrences are very frequent. In 80% of the patients, recurrence appears near the margin of the resection cavity, but in 20% of the cases, it is observed in a new location⁴⁸. There is no standard of care treatment for patients

with recurrence GBM. The therapeutic options include a new surgery, re-irradiation and/or systemic therapy. However, factors related to the risk of increasing morbidity like, location of the recurrence, low performance of the primary surgery and tumour volume must be evaluated before considering a second surgery. Bevacizumab (anti-angiogenic antibody against vascular endothelial growth factor-VEGF) and alkylating agents such as TMZ or lomustine are the most common options used for patients with recurrent tumour⁴⁹. Re-irradiation can also be considered in case of relapse, even though the previous radiation treatment has damaged normal brain tissue. The risk of necrosis has to be determined after stereotactic radiosurgery (SRS) and stereotactic radiotherapy (SRT)⁵⁰.

1.3 Glioblastoma Stem-like Cells (GSCs)

Glioblastoma presents a high degree of heterogeneity and plasticity within the tumour, being a major obstacle to treatments. Cancer stem-like cells (CSC) play an important role in tumour recurrence and resistance to therapy⁵¹. In the past, Glioblastoma stem cells (GSCs) have been identified using single-surface markers such as CD44, L1CAM, A2B5 and GFAP, CD133, CD15 for membrane markers and Nestin, SOX2, SALL2, ALDH1 for intracellular markers⁵². Moreover, they have been functionally identified as cells able to self-renew and produce a new heterogenous tumour (Figure 6)⁵³.

However, several aspects of the GSC definition have generated controversy in the last years. Nowadays, in the single-cell genomics era, researchers suggest that multiple cellular stages can be defined as GSC and these stages are able to interconvert to adapt to microenvironmental cues. It is suggested that the detection of different GSC markers are only able to isolate a distinct cellular state rather than a subpopulation of cells⁵⁴. Thus, data describing the stem marker expression would give a snapshot on time and do not consider the dynamic functional properties of GSC that displace different states⁵⁵. Therefore, the identification of GSC in GBM is still complicated, and although the use of cell surface markers is frequently used, researchers questioned if it is enough for GSC identification⁵⁵.

More recently, CXCR4 (CD184) chemokine receptor has been identified as another membrane protein highly expressed in GSCs and is the main focus of this project⁵⁶.

CXCR4 is a known mediator of cancer cell proliferation and results from the increased expression of HIF-1- α (hypoxia-inducible factor)⁵⁷.

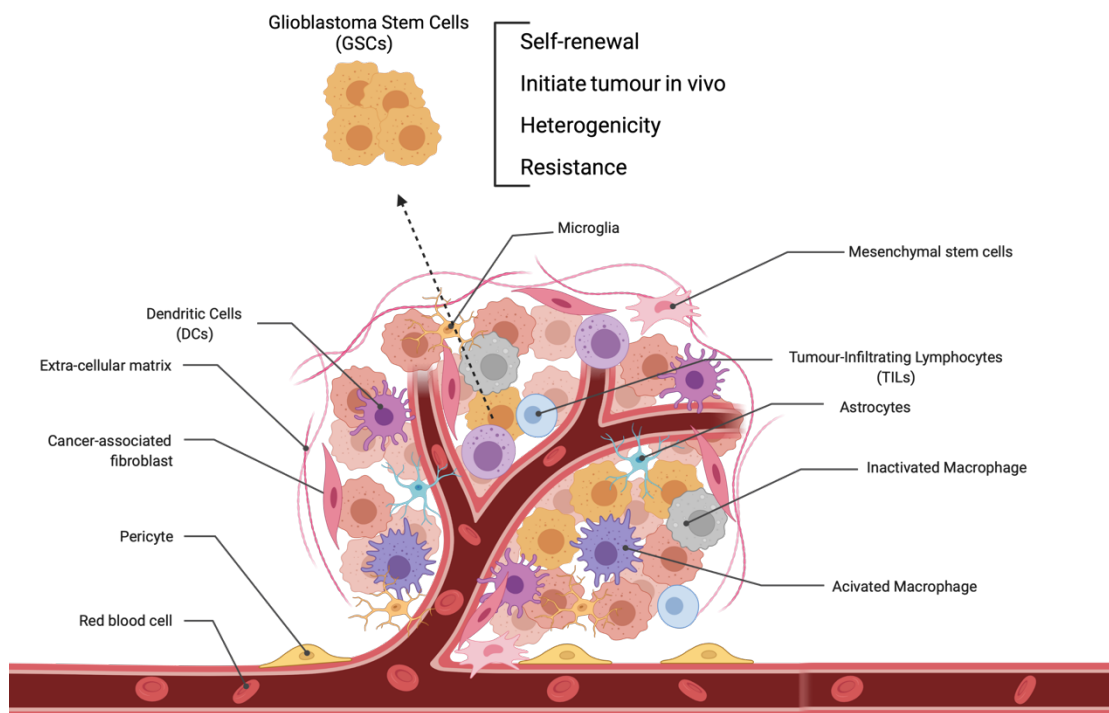


Figure 6: Overview of tumour microenvironment with the presence of glioblastoma stem-like cells. Tumour microenvironment is composed by stromal cells like fibroblast, microglia and astrocytes, mesenchymal cells, immune cells and GSC cells. (Figure created with [biorender.com](https://www.biorender.com))

1.3.1 GSC tumour niches

Preclinical studies demonstrate that GSCs can activate mechanisms to escape radiotherapy and protect themselves. One parameter that may influence the response to irradiation is the tumour microenvironment (TME). It is well known that apart from tumours cells, tumours are composed by other cells like endothelial cells, infiltrating inflammatory and immune cells. Together with extracellular matrix cytokines, nitric oxide and oxygen levels, these cells can participate in the resistance mechanisms. All these components are also exposed to the radiotherapy treatment, and the crosstalk between them may contribute to the tumour stem-like cells radio-resistance.

The microenvironment niche where the GSC can specifically reside plays a crucial role in homeostasis, regeneration, maintenance and repair⁵⁸. In addition, GSC niches

act as a communication centre where cells interact by direct cell-cell contact or paracrine pathway to maintain and protect the GSC cells from the immune system and therapeutic treatments. In glioblastomas, three specialised niches where vasculature plays a major role have been described⁵⁹.

a. The perivascular niche

Glioblastoma is known to be very angiogenic. The formation of disorganised blood vessels within the tumour, creating a supportive micro-environment for GSC growth maintenance and survival, is frequently observed. The creation of these new vessels in the tumour is due to the overexpression of vascular endothelial growth factor (VEGF). VEGF and other factors like FGF (fibroblast growth factor) and PDGF (platelet-derived growth factor) are overexpressed in GBM⁶⁰. Apart from the proliferation of already existing endothelial cells, the expansion of vasculature can result from the trans-differentiation of GSCs into endothelial cells and pericytes participating thereby directly in vessels formation by creating the support of microvasculature⁶¹. The vascular formation can also result from the recruitment of bone marrow-derived endothelial pericytes progenitors incorporated in growing vessels, although this mechanism appears to have a minor role⁶².

On the other hand, vascular abnormalities can disrupt the blood-brain barrier (BBB). This disruption induces barrier permeability allowing plasma and fluid to penetrate inside tumour tissue and produce cerebral oedema and interstitial pressure⁶³. Moreover, as a consequence of BBB disruption, immune cells like monocytes, pericytes and myeloid-derived suppressors cells (MDSC) can enter the brain and be found in the perivascular niche⁶⁴⁻⁶⁶ (Figure 7). The role of these cells in the GBM immune microenvironment will be explained in detail in the 1.4 section of this manuscript.

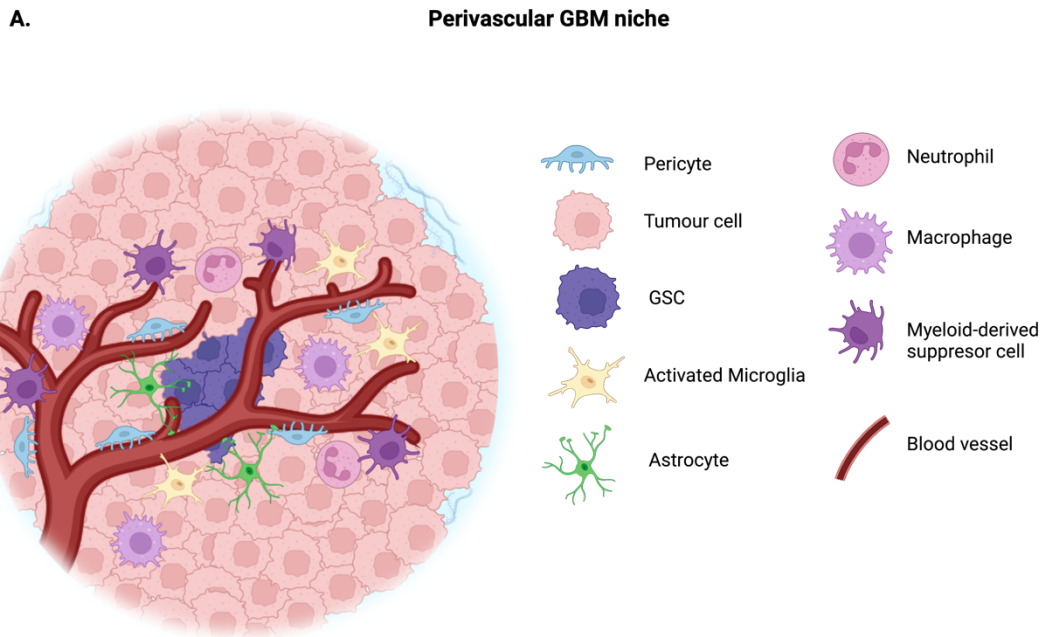


Figure 7: Illustration of the perivascular niche (PVN). Glioblastoma cell interactions with cells of the microenvironment create a supportive niche allowing GSCs proliferation, maintenance and survival. This niche is a multicellular structure made of endothelial cells, pericytes, macrophages, neutrophils and myeloid-derived suppressor cells (MDSCs) that interact with tumour cells and GSC. Macrophages are recruited by tumour cells and GSCs. (Adapted from Hambarzumyan D, et al., 2015, modified with [biorender.com](https://www.biorender.com))

b. The hypoxic niche

Some regions of the tumour are deprived of correct oxygen irrigation. This hypoxia can lead to the formation of pseudopalisading necrotic area⁶⁷. These necrotic regions are developed due to vessel collapse, vaso-occlusion by endothelial cell apoptosis, vascular regression and intravascular thrombosis⁶⁸. As explained in the 1.1.2 section, GBM cells elongate their nuclei and get aligned in rows as palisades around the necrotic centre¹⁴. Pseudopalisading necrosis and microvascular hyperplasia are two powerful predictors of poor prognosis and characterise the transition of high-grade astrocytoma to glioblastoma⁶⁹. Hypoxia modulates the HIF-1- α and HIF-1- β expression that becomes stable in low oxygen conditions, being upregulated in pseudopalisading tumour cells. At the same time, these cells overexpress VEGF and IL-8, which participate in survival, invasion and angiogenesis^{70,71}. GSCs are recruited to these regions and detected in perinecrotic biopsied samples. Thus, hypoxia induces stem characteristics by activating genes related to self-renewal and

dedifferentiation such as CD133, SOX2, OCT4, Nestin, CXCR4 and Klf4⁷². Moreover, these regions protect GSCs from chemotherapy and radiotherapy (Figure 8)⁷³.

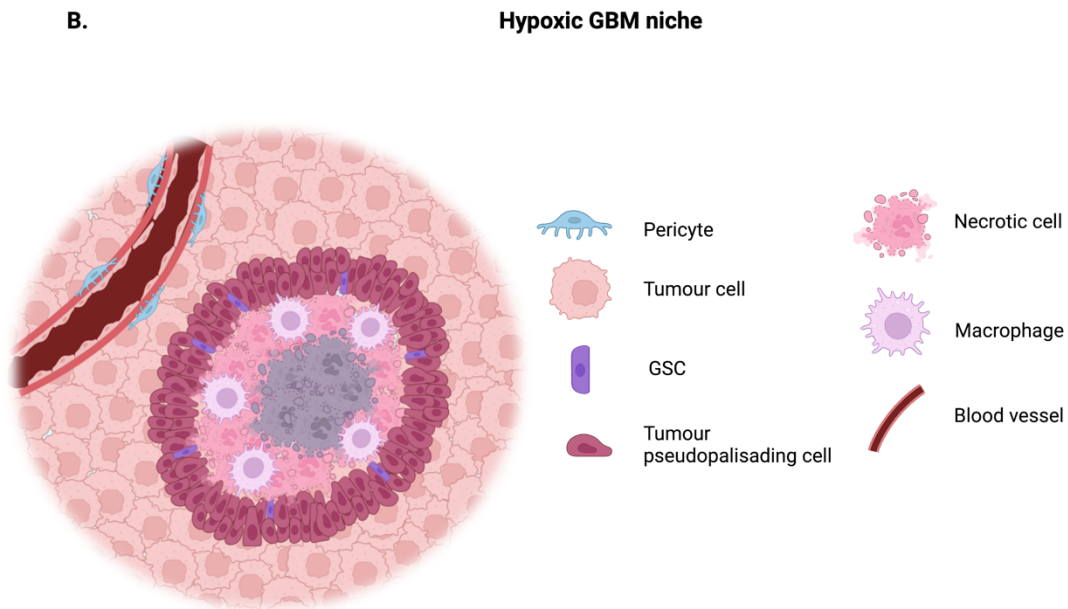


Figure 8: Illustration of the hypoxic GBM niche. Pseudopalisading regions with a necrotic core are characteristic of GBM. This structure creates a hypoxic niche for GSCs. Hypoxia induces the expression of HIF-1- α which promotes the expansion of GSCs and the recruitment of immune cells like Macrophages. (Adapted from Hambarzumyan D, et al., 2015, modified with [biorender.com](https://www.biorender.com))

c. The invasive niche

Tumour cells can migrate and invade normal parenchymal tissue. GSCs can migrate as single cells or through white matter and blood vessel tracks⁷⁴. During parenchyma invasion, the interstitial space is filled with a matrix composed of proteoglycans, hyaluronan and tenascins produced by astrocytes, forming a gelatinous substance filling throughout the brain space. Most of these secreted molecules are important for the attachment of cells. However, this dense ECM can be an obstacle to the migration of glioma cells⁷⁵. For this reason, glioma cells secrete proteases including matrix metalloproteinases (MMPs) type MMP1, MMP2 and MMP9 or recruit microglia, astrocytes and endothelial cells able to secrete more proteases. This combined protease activity degrades ECM to increase tumour invasion and migration and thus

increases glioma proliferation⁷⁶. In contrast to the perivascular niche, it confers a more functional vasculature and is associated with other host cells components like astrocytes, endothelial cells, pericytes and activated microglia (Figure 9)⁷⁷.

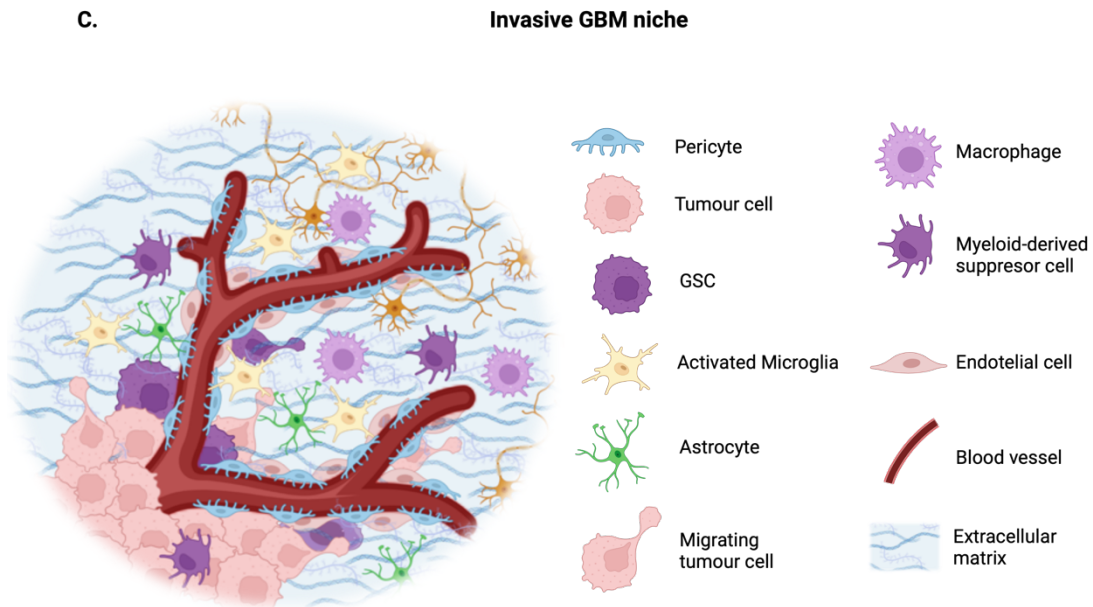


Figure 9: Illustration of the invasive GBM niche. Glioblastoma cells can migrate through blood vessels, defined as perivascular invasion. Cell types that form part of the invasive microenvironment involve endothelial cells, pericytes, activated microglia, reactive astrocytes and neurons. (Adapted from Hambardzumyan D, et al., 2015, modified with biorender.com)

1.3.2 Models of GSC development

The origin of cancer cells in glioblastoma is still not clear, and there are two main hypotheses proposed: the dedifferentiation theory and the stem cell theory²⁵.

- **The dedifferentiation theory**

In glioblastoma, the idea of an hierarchical organisation in which GSC reside at the apex and recreate intra-tumour heterogeneity by creating different types of progenies has been questioned. The dedifferentiation theory is based on the idea that GSC cells do not originate from the transformation of healthy stem cells. Instead, it suggests that, due to tumour cell plasticity and genome instability, non-GSC cells can dedifferentiate and acquire GSC-like properties by the combination of different gene mutations⁷⁸. Indeed, it has been demonstrated that genetic alterations can equally

create GSC cells from Neural Stem Cells (NSC) or from differentiated astrocytes⁷⁹. A more recent study shows that GBM can originate from different brain cells, including cortical astrocytes and neurons. Interestingly, the analysis of these cancer cells in early stages shows that expression of differentiation markers is progressively reduced, while stemness markers expression increases with tumour progression⁷⁸.

- **The Stem Cell theory**

Since 1992, it has been shown that neural stem cells (NSC) can also be found in adult brains⁸⁰. The two neurogenic niches for these NSC are the Subventricular Zone (SVZ) located in the walls of the lateral ventricles and in the subgranular zone (SGZ) of the *dentate gyrus* of the hippocampus^{81,82}. SVZ is the largest neurogenic niche in adult brain located in the lateral wall of lateral cerebral ventricles between the ependyma and a few rows of cells after the ependyma. The NSC located in this area are surrounded by ependymal cells, astrocytes, endothelial cells from blood vessels and oligodendrocytes⁸³. Brain parenchyma is formed by differentiated glial cells and neurons. In human brain, SVZ can be divided into four different layers: layer I is the ependymal layer that lines the ventricle and is composed of ependymal cells possessing atypical microvilli and basal expansions⁸⁴; layer II is the hypocellular layer characterised by the lack of cell bodies with an unknown function; layer III is the astrocytic ribbon layer that mainly contains astrocyte-like NSC and neuroblasts. Finally, the IV layer is composed of myelinated axons and oligodendrocytes⁸⁵.

The Stem Cell theory suggest that GSCs can come from the neural stem cell (NSC)-niche located in the SVZ⁸⁶. As previously explained, this region can produce neurons and glial cells through adult life⁸⁷. Quiescent type B cells (NSC) can give rise to highly proliferative cells (type C cells), also known as transit-amplifying progenitor cells, which differentiate in two progenitor cells: neuroblast (type A cells) and oligodendrocytes precursor cell (OPCs)⁸⁸. GSC are likely to arise from quiescent type B cells located in the SVZ. The most actively dividing cells in the adult brain are the OPCs, meaning that these progenitors are susceptible to being a progenitor of tumourigenesis. OPCs are plastic cells that can give rise to oligodendrocytes. Moreover, GBM expresses NG2 and PDGFR, two markers closely related to OPCs^{89,90}. Lee and colleagues have shown recently that glioma cancer cells can come from mutated SVZ cells. They found a clonal relationship between the SVZ and the

GBM derived tissue, proving that SVZ NSCs are the cells from which GBM cells can derive. Moreover, they demonstrated that astrocyte-like NSCs migrate from the SVZ to a distant region to form a glioblastoma^{85,91}.

Besides being the source of new GSC, SVZ can play the role of a protective niche for GSC cells that have migrated from the tumour mass. The migration of these GSC cells is related to the secretion of different factors and chemokines by the SVZ, including the CXCL12/CXCR4 axis⁹².

1.3.3 CXCR4/CXCL12 axis

In a normal healthy brain, the white matter tracks can guide the migration of NSCs or glial progenitor cells. However, several evidences have demonstrated a similar pattern for the migration of the GBM cells through the SVZ⁹². Some studies have demonstrated that injection of human GBM cells into immunocompromised mice brains can lead to GBM tumours which develop one month after injection. Those mice or *nude* mice are able to accept xenotransplantation due to their immune deficiency. Moreover, migration of GBM cells into the corpus callosum (CC) to reach the ipsi- and contralateral SVZ has been observed^{93,94}. Such GSCs migration from the Tumour Mass (TM) to the SVZ is mediated by a gradient of cytokines or other proteins. The first axis that seems to be involved in this migration is the CXCL12/CXCR4 axis⁹³. CXCL12 (Stromal cell-derived factor-1 or SDF-1) is a chemokine that interacts with the two G protein-coupled (GPCR) receptors, CXCR4 and CXCR7⁹⁵. It is involved in proliferation, tumour growth⁹⁶, epithelio-mesenchymal transition (EMT), regulates the expression of GSC markers and increases the resistance of the tumour to chemotherapy and radiotherapy⁹⁷. Moreover, CXCL12 is known to increase cell survival and facilitate DNA double strands break repair when it interacts with CXCR4 receptor^{98,99}. CXCR7 (also named ACKR3) was identified as a second receptor for CXCL12. In contrast to CXCR4, whose sole ligand is CXCL12, CXCR7 can bind CXCL12 and CXCL11, but its interaction with these ligands does not activate the G-proteins^{100,101}. CXCL12 interaction with CXCR4 can trigger the receptor homo- and heterodimerisation with CXCR7 depending on their respective co-expression level in the cell¹⁰⁰.

- **CXCR4/CXCL12 pathway**

CXCR4 is a membrane receptor with seven alpha-helical transmembrane regions and six extramembrane loops¹⁰². It was discovered in the late 90s as expressed on CD4+ T cells and served as a co-receptor for the human immunodeficiency virus HIV-1¹⁰³. CXCR4 binding with its ligand CXCL12 leads to a conformational change in the receptor that leads to the G-protein activation and dissociation of G-protein α and $\beta\gamma$ subunits¹⁰⁴. G-protein α -subunit induces the release of Ca^{2+} that consequently induces the activation of JAK/STAT, nuclear factor-kappa B (NF- κ B), Ca^{2+} dependent tyrosine kinase PYK2 and the (PIP3K)-Akt pathways that will lead to cell survival and proliferation¹⁰⁵. The G-protein $\beta\gamma$ subunits will induce the downstream activation of the protein kinase B (AKT)/mitogen-activated protein kinase (MAPK) pathway. This activation leads to specific genes expression, actin polymerisation, cell skeleton rearrangement and cell migration¹⁰⁶. During embryonic development, CXCR4/CXCL12 signalling is essential for the distribution and correct migration to the final destination of the CXCR4⁺ progenitor cells¹⁰⁷. CXCR4 internalisation is related to G-proteins' uncoupling and subset interaction with β -arrestin¹⁰⁸.

- **CXCL12/CXCR4 role in Glioblastoma**

Autocrine and paracrine CXCL12/CXCR4 signalling plays an important role in tumour development, cell proliferation and invasiveness of several cancers in humans. Nowadays, CXCR4 overexpression is related to more than 20 human tumours, including pancreatic, ovarian, prostate, breast, renal cell carcinoma, lymphoma, oesophageal, melanoma, neuroblastoma and GBM^{109–113}.

CXCR4 expression in cancer is associated with metastases, migration through a gradient of CXCL12 expressed in organs like lung, liver, brain lymph nodes and bone marrow¹¹⁴. In glioblastomas, this axis is overexpressed compared to adjacent healthy tissue, and expression of both CXCR4 and CXCL12 is correlated with the level of malignancy and poor prognosis^{115,116}. It has been shown that regions where CXCR4 is overexpressed, are hypoxic regions like in the pseudopalisading necrotic areas, as explained in 1.1.2 section and represented in figure 8. Hypoxia promotes GBM angiogenesis through the expression of HIF-1 α that induces the transcription of VEGF and cytokines that, in turn, simulates CXCL12 and CXCR4 upregulation¹⁰⁵.

Moreover, it has been shown that the spread of GSC cells in the brain is followed by the pattern known as “secondary structures of Scherer”, which gather blood vessels, white matter tracts and glial surface. Among those secondary structures of Scherer, GBM cells are organised around blood vessels where CXCL12 is highly expressed, inducing the migration of CXCR4+ GBM cells along white matter tracts¹¹⁷.

CXCR4 overexpression has been detected in GSCs derived from various cancers, including GBM¹⁰⁵. CXCL12/CXCR4 pathways in GSC induce an autocrine/paracrine signal triggering self-renewal, proliferation, migration, angiogenesis, chemo- and radio- resistance⁵⁷. Several studies have shown a higher expression of CXCR4 in GSCs compared with differentiated tumour cells of the same patient, this expression being highly heterogeneous amongst GSCs cultures¹¹⁸.

Goffart *et al.* demonstrated in 2015 that these CXCR4+ GSCs have a specific tropism for the SVZ in both human and mouse brains⁹⁴. They have indeed demonstrated the migration of GBM cells with stemness features through the *corpus callosum* (a secondary structure of Scherer) toward the SVZ, known to express CXCL12. SVZ appears thus as a potential reservoir of GSCs (Figure 10)⁹². As previously explained, the SVZ is a niche for NSC and GSCs, like healthy NSC, require a specific environment to maintain their stemness features. Moreover, CXCL12 secreted by SVZ activates the mechanism responsible for the GSCs’ extrinsic resistance to irradiation¹¹⁹. GSCs that migrate away from tumour mass are thus more resistant to therapy, are away from the tumour mass and the surgical resection main site and could then play a role in tumour recurrence⁹⁴. In line with this study, GSCs isolated from the SVZ appear to be more resistant to drug or/and radiotherapy than cells isolated from the TM¹²⁰.

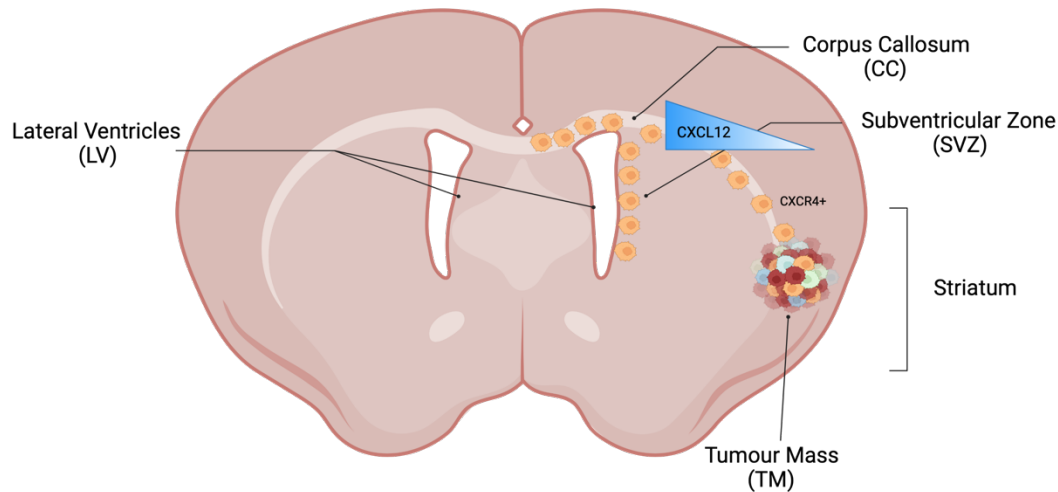


Figure 10: Mice brain representation of GBM cells migrating to the SVZ. Schematic representation of adult glioblastoma (GBM) tumour mass (TM) in the right striatum of the brain (schema drawn as coronal cut showing lateral ventricles). Some GBM cells overexpressing CXCR4 (orange cells) migrate to the subventricular zone (SVZ) of the lateral ventricles (LV) through the corpus callosum (cc) following the gradient of CXCL12 expression. (Created with [biorender.com](https://www.biorender.com))

Moreover, in the same study, they demonstrated the capacity of epithelial-mesenchymal transduction (EMT) induction of GSCs by CXCL12 when located in the SVZ. GSCs in SVZ show a higher expression of mesenchymal markers like vimentin, N-cadherin and EMT transcription factors¹¹⁹. Thus, all this information suggests that SVZ environment is able to attract GSCs in a CXCR4-dependant manner via a CXCL12 gradient. Once in the SVZ, GSCs create a reservoir of stem-like cells for tumour recurrence.

1.4 Importance of the Microenvironment and the Immune system

GBM is considered a “cold tumour”, which means that it is not likely to trigger a strong immune response. However, microenvironment presents a diversity of non-neoplastic cells that includes infiltrating and resident immune cells, endothelial vascular cells and other glial cells¹²¹. Analyses of the percentage of different immune cells present in GBM indicate that tumour-associated macrophages (TAMs) constitute the dominant infiltrate immune cells population. However, we can also find NK cells, regulatory T-cells (Tregs), tumour infiltrating lymphocytes (TILs), dendritic cells (DC) and Myeloid-Derived Suppressor cells (MDSCs)¹²².

1.4.1 *Tumour Associated Macrophages (TAMs) and Microglia*

TAMs represent 30%-40% of the cells in GBM and their interactions with tumour cells, and the microenvironment are important to promote tumour growth and progression^{123,124}. Knowing the crucial role of TAMs in GBM development, it is fundamental to understand the origin of these cells and their functional role.

Tumour-associated macrophages come from two different sources. They differentiate either from brain resident microglia and/or from bone marrow-derived monocytes¹²⁵. During mice's embryonic stage (day 8.5 and 9.5), some progenitor cells migrate from the Yolk sac to the central nervous system (CNS) and differentiate into microglia, maintained during adult life by self-renewing. Microglia is the only resident macrophage in the CNS in a healthy brain parenchyma¹²⁶, but the situation can change upon GBM development. As previously explained, in GBM the BBB is disrupted and allows the infiltration of monocytes recruited from the periphery and migrated into the tumour. One type of monocytes found in the GBM are the macrophages-DC precursors. These macrophages-DC precursors are differentiated into monocytes in the bone marrow and released into the circulating blood to reach peripheric organs¹²⁷. Thus, bone marrow-derived monocytes are highly plastic, and they can change to TAMs following the localisation of the tumour¹²⁸. Engineered mouse models (GEMMs) have demonstrated that the majority of TAMs (85%) come from infiltrating bone marrow-derived monocytes compared to the 15% that represent resident microglia¹²⁹. TAMs are more located in the perivascular areas, while resident microglia is located in peritumoural regions¹²⁵.

TAMs phenotype is achieved due to their interactions with immunogenic antigens, enzymes and cytokines. TAMs are not restricted to a defined M1/M2 population; indeed, they adopt a variety of activation states¹³⁰. Let's remember that the pro-inflammatory M1-like phenotype is characterised by the activation of enzymes like NADPH oxidase, inducible nitric oxide synthase (iNOS), the increase of STAT1, NF- κ B and TNF- α transcription, pro-inflammatory cytokines and chemokines secretion and finally, the expression of MHC I and co-stimulatory molecules like CD40, CD80 and CD86 that increase antigen presentation¹³¹⁻¹³³.

Anti-inflammatory/Pro tumour M2-like macrophages polarization is mediated by IL4 and IL13 expression produced by Th2 lymphocytes, leading to the activation of

STAT and secretion of TGF- β and IL10. It has been shown that there is a bidirectional interaction between M2 and GBM. GSC cells produce IL10, TGF- β and glucocorticoids¹³⁴ that stimulate the expansion of M2-like phenotype, which in turn will promote the proliferation of tumour cells. Thus, TAMs in glioblastoma mainly acquire the M2-like polarisation inducing an unbalance between M1-M2 population^{135,136}.

Knowing that TAMs are a significant population in GBM, it makes pro-tumoural M2 macrophages an interesting target for new therapies. Oncolytic virotherapy has been shown able to revert M2-like phenotype to M1-like and consequently revert the “cold” GBM microenvironment into “hot” and increase the capacity to respond to immunotherapies. This subject will be further discussed in detail in the second part of the introduction of this manuscript^{137–139}.

1.4.2 Regulatory T cells (Tregs)

Regulatory T-cells (Treg) have a major role in mediating immune tolerance and immune suppression and assure protection against autoimmunity¹⁴⁰. Treg can be classified according to their origin in the CNS: the natural Tregs (nTreg) that derive from the thymus and represent the majority of tumour infiltrating lymphocytes in the CNS (25%) and the induced Tregs (iTregs)^{140–142}. GBM recruits nTregs, and their presence induces immune suppression and tumour progression, leading to a poor prognosis. Treg recruitment in GBM is due to the secretion of CCL22 and CCL2 by GBM cells that bind the CCR4 on Treg surface^{143,144}.

1.4.3 Tumour-Infiltrating Lymphocytes (TILs)

TILs are represented by CD8⁺ (CTLs), CD4⁺ T helper cells and regulatory CD4⁺/FoxP3⁺ T cells (Treg)¹⁴⁵. The infiltration of CD8⁺T cells increases from low-grade to high-grade tumours due to the disruption of the BBB. In general, GBM presents a global T cells impairment and immunosuppressive function¹⁴⁶. In fact, patients with GBM display both a reduction of CD4⁺T cells levels and an upregulation of inhibiting receptors like CTLA-4, CD73 and CD39, inducing the decrease of T cell activity¹⁴⁵.

1.4.4 Dendritic cells (DC)

DCs are ubiquitous antigen presenting cells (APCs) responsible for coordinating several immune responses and forming self-tolerance to fight infections¹⁴⁷. The organisation of DC in the CNS is not fully understood, and there are several studies still ongoing to understand their role in GBM microenvironment. Some studies demonstrate that the DC exposition to GBM antigens increases the expression of Nrf2, which correlates to an immunosuppressive state. Thus, the inhibition of Nrf2 can increase the activity of DCs and T cells against GBM¹⁴⁸.

1.4.5 Myeloid-Derived Suppressor Cells (MDSCs)

One of the main characteristics of GBM is the abundance of MDSC in the TME. These cells, which derive from the bone marrow, are a key component of the innate immune system¹⁴⁹. Infiltration of MDSC cells in GBM induces the suppression of cytotoxic CD8⁺ T cells. Studies have shown that they are able to stop CD4⁺T cell memory functions. Their depletion improves mice survival and leads to the increase of T cell activation in patient PBMC's¹⁵⁰. GBM stimulates the expansion of MDSCs by the secretion of various cytokines and factors like IL-6, IL-10, VEGF, PGE-2, GM-CSF and TGF- β ¹⁵¹.

1.5 Current Immunotherapies

As previously said, GBM is highly heterogeneous, and its tumour microenvironment (TME) plays a key role in tumour progression and survival. Despite the introduction of TMZ as a current standard of care (SOC) treatment for GBM in 2005, the median of survival has only improved by a few weeks¹⁵². Moreover, anti-angiogenic treatments as bevacizumab, an inhibitor against vascular endothelial growth factor - A (VEGF-A), and hundreds of other treatments have been tested and have unfortunately failed¹⁵³. Indeed, despite many clinical trials conducted in the last decade, only a few have succeeded in improving only slightly the median of survival¹⁵⁴.

Thus, the lack of success leads to focus on the TME, which has considerable potential for new therapies against cancer. Immunotherapies seem to be successful for many aggressive cancers, and they are now being tested as potential new therapies for

GBM¹⁵⁴. This section, will focus on the several immunotherapies that are ongoing for glioblastoma and their impact on the TME (Figure 11).

- **Immune Checkpoint Inhibitors (ICIs)**

Immune checkpoint molecules are coinhibitory molecules that can attenuate the intensity and duration of T-cell immune response, allowing the maintenance of self-tolerance and preventing an uncontrolled immune response¹⁵⁵. The discovery of the immune checkpoint molecules like the programmed cell death protein 1 (PD-1) and its ligand PDL-1, the cytotoxic T-lymphocyte antigen 4 (CTLA-4), the T-cell immunoglobulin and mucin domain 3 (TIM-3)^{155–157} has recently modified the therapy of some cancers. Immune checkpoint inhibitors anti-CTLA-4 and anti-PD-1/PD-L1 demonstrate to be very successful for melanoma and non-small cell lung cancer (NSCLC)^{158,159}. CTLA-4 has been largely studied, and its capacity to repress T-cell activation results from its interaction with CD80 and CD86 (B7 proteins), creating a competition with the costimulatory molecule CD28 responsible for the activation of CD4⁺ T cells and CD8⁺ cytotoxic T cells (CTL)^{160,161}. In the case of cancer, prolonged T cell activation induces an increase in CTLA-4 expression on Treg and CTL. The interaction of CTLA-4 with B7 proteins leads to the reduction of T cell proliferation and survival¹⁶². In GBM, the immunosuppressive status correlates with the upregulation of PD-L1 in tumour cells and circulating monocytes or macrophages, which leads to a CD8⁺ and CD4⁺T cells inhibition¹⁶³. The prolonged T cell activation induces the expression of PD-1 on T cell surface, allowing the interaction with PD-L1 expressed on antigen presenting cells (APC) and tumour cells, triggering thereby T cell exhaustion¹⁶². This inhibitory mechanism, combined with the upregulation of other immune checkpoints and the infiltration of Treg is a key feature of GBM microenvironment^{164–166}.

The first immune checkpoint inhibitor (ICI) recognised for cancer immunotherapy was the Ipilimumab targeting CTLA-4 used for metastatic melanoma and now approved for other solid tumours¹⁶⁷. In mice models, anti-CTLA-4 has been shown to induce long term survival in 80% of the mice and reduce Treg presence in the tumour¹⁶⁸. On the other hand, anti-PD-1, targeting another important immune checkpoint was able to eliminate 44% of GBM tumours in mice when used alone and 100% when used in co-treatment with TMZ¹⁶⁹. Even if *in vivo* pre-clinical studies with ICI have been promising, results in GBM patients have been disappointing, as

shown in the checkmate 143 trial (the first major clinical trial for immunotherapy). A phase I trial addressing the safety of anti-CTLA-4 and anti-PD-1 in 40 patients with recurrence¹⁷⁰ shows that anti-PD-1 alone was better tolerated than anti-PD-1 and anti-CTLA4 combination. However, a phase III randomised trial comparing anti-CTLA-4 and anti-PD-1 administered to 360 GBM patients failed to improve the survival¹⁷¹. In general, ICIs do not demonstrate a benefit in GBM, and several hypotheses may explain this failure. As mentioned in the previous section, GBM is considered a “cold” tumour, presenting a downregulation of antigen presenting capabilities and a high percentage of TAMs. Immunologically “hot” tumours present high T cell infiltration and immune activation: they are thus able to respond correctly to the ICIs treatment¹⁷². Therefore, turning immunologically cold tumours into hot is crucial to improve the ICIs response. Moreover, GBM can adapt to ICI anti-PD-1 therapy and can upregulate alternative checkpoints like TIM-3, an inhibitory receptor able to suppress CTL and effector T cells. Thus, the treatment of anti-PD-1 combined with anti-TIM-3 may overcome this resistance¹⁷³.

- **Myeloid-Targeted Therapies**

As explained before, TAMs are the most abundant immune cells in GBM and are associated with the grade of malignancy. As previously said, TAMs are not restricted to a defined M1/M2 population¹³⁰. It is interesting to remember that GSCs can recruit TAMs by the secretion of cytokines and periostin^{174,175}. Moreover, TAMs can participate in the immunosuppression of TME by promoting T cell exhaustion by PD-L1/PD-1 signalling, and they do not present activator T cell molecules on their surface as CD80, CD86, and CD40^{176,177}. They also have been associated with resistance to anti-angiogenic treatments like bevacizumab and contribute to the suppression of APCs, DCs and Tregs¹⁷⁸. Altogether, these observations show that TAMs actively participate in immunosuppression and tumour progression and are thus a good target for new therapies. Indeed, several approaches targeting TAMs are currently under consideration. One of them aims to inhibit the colony stimulating factor 1 receptor (CSF-1R), important for macrophages differentiation and survival¹⁷⁹. However, studies using CSF-1R inhibitors alone or in combination with radiotherapy have generated little success¹⁸⁰. In contrast to the CSF-1R inhibitors, there is no information about the potential benefit of targeting specifically

macrophages phenotypes. Studies of MG (Yolk sac-derived tissue microglia) and MDM (monocyte-derived macrophages) allow the identification of different specific markers opening the possibility to distinguish and specifically target them¹⁵⁴. Interestingly, a GBM mouse model study has shown that MDMs but not MG are more efficiently recruited to the perivascular GSC niche of the tumour¹²⁹. Considering all this information, the reprogramming phenotypes of macrophages and the targeting of specific TAMs can be an effective approach to try to change the TME of GBM.

- **Vaccines**

Driven mutations and passenger mutations in tumour cells cause the presentation of tumour antigens to CD4⁺T and CD8⁺T cells by the major histocompatibility complex (MHC) expressed on the surface of cancer cells or antigen presenting cells (APCs)¹⁸¹. Vaccine based therapy allows dendritic cells (DC) to educate them, exposing them to a single high expressed tumour antigen or several of them. The functional role of DCs as APCs in the brain is being more recognised, and it has been shown that they can even arise from MG differentiation. DC-vaccines can be generated by *ex vivo* amplification of DC harvested from patients. Purified DC are expanded *ex vivo*, charged with tumour antigens, exposed to maturation stimuli, and reintroduced into the patient as a vaccine^{182,183}. For GBM, DC-vaccines have shown promising results in early clinical studies. However, it seems that DC vaccines efficacy depends on the GBM subtype. Mesenchymal GBM subtype treated with DC-vaccines seems to have a highest response with a higher increase of CD8⁺ T cells infiltration than in the other subtypes. Thus, molecular GBM subtype can be an important factor to be considered in future studies with DC-vaccines¹⁸⁴.

Neoantigen-targeted vaccines in GBM are very limited due to the high heterogeneity¹⁸⁵. As an alternative, personalised vaccines seem to be a better alternative for this type of cancer. This kind of approach involves, the characterisation of the tumour's mutational profile, then the selection of a patient-specific target, and finally, the production of the vaccine¹⁸¹. Preliminary results using personalised vaccines in newly diagnosed GBM have shown a positive effect¹⁸⁶. There are over 50 ongoing clinical trials with various forms of vaccines for GBM that are expected to be conducted in the following years¹⁵⁵. One example of these clinical trials is the use of a vaccine that will target IDH1 mutants in newly diagnosed

gliomas of grades 3 or 4. The most common mutation in IDH1 encodes for the so-called IDH1(R132H) mutant. IDH-1-vac is a specific peptide vaccine that, *in vivo*, triggers T helper cell response effective against IDH1 (R132H)¹⁸⁷.

- **CAR T Immunotherapies**

CAR T cell therapy is a personalised treatment of T cells that takes advantage of using the patient's T cells to engineer them to express chimeric antigen receptors (CARs), which target cancer cells. Specifically, CARs combine an intracellular T cell activation domain and an extracellular antigen-recognition domain, linked by a transmembrane domain and a hinge¹⁸⁸. This type of therapy was a hugely successful in blood cancers like acute lymphoblastic leukaemia (ALL) and diffuse large-B-cell lymphoma (DLBCL)^{189,190}. They are different generations of CARs, which have evolved to incorporate co-stimulatory domains such as CD28, 4-1BB, OX40 and ICOS, followed by the addition of cytokines expressing domains¹⁹¹. However, the efficacy of CAR T therapy in solid tumours remains complicated due to off-target effects, poor infiltration and high immunosuppressive TME¹⁸⁸. In the case of glioblastoma, there are some ongoing CAR T cell candidates that include CAR T cells against EGFRvIII, IL13R α 2 and HER2. Studies in orthotopically transplanted human GBM xenograft model have shown a survival increase of the mice up to 55 days by using EGFRvIII specific CAR T¹⁹². IL13R α 2 CAR T cell have been demonstrated to be well tolerated in clinical studies and has been structurally optimised to prevent off-target interaction¹⁹³. IL13R α 2 is overexpressed in 85% of the GBM, and it is related to a poor prognosis and a mesenchymal subtype¹⁹⁴. This IL13R α 2-specific therapeutic candidate has been shown to dramatically reduce the tumour and to trigger a sustained clinical response in a patient with seven highly aggressive recurrence GBMs¹⁹⁵. Finally, HER2 CAR T cells carefully engineered to improve tumour specificity and reduce off-target effects have also generated a good response in early phase clinical trials¹⁹⁶.

However, the capacity of GBM tumours to adapt through antigen escape mechanisms remains a major problem for CAR T cells therapy. Thus, it is useful to target multiple antigens or use CAR T cells combined with another therapeutic approach that can induce synergy to minimise the risk of resistance. Bispecific CAR directed against IL13R α 2 and HER has shown to induce tumour regression and increase survival in

mice model¹⁹⁷, and IL13R α 2 CAR T has been used in combination with nivolumab and ipilimumab for recurrent GBM¹⁸³.

Finally, CAR-NK cell therapy has started to be studied over the last few years. In GBM, NK cells are able to mediate tumour cell killing and their presence is associated with a good prognosis¹⁹⁸. CAR-NK treatment has the advantage that it can be administered to HLA-mismatched patients allowing the possibility of an off-the-shelf therapy¹⁹⁹. Unfortunately, the time and cost associated with the manufacturing of NK expansion are still a barrier to the CAR-NK therapy.

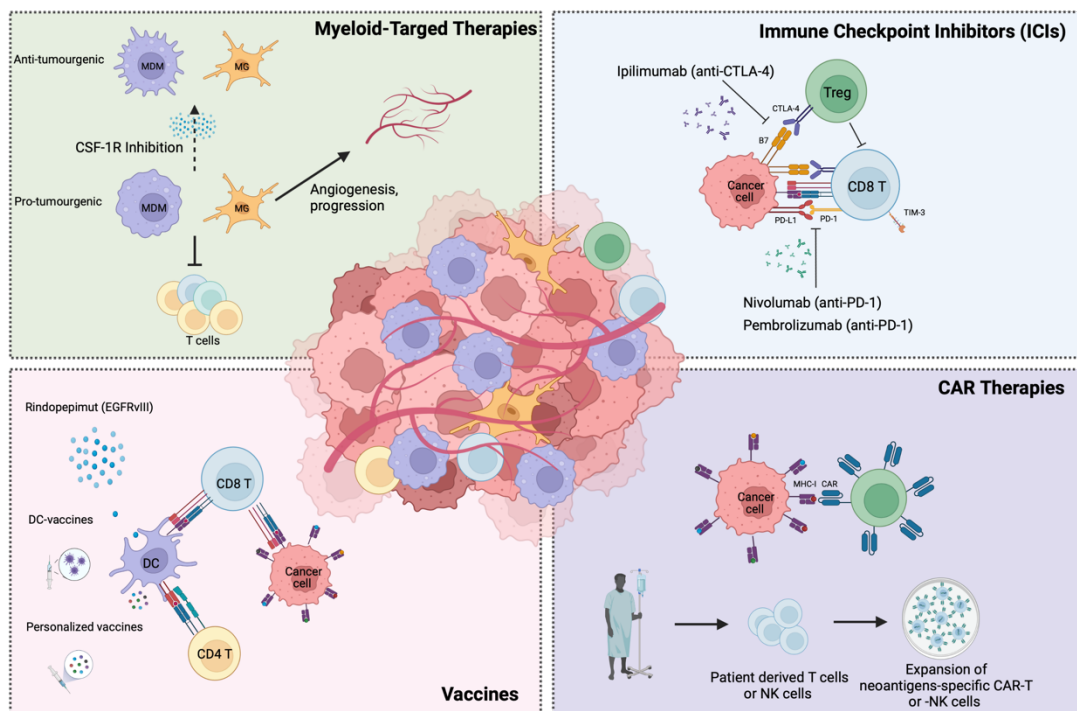


Figure 11: Four current glioma immunotherapies and mechanisms of resistance. Immune checkpoint inhibitors (ICIs) block the immune checkpoint PD-1 or CTLA-4 to restore T cell activity and antitumour activity. Myeloid target therapies like CSF-1R inhibitors can reprogram the immunosuppressed microglia (MG), or monocytes derived macrophages (MDMs) to become anti-tumourigenic. DC-vaccines are personalised vaccines able to educate T cells to specific neoantigens. Chimeric antigens receptors (CAR) therapy is based on patients T cells or non-patient NK cells genetically engineered for expressing CARs and further transferred to the patient. (Adapted from Yu and Quail, 2021 with [biorender.com](https://www.biorender.com)).

The last immune therapy to discuss is the oncolytic virus (OV) which is the main subject of the project and will be discussed in detail in the second part of the introduction.

2. Oncolytic virus therapy

2.1 Oncolytic virus types and characteristics

Oncolytic virus (OV) therapy relies on the use of viruses able to selectively replicate in cancer cells and kill them without damaging normal surrounding tissue and constitutes thus a new promising therapeutic approach²⁰⁰. OV are presented as an innovating cancer therapy with different mechanisms of action²⁰¹. Oncolytic viruses can be divided into two classes depending on their characteristics. One group corresponds to the viruses that have a natural tropism to cancer cells but are non-pathogenic in humans due to the immune system's sensitivity to detect them or their dependence to replicate only in the presence of an activated oncogenic pathway. In this group, we can include the parvovirus, myxoma virus (MYXV), Newcastle disease virus (NDV), reovirus and Seneca Valley virus (SVV). The second group corresponds to two types of viruses. On the one hand, viruses including, measles virus, poliovirus, and vaccinia virus, are genetically modified to be used as vaccine vectors. On the other hand, viruses such as Adenovirus (Ad), Herpes simplex virus (HSV), vaccinia virus (VV) and vesicular stomatitis virus (VSV) have been genetically engineered with deletions or mutations in genes that are necessary to replicate in normal cells but not in cancer cells^{202,203}.

As a result of the evolution of knowledge and available tools for genetic engineering, the OV field has rapidly evolved over the past 20-30 years, leading to a broad range of viruses that have been designed to ensure the infection in cancer cells only or sub-populations of cancer cells and to improve the safety²⁰¹. As a therapeutic tool, virotherapy presents many advantages as the low probability of developing resistance, the possibility of targeting multiple oncogenic pathways, replicating specifically in tumour cells, and the absence of pathogenicity (only minimal systemic toxicity has been detected). Importantly, the viral infection triggers an immune response not only against viral antigens but also against tumour antigens released upon virus-induced cell lysis, making it suitable to be used in combination with other immunotherapies like ICIs and CAR T cell therapy^{200,204}.

The first registered and approved OV was a picornavirus (Rigvir®) approved in Latvia in 2004 for melanoma treatment. This virus was not genetically modified but has been selected and adapted for melanoma. However, this oncolytic virus has not

been broadly used²⁰⁵. In 2005, the engineered adenovirus H101 (Oncorine[®]) was approved in China to treat neck cancer²⁰⁶, and in 2015, an engineered Herpes Simplex Virus (HSV-1), called Talimogene Laherparepvec (T-VEC, Imlygic[™]) was the first to be approved in USA and Europe for the treatment of non-resectable metastatic melanoma²⁰⁷. Finally, in 2021, DELYTACT[®], a modified oncolytic HSV-1 (G47 Δ) was recently approved in Japan for glioblastoma treatment²⁰⁸.

Several types of viruses with and without genetic alterations have been tested for their oncolytic properties and are currently in clinical trials (Table 1). Many DNA viruses (adenoviruses, HSV-1, parvoviruses, poxviruses, vaccinia virus and myxoma virus) or RNA viruses (Coxsackie virus, Maraba virus, measles virus, Newcastle disease virus, poliovirus, reovirus, retrovirus, Seneca Valley virus, Semliki Forest virus, Vesicular Stomatitis virus and Sindbis virus (SBV) are currently in clinical trials²⁰⁴.

Table 1: List of Oncolytic virus in clinical trials.

Virus	Genome size	Cell receptor binding	Host	OV name	Phase	Cancer type
DNA virus						
Adenovirus	dsDNA (35kb)	CAR	Human, animals	DNX-2401 ONCOS-102 AD-E6E7	III I I/Ib	Squamous cell carcinoma (SCCHN) ²⁰⁹ Solid tumours ²¹⁰ HPV-associated cancer ²¹¹
Herpesvirus HSV-1, HSV-2	dsDNA (154kb)	HVEM, Nectin-1	Human (HSV-1)	T-VEC, OH2, HSVG207, M032	I/II Ib I	SCCHN ²¹² Melanoma ²¹³ Glioma ²¹⁴
Parvovirus: B19PV, H1PV	ssDNA (5kb)	Sialic acid residues, P antigens	Human, animals	ParvOryx01	I/IIa	Glioblastoma multiforme (GBM) ²¹⁵
Poxvirus: VACV, MYXV	dsDNA (160-190 kb)	Heparan, laminin, chondroitin, integrin β 1, CD98	VACV (unknown) MYXV (rabbit)	Pexa-Vec, JX-594	Ib/II II	Metastatic melanoma ²¹⁶ Hepatocellular carcinoma ²¹⁷
RNA virus						
Alphavirus: Semliki Forest virus (SFV), Sindbis virus (SINV), M1	SS (+) RNA (11-12 kb)	Prohibitin, phosphatidyl serine, GAGs, ATP synthetase β subunit	SFV: rodents/humans SINV: birds	SFV-IL12, SINV AR339	I/II	Recurrent GBM ²¹⁸

Measles virus	SS (-) RNA (16 kb)	SLAMF1 (CD150), CD46, Nectin-4	Human	MV-NIS	I	Medulloblastoma, Recurrent Atypical teratoid/rhabdoid tumour ²¹⁹
New Castle disease virus (NDV)	SS (-) RNA (15 kb)	Sialic acid	Birds	MEDI5395	I	Advanced solid tumours ²²⁰
Coxsackievirus A21	SS (+) RNA (28 kb)	CAR, ICAM-1, DAF	Human	CVA21, CV-B3	I	Non-Muscle invasive Bladder Cancer ²²¹
Polio virus	SS (+) RNA (7.5 kb)	CD155	Human	PVSRIP0	II	Recurrent GBM ²²²
Seneca Valley Virus (SVV)	SS (+) RNA (7.5 kb)	Anthrax toxin receptor 1	Pig, cow	SVV-001	I	Carcinoid Neuroendocrine ²²³
Reovirus	dsRNA (23kb)	Sialic acid, JAM1	Human	Reolysin	II	Metastatic Breast Cancer ²²⁴
VSV	SS (-) RNA (11 kb)	LDLR	Cattle, horse, pigs	VSV-IFN β -NIS	I/II	Solid tumours, Non-Small Cell lung cancer, Neuroendocrine carcinoma ²²⁵
Maraba virus: MG1	SS (-) RNA (11 kb)	LDLR	Amazonian phlebotomine sand flies	MG1MA3	I/II	Advanced Metastatic Solid Tumours ²²⁶

2.2 Herpes Simplex Virus 1 (HSV-1)

Herpes Simplex Virus-1 belongs to the Herpesviridae family, further divided into three subfamilies: the alpha-, beta- and gamma-Herpesviridae. These three subfamilies are organised according to their biological characteristics, genomic sequences, tissue/cell type tropism and cells where they can establish latent infection. More specifically, alpha-Herpesviridae, including HSV-1, HSV-2 and Varicella Zoster Virus (VZV), are characterised by latency in neurons²²⁷.

HSV-1 prevalence is rather high, and approximately 45-90% of the population is positive for HSV-1. Primary infection occurs in an early stage of life, establishing a latent infection in the sensory neurons where the virus remains latent. Upon various stimuli, the latent viruses can periodically reactivate, causing new episodes of clinical disease and potential transmission to a new host²²⁸. In some cases, HSV-1 can be responsible for complications, the most serious one being herpes encephalitis, which occurs when the virus can reach the central nervous system (CNS). Although this complication is rare, it is associated with a high mortality rate²²⁹. Unfortunately, no vaccine is available, despite good knowledge of HSV-1 biology. However, very efficient antiviral treatments, in particular nucleoside analogues such as acyclovir (acycloguanosine), can limit the lytic infection but cannot eliminate the virus²³⁰.

2.2.1 Structure and Genome organisation

HSV-1 is an enveloped virus composed of a 152 kbp double-stranded DNA genome, with few variations between strains. The viral genome is organised as a unique long (U_L), and a unique short (U_S) fragments, both flanked by internal (IR_S/IR_L) or terminal and (TR_S/TR_L) repeated sequences (Figure 12)^{229,231}.

For HSV-1, approximately 80 genes have been identified by direct study of the transcripts and proteins or by the interpretation of the open reading frames (ORFs). Gene's nomenclature is based on the enumeration from the left of the genome orientation and annotation of the segment in which the sequence lies. Thus, R_L1 ; R_L2 , U_L1-U_L56 , R_S1 and U_S1-12 ²²⁹. As pictured in figure 12, this double-strand DNA genome is encased in an icosahedral capsid formed by 162 capsomeres made by six viral proteins. This capsid is surrounded by the tegument formed by 20-23 different viral tegument proteins related to structural and regulatory functions. Finally, the virus is covered by the viral envelope in which at least 12 different

glycoproteins (gB, gC, gD, gE, gG, gH, gI, gJ, gK, gL, gM and gN) are located (Figure 12)^{232,233}.

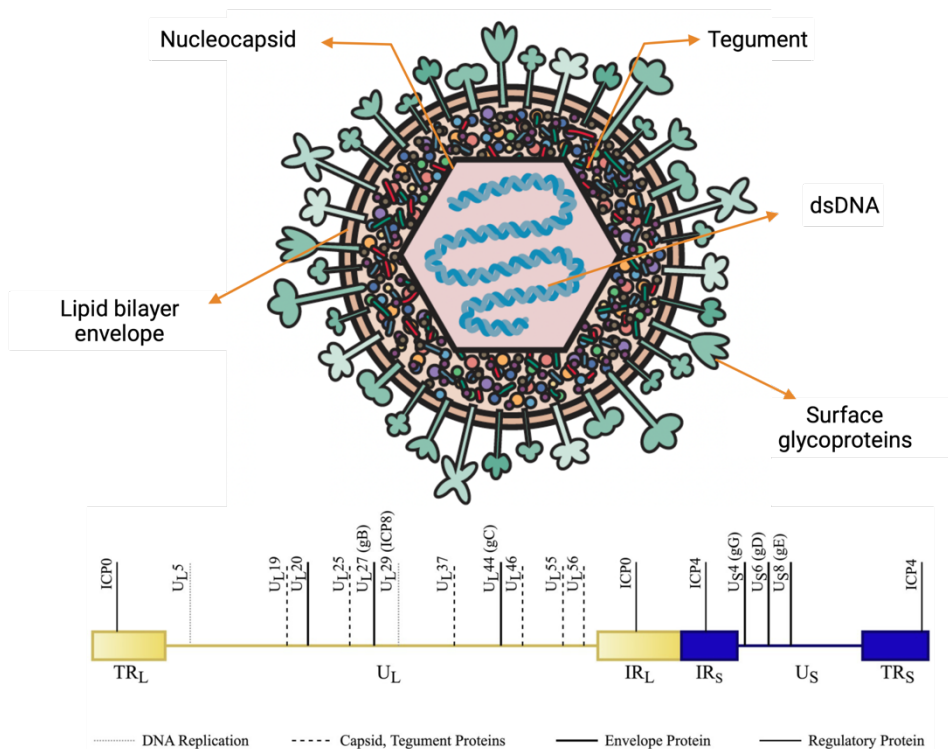


Figure 12: Schema of HSV-1 viral structure and genome. Schematic representation of viral parts. HSV-1 presents an icosahedral capsid surrounded by an amorphous layer of proteins called tegument. The envelope contains an outer lipid membrane derived from the host cell membrane containing different viral glycoproteins. Representation of the HSV-1 genome not drawn to scale showing the different segments. The terminal repeats (TR_L and TR_S), internal repeats (IR_L and IR_S) and the unique long (U_L) (yellow) and short (U_S) (dark blue) region are indicated. (Adapted from Flint Jane, L. *Principles of Virology 4ed. et al.*, 2007 and Krishnan, R. *et al.*, 2021).

2.2.2 Infectious cycle

2.2.2.1 Viral Entry

Entry of HSV-1 into the host cells is a multistage complex that requires the interaction of both viral surface proteins (glycoproteins) and surface cellular proteins. The presence of only four glycoproteins (gB, gD, gL, gH) and the cells receptors are sufficient to deliver viral content inside the cell²³⁴(Figure 15 step 1). In the first step, gB and/or gC first attach to the host cell surface by interaction with heparan sulphate proteoglycans (HSPGs) (Figure 13, step 1), allowing the so-called “viral surfing” of

the viral particle through the cell surface to reach the specific receptor for fusion (Figure 13, step 2). It is known that gC makes the first contact with HSPGs. However, in the absence of gC, gB is able to take its role. The binding of gD with its natural receptors is essential for fusion. gD natural receptors are the Herpesvirus entry mediator (HVEM), nectin-1 or nectin-2, cells adhesion molecules that belong to the immunoglobulin (Ig) superfamily and heparan sulphate harbouring specific modifications (3-O-S HS) catalysed by a particular isoform of 3-O-sulfotransferase (Figure 13, step 3). Indeed, HVEM was the first receptor identified. It corresponds to the tumour necrosis factor (TNF) receptor superfamily, and participates in the regulation of host immune responses. HVEM is expressed by a large variety of cells, including immune cells as T cells, B cells, dendritic cells, etc⁹². Nectin-1 and Nectin-2 belong to the immunoglobulin superfamily and form part of type I transmembrane glycoproteins. They are expressed in a large variety of cell types, and mediate cell-to-cell adhesion²³⁵. The interaction of gD with these receptors induces a conformational change of gD resulting in the displacement of its C-terminus of gD, leading to the uncovering of regions required for gD interaction with gH/gL that activates the mechanism of fusion²³⁶ (Figure 13 step 3). gH/gL requires two signals; one from the gD-cellular receptor binding and the other one from the integrin gH/gL-receptor (Figure 13 step 4). Once these two signals are received, gL disassociates from gH, allowing gH to bind to its receptor and activate gB. Thus, it is suggested that gL acts as an inhibitor of gH. Finally, activation of gB allows the creation of gB,gH/gL fusion complex that induces the formation of a fusion pore allowing the delivery of viral content into the host cell by membrane fusion (Figure 15 step 2a) or endocytosis (Figure 13 step 5), (Figure 15 step 2b)²³⁷. The choice between these two ways of fusion will depend on the cell type²³³.

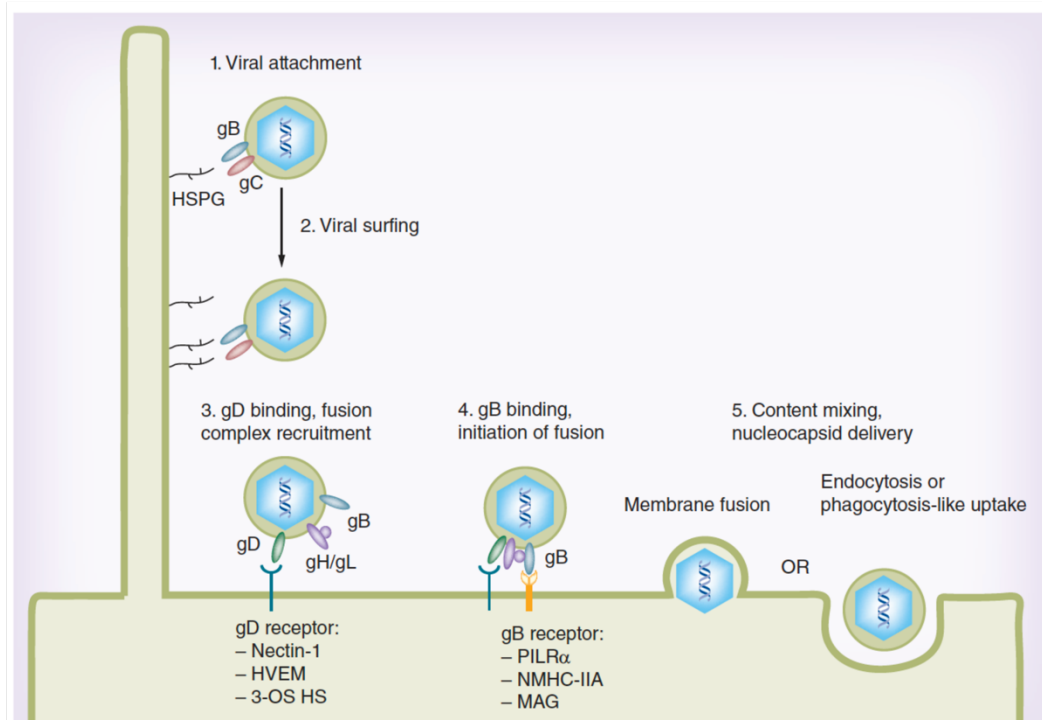


Figure 13: Schematic representation of HSV-1 entry. Four HSV-1 envelope glycoproteins coordinate to induce viral entry through membrane fusion. First, gB along with gC induces viral attachment to the cell surface by interaction with cell-surface heparan sulfate proteoglycans (Step 1 and 2). Then, gD interacts with one of its three entry receptors, HVEM, Nectin-1 or 3-OS-HS (Step 3). This triggers the conformational change of gD, allowing the formation of gH/gL/gB fusion complex (Step 4) that induces the merge of viral lipid envelope and cellular membrane (Step 5) (Adapted from Agelidis M, A. et al., 2015)

Once HSV-1 enters the cell, the nucleocapsid is transported to a nuclear pore as a result of the interaction between the inner tegument proteins and dynein motors to allow retrograde transport along the microtubule to the microtubule organizing centre (MTOC) (Figure 15 step 3). Finally, the capsid approaches to a nuclear pore where viral DNA is released into the nucleoplasm (Figure 15 step 4) ²³⁸.

2.2.3 Gene expression and protein synthesis

HSV-1 genes are expressed during productive infection in tightly regulated and sequentially ordered waves. They are classified as immediate-early (IE or α), early (E or β), and late (L or γ) (Figure 15, step 5). IE are the first genes to be transcribed by the host transcriptional machinery and stimulated by the VP16 tegument protein. This first step does not require the expression of *de novo* viral genes. The presence

of these IE proteins is required for early genes transcription and, finally, late gene transcription that occurs when the viral DNA genome replication has started. These late genes can be subclassified into leaky-late (γ_1) and true-late (γ_2), depending on how strict their requirement is for DNA replication. True-late genes expression depends strictly on viral DNA synthesis, and low levels of leaky-late genes expression can occur prior to DNA replication²³⁹.

IE genes code for four essential proteins in which ICP4 and ICP27 are essential for an effective infection. ICP4, which harbours a DNA-binding domain containing a relaxed sequence that binds to different promoters in the viral genome, is important for early and late gene transcription. ICP27 is a multifunctional protein that has a role in mRNA transport. Apart from these two essential IE proteins, it is important to highlight the role of ICP47, a small protein able to bind and inhibit the transporter associated with antigen processing (TAP), inhibiting thereby the antigen presentation by MHC-I²²⁹.

2.2.4 DNA replication, capsid assembly and egress

HSV-1 capsid is an icosahedral structure formed by 162 capsomeres, each of them containing six (hexamers) or five (pentons) of the major capsid protein VP5 (pUL19). VP26 allows the binding between VP5 hexons. However, triplexes formed by VP19C, and VP23 allow the binding between hexons and pentons. Finally, one vertex of the capsid forms the portal that allows the packing of viral DNA²⁴⁰ (Figure 14).

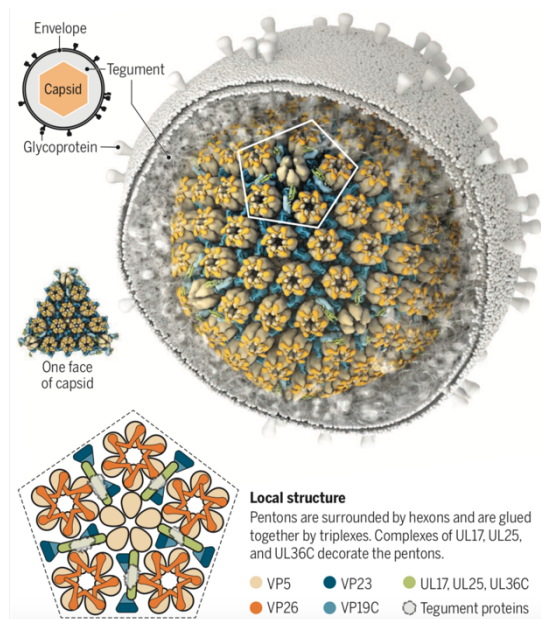


Figure 14: Schematic representation of HSV-1 capsid. HSV-1 capsid structure is composed of 20 faces and 12 vertices. A high-resolution image shows how 3000 proteins forming pentons, hexons and triplexes are arranged to form HSV capsid. Zoom in the local structure shows how VP5 hexons linked by VP26 are arranged around VP5 pentons and linked to them through VP19C and VP23 (Adapted from Heldwein, E. et al., 2018)

After the correct capsid assembly and DNA packaging, which happens in the nucleus (Figure 15 step 7), the capsids need to acquire the envelope, which is acquired after a complicated multi-step mechanism. First, the capsid buds through the inner nuclear membrane (INM) to the perinuclear space, acquiring thus a provisional envelope which then fuses with the outer nuclear membrane (ONM) (Figure 15 step 8), allowing the liberation of naked capsid into the cytoplasm. Once in the cytoplasm, naked capsids interact with Golgi vesicles, where tegument and glycoproteins become assembled by the budding into the vesicles. Protein-protein interaction between tegument and glycoproteins allows the anchor of the membrane to the tegument layer. Finally, these vesicles are transported to the cytoplasmic membrane, where the matured viral particles are released by exocytosis^{229,240}.

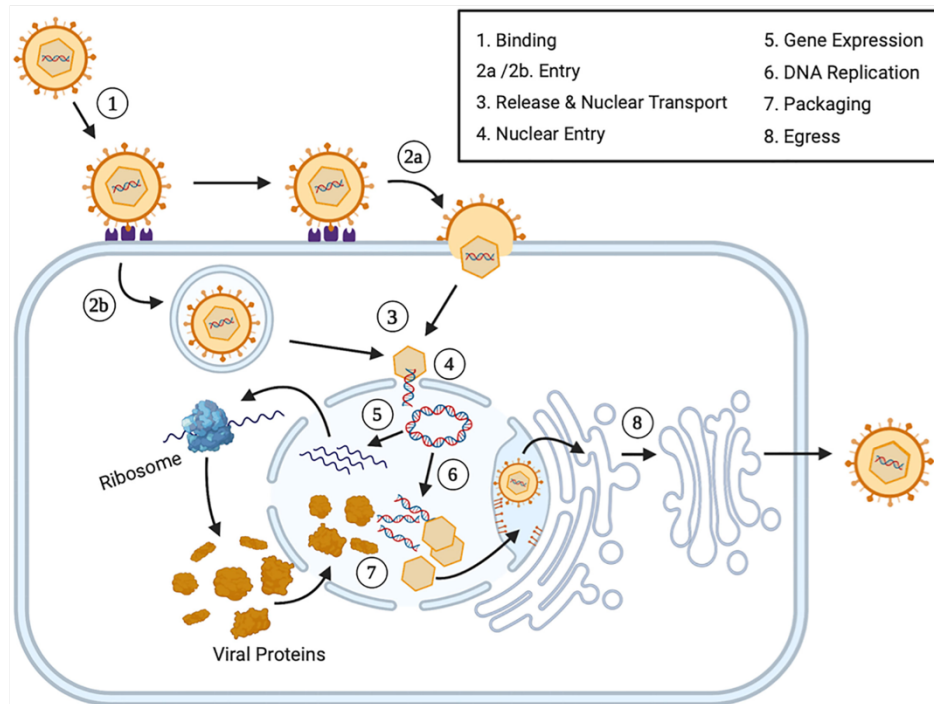


Figure 15: HSV-1 lytic cycle summarised schema. HSV-1 entry replication and assembly in a non-neuronal cell. Glycoprotein C bind to cell surface receptors leading to the interaction between gD and gB/gH/gL complex with the natural receptors HVEM and Nectin-1 (1). This interaction induces the fusion of the viral and host membrane to deliver the viral capsid wrapped with the tegument (2). After the strip of the outer tegument, the layer inner tegument layer can recruit dynein motors and allow the retrograde transport through the microtubules unit to reach the nuclear pore (3). Inside the nucleus, viral DNA undergoes transcription in three timely-regulated waves (IE, E and L) (4) and genome replication (5). The viral genome is then packed into an immature capsid, which supports a nuclear egress (6). The hypothesis of nuclear egress suggests that the nucleocapsids bud through the inner nuclear membrane (INM) to the peri-nuclear space, acquiring thus a primary envelope that fuses to the outer nuclear membrane (ONM). This primary envelope is thus lost, and naked capsids are released into the cytosol. The tegument proteins thus surround nucleocapsids while envelope glycoproteins are processed in the endoplasmic reticulum/ Golgi apparatus. The matured virus is transported via the trans-Golgi network (TGN) or the endosomes (7), where the virus acquires its full matured envelope in a secondary envelopment process. Finally, the virus is released by exocytosis (8) and released to the media/ extracellular region (Adapted from Vernoza. A, et al., 2021).

2.3 HSV as oncolytic virus

As mentioned in the 2.1 section, oncolytic viruses are currently tested in clinical trials and are considered highly promising for cancer treatment. Specifically, oncolytic Herpes Virus (oHSV) is one of the few viruses that have moved to phase III clinical trials. Two oHSV have even been approved for clinical applications (T-Vec in the USA for melanoma and DELYTACT in Japan for glioblastoma)^{241,242} HSV is a great candidate to be used as an oncolytic. On the one hand, it possesses a large genome with approximately 30 kbp code for non-essential genes allowing their deletion and/or their replacement by transgene²⁴³. On the other hand, it presents a good safety profile because it does not induce insertional mutations when it replicates. Moreover, it presents a great sensibility to antiviral treatments like acyclovir²⁴⁴. T-VEC is the only oHSV approved by FDA for melanoma treatment. This oHSV, armed with two copies of granulocyte-macrophage colony-stimulating factor (GM-CSF), has been used in 38 clinical trials that proved its safety and efficiency in several cancers²⁴⁵. In melanoma cancer, T-VEC treatment shows the recruitment of melanoma-specific CD8⁺T cells and a decrease of Treg involved in the immunosuppression²⁴⁶. For GBM in particular, many different oHSV have been developed and tested over the last years²⁴⁷. Indeed, DELYTACT (G47Δ HSV-1) has been approved in Japan as the first oHSV to be used in humans for GBM treatment. G47Δ virus is a third generation oHSV containing a triple mutation within its genome that induce and augments, a selective replication in GBM cells, leading to the induction of an antitumour immune response²⁴². However, despite the fast evolution of oHSV therapy and the great hopes it opens, it still presents some challenges such as suboptimal viral delivery, inefficient viral entry to cancer cells, limited viral replication, etc²⁴¹.

This section of the manuscript will focus on the current types of oHSV therapies and the strategies to overcome the existing treatments.

2.3.1 *Attenuations of oHSV for GBM treatment*

As previously mentioned, HSV codes for many non-essential genes that can be deleted. For treatment safety, some genes need to be removed to ensure a selective replication in cancer cells.

- **γ 34.5 double mutation**

During viral infection, the host cell detects type I IFNs through the IFN receptor triggering the expression of several interferon-stimulated genes (ISGs), among which the protein kinase R (PKR). Once activated, PKR phosphorylates the host translation initiation factor eIF2 α , inhibiting viral and host protein synthesis. However, HSV can overcome this mechanism of defence with ICP34.5 activity, which can bind both the host phosphatase PP1 α and eIF2 α . PP1 α is thus retargeted to eIF2 α and dephosphorylated it, restoring the mRNA translation²⁴⁸. Many oHSVs viruses are deleted from both copies of γ 34.5. The absence of ICP34.5 results in a conditional replication of oncolytic viruses in tumour cells with low PKR activity, such as human glioma cells (Figure 16)²⁴⁹.

Moreover, ICP34.5 has been shown to be responsible for HSV-1 neuropathogenicity, and its deletion improves oHSV safety. The first generation of oHSV (HSV1716 and R3616) with γ 34.5 diploid deletions has proven safer than the wild type virus and has higher oncolytic efficacy²⁵⁰.

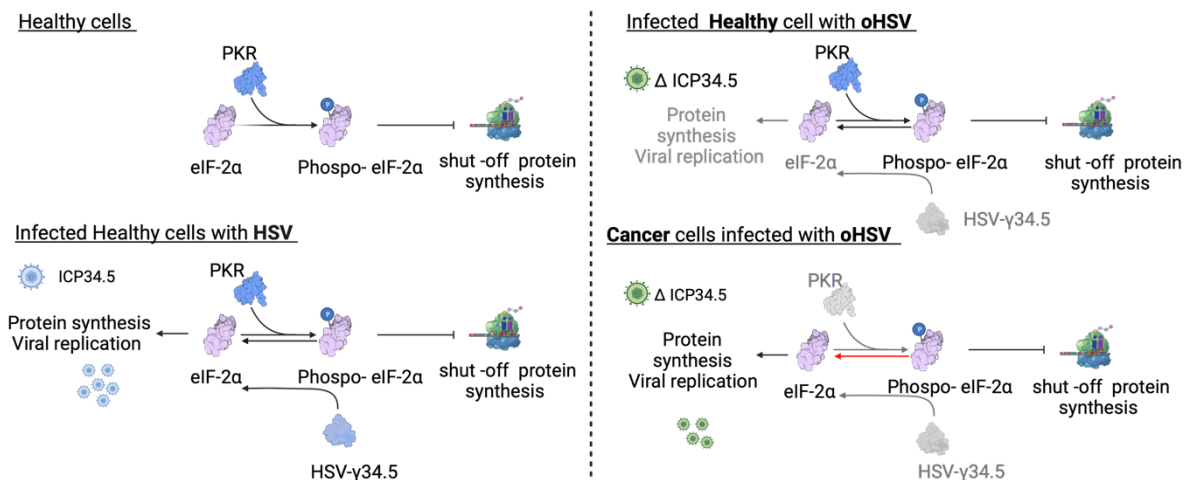


Figure 16: Schematic representation of the ICP34.5 role and the impact of its deletion in oHSV. PKR is responsible for eIF2 α phosphorylation in healthy cells and the subsequent shut-off of protein synthesis. In healthy cells infected with not attenuated HSV, viral ICP34.5 counteract the effect of PKR, leading to viral protein synthesis and viral replication. A healthy cell infected with an attenuated oHSV Δ ICP34.5 can stop protein synthesis due to eIF2 α phosphorylation by a functional PKR. Cancerous cells present a disrupted PKR-eIF2 α pathway. Thus, they cannot shut down viral protein synthesis even if infected with Δ ICP34.5 oHSV virus. Created with biorender.com

- **ICP6 mutation**

In the second generation of oHSV, the double deletion of ICP34.5 has been completed by the deletion/inactivation of UL39, coding ICP6, the larger subunit of the ribonucleotide reductase (RR). This enzyme converts ribonucleotides into deoxyribonucleotides required for viral genome synthesis. In non-dividing cells, the cellular ribonucleotide reductase is not active, but ICP6 can compensate to produce the deoxyribonucleotide pool and allow viral replication while the Δ ICP6 HSV is unable to replicate.²⁵¹ However, when cells are dividing, the cellular RR is active, and ICP6 expression is not required and the Δ ICP6 HSV can thus replicate (Figure 17)²⁵².

G207 was the first oHSV used in a clinical trial in the US for glioblastoma treatment²⁵³. Its attenuation results from both the diploid deletion of ICP34.5 and the inactivation of ICP6²⁵³. It is able to lyse human GBM cells, control tumour growth and increase the survival of orthotopic subcutaneous xenografts mice²⁵⁴.

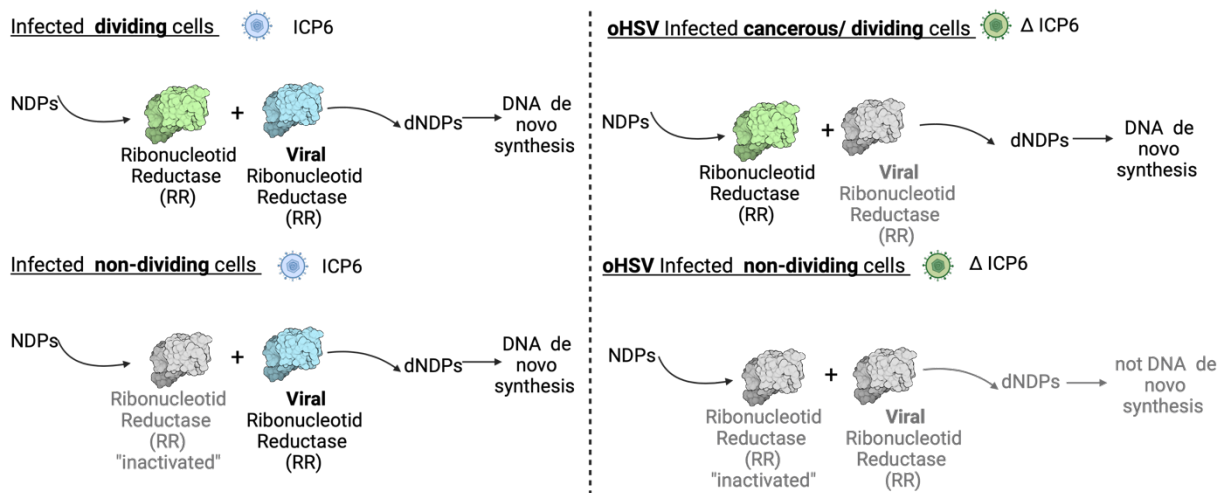


Figure 17: Schematic representation of ICP6 role in HSV and the impact of its deletion. In healthy dividing cells, ribonucleotide reductase (RR) converts ribonucleotides to deoxyribonucleotides for the ‘de novo’ DNA synthesis. In healthy non-dividing cells, RR is not active. When the non-attenuated HSV infects non-dividing cells, viral RR (ICP6) can take the role of cellular RR and lead the DNA ‘de novo’ synthesis allowing the viral genome replication. Upon infection with an Δ ICP6 oHSV, only cancerous cells (highly dividing) are able to induce the DNA ‘de novo’ synthesis due to the presence of active cellular RR. (Created with [biorender.com](https://www.biorender.com)).

- **ICP47 deletion**

In the third generation of oHSV, US12 coding for $\alpha 47$ gene (ICP47) has been deleted. The deletion of this gene has two advantageous consequences. On the one hand, as previously mentioned, ICP47 can bind to the transporter associated with antigen presentation (TAP) and induce the down-regulation of MHC I antigen presentation^{228,255}. Consequently, antigen presentation to CD8⁺ cells is impaired. Deletion of ICP47 restores the capacity to present endogenous antigens in the MHC I context (Figure 18 A)²⁵⁶.

On the other hand, besides this impact on the antigen presentation, ICP47 deletion places the US11 gene, normally expressed as a late gene, under the control of US12 promoter, allowing US11 to be expressed as an immediate-early protein instead of a late protein²⁵⁷. The high levels of US11 bind to the double stranded RNA, a PKR ligand, blocking thereby PKR activation and inhibiting the subsequent signalling pathway. In the presence of US11, eIF2 α is indeed not activated, and the protein synthesis is no more blocked (Figure 18 B). The early expression of US12 thus partly complements the poor replication of $\gamma 34.5$ deletions and is beneficial for oHSV replication, especially in glioblastoma stem-like cells (GSC), in which oHSV- $\Delta\gamma 34.5$ replication is very poor²⁵⁷.

G47 Δ oHSV presents the same deletions as G207 with the addition of the deletion of ICP47²⁴⁹. It shows higher efficacy *in vivo* than G207, reducing tumour growth and has been approved in Japan (DELYTACT) for GBM treatment²⁰⁸.

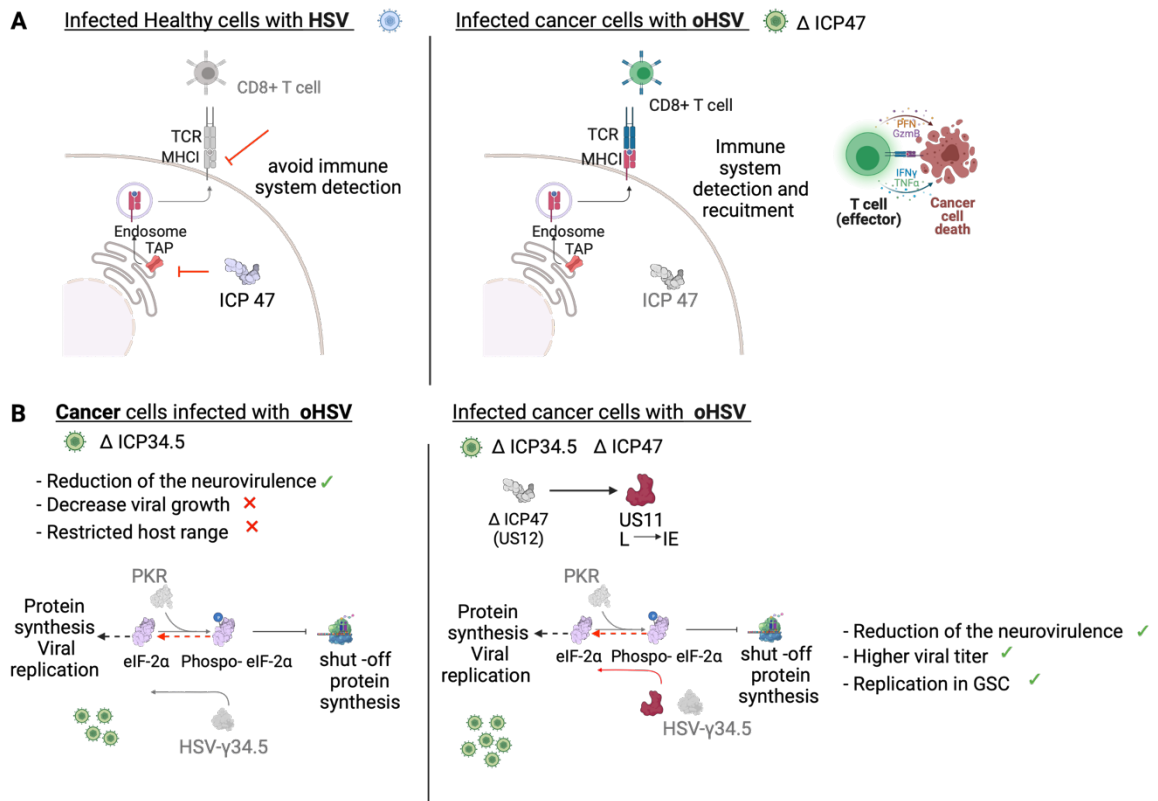


Figure 18: Schematic representation of ICP47 role and the impact of its deletion in oHSV infection. ICP47 blocks the transporter associated with antigens processing (TAP) and leads to an immune escape mechanism. In oHSV, when ICP47 is deleted, viral antigens can be efficiently presented by the MHC-I, and the infected cells are detected by CD8⁺ cells (A). Upon ICP47 (US12) deletion, US11, usually expressed as a Late gene is placed under pICP47 control, changing its expression to an Immediate-Early gene. Due to its capacity to bind dsRNA and thus compete with PKR activation, US11 can partly compensate for the loss of replication efficacy resulting from ICP34.5 deletion (B). (Created with [biorender.com](https://www.biorender.com))

2.3.2 oHSV Re-targeting oHSV for GBM therapy

Attenuated oHSV described above (Δ ICP34.5/ Δ ICP6/ Δ ICP47) have been demonstrated to be safe²⁵⁸. However, the sensitivity of oHSV to infect cancer cells is not optimal due to the different levels of expression of Nectin-1 between tumour cells²⁵⁹. For this reason, some oHSVs have been engineered to specifically infect cancer cells through the overexpression of their specific receptors²⁶⁰. As previously explained, HSV entry occurs in a multiple steps process in which essential glycoproteins gB, gD and gH/gL are required. gD is responsible for the interaction with HSV natural receptors HVEM and Nectin-1. oHSV-retargeting strategies are

thus based on modifying the gD regions shown to be important for interactions with the receptors²⁶¹.

Specifically, gD structure is composed of a V-like Ig domain with N- and C-terminal extensions (Figure 19). The N-terminus of gD is flexible and able to refold the 20 N-terminal amino acids of gD to form a hairpin that interacts with the HVEM receptor. Specifically, HVEM contact residues in gD are from the aa 7 to the aa 15 and for the aa 24 to the aa 32²⁶². In the unliganded molecule, this N-terminal hairpin is filled by the C-terminal region²⁶³. Interaction with the Nectin-1 receptor occurs by binding to an epitope, part of it also located in the N-terminal, also buried by the same C-terminal region when there is no interaction. There are 21 amino acids involved in gD/Nectin-1 interaction, 7 in the N-terminal extension, 13 in the C-terminal and 1 in the Ig core. Specifically, it seems that tyrosine 38 is essential for the binding to nectin-1 and to cell fusion²⁶⁴. The interaction of gD with either of its natural receptors disrupts the interaction of the Ig-core and C-terminal region, inducing an unwrapping of the glycoprotein and exposure of the last 50-residues of C-terminal region, also named pro-fusion domain²⁶⁵. After gD conformation change, pro-fusion domain interacts with gH/gL heterodimer and/or trimer gH/gL/gB. Finally, gB is triggered to insert its fusion loops into the cell membrane leading to membrane fusion²⁶⁶.

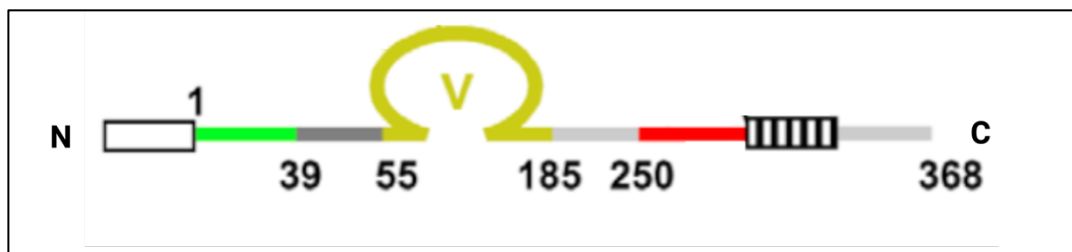


Figure 19: Schematic structure of gD. N- terminal and C-terminal are indicated by an N or a C, respectively. The signal peptide is shown in a white box and transmembrane region as a hatched box. gD Ig core is shown in yellow, residues that form HVEM hairpin in green, residues 39 to 55 from N-terminal in dark grey, residues from the C-terminal region, 185-250 are in light grey and residues implicated in Nectin-1 interaction in red (Adapted from Giovine. P, et al., 2011)²⁶⁶.

Given this information, most retargeted HSV-1 known in literature focuses on gD modifications. Epidermal growth factor receptor (EGFR) is overexpressed in 60% of primary GBMs²⁶⁷, and this is why an oHSV was specifically engineered to target EGFR⁺ cells. Retargeted KNE oHSV was created by deleting the HVEM region of

interaction in gD (A.A. 2-24), which was replaced by a single chain fragment (scFV) antibody against EGFR. KNE was shown to be safe and significantly reduce tumour growth and prolong the survival of mice in an orthotopic GBM xenograft mice model²⁶⁸. Another retargeted oHSV (R-LM113) has been designed to target human epidermal growth factor (HER2)²⁶⁹. As EGFR, HER2 is overexpressed in 80% of primary GBM approximately and is not expressed by neurons or glial cells²⁷⁰. R-LM113 has proven its efficacy against HER2⁺ murine GBM xenografts, increasing the median of survival of 21 days compared to the control group²⁷¹.

These two examples of oHSV retargeting demonstrate that this approach is a way to increase oHSV specificity to tumour cells or a sub-population of them, enhancing oncolytic activity²⁷². However, further clinical trials are required to validate the safety and efficacy of this new generation of oHSV.

2.3.3 *Armed oHSV for GBM*

Even if it has been shown, in preclinical or clinical trials, that oHSV virotherapy by itself can achieve promising results, oHSV infection alone appears to be not potent enough to eliminate a 100% of the tumour.

As previously mentioned, the HSV genome codes for many non-essential genes, which can be replaced by foreign DNA sequences presenting therapeutic potential. oHSV can thus be armed with transgenes whose product may have immunomodulatory, tumour suppressors or antiangiogenic properties, for example²⁷³.

- **Arming with cytokines**

The reduced capacity of oHSVs to activate the immune system is generally due to the immunosuppressive TME found in GBM²⁷⁴. Some oHSV have been armed with different cytokines to stimulate the immune system to overcome this problem. The ability of oHSV to specifically replicate in cancer cells allows to deliver within the tumour itself molecules able to modify the TME properties²⁷³.

IL-12 is a cytokine playing an important role in modulating of the immune system response. It regulates the innate and adaptive response by inducing Th1 differentiation, stimulating the growth and cytotoxicity of NK cells, increasing IFN- γ production and inhibiting angiogenesis²⁷⁵. Murine IL12 (mIL12) was inserted in the G47 Δ backbone by Cheema and colleges²⁷⁶. The so-called G47 Δ -mIL12 oHSV

has shown significant inhibition of angiogenesis and an increased survival in an orthotopic U87 or patient-derived tumourspheres xenograft model. To be able to see the impact on the immune system, the authors also used an immunocompetent orthotopic mouse model where 005 GSC-derived were engrafted. Intratumourally injection of G47Δ-mIL12 induced a significant survival increase compared to the injection of the unarmed oHSV. This increased survival was associated with the reduction of GSC cells and Treg cells²⁷⁶. As IL12, other cytokines like FMS-like tyrosine kinase 3 ligand (Flt3L) were tested to arm oHSVs. Flt3L is a cytokine and growth factor associated with the development of hematopoietic precursors into dendritic cells (DCs) and its mobilization out of the bone marrow. G47Δ-Flt3L had a significant impact on local and systemic immunity, driving a more potent antitumour effect when compared with the parental G47Δ²⁷⁷.

Besides their role in triggering the immune response or angiogenesis, cytokines can also trigger apoptosis. In this context, the tumour necrosis factor-related apoptosis-inducing ligand TRAIL emerges as a promising arming strategy due to its capacity to induce tumour-specific apoptosis in a death receptor-dependent manner.

oHSVs have thus been armed with a soluble form of TRAIL (sTRAIL) shown to have a higher apoptotic effect compared to TRAIL itself²⁷⁸. However, when used in clinical trials, its systemic delivery was associated with off-target toxicity and poor efficacy due to its short half-life²⁷⁹. Moreover, GBM shows a heterogenic response to TRAIL, some of them being resistant to TRAIL-mediated apoptosis²⁸⁰. Interestingly, Tamura K et al. demonstrates by intracranial injection that oHSV and sTRAIL can synergise, and sTRAIL-arming may overcome the resistance to TRAIL²⁷⁸. Importantly, it has also been shown that oHSV-TRAIL is able to overcome TMZ resistance in GBM. Intracranial treatment of recurrent human GSC with oHSV-TRAIL leads to considerable tumour growth inhibition. Thus, local expression of TRAIL by an oncolytic HSV is a promising strategy to avoid toxicity resulting from systemic delivery and overcome resistance to TMZ-chemotherapy²⁸¹.

- **Arming with angiogenesis inhibitors**

oHSV expressing angiogenic inhibitors improved survival compared to the unarmed virus. oHSV-arming with the murine angiostatin (mAngio) (G47Δ-mAngio) showed an extended median of survival compared to unarmed G47Δ²⁸². This improvement is linked to the decrease of tumour vascularity (CD31⁺ vessels), the increased presence

of anti-viral macrophages and the reduction of vascular endothelial growth factor (VEGF) expression²⁸³. Another oHSV armed with an endostatin-angiostatin fusion gene coding for an angiogenic inhibitor demonstrated the reduction of the microvessel density (MVD) in a subcutaneous and intracranial GSC-derived xenograft model, as well as an improvement of median survival compared to the control unarmed oHSV²⁸⁴.

- **Arming with immune checkpoints inhibitors**

As explained before tumour microenvironment (TME) plays a crucial role in GBM progression and maintenance. As explained in the 1.5 section, GBM is known to have a “cold” TME by the overexpression of PDL-1 and CTLA-4. The treatment of GBM with anti-PD-1 shows the inhibition of PD-1/PDL-1 interaction, preventing T cell exhaustion. However, the use of anti-PD-1 is limited by the difficulties to cross the blood-brain barrier (BBB) and the presence of a high immunosuppressive TME characterised by a low number of tumour-infiltrating lymphocytes (TILs)²⁸⁵. The local injection of an oHSV armed with an anti-PD-1 is able to overcome these challenges, as demonstrated by *Passaro et al.* who created an oHSV armed with a scFv against PD-1 (MG34scFvPD-1). In a syngeneic immunocompetent model, the in situ expression of anti PD-1 scFv triggers a durable immune response and long-term memory protection²⁸⁶.

Finally, many different oHSV have been developed, and some of them are currently under clinical trials to validate their safety and efficacy in patients (Table 2)²⁴⁷.

Table 2: List of several oHSVs engineered for GBM treatment

	oHSV	Strain	Deletion	Reporter gene	Targeting	Arming	Model
Unarmed/ Attenuated	dlspk	F	-TK	-	-	-	U87 ²⁸⁷
	hrR3	F	Δ ICP6,	+ lacZ	-	-	U87 ²⁸⁸
	HSV1716	17+	-/- γ 34.5	-	-	-	NT2 ²⁸⁹
	HSV3616	F	-/- γ 34.5	-	-	-	U87 ²⁹⁰
	G207	F	-/- γ 34.5, Δ ICP6,	+ lacZ	-	-	U87 ²⁵¹
	G47 Δ	F	-/- γ 34.5, Δ ICP6, Δ ICP47	+ lacZ	-	-	U87 ²⁵⁶
	rQNestin34.5v2	F	- γ 34.5, Δ ICP6,	+eGFP	-	-	U87 Δ EGFR ²⁹¹
	HSVQ I	F	- γ 34.5, Δ ICP6,	+eGFP	-	-	U87 Δ EGFR ²⁹¹
	C130	AD169/ F	-/- γ 34.5, HCMV-TRS1	-	-	-	U87 ²⁹²
	C134	AD169/F	-/- γ 34.5, HCMV-IRS1	-	-	-	U87 ²⁹²
	C101	F	-/- γ 34.5,	+eGFP	-	-	U87 ²⁹²
	MG18L	F	-US3, Δ ICP6,	+ lacZ	-	-	BT74 ²⁹³

Retargeted	R-LM113	F	-	+eGFP	hHER2	-	mGBM-HER2 and BALB/c- HGG-HER2 ^{271,294}
	R-115	F	-	+eGFP	hHER2	mIL-12	mHGG ^{pdgf} - hHER2 ²⁹⁵
	K-NE	KOS	-	-	EGFR	-	GBM30 ²⁶⁸
	KGE-4: T124	KOS	-	-	EGFR	4 miR-124 target sites in ICP4	GBM30 ²⁹⁶
	KMMP9	KOS	-	-	EGFR/EG FRvIII	4 miR-124 +MMP9	GBM30 ²⁹⁷
Armed with cytokines	G47Δ-mIL12	F	-/- γ 34.5, ΔICP6, ΔICP47	+ lacZ	-	mIL12	005 GSC ²⁷⁶
	M002	F	-/- γ 34.5,	-	-	mIL12	Patient's GBM tumours ²⁵⁹
	oHSV-Flt3L	F	-/- γ 34.5, ΔICP6, ΔICP47	+ lacZ	-	Flt3L	CT-2A ²⁷⁷

	oHSV-TRAIL	F	-/- γ 34.5, Δ ICP6, Δ ICP47	+ lacZ	-	TRAIL	LN229-FmC GBM and GSC31 ^{278,281}
Angiogenic inhibitors	G47 Δ -mAngio	F	-/- γ 34.5, Δ ICP6, Δ ICP47	+ lacZ	-	+mAngio	U87 ^{282,283}
	VAE	F	-/- γ 34.5, Δ ICP6,	-	-	+endo- angio	Human GSC lines ²⁸⁴
	RAMBO	F	-/- γ 34.5, Δ ICP6,	-	-	+Vstat120	U87 Δ EGFR MGG23 ²⁹⁸
Armed with ICIs	NG34scFcPD-1	F	-/- γ 34.5, Δ ICP6,	-	-	+GADD +scFvPD- 1	GL261N4 CT-2A ²⁹⁹

Abbreviations: (-) single deletion, (-/-) diploid deletion, Δ , mutation or inactivation of the gene, (+) insertion.

2.4 oHSV in combination with other treatments

Oncolytic virotherapy has been shown to be very efficient as new therapy but not sufficient to get rid of GBM tumour. Its potential synergy with other treatments like chemotherapy, radiotherapy or immunotherapy should thus be considered.

2.4.1 oHSV and standard therapies

oHSV as a single agent has been tested in different cancer clinical trials alone or/and combined with other treatments. The combination of oHSV with a standard of care treatments (SOC) as chemotherapy and radiotherapy is able to kill more cancer cells than each treatment alone³⁰⁰. Chemotherapy, particularly Temozolomide (TMZ), is one of the most common treatments for GBM. However, it presents some limitations as a dose-limiting toxicity (DLT) and resistance. In contrast, virotherapy does not seem to induce resistance and presents a large therapeutic index (TI) with reduced toxicity. Preclinical and clinical studies are thus essential to determine if the interaction between treatments can have a higher efficacy while reducing toxic effects into normal tissue and therefore be beneficial for the patients³⁰⁰. TMZ and G207 oHSV were shown to synergise and improve TMZ sensitivity to U87 cells due to the upregulation of GADD34 by TMZ treatment. In TMZ-resistant cells, the synergy was observed only when the cells were MGMT-wild type due to the RR upregulation in these cells. More importantly, the combined therapy works in an antagonist way in normal astrocytes *in vitro*³⁰¹.

oHSV treatment has also been shown to synergise with radiotherapy, which is a standard of care treatment in several preclinical studies. Indeed, studies have shown that ICP0, an IE viral protein able to inhibit the repair of DNA double-strand breaks, is able to sensitise radioresistant human GBM cells lines, which thus become more sensitive to radiotherapy³⁰².

2.4.2 oHSV and immune checkpoints inhibitors

As explained in 1.5 section, immune checkpoint inhibitors (ICIs) play an essential role in regulating the anti-tumour response in GBM, known to represent a 'cold' tumour microenvironment (TME). Due to the 'cold' TME, ICIs treatments have a very limited impact and do not lead to an activation of the immune system in GBM³⁰³. More specifically, phase III clinical trials where anti-PD1 (nivolumab), anti-PDL-1, and anti CTLA-4 were systemically administered failed to show an improvement in

patients or in GSC-derived tumours in mice treated. Combined administration of anti-PD1 and anti-CLTA-4 showed only a modest improvement in mice survival³⁰⁴.

In melanoma, T-VEC can activate T-cell response with an increase in CD8⁺T cell infiltration and IFN- γ expression, thus shifting the TME from 'cold' to 'hot'. This additional activity of viral infection allows the consideration of combining virotherapy with ICIs³⁰⁵. Indeed, T-VEC combined with anti-PD-1 in a phase IB clinical trial on melanoma has shown to increase up to 33% the response rate in patients compared to anti-PD1 alone³⁰⁶.

However, in a syngeneic GBM model resulting from the engraftment of murine 005 GBM cells in C57Bl/6 mice, G47 Δ -mIL12 combined with anti-CTLA-4 induces the infiltration of CD3⁺T cells, increases the effector T/Treg ratio but unfortunately induces a modest increase of survival compared to the G47 Δ -mIL12 alone. G47 Δ -mIL12 combined with anti-PD-1 or anti-PD-L1 also showed a limited increase in survival, suggesting that, contrary to the synergy observed in melanoma, the effect of the combined treatment is insufficient to have an impact probably due to the 'cold' TME characterizing the GBM in the mice model³⁰⁴. However, the addition of anti-CTLA4 (that affects immune priming) to anti-PD-1 (important for T cells activation) and G47 Δ -mIL12 show a clear synergy with the triple combined treatment allowing to cure 77% of mice. Importantly, all cured mice display immunological memory protection as demonstrated by the absence of tumour formation upon challenging tumour cell engraftment²⁷⁷. In this setting, local expression of IL12 is important since ICIs and non-armed G47 Δ combined treatment does not show an improvement. The efficacy of the triple treatment correlates with a reduction of tumour cells, an increase of infiltrating T effector cells (CD3⁺, CD8⁺), a proliferation of T cells (CD3⁺Ki67⁺), a reduction of Treg (CD4⁺FoxP3⁺), a reduction of PD-L1⁺ cells, an influx of macrophages (CD68⁺) and their polarization to anti-tumour M1-like phenotype³⁰⁴. CD4⁺, CD8⁺ T cells and macrophages are essential for the efficacy of this triple therapy, with CD4⁺ T cells playing a critical role. This successful triple therapy that switches the TME from 'cold' to 'hot' is very encouraging and might be translated to clinical trials³⁰⁷.

2.5 Impact of viral infection on GBM immune system

oHSV virotherapy plays an important role in the modulation of TME. oHSV lytic infection leads to the release of tumour antigens providing an immunogenic context able to turn the ‘cold’ and immunosuppressing TME into ‘hot’ and immunostimulatory TME³⁰⁸. oHSV are also able to promote immunogenic cell death (ICD) like necrosis, necroptosis, pyroptosis, autophagic cell death and apoptosis, inducing the release of danger-associated molecules patterns (DAMPs) and pathogen-associated molecular patterns (PAMPs). These DAMPs and PAMPs are recognised by NK and DCs cells, leading to the activation of several immune signals (Figure 20)³⁰⁹. Indeed, oHSV infection of squamous cell carcinoma (SCC) induces the increase of ATP and high mobility group box 1 (HMGB1) release. Moreover, infection induces the translocation to the cells surface of calreticulin (CRT) used as an “eat me” signal ³¹⁰.

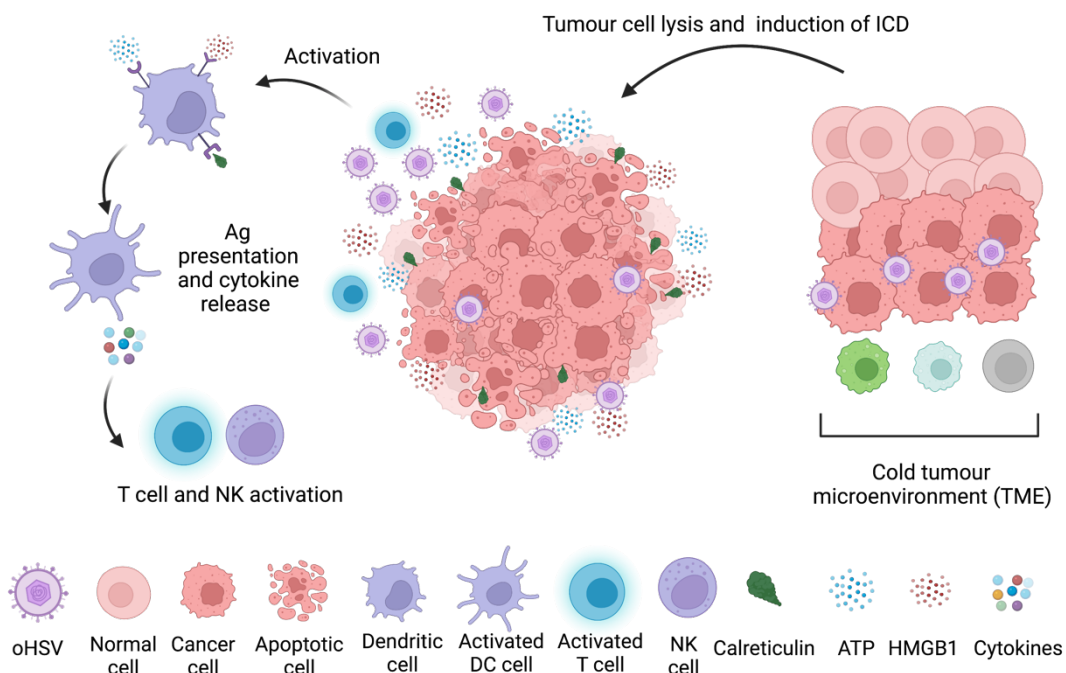


Figure 20: Mechanism of oHSV inducing antitumour immunity. Attenuated oHSV selectively replicates in tumour cells. Infected tumour cells undergo apoptosis and immunogenic cell death (ICD). ICD induces the expression of calreticulin (CRT) and the secretion of damage associated molecular patterns (DAMPs) like ATP and HMGB1. DAMPs are able to interact with DCs and attract them to the tumour area to engulf and present tumour antigens on their surface. The activated DCs secrete cytokines that will stimulate and activate CD8⁺T (CTL) cells and NK cells that will specifically kill tumour cells. (Adapted from Adrak, N. et al., 2021 with [biorender.com](https://www.biorender.com))

2.5.1 *Innate immune response activation and impact*

Activation of the innate and adaptive immune system has been largely studied over the last years. As previously said, HSV is able to induce the activation of host antitumour immune response through the expression of antiviral molecules and recruitment of surrounding immune cells³¹¹.

DCs play a pivotal role in viral clearance and antitumour activity³¹². Viral compounds like DNA, RNA, PAMPs and DAMPs derived from dying tumour cells bind to toll-like receptors (TLR) and other innate immune receptors of the DCs, leading to their maturation. Mature DCs induce the release of cytokines like IL-12, which drive their migration to local lymph nodes where T cells are primed against viral antigens³¹³. An early infection leads to the recruitment of innate lymphoid cells that induce an early, non-specific signal. The recognition of PAMPs by the innate pattern recognition receptors (PRRs) stimulates the expression of type I interferon through the stimulator interferon gene signalling pathway (STING)³¹⁴.

Innate immunity can be more efficiently stimulated by the increased expression of MHC class I and II and co-stimulatory molecules like CD40, CD80, CD83 and CD86 expressed on DCs cells, allowing the connection between innate and adaptive immunity³¹⁵. Viral components detected by PRRs, promote the release of cytokines such as IL-1 β , IL-6, IL-12 and TNF and chemokines like IL-8 and CCL2 by DCs cells³¹⁶. Thus, oncolytic virus therapy is able to override the local immune suppressive state found in a 'cold' TME environment by the induction of an antiviral response enabling a stronger innate immune response and promoting the transition to the adaptive antitumour response.

2.5.2 *Adaptive immune response activation and impact*

As previously said, DCs present antigen to the CD4⁺T and CD8⁺T cells through the MHC class II and MHC class I, respectively. Antigen presentation leads to the priming and activation of antigen-specific T cells. Subsequently, activated T cells start a clonal expansion in the lymph node and migrate again to the tumour by chemokines gradient such as CXCL9 and CXCL10³¹⁷. Ideally, tumour cells expressing MHC I loaded with tumour specific antigens are detected by CD8⁺T cells. Thus, in the context of oncolytic virus treatment, the first T cell response may be specific to viral infection. However, the presence of soluble tumour antigens and

dying tumour cells promotes the cross-presentation of tumour antigens to T cells which migrates to the tumour region due to the virus-mediated inflammation³¹⁸.

As said in the 2.2.3 section, HSV-1 can prevent antigen presentation by blocking the transport associated with antigen processing (TAP). ICP47 viral protein competes and blocks the peptide transportation by TAP and subsequently impairs the presentation of endogenous antigens by MHC-I and thus T cells activation. However, G47 Δ oHSV in which ICP47 is deleted no longer blocks MHC I presentation and allows antigen uptake and presentation by DCs compared to the G207 in which ICP47 is expressed³¹⁹.

Moreover, besides the classical antigen presentation pathway, soluble extracellular antigens can be released and presented by MHC I through an alternative pathway called cross-presentation³²⁰. Cross-presentation is carried out by DCs and plays an important role in the T cell response against tumour associated antigens. The presence of viral antigens resulting from oHSV-mediated oncolysis is able to increase this cross-presentation³²¹. Moreover, even if T cell activation requires three specific signals, viral antigens can usually generate all three T cell activation signals and trigger the T cell activation and recruitment³²². All preclinical data, suggest that OV can overcome the defect in antigen presentation and lead to T cells priming and activation in tumours.

2.6 Clinical evolution of oHSV for glioblastoma

Among all the oncolytic viruses that are currently in clinical trials, herpesviruses are the most tested and investigated. Several genetically engineered oHSV have been developed for the treatment of different cancers, including GBM (Table 3). oHSV that are in clinical trials for GBM or other cancers are; HVS1716, G207, HF10, NV1020, G47 Δ (the first oHSV approved in Japan for glioblastoma), M032, C134, rQNestin34.5v2 and T-VEC (the first oHSV approved by the FDA for melanoma)³²³. Depending on the clinical trial strategy, virus can be administered by injections in multiple areas within the tumour, by repeated intratumour injection or by intravenous administration³²⁴.

Early trials with HSV-1716 ($\Delta\gamma$ 34.5) were done for the treatment of recurrent glioblastoma²⁵¹, and it was tested in phase I clinical trial for stage IV melanoma and recurrent glioma³²⁵. In a first study, nine patients with recurrent high-grade glioma

(HGG) received stereotactic injections of 10^3 - 10^5 plaque forming units (pfu)/ml in scaling doses. Four of the nine patients survived longer than 14 months, and no evidence of HSV reactivation was observed³²⁶. In a second study, 12 HGG patients received an intratumour injection of 10^5 pfu/ml, and after 4-9 days, tumours were resected to evaluate viral replication. Viral DNA was detected in 10 of 12 patients in the injected area, and immune response was detected in 2 patients. This second study thus demonstrated the safety of HSV-1716 in HGG³²⁷. In a third study, 12 recurrent or new diagnosed HGG were under maximal surgical resection, after which they received 10^5 pfu/ml into 8 or 10 sites of the resected cavity. Three patients were stable for 15-22 months following the therapy and demonstrated a reduction of the residual tumour over a 22-month period³²⁸.

G207 ($\Delta\gamma34.5/\Delta$ ICP6) was evaluated in four phase I/Ib clinical trials, which validate its safety when used alone or in combination with radiotherapy for malignant glioma or recurrent GBM treatment³²⁹⁻³³². A first phase Ib clinical trial was performed with 21 HGG patients who received an intra-tumoural injection of 3×10^9 pfu/ml in five sites. Eight patients show a decrease in tumour volume one month after inoculation. Based on the results of this first trial, six recurrent GBM patients were enrolled in a second phase Ib trial and received 1.15×10^9 pfu/ml by stereotactical intra-tumoural injection. Viral replication and antitumour activity were detected in all patients³³¹. Another phase I study demonstrates the safety of G207 and radiation. Patients were treated with a stereotactic injection of 1.15×10^9 pfu of G207 and then irradiated with 5Gy. The combination of these two treatments was safe, and the median of survival significantly increased from 2.5 months without treatment to 7.5 months after G207 treatment³²⁹.

G47 Δ (G207 backbone further deleted for ICP47) has been evaluated in phase I/IIa clinical trial in which 21 GBM patients were enrolled. This trial demonstrates the treatment safety³³³. A phase II clinical trial in which 1×10^9 pfu was injected in the tumour two times for two weeks and then every four weeks for a maximum of 6 injections validates the antitumour efficacy in recurrent GBM patients. The patients well tolerated this treatment³³². rQNestin34.5v2, a modified version of G47 Δ in which ICP34.5 expression is controlled by the nestin promoter (overexpressed in GBM) and C134 virus (a chimeric HSV virus that expresses the HCMV PK-evasion genes) are also under clinical trials³³⁴. M002 virus (G47 Δ armed with mIL12)

demonstrates promising results in a mice model. Thus, a version armed with human IL12 was created (M032) and is currently under clinical trials with patients that present recurrent or progressive GBM³³⁵.

Besides their application in GBM treatment, oncolytic herpesviruses like HF10, NV1020 and T-VEC, have also been used for other cancers such as melanoma, breast cancer and gastric cancer. HF10 oHSV results from spontaneous mutations leading to the defective expression of UL43, UL49.5, UL55, UL56 and LAT genes and the increased expression of UL53 and UL54. It has been used for disseminated fibrosarcoma treatment³³⁶. Although the first tests in metastatic breast and subcutaneous metastases demonstrate no tumour reduction, around 30-100% of the cells die upon infection. Moreover, compared to normal tissue, tumours infected with HF10 demonstrate an increase of CD8⁺T cells and macrophages³³⁷. NV1020 is an R7020 strain HSV-1 virus that was initially developed as a vaccine for HSV-2 treatment. It harbours different modifications like the deletion of one allele of ICP0, ICP4, ICP34.5 and UL56 genes to reduce neurovirulence, and the deletion of thymidine kinase (tk) gene³³⁸. It was used in preclinical trials for pleural, gastric, hepatic cancer, head and neck squamous cell carcinoma^{339,340}. Finally, T-VEC results from the deletion of γ 34.5 and ICP47 and the insertion of GM-CSF gene to induce an immunogenic response³⁴¹. A phase II trial, with patients presenting unresected stage IIIc and IV of melanoma, demonstrate a clinical response in 20% of the patients and a complete response in 13% of the patients²⁴⁶. Additional clinical trials show that T-VEC can synergise with immune checkpoint inhibitors³⁴².

Despite encouraging results, new oHSVs are still under development, for which clinical trials are currently ongoing to determine the safety and tolerance of the virotherapy alone or combined with other treatments such as chemotherapy, radiotherapy or ICIs³²³.

Table 3: Clinical studies with oHSVs for brain tumours

oHSV type	Co-treatment	Cancer type	Viral dose (pfu)	Clinical phase	Country	Status	Main findings	Ref or NTC number
HSV1716	N/A	Recurrent malignant glioma	10^3 - 10^4 - 10^5	N/A	UK	Completed	First starting dose established	<i>Rampling, R. et al., 2000</i> ³²⁶
	N/A	HGG	10^5	N/A	UK	Completed	HSV1716 replication without toxicity	<i>Papanastassiou, V. et al., 2002</i> ³²⁷
	N/A	HGG	10^5 - 10^6	N/A	UK	Completed	No toxicity after viral injection into the resected cavity	<i>Harrow, S. et al., 2004</i> ³²⁸
	Dexamethasone	Refractory of HGG	N/A	I	US	Completed	No toxicity after injection into the resected cavity	NCT02031965
G207	N/A	Recurrent malignant glioma	3×10^9	Ib/II	US	Completed	Correct replication without toxicity after intra-tumour injection	<i>Market, J M. et al., 2000</i> ³³¹ NCT00028158
	N/A	Recurrent GBM	$1,5 \times 10^9$	Ib	US	Completed	No toxicity after viral injection pre- and- post tumour resection	<i>Market, J M. et al., 2009</i> ³³²

	Radiation	Recurrent malignant glioma	1x10 ⁹ followed by 5Gy radiation	I	US	Completed	Correct safety of single dose therapy combined with radiation	<i>Market, J M. et al., 2014</i> ³²⁹
G207	Radiation	Recurrent/ progressive supratentorial brain tumours	1x10 ⁶ or 3x10 ⁹ followed by 5Gy radiation	I	US	Active, not recruiting	N/A	NCT02457845 <i>Walters, M. A. et al., 2017</i> ³⁴³
	Radiation	Recurrent/ Refractory cerebellar brain tumours	1x10 ⁶ followed by 5Gy radiation	I	US	Recruiting	N/A	NCT03911388 <i>Bernstock JD. et al., 2020</i> ³⁴⁴
	Radiation	Recurrent HGG	1x10 ⁸ followed by 5Gy radiation	II	US	Not yet recruiting	N/A	NCT04482933
G47Δ	N/A	Progressive GBM	N/A	I/II	Japan	Recruiting	N/A	UMIN000002661
	N/A	Recurrent or residual GBM	1x10 ⁹	II	Japan	Recruiting	N/A	UMIN000015995
M032	N/A	Recurrent/progressive GBM	N/A	I	US	Active, not recruiting	N/A	NCT02062827
rQNestin 34.5v2	Cyclophosphamide	Recurrent malignant glioma	N/A	I	US	Recruiting	N/A	NCT03152318
C134	N/A	Recurrent GBM	N/A	I	US	Recruiting	N/A	NCT03657576

Abbreviations: N/A, not applicable.

II. AIM OF WORK

Glioblastoma is one of the most common and aggressive primary brain tumours in adults. Despite the improvement of standard treatments, glioblastoma patients have a poor prognosis due to the capacity of tumour cells to be resistant to radio- and/or chemotherapy (TMZ) and more broadly resistant to apoptosis. The expression of CXCR4, a stemness marker frequently overexpressed in cancers, including in Glioblastoma (GBM), usually correlates with the capacity of tumour cells to migrate and become resistant. Importantly, these cells harbour stemness features and are considered Glioblastoma stem-like cells (GSCs), partly responsible for recurrences. These CXCR4⁺ GSCs appear, therefore, as a good target for therapeutic approaches.

The main idea of this project is to create a CXCR4-retargeted oncolytic herpesvirus (oHSV) by the insertion of an anti-CXCR4 nanobody or CXCL12 ligand in the glycoprotein D of an attenuated HSV-1 (Δ ICP34.5; Δ ICP6; Δ ICP47) to target GBM cells that overexpress CXCR4 receptor. Moreover, it has been demonstrated that the combination of TRAIL treatment and oHSV infection is able to induce apoptosis in GBM resistant cells. Thus, we armed the virus with a soluble form of TRAIL (sTRAIL) under the control of the nestin promoter, a stemness marker to overcome the resistance of these GSC cells to apoptosis.

To answer these questions, we worked with glioblastoma cell lines and four different patient-derived cells. An orthotopic GBM model with U87MG CXCR4⁺ cells was used to validate the capacity of the new virus to reduce tumour volume and increase survival.

Part of this data has been submitted in a manuscript entitled:

“Nanobody-based retargeting of an oncolytic herpesvirus for eliminating CXCR4⁺ GBM cells: a proof-of-principle”¹

Judit Sanchez Gil¹, Maxime Dubois¹, Virginie Neirinckx², Arnaud Lombard^{2,3}, Natacha Coppieters², Paolo D’Arrigo¹, Damla Isci², Therese Aldenhoff², Benoit Brouwers², Cédric Lassence¹, Bernard Rogister^{2,4}, Marielle Lebrun¹ and Catherine Sadzot-Delvaux¹.

¹ Laboratory of Virology, GIGA Infection, Inflammation and Immunity (GIGA I3), University of Liège, Liège, Belgium

² Laboratory of Nervous system Disorders and Therapy, GIGA-Neurosciences, University of Liège, Belgium

³ Department of Neurosurgery, CHU of Liège, Liège, Belgium

⁴ Department of Neurology, CHU of Liège, Liège, Belgium

¹ This paper has been accepted on May 18, 2022.

III. MATERIALS AND METHODS

1. Cell lines

VERO cells (ATCC, #CCL-81) and human glioblastoma U87MG (ATCC # HTB-14) cells were maintained in Dulbecco's modified Eagle minimal essential medium (DMEM, Lonza, Verviers, Belgium) supplemented with 10% fetal bovine serum (FBS). J1.1-2 cells are HSV-1 resistant baby hamster kidney cells lacking HVEM and nectin-1 receptors. J/A and J/C cells are J1.1 transduced with HVEM and nectin-1, respectively (kind gift of Pr. G. Campadelli-Fiume (University of Bologna, Italy)). They were cultured with DMEM supplemented with 5% of FBS. J/A and J/C cells were treated with 400 µg/ml of G418 (Invivogen, Belgium). VERO CXCR4⁺ and U87MG CXCR4⁺ obtained by transduction of a lentivirus (Viral Vector platform, University of Liege) were treated with 20 ng/ml and 10 ng/ml of blasticidin, respectively.

Primary GBM primary cultures (T08, T013, T018 and T033) were established from freshly resected human glioblastoma tissue obtained from GBM patients. They were cultured as tumourspheres in stem cell medium (DMEM/F-12 with GlutaMAX (Gibco) supplemented with B27 (1/50) without vitamin A (Gibco), 1% Penicillin-streptomycin (Lonza, Verviers, Belgium), 1 µg/ml of heparin (n 7692.1, Carl Roth, Belgium), human EGF (20 ng/ml) and bFGF (20 ng/ml) (Peprotech). This primary GBM cultures were kept in culture until a maximum of 20 passages.

2. Construction of a recombinant oHSV by Two-steps recombination technique

Recombinant viruses were engineered in fHsvQuik-1 Bacterial artificial chromosome (BAC) containing an attenuated strain F HSV-1 ($\Delta\gamma34.5$, ΔUL39 , GFP; kind gift from A. Chiocca, University of Pittsburg, USA). Recombinants were obtained by the two-step "en passant" Red recombination technique³⁴⁵. Schematic representation with the two main recombination steps is showed in the appendice section (Supplemental figure 5). ICP47 deletion was done as described by Todo T et al., 2001³⁴⁶. The detargeting of gD from its natural receptors was performed as explained by Uchida et al. 2012²⁶⁸. Briefly, for the retargeting, we deleted from the amino acid 2 to the amino acid 24 of gD coding sequence and we inserted a patented

sequence coding for a nanobody against human CXCR4 receptor (CXCR4-NB; WO 2016/156570 A1) flanked by two linkers (G₄S)₃ to increase the flexibility of the nanobody. We also introduce a punctual mutation in tyrosine 38 to eliminate the region of interaction with Nectin-1 receptor. In addition, a second version of the retargeting was done by the insertion of the CXCL12 ligand coding sequences instead of the Nanobody sequence. The “arming” sequence containing a soluble form of TRAIL (sTRAIL)³⁴⁷ under the nestin promoter was inserted before the ICP6 promoter, as shown in figure 23 in the results section. A double mutation (D285N and A549T) was inserted within gB to compensate the loss of infectivity generally observed upon gD retargeting³⁴⁸. Selected clones were validated by sequencing the modified region. Later, a restriction fragment length polymorphism (RFLP) pattern of the clones by EcoRV digestion (Supplemental figure 6), and a fully sequencing of the BAC were done in the selected clones to verify that there was not any spontaneous mutation. All the plasmids, RFLP, part of the sequencing, BAC and primers used for the cloning are cited in the Appendices section.

For the production of the viral particles, the BAC was purified by a maxiprep and CXCR4+ Vero cells were plated in a 6 well at 40% confluence to be transfected with 3µg of BAC using JETPEI (Polyplus, Illkirch – FRANCE). Viral replication was detected 48h after transfection by the visualization of fluorescent foci. Viruses were produced and concentrated as previously described³⁴⁹. Briefly, cells were infected at low MOI (0.005) and cultured for four to five days at 33°C. The day before the experiment, cells were treated with 0,45 M of NaCl and 100 µg/ml of dextran sulfate. Supernatant was collected and centrifuged at 2200 g for 10 min at 4°C, then filtered with 0,8 µm filter to discard cell debris. Then, viral particles were ultracentrifuged at 47.850g at 4°C using Beckman SW27 rotor. The centrifugated virus was resuspended in PBS with 10% glycerol, aliquoted in 1.5 tubes and stored at -80°C. Plaque assay in VERO CXCR4+ was used to titrate the virus and determine the amount of PFU/ml³⁵⁰.

3. Viral growth assay

U87MG CXCR4+ or VERO CXCR4+ cells were plated in a 12 well and infected with oHSV/gD, oHSV/Nb-gD and oHSV/Nb-gD:sTRAIL at an MOI of 1 for 24, 48

or 72h. Supernatant was then harvested, and titer (PFU/ml) was determined by plaque assay.

4. Entry assay

J1.1-2, J/A and J/C cells were plated in a 24 well-plate the day before infection. Cells were infected with an MOI of 1, 0.1 and 0.01. After 48h, cells were fixed with paraformaldehyde 4% and washed with PBS. Images were collected with the Incucyte® S3 (Sartorius).

5. RT-qPCR

Total RNA was isolated using the kit RNA isolation Nucleospin® RNA (Macherey-Nagel) according to the manufacturer's protocol. 500 ng of RNA were reverse transcribed using RevertAid H Minus First Strand cDNA Synthesis Kit (Thermo Scientific, Lithuania) with Random primers (for gD or sTRAIL transcripts detection) or oligo-dT primers (for stemness markers transcripts detection). TBPH or 18S were used as controls. RT-qPCR reaction samples were prepared as follows: 4 µl of the diluted cDNA (2,5 ng in total for gD and sTRAIL or 10 ng in total for stemness markers) were mixed with 5 µl of SYBR green (TAKYON, Eurogentec, Liege, Belgium) and 100 µM of primers in a final volume of 10 ul. Primers used for transcripts detection are described in Table 4. Quantitative real-time PCR was done using the Roche LightCycler 480 (3 min. at 95°C of activation; 45 cycles: Denaturation 95°C, 3 sec, Hybridization and Elongation 60°C 25 sec).

Table 4: List of primers used for RT-qPCR

Primer name	Forward	Reverse
HSV-1 gD	GCCCCGCTGGA ACTACTATG	TTATCTTCACGAGCCGC-AGG
sTRAIL	CATCGAGAACGAGATCGCCC	TGTGTTGCTTCTTCCTCTGGT
CXCR4	ACAGTCAACCTCTACACAGT-GTCC	GCCAACATAGACCACCTTTTCA-GCC
SOX2	AGTCTCCAAGCGACGAAAAA	TTTCACGTTTGCAACTGTCC
POU3F2	CTGACGATCTCCACGCAGTA	GGCAGAAAGCTGTCCAAGTC

SALL2	ACTCCTCTGGGGTGACCTTT	GGAGTGGTAGTGGAGGTGGA
Nestin	CAGGAGAAACAGGGCCTACA	TGGGAGCAAAGATCCAAGAC
18S	AACTTTCGATGGTATCGCCG	CCTTGGATGTGGTAGCCGTTT
TBPH	ACAGCCTGCCACCTTACG	TGCCATAAGGCATCATTGGACTA

6. Flow cytometry

For CXCR4 detection by Flow Cytometry, cells were plated in 6 well-plate two days before analysis or cultured as spheroids. Spheroids and cells cultured as monolayers were washed with PBS and dissociated by incubating the cells for 10 min at 37°C with Accutase (Biowest, Nuaille, France). Once the cells were dissociated, they were centrifugated at 350g for 5 min at 4°C and washed with Flow Buffer (PBS with BSA 1%, EDTA 1mM and Azide 0,1 %). 5 µl of anti-CXCR4 APC-conjugated (#146507 Biologend, Amsterdam, The Netherlands) were added to 1×10^5 cells in 100ul of Flow buffer (dilution 1/20) and kept at 4°C for 1 hour in the dark. Cells were washed by adding 1 ml of Flow Buffer and centrifugated at 400g for 4 min at 4°C. After a second wash, cells were resuspended in 200 µl of Flow buffer and directly analysed with the FACS CANTO II (BD biosciences). Data were analysed with FlowJo software.

7. Annexin V/DAPI apoptosis test

For Annexin V/DAPI apoptosis assay, 92.000 cells were plated in a 12-well plate and infected with an MOI of 1, 5 or 10 for 72 hours or with a MOI of 5 for 24, 48 and 72 hours. Cells were collected and resuspended in 140 µl of Binding Buffer 1X (Cat 556454, BD Pharmingen). 10 µl of DAPI (1:100; Invitrogen) and 5µl of Annexin V-PE (AB_2869071) were added, and cells were incubated for 15 min at RT in the dark. Finally, 200 µl of Binding buffer 1x was added, and samples were directly analysed with the FACS FORTESSA™ (BD biosciences). Data were analysed with FlowJo software.

8. Viability assay

U87MG and U87MG CXCR4⁺ cells were plated in a 12 well. They were infected with the different viruses at an MOI of 5 or treated at a concentration of 1000ng/ml or 100ng/ml with human recombinant sTRAIL expressed in *E. coli* (T9701, Sigma-aldrich). A viability reading was done at 24, 48 and 72h post-infection using a metabolic activity assessment, Resazurin assay. On the day of the lecture, resazurin was prepared at 20% (v/v) with DMEM-10% FBS. The media of each well was removed, and 500 μ L of the diluted resazurin was added. Cells with resazurin were incubated for 4h at 37°C. The metabolised media was transferred into a 96-well flat-bottom black plate. The plate was read using the multi-mode microplate reader (FilterMax F5) to determine cell viability (λ ex= 535 nm; λ em= 595 nm). Obtained results are expressed as a percentage of the control.

9. Cryosection and Immunofluorescence of patient-derived tumourspheres

Tumourspheres were infected for 48 hours with 10⁶ pfu/ml. Forty-eight hours post-infection, cells were washed and fixed with PFA 4% for 20 minutes and incubated overnight with 20% PBS-sucrose before being embedded with coloured OCT (Neg-50™). Spheroids were cut into 5 μ m-thick cryosections (Microm HM 560, ThermoScientific) and placed onto SuperFrost slides (Thermo Scientific). Sections were permeabilised with 0,3% Triton X-100 PBS solution for 10 min, and unspecific binding sites were blocked with 5% BSA for 30 min. Spheroids sections were incubated overnight at 4°C with primary antibodies diluted in 5% BSA (rabbit anti-CXCR4 (Abcam n°124824, 1:200); mouse anti-nestin (sc-23927, Santa Cruz, 1:250). After two washes, slides were incubated for 1h at RT in the dark with secondary antibodies (goat anti-mouse Alexa fluor 633 and goat anti-rabbit Alexa fluor 488 diluted 1:500). Nuclei were stained by incubation with Hoechst for 10 min at 1:50000. Finally, Mowiol (Sigma) was added, and sections were covered by a coverslip. Staining was analysed with Nikon A1R confocal microscope. Figures were composed and examined with ImageJ software.

10. Western Blot assay

Cells were lysed with RIPA modified buffer (50mM of Tris-HCl, 150mM of NaCl, 1mM of EDTA, 1% NP40 and 0,25% of DOC). 80 μ g of proteins were loaded on a

6 (for PARP and gD detection) or 12% (for caspase 3 and α -tubulin detection) SDS-acrylamide gel. After electrophoresis, proteins were transferred on a PVDF membrane (GE Healthcare) according to standards protocols. Mouse anti-gD was used to determine viral infection level (1:1000, sc-21719, Santa Cruz), rabbit anti-PARP (1:1000, 9532, Cell Signaling) and mouse anti-caspase 3 (CC3) (1:1000, ALX-804-305, Enzo Lifesciences) were used to detect the activation of the apoptotic pathway. Mouse anti α -tubulin (1:2000, cat n° T6199, Sigma) was used as loading control. Anti-rabbit- IgG HRP linked (7074, Cell Signaling) and anti-mouse- IgG HRP linked (7076, Cell Signaling) were used as secondary antibodies. Signals were revealed using ECL and imaged with LAS4000 CCD camera (GE Healthcare).

11. *In vivo* experiments

Adult 6 weeks female immunodeficient Crl:NU-Foxn1nu mice (Charles River Laboratories, Brussels, Belgium) were used for xenograft experiments. The athymic nude mice were housed in sterilised, filter-topped cages at the animal facility at the University of Liège, and all experiments were performed as previously approved by the Animal Ethical Committee of the University of Liège, in accordance with the declaration of Helsinki and following the guidelines of the Belgium Ministry of Agriculture in agreement with European Commission Laboratory Animal Care and Use Regulation. Intrastratial grafts were performed following the previously described procedures³⁵¹. Briefly, 50.000 U87MG CXCR4+Luc+ cells resuspended in 2 μ l of PBS were injected into the right striatum of mice previously anaesthetised with an intraperitoneal injection of a Rompun (Sedativum 2%, Bayer, Brussels, Belgium) and Ketalar (Ketamin 50 mg/mL, Pfizer, Brussels, Belgium) solution (V/V) prepared just before injection. The injection was performed according to stereotactic coordinates (0.5 mm anterior and 2.5 mm lateral from the bregma and at a depth of 3 mm), allowing a precise and reproducible injection site. Later, oncolytic viruses resuspended in 2 μ l of PBS were injected, under similar anaesthesia, within the tumour using the same stereotactic coordinates. Mice's health status was evaluated daily, and mice were weighed regularly.

12. Bioluminescence assay in vivo experiments

Immunodeficient nude mice bearing intracranial U87MG CXCR4+Luc+ xenografts were injected intraperitoneally with Beetle Luciferin Potassium salt (E1605,

Promega) (150 mg/kg). Under anaesthesia using 2.5% isoflurane, mice were imaged with a camera-based bioluminescence imaging system (Xenogen IVIS 50®; exposure time 1 min or 30s, 15 min after intraperitoneal injection). Signals were displayed as photons/s/cm²/sr. Regions of interest were defined manually, and images were processed using Living Image and IgorPro Software (Version 2.50). Raw data were expressed as total counts/sec or total counts/min.

13. Intracardiac perfusion of PFA 4% in mice

Mice received an intraperitoneal injection of 140mg/kg of Euthazol Vet (Kela) diluted 1/6 in NaCl 0,9%. After checking the correct function of anaesthesia, mice were placed correctly to proceed with the intracardiac perfusion. The thoracic cage was removed, and 50ul of heparin were injected into the left ventricle. A catheter was placed at the same place, and the right atrium was cut. After cleaning the mice with saline solution (NaCl 0,9%) the mice were fixed entirely using PFA 4%. The brain was removed from the skull with dissection tools and fixed again overnight at 4°C with 4% PFA. The next day PFA was removed, and brains were stored at 4°C in a 30% PBS-Sucrose solution until cryosection.

14. Brain tissue processing and tumour volume measurement

For RT-qPCR brains were not fixed with PFA 4% as previously explained. Brains were just cleaned with saline solution (NaCl 0,9%) and removed from the skull with dissection tools. Right hemispheres were cut into three parts (Frontal, middle and occipital) and stocked at -80°C to perform an RNA extraction using the kit RNA isolation Nucleospin® RNA (Macherey-Nagel) according to the manufacturer's protocol.

Regarding tumour volume analysis, cryosections of the brains were done in the Microm HM 560 (Thermoscientific) at 14 µm of thickness and placed onto SuperFrost slides (Thermo Scientific). Previously to staining, slices were permeabilised again with 4% PFA for 15 min at RT and dried overnight. Tumour volume analysis was performed by Immunohistochemistry for human vimentin detection (Mouse anti-human vimentin, MAB3400, Merck, 1:200) with POLYVIEW®PLUS HRP-DAB kit for detection (Enzo Life Sciences, Brussels, Belgium). Tumour was delineated based on anti-vimentin positivity. 10 to 12 serial

brain sections were analysed using the Mercator software (ExploraNova, La Rochelle, France). 3D reconstitution and extrapolation of tumour volume were performed using Map3D software.

15. Statistical analysis

All statistical analyses were performed using GraphPad Prism 9. Data are displayed as Mean \pm SEM. Depending on the experiments, paired t-Test, one-way or two-way ANOVAs were performed as indicated in the figure legends. Statistical significance of survival assay was analysed by log-ranked (Mantel-Cox) test.

IV. RESULTS

1. Construction of a retargeted oncolytic herpesvirus

As said in the introduction, the role of GSCs in GBM malignancy and recurrence is crucial. Knowing the importance of the CXCL12/CXCR4 pathway and the capacity of the CXCR4⁺ cells to migrate from the tumour mass, we decided to create an oHSV able to target CXCR4⁺ GSCs specifically. We decided to engineer two types of retargeted oHSV. The two oHSV were first detargeted from HVEM and nectin-1, the natural receptors before being retargeted to CXCR4 (Figure 21). These modifications were introduced within fQuick-1 (kind gift from Prof. EA. Chiocca), a BAC containing the attenuated HSV-1 genome (Strain F; Δ ICP34.5/ Δ ICP6/EGFP⁺) (Scheme of the BAC in Annexes). This backbone was further deleted from US12 coding for ICP47. This deletion is important to overcome the attenuation resulting from γ 34.5 deletion partly³⁵². The two types of detargeting/retargeting were achieved by replacing the residues 2-24 of gD of the HVEM-binding domain by either an anti-human CXCR4 nanobody³⁵³ or by the CXCL12 coding sequence. In addition, residue 38 of gD was mutated (Y38C) to impair gD interaction with nectin-1, another natural receptor³⁵⁴. Finally, two mutations (D285N and A549T) shown to improve the fusion capacity of glycoprotein B (gB) were introduced in UL27³⁴⁸. After transfection of these constructions into VERO cells, previously transduced with the human CXCR4, oHSVs were produced in the supernatant and further purified and titrated. They are referred as oHSV/gD (non-retargeted) oHSV/CXCL12-gD (CXCL12-retargeted) oHSV/Nb-gD (CXCR4-retargeted).

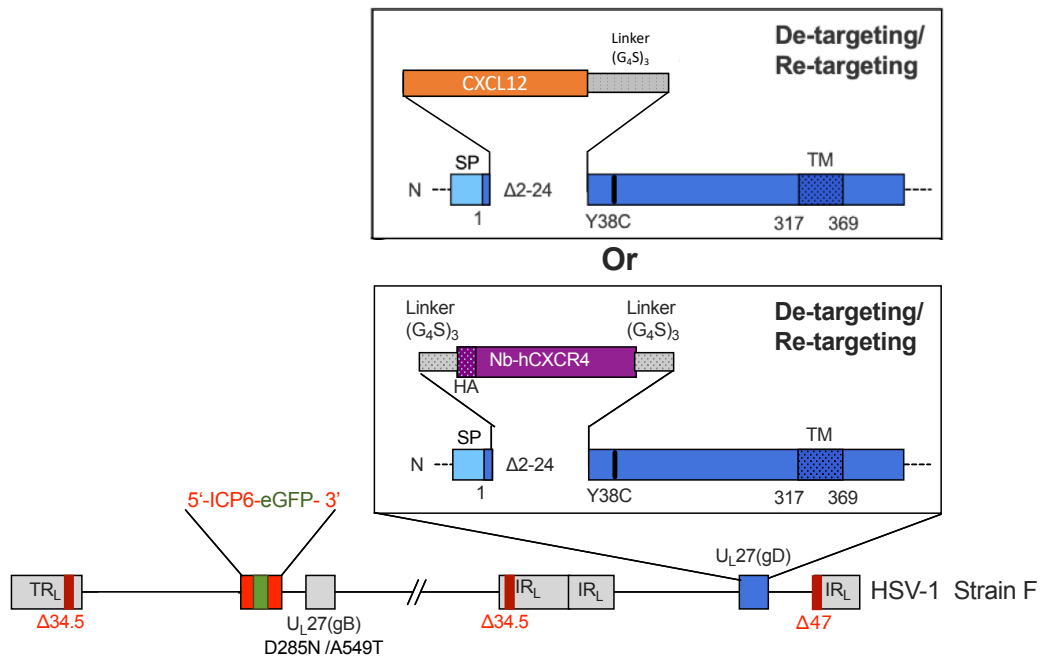


Figure 21: Schematic representation of the structure of the retargeting. oHSV backbone contains the same deletions as the G47Δ backbone (-/- ICP34.5/ΔICP6/ΔICP47). Retargeting of the virus is achieved by integrating either an anti CXCR4-nanobody sequence flanked by two linkers (G₄S)₃ into gD sequence or the insertion of CXCL12 coding sequences followed by a linker(G₄S)₃. A double mutation in gB (D285N/A549T) was done to improve viral fusion capacity.

2. In vitro efficacy of the CXCR4-retargeting

J1.1-2 hamster cells are resistant to HSV due to the lack of HVEM or nectin-1 expression at the cell surface³⁵⁵. Thus, they were used to verify the detargeting efficacy of the two new constructions. These were infected with oHSV/Nb-gD or oHSV/CXCL12-gD at different MOI (0.01, 0.1 and 1). oHSV/gD was inoculated in parallel as a control. In addition, J/A and J/C expressing respectively human HVEM³⁵⁶ or nectin-1³⁵⁷ (kind gift from Pr. G. Campadelli Fiume) were infected in parallel with the different oHSVs. Contrary to oHSV/gD, which led to multiple infectious foci in J/A and J/C, no foci were detected upon oHSV/Nb-gD retargeted viral infection, demonstrating that oHSV/Nb-gD was properly detargeted. However, although the detargeting strategy was the same for both retargeted viruses, oHSV/CXCL12-gD was still able to interact with Nectin showing multiple infection

foci in J/C (Nectin⁺ cells) (Figure 22A). Consequently, we decided to stop the oHSV/CXCL12-gD virus study and continue the analysis of oHSV/Nb-gD.

To evaluate the capacity of oHSV/Nb-gD to infect CXCR4⁺ cells specifically, glioblastoma U87MG cells which express CXCR4 at a very low level (Fig 22B) were transduced with a lentivirus expressing the human CXCR4. The expression of CXCR4 on the U87MG CXCR4⁺ cell surface was confirmed by flow cytometry (Figure 22B). U87MG and U87MG CXCR4⁺ were infected with oHSV/gD or oHSV/Nb-gD (MOI: 0.1). Contrary to oHSV/gD, which entered and replicated in both cell lines independently of CXCR4 expression, oHSV/Nb-gD only generated infectious foci in U87MG CXCR4⁺ cells while no foci were observed in U87MG (Figure 22C, GFP pictures). These observations were supported by a significant increase in gD transcripts as measured by RT-qPCR, confirming that oHSV/Nb-gD infects cells in a CXCR4-dependent manner (Figure 22C). Finally, the growth capacity of both viruses was evaluated in U87MG CXCR4⁺ cells, and no statistical difference was observed (Figure 22D).

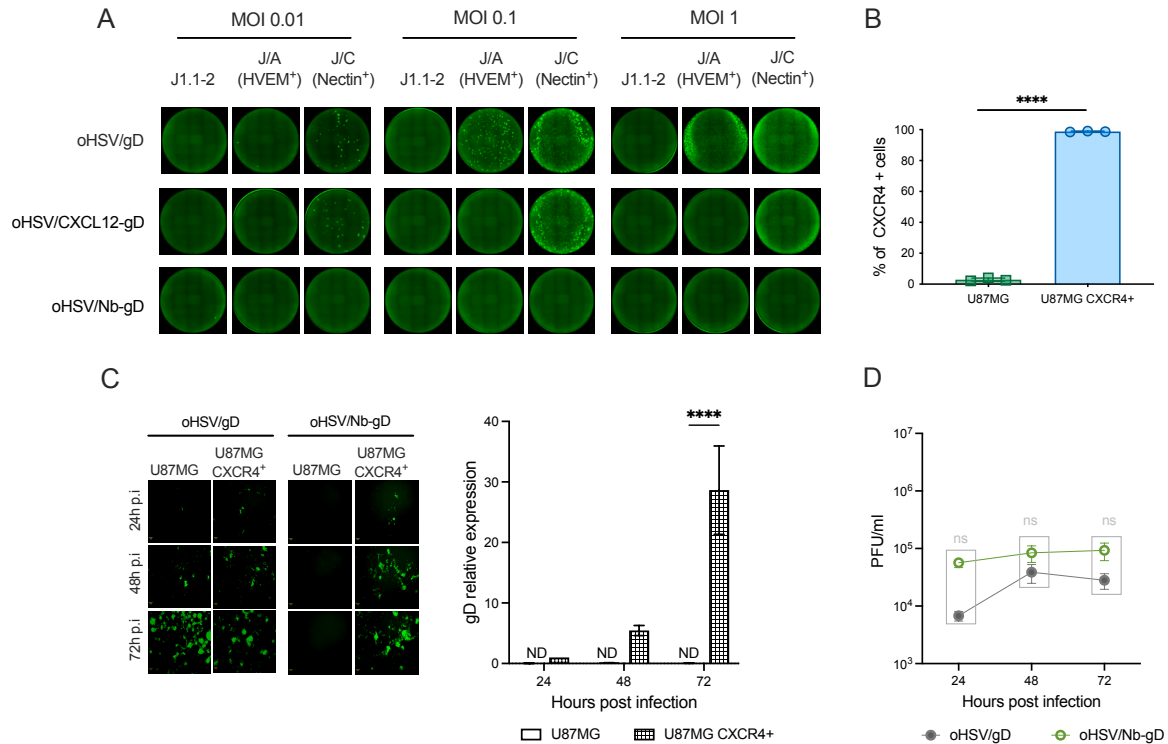


Figure 22: Efficacy of the oHSV de-targeting and re-targeting. J1.1-2, J/A (J1.1 HVEM⁺) and J/C (J1.1 Nectin⁺) cells were infected for 48 hours at an MOI of 0.01, 0.1 and 1 with the recombinant oHSV expressing either gD WT (oHSV/gD) or gD modified by the insertion of either CXCL12 (oHSV/CXCL12-gD) or an anti-CXCR4 nanobody (oHSV/Nb-gD) (A). CXCR4 expression on U87MG and U87MG transduced with hCXCR4 was analysed by flow cytometry (B). U87MG and U87MG CXCR4⁺ cells were infected for 48 hours with oHSV/gD or oHSV/Nb-gD (MOI 0.1). RT-qPCR analysed gD expression in U87MG and U87MG CXCR4⁺ infected cells at 24, 48 or 72 hpi and is expressed as the fold induction with the expression in cells infected with an MOI of 0.1 for 24h considered as equal to 1 (C). For B and C, bars represent the mean \pm SEM of 3 independent experiments. Statistical significance was determined by t-Test (B) or two-way ANOVA (C). (**** $p < 0,0001$). A growth curve assay evaluated the replication efficacy of oHSV/Nb-gD and oHSV/gD virus. U87 CXCR4⁺ cells were infected at an MOI of 1, and the supernatant was harvested at 24, 48, and 72 hours post-infection and used for titration as previously described³⁵⁰ (D). The number of foci was calculated based on Incucyte® imaging. Bars represent the mean \pm SEM (PFU/ml) of three independent experiments. The lack of statistical difference is confirmed by unpaired t-test analysis.

3. Construction of an armed oncolytic herpesvirus

Viruses were further armed with a transgene expressing a soluble form of TRAIL (sTRAIL)³⁴⁷ under the control of a nestin promoter. Specifically, the arming sequence was created by the NH₂-terminal fusion of the extracellular region of TRAIL sequence (114-281 aa) to a sequences coding for (i) an isoleucine zipper, (ii) the extracellular domain of Flt3L, proven able to aid in the secretion of various cellular proteins and (iii) the isoleucine zipper to favour TRAIL trimerization, which is important for enhancing death signalling when it binds to its receptors (Figure 23). Due to the negative results corresponding to oHSV/CXCL12-gD retargeting. This virus was no longer used in this project, and consequently, it has not been armed with sTRAIL transgene.

After transfection of these constructs into VERO cells previously transduced with the human CXCR4, armed oHSVs were produced in the supernatant and further purified and titrated. They are referred as oHSV/gD:sTRAIL (non-retargeted; sTRAIL armed) and oHSV/Nb-gD:sTRAIL (CXCR4-retargeted; sTRAIL-armed).

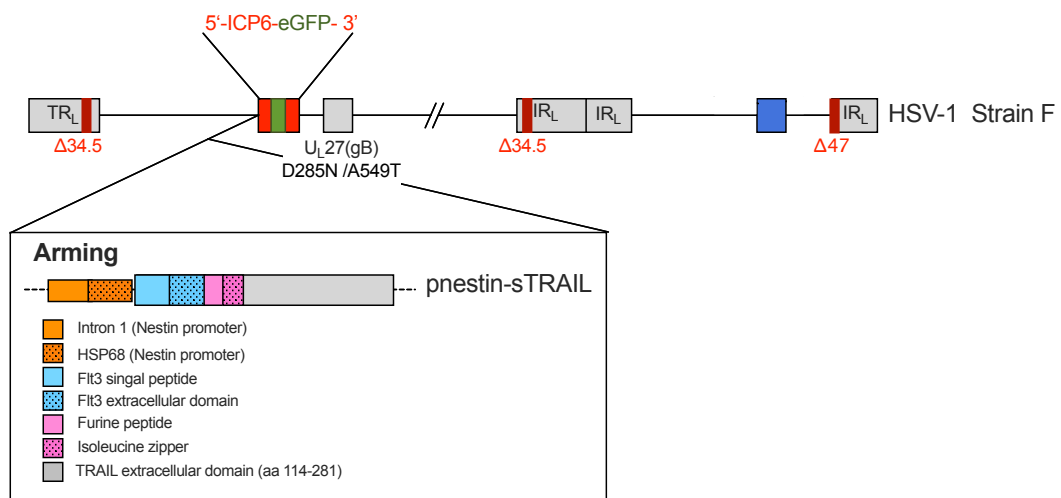
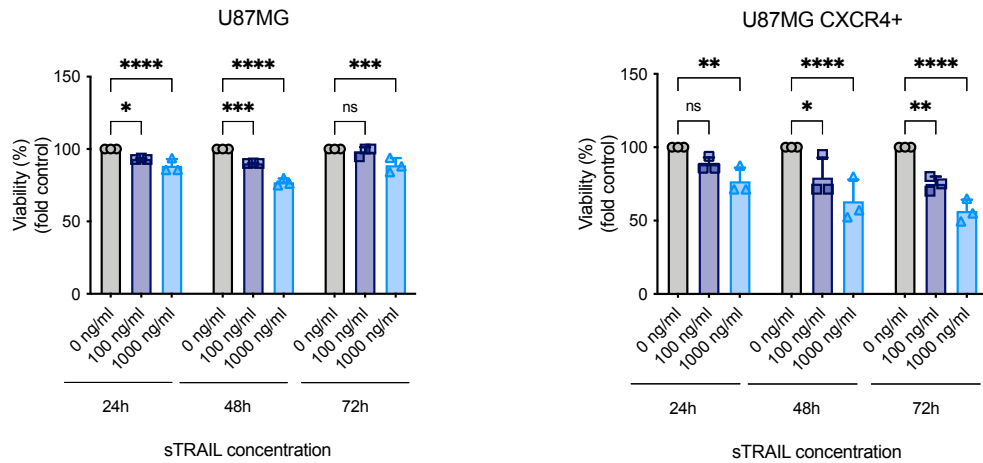


Figure 23: Schematic representation of arming strategy. Arming is achieved by insertion of the gene coding for the extracellular domain of TRAIL (aa 114-281), the Flt3 signal peptide and its extracellular domain, the furine peptide and the isoleucine zipper. All this synthetic construction is controlled by the represented nestin promoter and inserted before GFP expression in (-/- ICP34.5/ Δ ICP6/ Δ ICP47) backbone.

4. *In vitro* viability upon sTRAIL treatment or oHSV infection

Sensitivity to oHSV or sTRAIL-mediated oncolysis differs between cell lines. For this reason, we wanted to determine the sensitivity of U87MG and U87MG CXCR4⁺ to purified sTRAIL and viral infection. U87MG and U87MG CXCR4⁺ were treated with different concentrations of sTRAIL, and their viability was evaluated at different time points using a Resazurin assay (Figure 24A). Results reveal that both U87MG and U87MG CXCR4⁺ cells were sensitive to sTRAIL. Cells were then infected with our four different oHSV (oHSV/gD, oHSV/gD:sTRAIL, oHSV/Nb-gD or oHSV/Nb-gD:sTRAIL; MOI: 5). Results showed that both U87MG and U87MG CXCR4⁺ cells were sensitive when infected with oHSV (Figure 24B), decreasing the viability up to 15-20% 72h post-infection (hpi). Viability of the U87MG infected with the retargeted oHSV/Nb-gD or oHSV/Nb-gD: sTRAIL is not affected, confirming that they are not infected due to the low level of CXCR4 at the cell surface (Figure 24B).

A



B

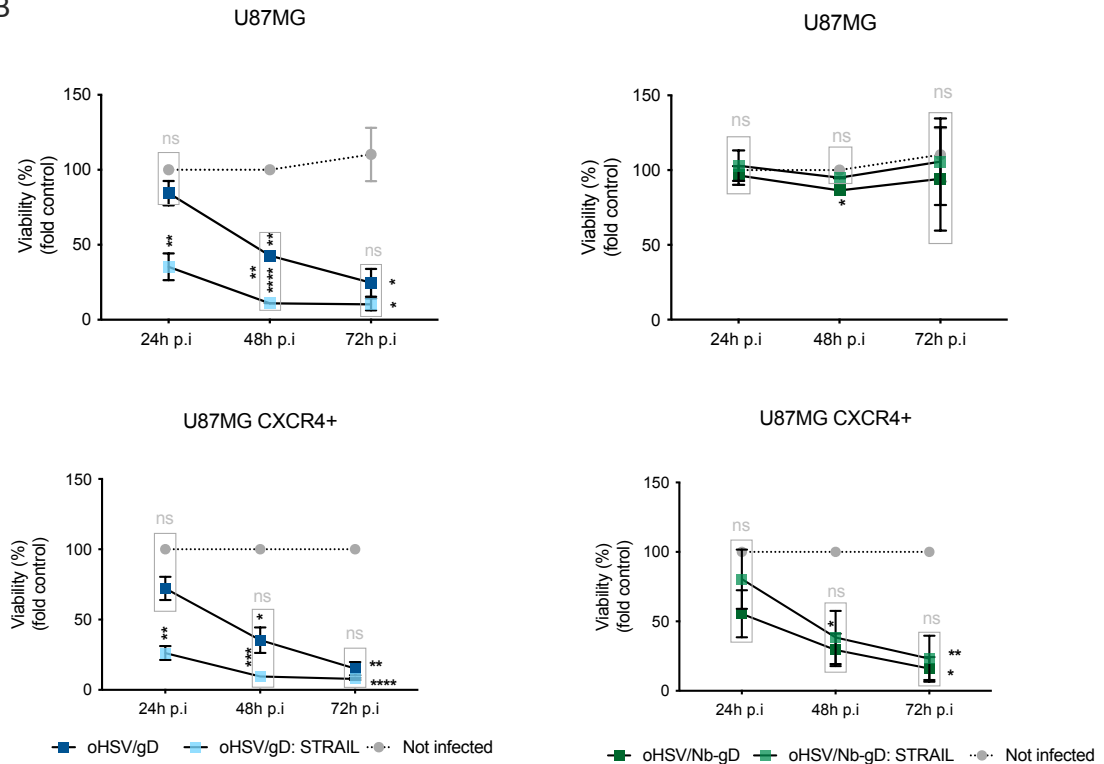


Figure 24: In vitro analysis of sTRAIL and oHSV. The impact of viral infection on U87MG and U87MG CXCR4⁺ cells was evaluated by measuring the cell viability with a Resazurin assay (A). U87MG and U87MG CXCR4⁺ cells were treated with different sTRAIL concentrations (0, 100 or 1000 ng/ml), and viability was analysed at different time points. Values are represented as a percentage of the control (not treated cells). Bars represent mean ± SD (B). Cells were infected with the four different oHSV at an MOI of 5, and the viability was analysed at 24, 48 and 72h post-infection (hpi). Values are represented as a percentage of the control (not infected cells). Statistical significance was determined by 2-way ANOVA with Bonferroni's multiple comparisons test (* $p < 0.05$, ** $p < 0.001$).

5. *In vitro* efficacy of sTRAIL-arming

A growth curve was done by infecting U87MG CXCR4⁺ with oHSV/Nb-gD and oHSV/Nb-gD:sTRAIL to determine if the arming induce a decrease in viral replication. Results show that the armed- and non-armed oHSV grew with the same efficacy, demonstrating that arming does not impair oHSV replication (Figures 25A). The efficacy of sTRAIL to trigger the apoptosis pathway was analysed either by western blotting or annexin V/DAPI assay. West-blot analysis shows that the expression of sTRAIL upon infection of U87MG CXCR4⁺ by oHSV/Nb-gD:sTRAIL led to the cleavage of PARP and caspase 3, while no cleavage was observed upon oHSV/Nb-gD infection. The level of infection was observed by the blotting of viral gD (Figure 25B). The annexin V/DAPI assay performed on cells infected with an MOI of 5 further confirmed apoptosis in U87MG CXCR4⁺ cells, but the sTRAIL-induced apoptosis was detectable at a later time point (48 hpi) and became significant only at 72hpi with an average of 36% of apoptotic cells compared to 12% with oHSV/Nb-gD (Figure 25C). Interestingly, the viability of the cells measured by a resazurin assay was not statistically different between armed and non-armed virus infections. Finally, induction of apoptosis by oHSV/Nb-gD:sTRAIL was dose-dependent, as shown in Figure 25D, where an annexin V/DAPI assay was performed on U87MG CXCR4⁺ cells infected at different MOIs (MOI:1,5,10) after 72 hours.

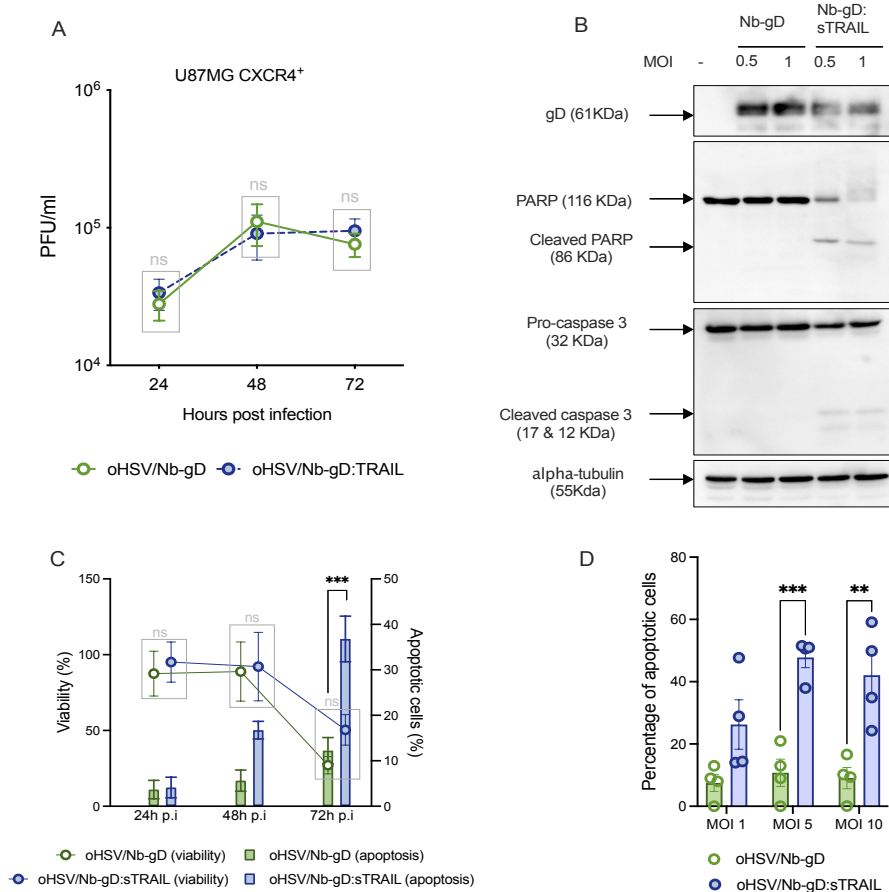
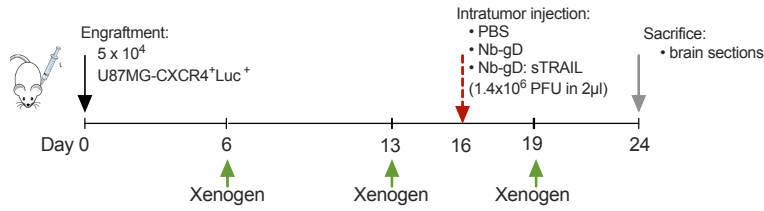


Figure 25: Efficacy of oHSV arming. The replication efficacy of the non-armed (oHSV/Nb-gD) and sTRAIL-armed (oHSV/Nb-gD:sTRAIL) oncolytic viruses was evaluated with a growth curve assay by infecting U87MG CXCR4⁺ at an MOI of 1 (A). The supernatant was harvested at 24, 48 and 72 hpi and used for titration as previously described³⁵⁰. The number of foci was calculated based on Incucyte imaging. Bars represent the mean \pm SEM (PFU/ml) of 3 independent experiments. Paired t-test confirms the lack of statistical difference. Apoptosis was evaluated by PARP and caspase 3 cleavage analysis by Western blot (WB) (B) and annexin/DAPI detection in flow cytometry (C). Apoptosis was also measured by flow cytometry. U87MG CXCR4⁺ cells were infected by oHSV/Nb-gD or oHSV/Nb-gD:sTRAIL at an MOI of 5, and apoptosis level was analysed at 24, 48, and 72 hours post-infection (hpi) by quantification of annexin V and DAPI positive cells by flow cytometry. The percentage of apoptotic cells corresponds to early (Annexin V⁺/DAPI⁻) and late apoptotic (Annexin V⁺/DAPI⁺) cells. In parallel, cells were incubated with resazurin to evaluate the viability upon treatment. U87MG CXCR4⁺ cells were infected for 72h by oHSV/Nb-gD or oHSV/Nb-gD:sTRAIL at indicated MOI, and apoptosis level was analysed by quantification of annexin V and DAPI positive cells by flow cytometry (D). Bars and dots represent the means \pm SEM of three independent experiments. Statistical significance was determined by ordinary 2-way ANOVA with Bonferroni's multiple comparisons of means (* $p < 0.05$, ** $p < 0.001$).

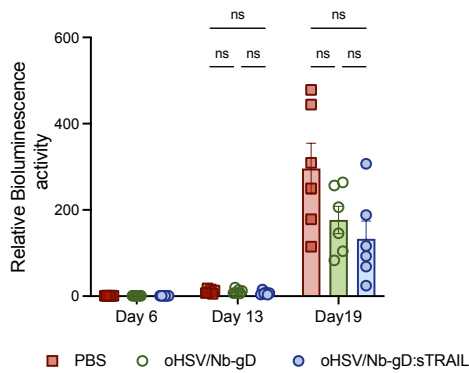
6. Therapeutic efficacy of oHSV/Nb-gD and oHSV/Nb-gD:sTRAIL using and orthotopic xenograft U87MG CXCR4+ GBM model

The capacity of oHSV/Nb-gD and oHSV/Nb-gD:sTRAIL to impact tumour growth and mice survival was evaluated *in vivo* in an orthotopic xenograft GBM model. A first experiment (Exp 0) was set up with engraftment of 5×10^4 U87MG CXCR4⁺Luc⁺ into the right striatum under stereotactic control (Figure 26A). Based on our expertise on U87MG Luc⁺ engraftment in this model³⁵¹, PBS or oHSVs (1.4×10^6 PFU in 2 μ l) were injected within the tumour on Day 16. Weekly bioluminescence analysis revealed a very quick increase of the tumours even after oHSV intra-tumoural injection, although the tumours grew faster in PBS-treated mice than in the mice treated with oHSV/Nb-gD or oHSV/Nb-gD:sTRAIL (Figure 26B). However, there was no statistical difference between PBS and oHSV-treated mice. Both control and oHSV-treated mice's health status evolved rapidly with a continuous weight loss of all mice from day 19 (Figure 26C). On day 24, the control mice's weight loss was critical, justifying the sacrifice of all mice. Although this experiment was not conclusive regarding oHSV efficacy, it revealed that U87MG CXCR4⁺Luc⁺ tumours grew much faster than U87MG, which confirmed the role of CXCR4 in tumour progression.

A



B



C

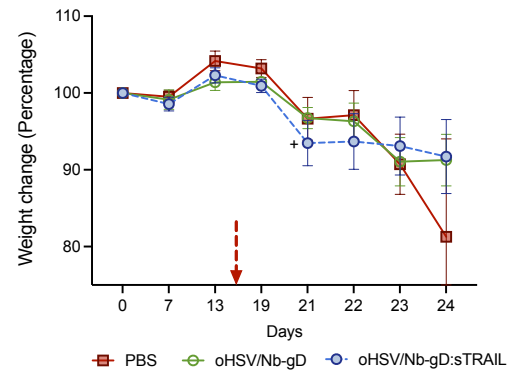


Figure 26: In vivo efficacy of oHSV/Nb-gD and oHSV/Nb-gD:sTRAIL (Exp 0). Schematic representation of the experimental setting of the first in vivo experiment. U87MG CXCR4+Luc+ cells (5×10^4 cells in $2\mu\text{l}$) were injected on Day 0 into the right hemisphere of the brain under stereotactic coordinates. Viral suspension (1.4×10^6 PFU in $2\mu\text{l}$) or PBS was injected within the tumour on day 16 as indicated by the red arrow. Mice were sacrificed on day 24 (A). Bioluminescence activity of mice was recorded with Xenogen IVIS 50 on day 6, 13 and 19. For each mouse, evolution of the bioluminescence is calculated regarding the bioluminescence on day 6 considered as equal 1 (B). Bars represent the means \pm SEM. Statistical significance was determined by two-way ANOVA with Bonferroni's multiple comparisons of means. Mice were weighed every two days and weight change is expressed as a percentage with the weight on day 0, considered as equal to 100% (C). Graph represents the mean \pm SEM (PBS, $n=7$; oHSV/Nb-gD, $n=6$; oHSV/Nb-gD:sTRAIL, $n=6$). (+: One mice from the oHSV/Nb-gD:sTRAIL died at day 21). Data represent the means \pm SEM. Statistical significance was determined by mixed-effects analysis with Bonferroni's multiple comparisons of means. There was no statistical difference between groups neither for the weight nor for the relative bioluminescence activity.

The experiment was thus repeated, considering the fast growth of CXCR4⁺ tumours. U87MG CXCR4⁺Luc⁺ GBM cells were engrafted, and PBS or oHSVs (1.4 x 10⁶ PFU in 2µl) were injected on day 7 instead of day 16 after engraftment (Figure 27A). Mice were weighed every two days, and bioluminescence analyses were performed weekly to evaluate the tumour size. On day 22, mice were anaesthetised and either perfused with saline solution only (for RNA extraction from brain tissue) or followed by paraformaldehyde fixation to allow immunostaining analyses. In contrast to oHSV-treated mice, which showed a transient weight loss just after the virus injection before a continuous weight gain until the end of the experiment, PBS-treated mice maintained their initial weight but displayed an evident weight loss from day 20 on (Figure 27B). On day 6, the size of the tumours was homogeneous, and no significant difference in bioluminescence signal was observed (Figure 27C). However, contrary to the PBS-treated mice signal, which dramatically increased up to day 20, the signal remained unchanged or even decreased in oHSV-treated mice, becoming even undetectable in some mice at day 13. Between day 13 and day 20, the signal slightly increased in several mice, although the differences were not statistically significant. All tumours in oHSV-treated mice remained statistically smaller than in the PBS-treated group (Figure 27C). All mice were sacrificed on day 22, and brains were harvested for either anti-human vimentin immunohistochemical staining and tumour size measurement (5 mice/group) or RNA extraction and RT-qPCR analyses (4 mice/group). The size of the tumour, calculated by measuring the area positive for human vimentin on serial sections and 3D volume reconstruction, clearly showed a significant impact of both oHSV/Nb-gD and oHSV/Nb-gD:sTRAIL oncolytic treatment, even if no significant difference was observed between the two viruses (Figure 27D and E). For RNA extraction, the right hemispheres, in which the cells were engrafted, were divided into three parts (frontal, middle, and occipital). Human CXCR4 expression, reflecting the presence of human GBM cells, was evaluated in each block individually and expressed as the relative expression to the level of expression in the middle part of PBS-treated mice brains (Figure 27F). Overall human CXCR4 expression was significantly decreased in oHSV-treated mice compared to PBS-treated mice. In both oHSV-treated groups, differences in the level of expression of hCXCR4 were observed between the 3 blocks, with a higher abundance of human transcripts detected in samples corresponding to the frontal and middle samples, covering the initial site of engraftment. RT-qPCR for human nestin

and TBPH confirm these results (data not shown). Unfortunately, at the end of the experiment (15 days after treatment), we were unable to detect gD or sTRAIL neither by immunohistochemistry nor by RT-qPCR (data not shown). This experiment was repeated with the same settings. Mice were sacrificed two days after virus injection to validate whether the virus replicates and sTRAIL is expressed in the tumour. Right hemispheres were divided into three parts (frontal, middle, and occipital), and RNA was extracted. gD and sTRAIL relative expression measured by RT-qPCR demonstrated the presence of gD transcripts in brains injected with oHSV/Nb-gD and oHSV/Nb-gD:sTRAIL while sTRAIL transcripts were detected only in the oHSV/Nb-gD:sTRAIL group (Figures 27G and H).

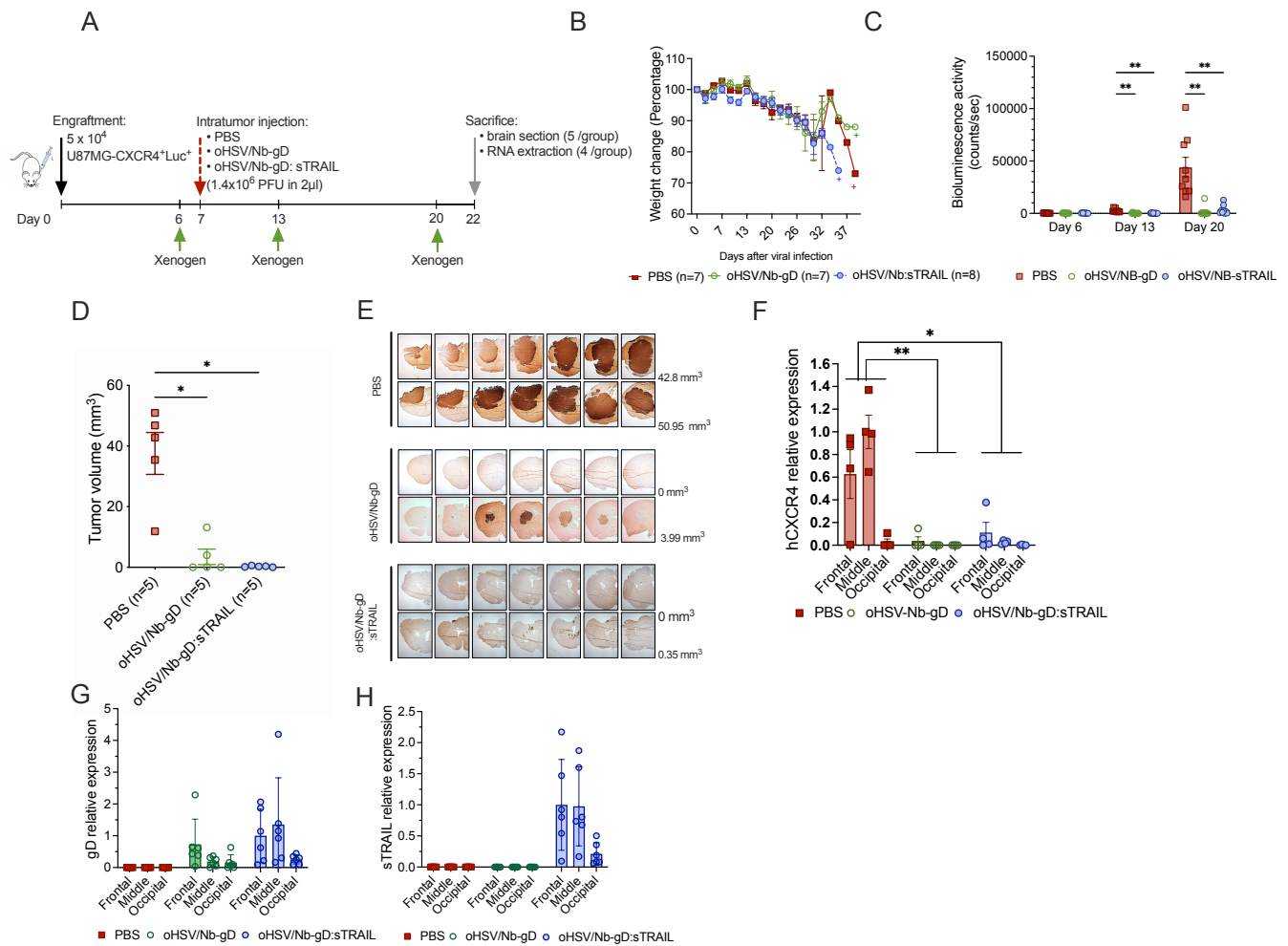


Figure 27: In vivo efficacy of oHSV/Nb-gD and oHSV/Nb-gD:sTRAIL. Schematic representation of the experimental settings (A). Mice were weighed every two days. Weight change is expressed as a percentage of the weight on day 0, considered as equal to 100% (B). Bioluminescence activity of nude mice engrafted with U87MG CXCR4⁺Luc⁺ cells was recorded with Xenogen on day 6, 13 and 20 after engraftment and virus of PBS was injected into the tumour on day 7 (n=9) (C). Mice were sacrificed on day 22. Brains from 5 mice were sectioned for immunostaining for tumour volume measurement by 3D reconstruction (D and E). Brains from the 4 other mice were frozen for RNA extraction and RT-qPCR analysis of hCXCR4 expression (F). For each transcript, relative expression is expressed with PBS-treated mice considered as a baseline and equal to 1. For tumour volume measures and qRT-PCR, bars represent the means \pm SEM. Statistical significance was determined by one-way ANOVA with Bonferroni multiple comparisons of means (* $p < 0.05$, ** $p < 0.01$, *** $p < 0.001$, **** $p < 0.0001$). The same in vivo experiment was repeated by sacrificing the mice (6 in each group) two days post-injection. Brains were divided into 3 parts (frontal, middle and occipital) which were frozen and treated independently for RNA extraction and RT-qPCR analysis of gD (G) or sTRAIL (H) expression. For each sample, relative expression is expressed with oHSV/Nb-gD:sTRAIL frontal sample considered as the baseline. Bars represent the means \pm SEM of 6 mice.

Finally, a survival assay was set up with similar experimental settings (Figure 28A). U87MG CXCR4+Luc+ cells were injected under stereotactic control and viral suspension, or PBS was injected within the tumour on day 7. Tumour size was evaluated by bioluminescence analyses just before (day 5) or six days after treatment (day 13), and mice were weighed every two days and sacrificed when the weight loss was $\geq 20\%$ and/or mice presented severe clinical signs. From day 19, all PBS-treated mice lost weight continuously while all oHSV-treated mice still gained weight (Figure 28B). At the end of the experiment, the oHSV-treated mice still alive were still gaining weight. As in the previous experiment, the bioluminescence signal before treatment was similar in all treated groups (Figures 28C and 28D). However, one week after the intratumour injection, tumours in the PBS group were significantly bigger than in both oHSV-treated mice, for which the signal was very low and even undetectable in 4/6 mice and 3/5 mice in oHSV/Nb-gD and oHSV/Nb-gD:sTRAIL, respectively (Figure 28C). Again, tumours of both oHSV-treated mice were significantly smaller than those of the control group, but no significant difference was observed between oHSV/Nb-gD and oHSV/Nb-gD:sTRAIL treated mice (Figure 28D). More importantly, while all PBS-treated mice died between day 21 and 27, the oHSV-treated mice's death was delayed with the first deaths observed on day 31 (Figure 28E). At day 61, one oHSV/Nb-gD (out of 6) and two oHSV/Nb-gD:sTRAIL (out of 5) treated mice were still alive.

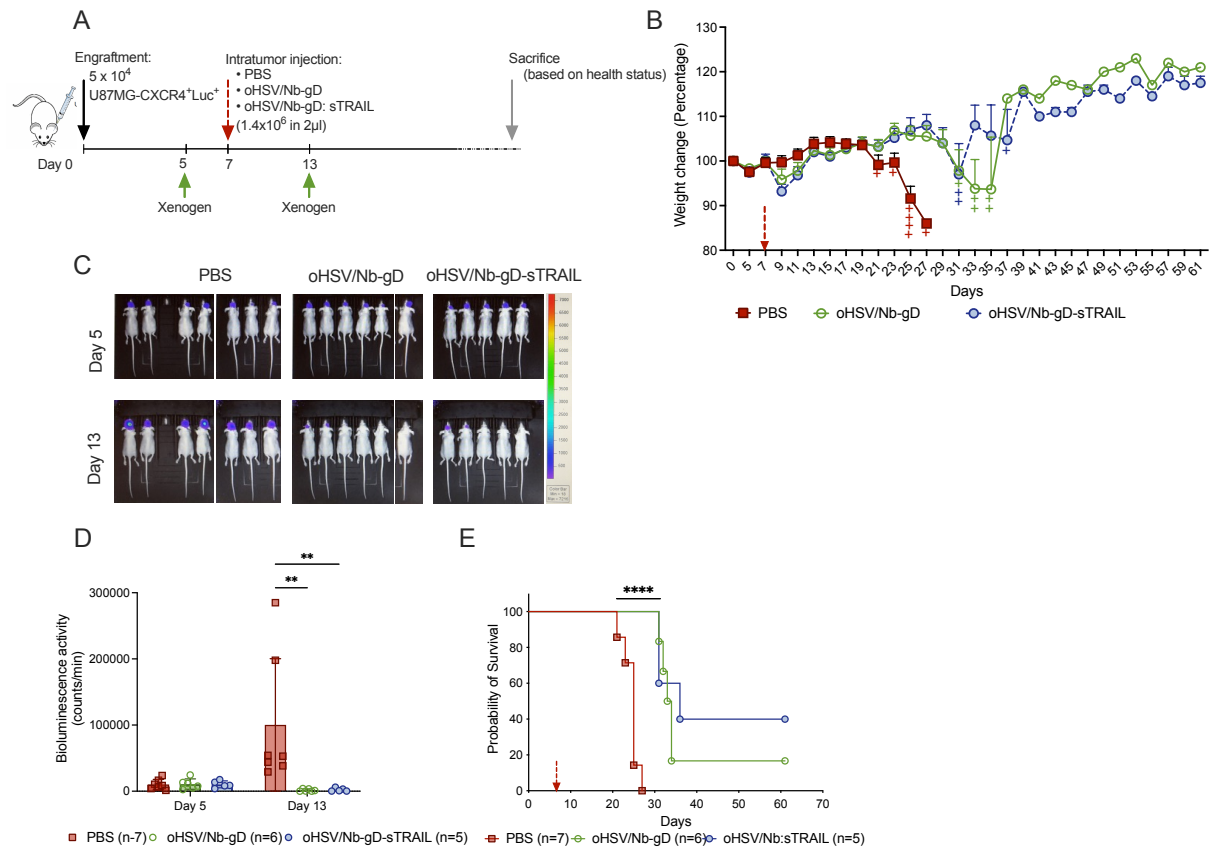


Figure 28: Survival assay upon oHSV/Nb-gD or oHSV/Nb-gD:sTRAIL treatment. Schematic representation of the experimental settings (A). Mice were weighed every two days, and weight change is expressed as a percentage of the weight on day 0, considered equal to 100% (B). Graph represents the mean \pm SEM (at the beginning of the experiment PBS n=7, oHSV/Nb-gD n=6, oHSV/Nb-gD:sTRAIL n=5). Bioluminescence imaging of mice was recorded with IVIS 50TM Xenogen on day 5 (two days before treatment) and day 13 (6 days after treatment). Mice from each group were not systematically in the same cage. Pictures have thus been edited to regroup the mice from each group based on their identification tattoo (C). Bioluminescence activity of nude mice engrafted with 5×10^4 U87-CXCR4 Luc⁺ cells were recorded with Xenogen on day 5 (two days before treatment) and day 13 (6 days after treatment) (D). Bars represent the means \pm SEM. Statistical significance was determined by 2-way ANOVA with Bonferroni multiple comparisons of means (** $p < 0.01$). Probability of survival of mice treated with PBS (n=7), oHSV/Nb-gD (n=6) or oHSV/Nb-gD:sTRAIL (n=5). The red arrow indicates the day of treatment (Day 7) (E). Statistical significance was determined by log-ranked (Mantel-Cox) test (**** $p < 0.0001$).

7. Infection of patient derived Glioblastoma stem-like cells

As previously said in the introduction, GSCs play an important role in recurrence and tumour progression. GBM harbour a very high heterogeneity inside the tumour and between different tumours. To consider this heterogeneity, the efficacy of oHSV/Nb-gD and oHSV/Nb-gD:sTRAIL was further evaluated on four different GSCs cultures (T08, T013, T018 and T033) directly established from residual GBM tissue obtained after surgical resection (Department of Neurosurgery, CHU Liège, Belgium) and maintained as tumourspheres. When cultured as tumourspheres, these patient-derived cells expressed stemness markers as demonstrated by quantifying SOX2, POU3F2 and SALL2 by RT-qPCR (Figure 29A). Importantly, when analysed by flow cytometry, both the proportion of cells expressing CXCR4 and the median fluorescence index (MFI) were highly variable. While less than 4% of T08 cells were positive for CXCR4, around 75% of T033 expressed this chemokine receptor, T013 and T018 being intermediate (Figure 29B). Moreover, the median fluorescence index (MFI) on T033 was significantly higher than on the other primary GSCs (Figure 29C).

Tumourspheres were infected with oHSV/Nb-gD (10^6 PFU/ml). Forty-eight hours post-infection, the GFP signal was clearly visible by epifluorescence microscopy, and its intensity reflected the level of expression of CXCR4 with a very low GFP signal in T08 and a brighter in T033 (Figure 29E, left panels). Confocal microscopy on tumoursphere sections confirmed that only very few T08 cells were GFP⁺ while more infected cells were observed in T013, T018 and T033 tumourspheres (Figure 29D). Although no clear co-localization between GFP and CXCR4 was observed at the cellular level, infected cells were usually observed in the CXCR4⁺ area.

Some tumourspheres were dissociated after 48hpi for FACS analyses (Figure 29E) or RNA extraction and RT-qPCR (Figure 29G). The percentage of infected cells with oHSV/Nb-gD virus measured by FACS analyses clearly showed a statistical difference between T08 and T033 cells (respectively 3,2% and 22,6 % GFP⁺ cells on average) (Figure 29E). Indeed, the level of infection correlates with the level of CXCR4 expression ($R^2= 0.7799$ (Figure 29F)). RT-qPCR analyses confirmed these observations with the level of expression of gD and sTRAIL increasing in a CXCR4-dependent manner (Figure 29G and H).

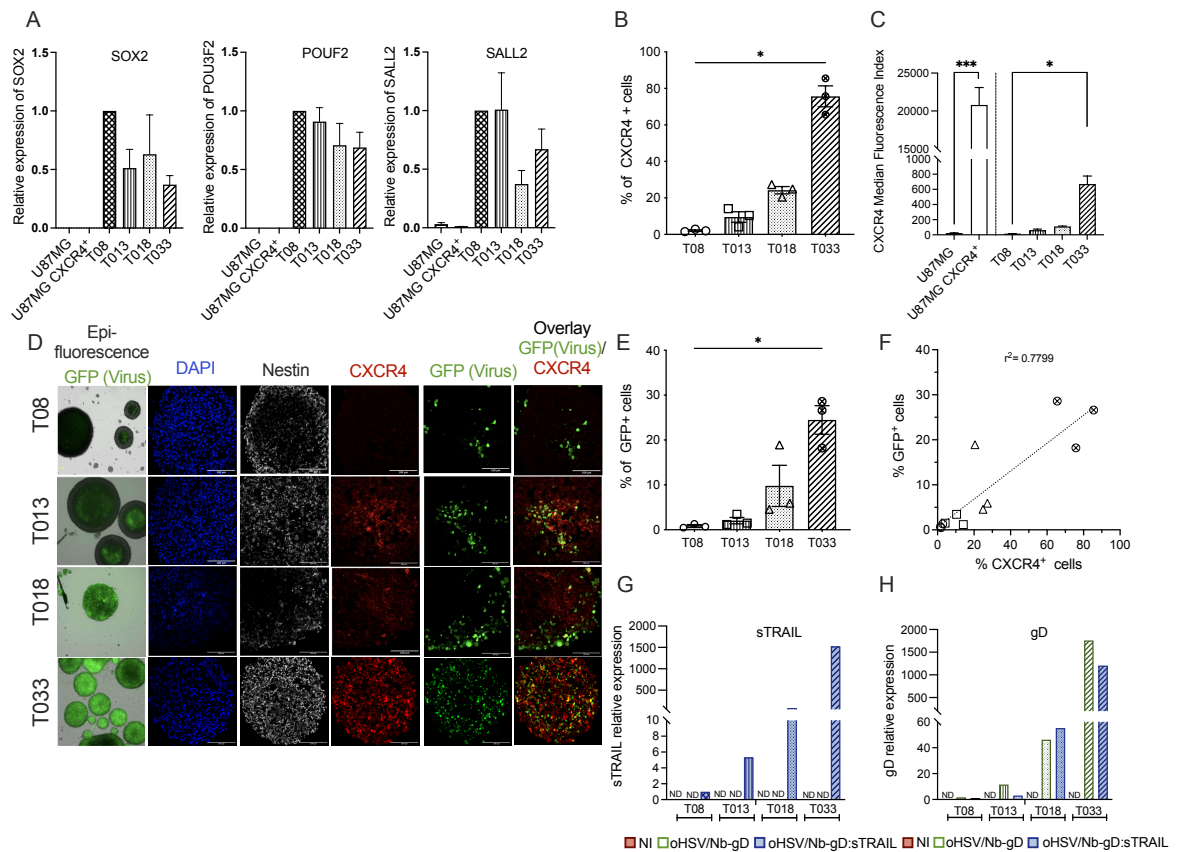
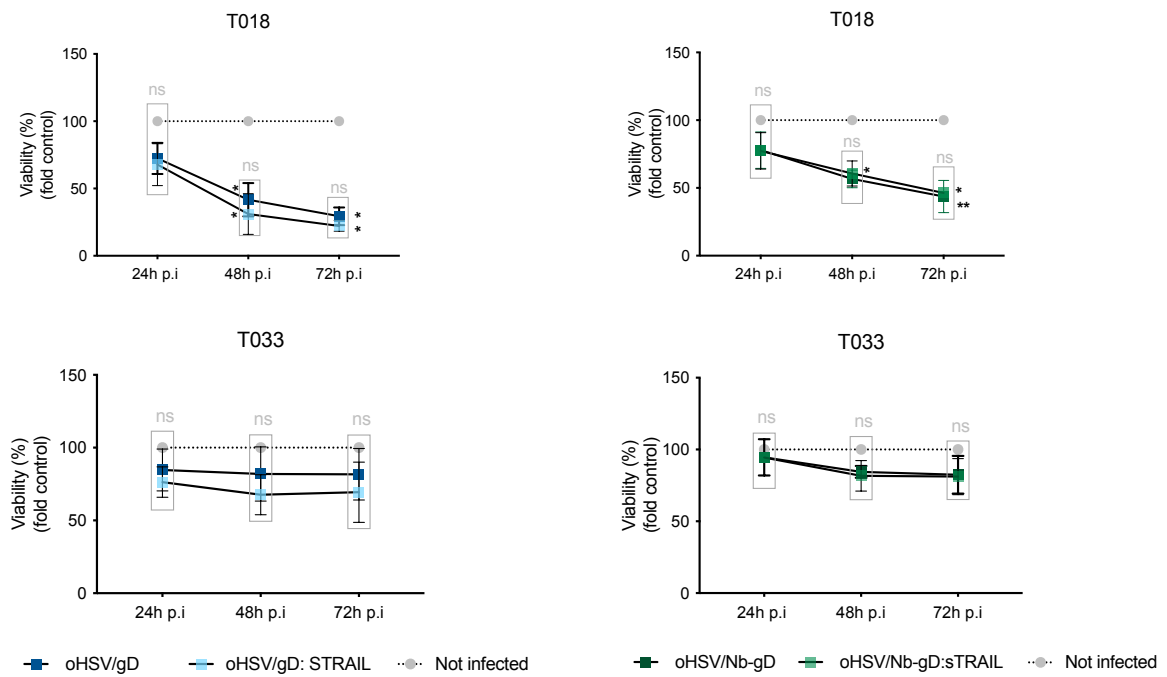


Figure 29: Efficacy of the CXCR4-retargeting and sTRAIL arming in GBM patient-derived cells. T08, T013, T018 and T033 were cultured as neurospheres. The expression of stem markers was analysed by RT-qPCR (A). Tumourspheres were dissociated for flow cytometry quantification of the percentage of CXCR4 positive cells (B) and for the MFI of CXCR4 (C). Bars represent the means \pm SEM of three independent experiments. Statistical significance was determined by Krustall-Wallis test (* $p < 0.05$). (D to H) Tumourspheres infected for 48h by oHSV/Nb-gD or oHSV/Nb-gD:sTRAIL with 10^6 PFU/ml were either analysed by epifluorescence for GFP detection (left panels) or fixed for immunostaining of nestin (white) or CXCR4 (Red) and GFP detection (green). Nuclei were labelled with DAPI (Blue). Images were recorded with NIKON AIR confocal microscope. Magnification: 40x. (D) Infected tumourspheres with oHSV/Nb-gD virus were dissociated, and the percentage of GFP⁺ cells was evaluated by flow cytometry (E). Bars represent the means \pm SEM of three independent experiments. Statistical significance was determined by ordinary 2-way ANOVA with Bonferroni's multiple comparisons of means (* $p < 0.05$, ** $p < 0.001$). The correlation between GFP and CXCR4-positivity was further analysed (F). In parallel, the expression of gD and sTRAIL was analysed by RT-qPCR as illustrated by a representative experiment with gD (G) and sTRAIL (F) expression level in oHSV/Nb-gD:sTRAIL infected T08, considered as the baseline. (ND: not detected).

8. *In vitro* sensitivity to oHSV infection and sTRAIL apoptotic effect in tumourspheres

As for U87MG and U87MG CXCR4⁺ cells, the impact of oHSVs infection was analysed in two patient-derived cultures (T018 and T033). Tumourspheres were infected with the four different viruses at an MOI of 5 to further analyse viability at different time points (Figure 30A). Results show that T018 was sensitive to oHSV infection even if its level of infection was low with the retargeted due to the percentage of CXCR4⁺ cells. Surprisingly, despite presenting the highest level of infection, T033 viability was not affected, indicating that T033 cells are resistant to the four oHSV, independently of the retargeting or arming features. No statistical difference was observed between infected and non-infected cells. The capacity of purified sTRAIL to induce apoptosis in these two primary GSCs lines was analysed in parallel (Figure 30B). Tumourspheres were treated at different concentrations of sTRAIL, measuring their viability at different time points. Results showed a significant difference between T018 tumourspheres treated or not, validating the results obtained with the sTRAIL-armed oHSV. However, sTRAIL had no significant effect on T033 tumourspheres, demonstrating resistance to sTRAIL treatment.

A



B

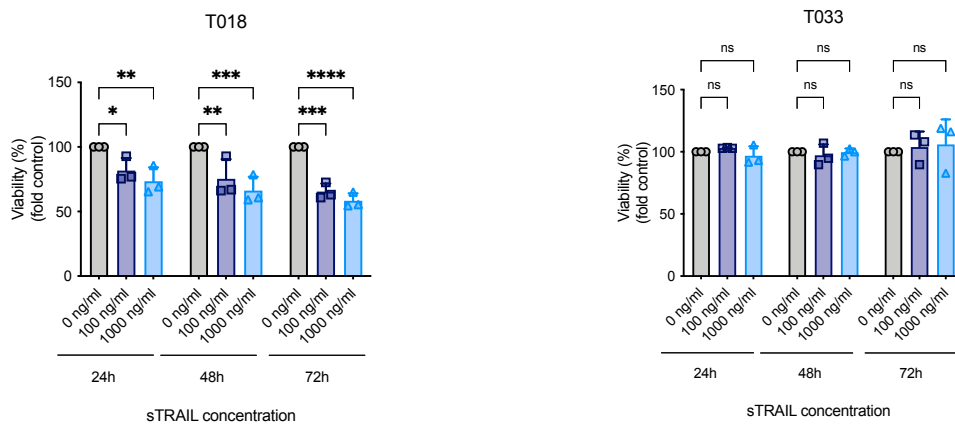


Figure 30: In vitro viability and sTRAIL sensitivity of patient-derived cells. A resazurin assay evaluated the viability of T018 and T033 tumourspheres to determine the impact of the viral infection in patient-derived cells. Tumourspheres were infected with the four different viruses at 10^6 pfu/ml and analysed at 24, 48 and 72h pi. Values correspond to percentage according to the viability of non-infected cells at 24h (A). T018 and T033 were treated at different sTRAIL concentrations (0, 100 or 1000 ng/ml), and viability was analysed at different time points with a Resazurin assay as well (B). Values are represented as the percentage of the mock-treated cells at 24h. Bars represent mean \pm SD. Statistical significance was determined by 2-way ANOVA with Bonferroni's multiple comparisons test (* $p < 0.05$, ** $p < 0.001$).

To understand the different sensitivity to sTRAIL, the level of sTRAIL death receptors (DR4 and DR5) expressed by T018 et T033 was analysed by flow cytometry. DR4 and DR5 expression on U87MG and U87MG CXCR4⁺ cultured as tumourspheres was also analysed as a control. (Figure 31A). There was no statistical difference for DR4 expression, while DR5 analysis showed a significantly lower expression in T033 than in the other cells. Considering that in armed-oHSV, nestin promoter drives sTRAIL expression, the nestin level was evaluated by RT-qPCR (Figure 31B). A significant difference was observed between U87MG and primary GSCs. More importantly, the level of nestin expression was statistically lower in T033 than in T018, suggesting that sTRAIL might be less expressed in T033. Unfortunately, sTRAIL expression was not analysed in this experiment.

Finally, the level of apoptosis induced by the arming was measured by an Annexin V/ DAPI assay on T018 and T033 cells infected for 96h at 10⁷ pfu/ml (Figure 31C). In T018, apoptosis level was significantly higher upon oHSV/gD:sTRAIL than oHSV/gD infection. However, apoptosis level was relatively low in T018 cells infected with the retargeted viruses, which agrees with the low percentage of T018 cells expressing CXCR4 at the cell surface (Figure 26B). Following the data obtained from the viability assay, apoptotic cells were not detected in cells from T033 tumourspheres, regardless of the virus used for infection.

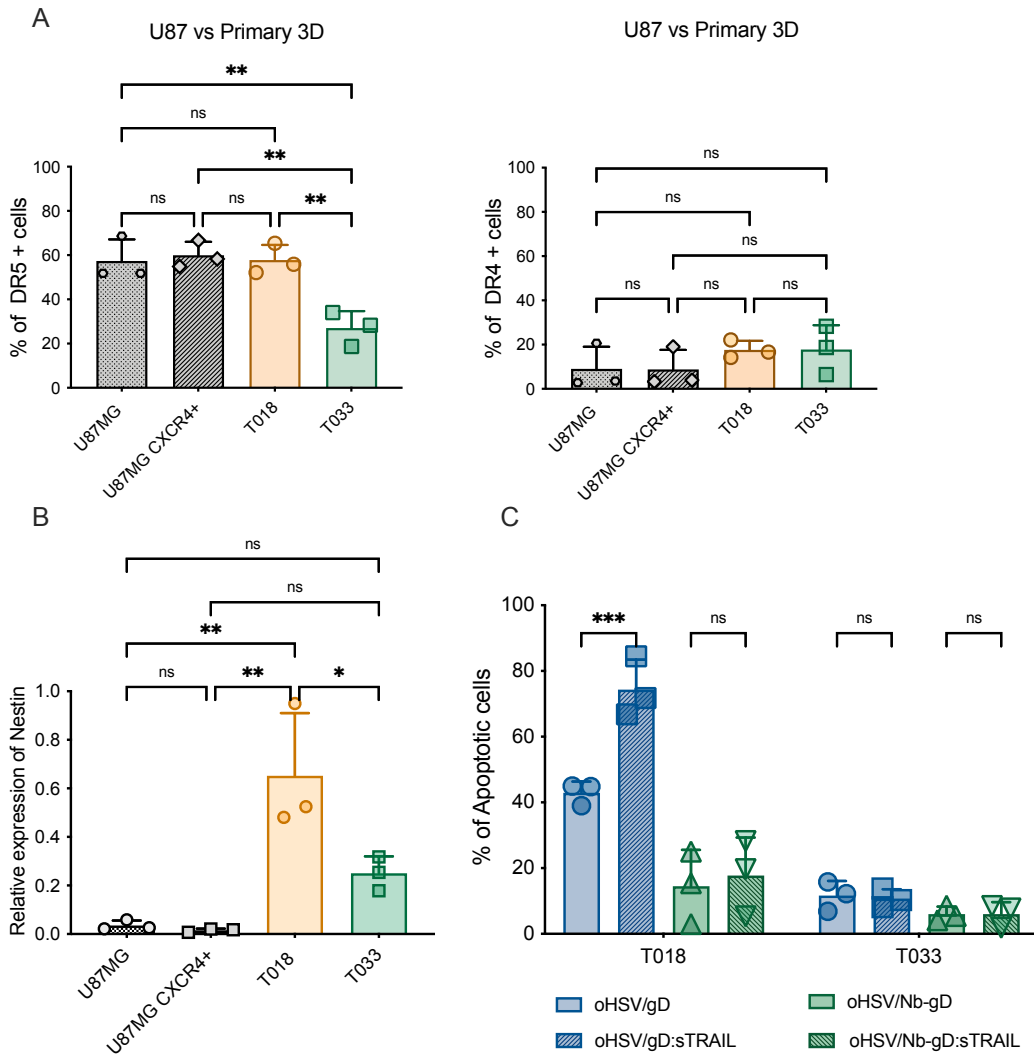


Figure 31: Death receptors, Nestin expression and apoptosis level analysis upon oHSV infection. U87MG, U87MG CXCR4⁺ and patient-derived tumourspheres (T018 and T033) were cultured as tumourspheres. The percentage of cells expressing Trail receptor 1 (DR4) and Trail receptor 2 (DR5) at the cell surface was evaluated by flow cytometry. Results are expressed as the percentage of cells expressing the receptor (A). Relative expression of nestin was analysed by RT-qPCR and expressed compared to the level of CXCR4 transcripts in U87MG, considered equal to 1 (B). Bars represent the means \pm SD. Statistical significance was determined by one-way ANOVA with Bonferroni multiple comparisons of means ($*p < 0.05$, $**p < 0.01$, $***p < 0.001$). Finally, cells were infected for 96 h with the four oHSVs at 10^7 pfu/ml. They were then dissociated, and apoptosis level was analysed by quantifying annexin and/or DAPI, positive cells by flow cytometry. The percentage of apoptotic cells corresponds to early (Annexin+/DAPI-) and late apoptotic (Annexin+/DAPI+) cells (C). Bars represent the means \pm SD of 3 independent experiments. Statistical significance was determined by 2-way ANOVA with Bonferroni's multiple comparisons of means ($*p < 0.05$, $**p < 0.001$).

9. Therapeutic efficacy of oHSV/Nb-gD and oHSV/Nb-gD:sTRAIL using and orthotopic xenograft GSC-like GBM model

A survival assay with T033 was done in parallel with the *in vitro* viral and sTRAIL sensitivity assays. Experimental settings for T033 luc⁺ cells orthotopic engraftment in nude mice and further virus injection are described in Figure 32A. Cells were injected under stereotactic control and viral suspension, or PBS was injected within the tumour on day 25 or day 32. Tumour size was evaluated by bioluminescence analyses on day 21, just before virus injection, as well as on days 32 and 41 (corresponding to days 7 and 13 after viral injection, respectively). Mice were weighed every two days and sacrificed when the weight loss was $\geq 20\%$ and/or their behaviour was abnormal. From day 21, all mice lost weight continuously with no significant difference between PBS and oHSV-treated mice (Figure 32B). Bioluminescence signal before treatment was similar in all treated groups (Figures 32C). Unfortunately, one week after the viral intratumour injection, no significant difference in bioluminescence signals was observed between PBS and oHSV-treated mice. Only oHSV/Nb-gD treated mice seemed to have a reduction in luciferase signal compared to the PBS at day 7 post-treatment. However, this difference was not significant, and the bioluminescence signal increased on day 13 post-treatment. In accordance with the bioluminescence activity, most of the mice died 30 to 40 days after viral injection, with no significant differences in survival between PBS and oHSV-treated groups (Figure 32D).

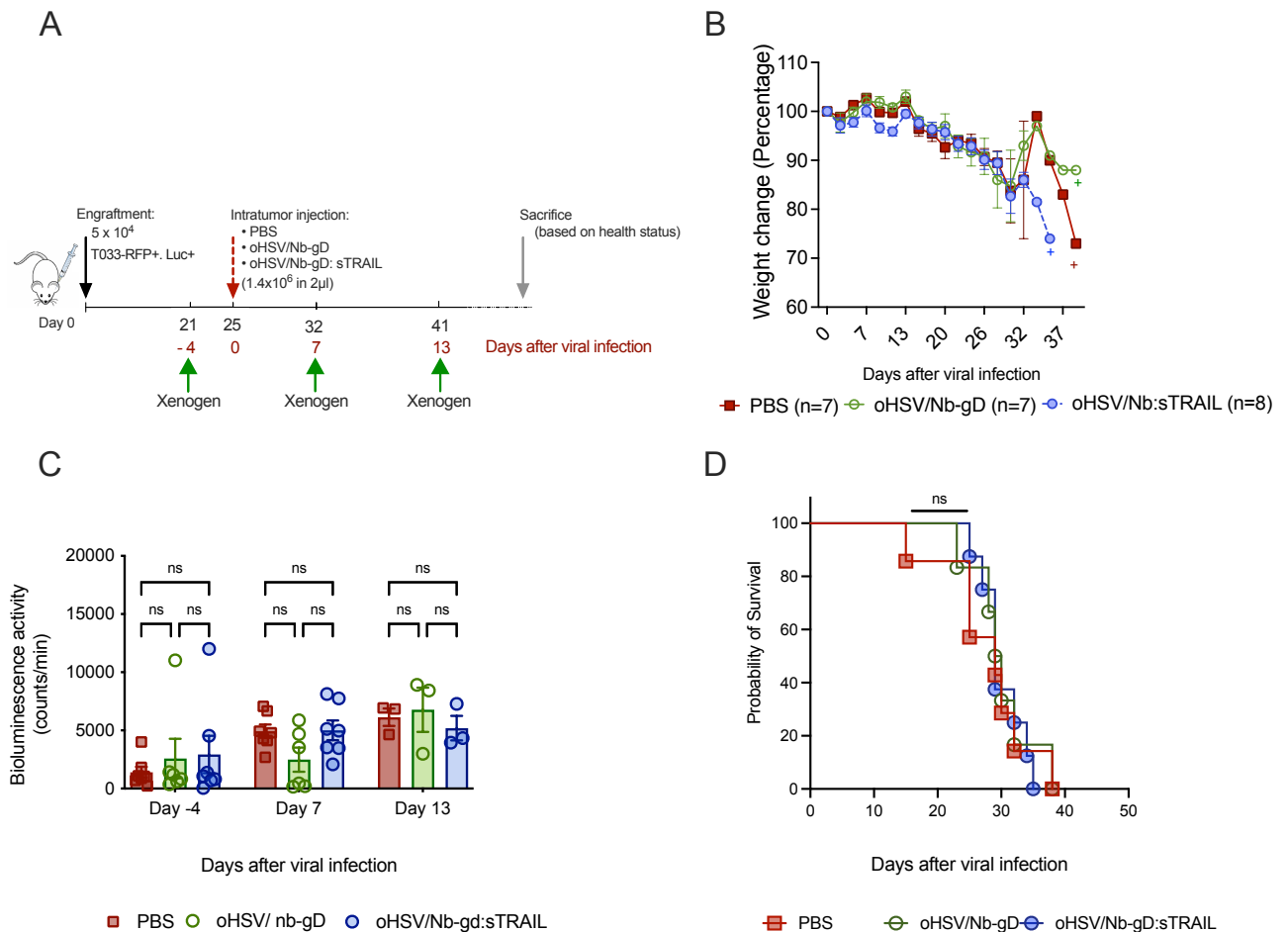


Figure 32: Survival assay upon oHSV/Nb-gD or oHSV/Nb-gD:sTRAIL injection in T033 patient-derived cells tumour in an orthotopic murine model. Schematic representation of the experimental settings (A). Mice were weighed every two days, and weight change is expressed as a percentage of the weight on viral injection day (Day 0), considered equal to 100% (B). Graph represents the mean \pm SEM (PBS n=7, oHSV/Nb-gD n=7, oHSV/Nb-gD:sTRAIL n=8). Bioluminescence activity of nude mice engrafted with 5×10^4 T033 Luc+ cells were recorded with Xenogen on day 21 (four days before treatment), on day 32 (7 days after treatment) and 41 (13 days after treatment) (C). Bars represent the means \pm SEM. Statistical significance was determined by 2-way ANOVA with Bonferroni multiple comparisons of means (** $p < 0.01$). Probability of survival of mice treated with PBS (n=7), oHSV/Nb-gD (n=7) or oHSV/Nb-gD:sTRAIL (n=8) (D). Viral injection day is considered day 0. Statistical significance was determined by log-ranked (Mantel-Cox) test (**** $p < 0.0001$).

V. DISCUSSION

Glioblastoma (GBM) remains the most aggressive adult brain cancer. Unfortunately, the prognosis remains dismal despite improvements in the current treatments such as surgical resection, chemo, or radiotherapy. The most important cause of this failure is the high recurrence rate, mostly due to a GBM sub-population of cells considered Glioblastoma-stem cells (GSCs)³⁵⁸. GSCs display stemness features, being more resistant to radio and chemotherapies, and can generate a tumour when injected into healthy mice's brains. Targeting GSCs which play a crucial role in cancer progression appears as an opportunity for new therapeutic approaches. A wide variety of therapeutic strategies aiming to target GSCs, have been evaluated in preclinical models and are being clinically translated³⁵⁹. Considering the biological complexity of those cells, the main hurdle is to target GSCs without impairing normal tissue. In the last years, oncolytic viruses are emerging as new therapy for several cancers. Specifically, oncolytic herpes virus (oHSV) is the first virus approved by the FDA for cancer treatment³⁶⁰.

1. Creation of an oHSV CXCR4 retargeted and armed with sTRAIL

Several modified oHSV have been tested in periclinical models. Some of them demonstrate safety and succeed in clinical trials. Attenuation of HSV by the deletion of several genes has been shown to be necessary for the safety of the treated patients. In this project, the HSV backbone used was attenuated for the neurovirulence (ICP34.5 -/- deletion) and for limiting the replication to dividing cells (ICP6 deletion). Before the retargeting and arming modifications, ICP47 was deleted following the strategy previously described by *Todo T, et al.*²⁵⁶. As detailed in the introduction, ICP47 deletion leads to two main advantages for oHSV treatment. On the one hand, ICP47 viral protein is able to block the antigen processing protein (TAP), preventing its presentation onto MHC I. Thus, this deletion allows the detection of infected cells by the immune system³⁴¹. On the other hand, the deletion of ICP47 places the US11 gene under the control of the ICP47 promoter, changing its expression from a true late (TL) gene to an immediate-early (IE). IE expression of US11 leads to the complementation of ICP34.5 deletion in non-permissive cells like primary GSC keeping eIF2 dephosphorylated and protein translation unblocked.

Altogether, the deletion of ICP47 enhances an immune response against viral infection and the replication in GSC cells²⁵⁴.

1.1 Retargeting strategy

One of the main objectives of this project was to create an oHSV that specifically targets the CXCR4 receptor, a GSC marker. CXCR4, which GSCs overexpresses, can trigger proliferation, tumourigenesis, and migration. Our approach, which aims to target GSCs specifically, is entirely different from other works that target proteins such as the Epidermal Growth Factor Receptor (EGFR), the IL13-R, or the urokinase Plasminogen Activator Receptor (uPAR), described to be overexpressed in cancer tissues without any specificity for the GSCs^{361–363}. Moreover, contrary to the oHSVs described in this project which are generated in an attenuated HSV backbone, all these retargeted viruses were engineered in a non-attenuated wild-type HSV aiming to reach a higher level of viral replication. As expected, these retargeted viruses allowed a high replication level. However, their safety relies only on the control of their entry into cancer cells, and a low level of expression of the target of interest on healthy cells is thus a prerequisite. Similarly, the CXCR4-retargeted oHSVs entry depends on the virus's capacity to specifically interact with a receptor, but its attenuated character limits its replication in non-cancer cells, improving its safety.

As previously said, two types of retargeting were created with a similar strategy. Specifically, retargeting of HSV requires the replacement of the domain of interaction of glycoprotein D with its natural receptors HVEM and Nectin-1 by a specific sequence allowing the interaction with a protein of interest that can be used as a receptor. We have chosen two different approaches to retarget the virus: 1) the insertion of a sequence coding for CXCL12, the natural ligand of CXCR4, or 2) the insertion of a sequence coding for a nanobody that specifically recognises CXCR4. Although single-chain antibodies (scFv), cytokines, or specific ligands have been described for their efficacy in retargeting oHSV^{361–363}, nanobodies are not yet documented. However, nanobodies, corresponding to a single heavy variable domain of camelid antibodies, can be easily obtained by screening either immune or artificial libraries characterised by a vast diversity and constitute an interesting tool for oHSV customization. We thus considered as a proof-of-principle the use of a genetically

engineered oHSV whose gD is modified by the insertion of a nanobody able to recognise the CXCR4 receptor.

Retargeting results showed that, even if detargeting strategies were identical and both constructions had a punctual mutation in tyrosine 38 (Y38C) to disrupt the interaction with the nectin-1 receptor, oHSV/CXCL12-gD virus was still able to interact with Nectin-1 and infect J/C (Nectin+) cells. Indeed, even if Y38 is essential for nectin-1 binding and cell fusion, it is not the only responsible. It is known that 21 amino acids of gD are involved in gD/nectin-1 interaction. Specifically, 7 are located in the N-terminal region, 13 in the C-terminal, and 1 in the Ig core of the glycoprotein²⁶⁴.

Our retargeting strategy was based on the strategy described by *Uchida et al.* where a sequence of 744 bp coding for an scFv against EGFR receptor was inserted between aa 2 and 24³⁶⁴. The only difference between oHSV/CXCL12-gD and oHSV/Nb-gD construction is the length of the inserted sequence being 318bp and 507bp, respectively. We could suggest that the short length of CXCL12 insertion, compared to our nanobody or Uchida and colleague's scFv, could impact gD structure, changing the region of interaction with Nectin-1 receptor and being no longer Y38 the amino acid essential for binding and cell fusion.

This hypothesis could explain why even if the tyrosine 38 is mutated in both strategies, oHSV/CXCL12-gD can still interact with the Nectin-1 receptor and oHSV/Nb-gD is not. However, a deep study of the CXCL12-gD crystalised structure should be done to understand better whether the region of gD/Nectin-1 complex interaction in this new construction is modified.

By opposition, we demonstrate that oHSV/Nb-gD could no longer detect its natural receptors HVEM or Nectin-1 and specifically infects CXCR4⁺ cells in a CXCR4-dependent manner. Moreover, it has been validated by a growth curve that there was no significant difference in viral production between oHSV/gD and oHSV/Nb-gD.

1.2 Arming strategy

Concerning the arming strategy, we followed the approach described by *Shah K. et al.* in which a secretable form of TRAIL (sTRAIL). It has been shown that the expression of both the full-length and the secretable form of TRAIL, can induce apoptosis selectively in GBM cells while sparing normal cells. This selective apoptosis is related to the lack of expression of DR4 and DR5 death receptors of sTRAIL in normal cells compared to the overexpression in glioblastoma cells³⁶⁵.

sTRAIL was created from the fusion of the extracellular region of TRAIL sequence (NH₂-terminal, 114-281 aa) to a sequence coding for an isoleucine zipper and the extracellular domain Flt3L³⁴⁷. Specifically, isoleucine zipper, a variant of leucine zipper, was inserted to favor TRAIL trimerization, necessary for enhancing of death signaling by binding to its receptor³⁶⁶. Furthermore, the addition of the extracellular domain of the human receptor tyrosine Kinase, Fms-like tyrosine kinase 3 ligand (Flt3L/hFlex) can help the secretion of several proteins³⁶⁷ and studies showed that Flt3L administrated alone or with other cytokines, is able to inhibit efficiently the proliferation and metastasis of some cancers, like liver, lung and breast cancer in murine models³⁶⁸. Thus, Flt3L was inserted to increase the secretion of sTRAIL and trigger apoptosis. Finally, a furin peptide was added between the FLt3L and the isoleucine zipper sequences to induce the cleavage of FLt3L and sTRAIL sequences³⁶⁹ and thereby generate two functional biological products: FLt3L that stimulates dendritic cells (DC) and sTRAIL able to induce apoptosis³⁶⁷. Although the release of sTRAIL and its role in apoptosis was sought in this study, it would be interesting in the future to evaluate the role of FLt3L in DC activation and anti-tumour immunity activity.

In contrast to the already existing virus oHSV-sTRAIL, whose expression is driven by the HSV immediate early promoter IE 4/5^{370,371}, sTRAIL expression in oHSV/Nb-gD:sTRAIL is driven by the nestin promoter. Apart from NSC and progenitor cells, differentiated mature brain cells do not express nestin. However, it is recognised as a GSC marker, and its overexpression is correlated with a poor prognosis playing a role in the aggressiveness, metastasis, and self-renewal in tumour cells³⁷². *Kambara, H et al.* showed that the use of nestin as a specific promoter for protein expression in glioblastoma cells was safe enough by creating rQNestin34.5, an oHSV in which ICP34.5 expression was under the control of nestin promoter³⁷³. Finally, this construction was inserted in oHSV/gD (non-retargeted oHSV) and in oHSV/Nb-gD (nanobody-retargeted oHSV) creating the oHSV/gD:sTRAIL virus and the oHSV/Nb-gD:sTRAIL viruses respectively.

This project has validated that viral replication capacity between oHSV/Nb-gD and oHSV/Nb-gD:sTRAIL is comparable, demonstrating that sTRAIL expression does not impact viral production. In addition, we have shown *in vitro* that infection of U87MG CXCR4⁺ cells with armed oHSV/Nb-gD:sTRAIL triggers apoptosis more

efficiently than the non-armed oHSV/Nb-gD. These results correlate with results obtained in sTRAIL sensitivity analysis, where U87MG and U87MG CXCR4+ showed a decrease in viability when treated at different concentrations of sTRAIL. However, even though sTRAIL-arming triggers apoptosis *in vitro*, it does not significantly improve the virotherapy efficacy when used in the xenograft model. Moreover, as shown by others^{370,371}, sensitivity to viral death due to infection can be cell-dependent. Viability test in infected U87MG and U87MG CXCR4+ cells show a high sensitivity to oHSV-induced death, hiding the effect of sTRAIL-induced apoptosis when high MOIs are used. This high sensibility to oHSV-mediated death can explain the lack of difference *in vivo* between mice treated with oHSV/Nb-gD and oHSV/Nb-gD:sTRAIL in a U87MG CXCR4+ model. Even if there was no difference between treatments, oHSV/Nb-gD and oHSV/Nb-sTRAIL viral infection have a significant impact on tumour growth and mice survival when compared to the PBS group. However, tumour cells were not totally cleared. Sparse tumour cells or small tumours were still observed 2 weeks after treatment. Indeed, in our first experiment (Exp 0), we demonstrate that U87MG CXCR4+ cells engrafted in the xenograft model have very rapid growth kinetics. This rapid growth could be the reason why we did not see any effect in viral infection in our first experiment, suggesting that it was too late to inject the virus two weeks after cell engraftment. Such rapid growth can hamper the total elimination of the tumour after a single viral injection and explain the regrowth. In this context, it would be worth to evaluate the impact of repeated injections or of a continuous delivery of the virus through a mini osmotic system³⁷⁴. Finally, some mice were sacrificed 48h post-intra-tumoural injection to detect viral or sTRAIL transcripts and validate a correct viral replication³⁷⁵. RT-qPCR results showed a correct detection of gD and sTRAIL mRNA levels in treated mice. However, another RT-qPCR performed in some mice sacrificed two weeks after viral injection, did not allow the gD mRNA detection (data not shown), demonstrating a clearance of oHSV infection after viral injection. It could be possible that immune response plays a role in this clearance. Indeed, a study with U87ΔEGFR cells in an immunosuppressed mice model infected with rQnestin34.5, observe an antiviral response from macrophages and microglia³⁷⁶. They demonstrate that macrophages and microglia in oHSV treated mice were polarised towards M1 pro-inflammatory phenotype expressing high levels of TNFα.

TNF α is able to induce apoptosis in infected tumour cells and inhibit viral replication³⁷⁶. Their results suggest that oHSV therapy combined with TNF α inhibitors approved by the FDA could improve the efficacy of oHSV therapy in a future³⁷⁷. Apart from TNF α , other signals such IL-1b, IL-6, interferon, and nitric oxide are released to control the oHSV infection³⁷⁸. Thus, in our study, even if we work with nude mice, innate responses as macrophages and microglia can impact viral replication.

2. Efficacy of oHSV/Nb-gD and oHSV/Nb-gD:sTRAIL in tumourspheres

As previously said, GSC cells play an important role in tumour recurrence and aggressiveness. Several studies have identified the existence of cancer stem cells in solid tumours³⁷⁹. These cells are related to a poor prognosis, present stemness features, are resistant to radiotherapy and chemotherapy, and can create tumours when injected into mice. Therefore, the development of therapies targeting GSC could offer a new strategy to improve GBM prognosis. GSCs can be recognised by the expression of different markers like CD133, Nestin, SOX2, SALL2, and CXCR4^{359,380}. CXCR4, which is upregulated in response to an increased expression of hypoxia-inducible factor HIF-1- α , may play an important role in regulating the proliferation and migration of GSC⁵⁷. Indeed, *Goffart N, et al.* demonstrated *in vitro* and *in vivo* that GB138 Glioblastoma GSC cells overexpressing CXCR4 could migrate from the tumour mass (TM) to the subventricular zone (SVZ) through a CXCL12 gradient. Moreover, they observed that in mice treated with AMD3100, a CXCR4 specific antagonist, the migration of these cells was disrupted⁹⁴. Altogether, these data suggest that CXCR4 can be a potential target to promote a reduction of migration and proliferation. In this context, one of the main goals of this project was to target some of these GSC cells, overexpressing CXCR4, and reduce the percentage of migrating cells left after surgical resection.

After validation of retargeting and sTRAIL arming in a U87MG CXCR4+ model, we decided to analyse the capacity of these viruses to replicate and to induce apoptosis in different patient-derived cells. We obtained four different GSC patient-derived cells as a result of the collaboration with the Laboratory of Nervous System Disorders and Therapy (GIGA Neurosciences). They were able to isolate human

samples after surgical resection and keep it in culture in a stem cell culture medium. First, we validate the level of stemness by analysing different stemness markers by RT-qPCR. Results show a difference in stemness level between the GSC cells compared to the non-expression in U87MG and U87MG CXCR4⁺ cell lines. Moreover, the percentage of CXCR4⁺ cells analysed by flow cytometry correlates with the percentage of infected cells by the oHSV/Nb-gD, demonstrating its capacity of infection in a CXCR4 dependent manner. We could expect that due to the compact 3D structure of GSC tumourspheres, virus's capacity to reach all CXCR4⁺ cells would be compromised. However, immunofluorescence results performed on tumoursphere sections show that oHSV/Nb-gD virus could reach the CXCR4⁺ cells even if they were located at the centre of the sphere. However, tumourspheres are created from the dissociation of patient-derived glioma cells, leading to a clonal expansion³⁸¹. This clonal expansion spontaneously leads to the production of cancerous spheres from single cells, retaining a minimum degree of heterogeneity but losing the intra-tumour distribution due to single-cell dissociation step³⁸¹. Thus, the tumourspheres model system seems to have some limitations when analysing the impact of oncolytic viruses in a heterogeneous population. Glioblastoma organoids (GBO) technique avoids single-cell dissociation and uses serum-free and EGF/bFGF free media³⁸². This culture strategy allows GBOs to maintain native cell-cell interaction and parental tumour heterogeneity³⁸¹. Moreover, this GBO culture strategy also keeps alive tumour-associated non-cancerous cells. Thus, our lab started to culture GBOs directly from patient samples, and the oHSV created in this project will be tested soon.

After validating infection capacity in GSC, we wanted to determine their sensitivity to oHSV or sTRAIL-induced death. Analysis was done with the two patient-derived cells that express the most CXCR4⁺ (T018 and T033) to have the highest oHSV/Nb-gD infection possible. Viability test by infection of T018 and T033 with our four different virus, oHSV/gD oHSV/gD:sTRAIL, oHSV/Nb-gD and oHSV/Nb-gD:sTRAIL shows that T018 GSC cells were sensitive to oHSV-mediated cell death. However, there was no significant difference in cell viability between armed and not armed viruses. These results correlate with the U87MG and U87MG CXCR4⁺ viability test, where oHSV-mediated death hides the effect of sTRAIL-induced apoptosis when high MOIs are used.

Surprisingly, even if the T033 infection level was high, any significant decrease in cell viability was observed with any of four viruses. These results suggest that T033 cells seem to be oHSV-death resistant. Indeed, it has been shown that some established cell lines and patient-derived can be resistant to oHSV-mediated oncolysis³⁷¹. During HSV-1 replication, there is a balance between pro- and anti-apoptotic processes during infection. This constitutes a sensitive balance of apoptotic signals, allowing the cells to produce progeny prior to HSV-mediated cell death³⁸³. However, the altered cell pathway linked to the oHSV death resistance is not well known, even if some articles mention a relationship between oHSV sensibility and p53 altered pathways³⁸⁴. Indeed, p53 is one of the most common mutated genes in cancer. Its mutation in GBM is related to progression, invasion, reduction of apoptosis, increasing proliferation and higher stem-like phenotype. Numerous studies demonstrate that p53 mutation in cancer cells reduces HSV-1 viral replication *in vitro* and *in vivo*³⁸⁵.

In this context, the use of oHSV as a single agent in clinical trials demonstrates safety. However, they induced a partial response, suggesting that GBM presents a heterogeneity to the oHSV response, with some cells resistant to oHSV oncolysis and induced apoptosis. T018 oHSV sensitive and T033 oHSV resistant were treated at different concentration of soluble TRAIL to determine its sensibility. We obtained the same results as *Tamura K*, and colleagues, who identified some patient-derived cells that were either resistant to TRAIL-mediated apoptosis or resistant to both oHSV death and TRAIL³³⁹. In our case, T033, which shows to be resistant to HSV-mediated death, also demonstrated an apparent resistance to sTRAIL treatment compared to T018, which were HSV sensitive and sTRAIL sensitive. However, in contrast to our results, they demonstrate that the combination of both treatments by the infection of an oHSV-TRAIL³³⁹ could induce apoptosis in sTRAIL and oHSV resistant GSC. In our case, Annexin V test analysis in T018 and T033 GSC cells infected with our four viruses shows that only the T018, which are already sensitive to TRAIL, has an increase of apoptotic cells when the virus is armed. We expected an increase of apoptosis in T033 when the virus was armed, as demonstrated with the oHSV-TRAIL virus. The main difference between the oHSV-TRAIL construction and our oHSV/gD:sTRAIL construction is the promoter controlling sTRAIL expression. As previously said, the oHSV-TRAIL virus express TRAIL under the control of viral HSV immediate early promoter IE 4/5 while in our

oHSV/gD:sTRAIL and oHSV/Nb-gD:sTRAIL virus, sTRAIL is expressed under the control of nestin promoter. Although nestin is overexpressed in most GBM³⁵⁹, it might not be activated at the same level in all GBM cells. Thus, the level of expression of sTRAIL in the infected cells with our virus could be compromised by a lower nestin expression. RT-qPCR results show that T033 cells express a significantly lower amount of nestin than T018, suggesting that sTRAIL could be expressed at a deficient level in these cells. This low nestin expression partly explain the absence of apoptosis in T033 infected with the oHS/gD:sTRAIL or the oHSV/Nb-gD:sTRAIL. An ELISA test to determine the level of sTRAIL produced in different GSCs cells needs to be done to validate this hypothesis. A stronger promoter, like CMV, controlling sTRAIL expression will be considered soon. This new promoter could help to generate a better secretion of sTRAIL and a higher induction of apoptosis while still targeting CXCR4+ GSC cells.

Another hypothesis to answer the resistance to TRAIL could be the level of death receptors expressed on the cell surface. There are four different death receptors that TRAIL interacts with, but only two (TRAIL-R1 or DR4 and TRAIL-R2 or DR5) can to induce an apoptotic signal³⁸⁶. The other two receptors (TRAIL-R3 or DcR1 and TRAIL-R4 or DcR2) act as decoys. DcR2 presents a truncated non-functional death domain, and the DcR1 lacks its transmembrane and death domain. The percentage of cells expressing DR4 and DR5 were analysed in GBM cell lines and T018 and T033 patient-derived cells by flow cytometry. Results show a low expression of DR4 in all the cells (around 10 % of DR4⁺ cells) and no significant difference between them. On the contrary, DR5 is highly expressed (around 60% of DR5⁺ cells) except in T033 where its expression is significantly lower than the others. Indeed, *Bellail A, et al.* shows that most of GBM primary GSCs were resistant to TRAIL-induced apoptosis because of the overexpression of cellular FADD-like interleukin-1 β -converting enzyme-inhibitory protein (c-FLIP) and the lack of DR4 and DR5 death receptors expression³⁸⁷. However, it has been shown that treatment with cisplatin leads to an upregulation of DR5 receptor in the cell surface and a downregulation of c-FLIP, restoring a correct TRAIL apoptotic pathway in tumourspheres³⁸⁸. Thus, we could suggest that combining our oHSV/gD:sTRAIL or oHSV/Nb-gD:sTRAIL with cisplatin could induce apoptosis in TRAIL-resistant primary GSCs.

Another interesting point to highlight is the low level of nestin expressed by U87MG and U87MG CXCR4+ detected by RT-qPCR. This result suggests that the expression

of sTRAIL by these cell lines should be low, leading to poor induction of apoptosis. However, as previously said, infected U87MG CXCR4⁺ with oHSV/Nb-gD:sTRAIL leads to a correct induction of apoptosis. Knowing that U87MG are sensitive to sTRAIL and present a high expression of DR5 receptor, we could suggest that the few sTRAIL expressed by these cells is enough to induce a significant apoptotic effect. However, it is crucial to analyse the level of secreted sTRAIL by ELISA to validate this hypothesis. Nevertheless, another suggested hypothesis is the possibility of a failure in promoter specificity. Even if we have inserted the same sequence for nestin promoter as rQNestin34.5 virus, the region of insertion in the BAC is different, suggesting that maybe transgene was inserted near an enhancer or viral promoter that could impact sTRAIL expression regardless of nestin promoter. Therefore, an ELISA or Annexin V/DAPI apoptotic test need to be done in nestin negative human cells like Astrocytes to validate that they do not express sTRAIL when nestin is not expressed.

Finally, we wanted to validate if our retargeted and armed virus oHSV/Nb-gD:sTRAIL was able to reduce tumour volume and increase survival in mice with tumours from T033 primary-derived GSC culture. Using patient-derived cells models *in vivo* is essential to work with similar patient conditions and facilitate the individualised study of GBM response to these new treatments. Unfortunately, due to the lack of time, the T033 *in vivo* experiment was done in parallel to the *in vitro* validation, where it has been shown that T033 cells were resistant to sTRAIL and oHSV-mediated death. *In vivo* experiment was done with T033 due to its high percentage of CXCR4⁺ cells allowing a higher infection with oHSV/Nb-gD:sTRAIL. According to our results obtained *in vitro*, there was no difference between the PBS group and the groups treated with oHSV/Nb-gD or oHSV/Nb-gD:sTRAIL. We could suggest that one of the reasons for the non-difference between the PBS group and treated groups is that, as shown *in vitro*, T033 cells are resistant to HSV-mediated cell death, and even if there were highly infected, their viability did not decrease. On the other hand, it could be that there was any viral infection after intratumour injection. To confirm that, some mice should be sacrificed at early time points like 2- and 4-days post infection³⁷⁵ as done in the *in vivo* U87MG CXCR4⁺ experiment where an RT-qPCR was done detecting a correct gD and sTRAIL mRNA level in treated mice.

Another option to validate that we had a correct viral replication in nude mice brains would be using the GFP signal obtained in cells when infected by our virus with a GFP sequence. The combination of bioluminescence and fluorescence imaging is frequently used for *in vivo* models³⁸⁹. This double analysis can be complementary to each other and gives different information. Indeed, in our model, a combination of GFP and luciferin signals would inform us about the level of infection and tumour size, respectively. However, attention must be drawn to the fact that the signal must pass through the skull in brain imaging, and if the GFP signal is not strong enough, a correct signal cannot be detected. Finally, another option would be to tag the virus with another luciferase than the one used by cells, as done by *Tamura K, et al., 2012*³³⁹, where they used *Renilla luciferase* (Rluc) for viral infection and *Firefly luciferase* (Fluc) for cells.

3. What about the immune system and TME role?

The role of the tumour microenvironment (TME) and especially innate immune response should not be underestimated. A deeper characterisation of the tumour microenvironment upon virotherapy will give important information that might help to improve virotherapy. Due to the nanobody sequence used in this project only recognising human CXCR4, we worked with an orthotopic xenograft model, presenting the innate immune system. Unfortunately, due to a lack of time in the project, we could not study the innate immune response after infection with oHSV/Nb-gD and oHSV/Nb-gD:sTRAIL. Studies analysing the impact of the innate immune system using oHSV therapy have shown a rapid activation of natural killer (NK) cells. Indeed, Glioblastoma cells infected with oHSV upregulate Nkp30 and Nkp46 ligands that interact with NK cytotoxicity receptors³⁹⁰. The recognition of these ligands induces an *in vivo* antiviral response leading to a viral clearance³⁹⁰. This rapid NK response could explain the results obtained by RT-qPCR, where after two weeks of viral infection, we did not detect viral RNA in mice brains samples. Moreover, a part of the NK role, it has been shown that the depletion of microglia and infiltrating macrophages reduces anti-viral response and increases 10-fold intra-tumoural oncolytic virus³⁹¹. Indeed, treatment of oHSV with cyclophosphamide (CPA), which depletes both microglia (CD68+) and peripheral macrophages (CD163+) cells, is currently under a phase I clinical trial for multiple melanoma³⁹².

Indeed, one of the key points working with oncolytic viruses is its capacity to change the TME from “cold” to “hot”, leading to an infiltration of T cells and enhancing a response to immunotherapies. Tumour associated macrophages (TAMs) are one of the most abundant in TME. They can enhance tumour cell migration and invasion in brain tumours³⁹³. TAMs phenotype which, is based on the cytokines, factors, and proteins that are present in the TME, can vary between M1-like and M2-like³⁹⁴. Previous studies demonstrate that the modification of the TME by polarisation of TAMs towards an M1-like phenotype, can enhance antitumour efficacy. Indeed, an oHSV armed with IL-12 demonstrate its capacity to increase INF- γ and reduce Tregs³⁹⁵. Thus, in the near future, the combination of our oHSV/Nb-gD with IL-12 or another cytokine could be helpful to increase the antitumour effect. Moreover, studies have shown promising results in clinical trials with the oHSV T-VEC and other oHSV. However, there are still many challenges that need to be studied to improve oncolytic virus therapy³⁹⁶.

One crucial issue that must be carefully addressed when targeting tumour cells is that healthy cells might express the target of interest and thus be infected by the oncolytic virus. In our case, CXCR4 is known to be overexpressed in several cancers, being a mediator of cancer cell proliferation and invasion⁵⁷. CXCR4 could be expressed in different cell types like macrophages, myeloid cells, vascular cells and neoplastic cells³⁹⁷. For this reason, our project is based on a retargeted but also attenuated virus to maintain safety and reduce off-target toxicity. CXCR4 expression is known to be located in normal endothelial cells and is enriched in blood vessels formed in GBM hypoxic areas due to necrosis. The inhibition of CXCR4 using plerixafor combined with bevacizumab, an anti-vascular drug, is proposed as an anti-vascular treatment against GBM³⁹⁸. Thus, the idea of targeting these CXCR4+ endothelial cells with our oHSV/Nb-gD seems beneficial to reduce tumour vascularity. On the other hand, it has been reported that the expression of CXCR4 by macrophage population is mainly done by tumour associated macrophages (TAMs) with an M2-like pro-tumoural phenotype³⁹⁹. Thus, even if a tight distinction cannot be made between M1- and M2-like, TAMs in GBM seems to present more functions of M2-protumoural profile. Consequently, the capacity of the CXCR4-retargeted virus to infect and potentially destroy these cells, would certainly be helpful.

Furthermore, as previously said in the introduction, neural stem cells (NSC) are located in the SVZ niche, and the secretion of CXCL12 by blood vessels and the CXCL12/CXCR4 autocrine/paracrine loop play a crucial role in the maintenance of stemness and quiescent in adult brain⁹⁴. Consequently, the potential infection of this NSC located in SVZ by the retargeted virus might be detrimental. It is thus crucial to address this question very carefully. Unfortunately, one of the main problems of this project, which sequences is based on the patent WO 2016/156570 A1, is that the anti-CXCR4 nanobody used does not recognise murine CXCR4 which limits the questions that could be addressed. However, our laboratory is currently screening a nanobody library to identify nanobodies that recognise human and murine receptors. Such nanobodies would not only allow to address important issues, such as the eventual targeting of healthy cells but also evaluate the importance of the immune response, particularly the adaptive immune response which requires a syngeneic GBM mice model.

However, despite some limitations, the retargeting of oHSVs by the insertion of a nanobody appears highly encouraging and constitutes an interesting approach that will allow to face the high heterogeneity of GSCs. Therefore, this project must be considered a proof-of-principle and support the idea that a set of nanobodies specific for GSCs markers may be used to customise oHSVs and constitute thus a first step towards personalised virotherapy of GBM able to complement the actual therapeutic options.

VI. CONCLUSION AND PERSPECTIVES

This PhD project was based on the creation of a new Oncolytic Herpes Virus (oHSV) able to replicate in glioblastoma CXCR4⁺ cells and to induce their apoptosis by the secretion of a soluble form of TRAIL (sTRAIL) expressed under the control of a nestin promoter, a glioma-stem cell (GSC) marker.

We first validated the capacity to create a new type of HSV retargeting by the addition of nanobody sequences instead of light chain antibodies (ScFv), as previously done in the literature. This validated strategy opens the possibility of creating new nanobodies for specific targets and new oHSV targeting other GSC markers. As a result of the collaboration with the Laboratory of Nervous System Disorders and Therapy (GIGA Neurosciences), we have been able to work with patient-derived cells cultured as tumourspheres. We demonstrate the heterogeneity of CXCR4 expression and the capacity of our virus to infect them.

The arming of the oHSV with a soluble form of TRAIL (sTRAIL) demonstrates the capacity to increase apoptosis in GBM cell lines, as previously described in the literature. Unfortunately, we did not obtain an apoptotic effect when working with primary GSC cells resistant to TRAIL and oHSV death. Opposite to the results showed in the literature, we did not observe a synergic effect between oHSV and sTRAIL to overcome resistance and induce apoptosis. A better study of the molecular mechanism of certain tumour cells, such as T033, to overcome death by viral infection and TRAIL needs to be addressed. Moreover, it seems that the expression of sTRAIL under the nestin promoter is not optimal. sTRAIL proper secretion needs to be validated by ELISA. Indeed, we showed that the level of nestin expression in GSCs tumourspheres is highly heterogenous. In consequence, changing the promoter to a stronger one is ongoing and may help overcome this problem. The specificity of the nestin promoter still needs to be validated by the infection of astrocytes, which are nestin negative, by oHSV/Nb-gD:sTRAIL to demonstrate that there is no activation of the apoptosis.

Unfortunately, because the nanobody sequences inserted in our retargeting only recognises the CXCR4 human form, we were unable to work in a syngeneic murine model where the immune system is not compromised. Therefore, our laboratory is working on creating of a new nanobody sequence against human and murine CXCR4. In that way,

we could study the role and impact of this new oHSV on the immune system. Finally, as a result of the collaboration with the Neurosurgery department (CHU Liège) and the Laboratory of Nervous System Disorders and Therapy (GIGA Neurosciences), we are optimizing the creation of patient-derived multicellular organoids obtained directly from patient tumours. The difference between the already obtained patient-derived tumourspheres and these new organoids is that the tumourspheres culture leads to an enrichment of stem cells compared to the organoids culture, where we are able to keep intra-tumour heterogeneity and retain many key features and markers of their parental tumours. Thus, the use of organoids will allow us to create and test personalised oHSV therapy in the future.

In conclusion, the present manuscript validates the use of nanobodies as a proof-of-principle as a new retargeting strategy in the oHSV field and opens a window to create and test a personalised set of oHSV against glioblastoma stem cells.

VII. BIBLIOGRAPHY

1. Louis, D. N. *et al.* The 2021 WHO classification of tumors of the central nervous system: A summary. *Neuro. Oncol.* **23**, 1231–1251 (2021).
2. Patel, A. P. *et al.* Single-cell RNA-seq highlights intratumoral heterogeneity in primary glioblastoma. *Science (80-.).* **344**, 1396–1401 (2014).
3. Neftel C, Laffy J, Filbin MG, Hara T, Shore ME, Rahme GJ, Richman AR, Silverbush D, Shaw ML, Hebert CM, Dewitt J, Gritsch S, Perez EM, Gonzalez Castro LN, Lan X, Druck N, Rodman C, Dionne D, Kaplan A, Bertalan MS, Small J, Pelton K, Becker S, Bonal D, Ngu, S. M. An integrative model of cellular states, plasticity and genetics for glioblastoma. *Cell.* **178**, 835–849 (2019).
4. Ostrom, Q. T. *et al.* CBTRUS statistical report: Primary brain and central nervous system tumors diagnosed in the United States in 2006-2010. *Neuro. Oncol.* **15**, (2013).
5. Hanif, F., Muzaffar, K., Perveen, K., Malhi, S. M. & Simjee, S. U. Glioblastoma multiforme: A review of its epidemiology and pathogenesis through clinical presentation and treatment. *Asian Pacific J. Cancer Prev.* **18**, 3–9 (2017).
6. Thakkar, J. P. *et al.* Epidemiologic and molecular prognostic review of glioblastoma. *Cancer Epidemiol. Biomarkers Prev.* **23**, 1985–1996 (2014).
7. TAMIMI, A. F. & JUWEID, M. Epidemiology and Outcome of Glioblastoma. *Glioblastoma* 143–153 (2017) doi:10.15586/codon.glioblastoma.2017.ch8.
8. Urbanska, K., Sokolowska, J., Szmidt, M. & Sysa, P. Glioblastoma multiforme - An overview. *Wspolczesna Onkol.* **18**, 307–312 (2014).
9. Schultz, S. *et al.* Fine needle aspiration diagnosis of extracranial glioblastoma multiforme: Case report and review of the literature. *Cytojournal* **2**, 1–6 (2005).
10. Rickert, C. H. *et al.* Glioblastoma with adipocyte-like tumor cell differentiation - Histological and molecular features of a rare differentiation pattern. *Brain Pathol.* **19**, 431–438 (2009).
11. D’Alessio, A., Proietti, G., Sica, G. & Scicchitano, B. M. Pathological and molecular features of glioblastoma and its peritumoral tissue. *Cancers (Basel).* **11**, (2019).
12. Rojiani, A. M. & Dorovini-Zis, K. Glomeruloid vascular structures in glioblastoma multiforme: An immunohistochemical and ultrastructural study. *J. Neurosurg.* **85**, 1078–1084 (1996).

13. Coomberl, B. L., Stewart, P. A., Hayakawa, K., Farrell, C. L. & Del Maestros, R. F. Quantitative morphology of human glioblastoma multiforme microvessels: structural basis of blood-brain barrier defect. *J. Neurooncol.* **5**, 299–307 (1987).
14. La, M. Palisades and Pseudopalisades. *Ajnr. Am. J. Neuroradiol.* 2037–2041 (2006).
15. Liu, S. *et al.* Relationship between necrotic patterns in glioblastoma and patient survival: Fractal dimension and lacunarity analyses using magnetic resonance imaging. *Sci. Rep.* **7**, 1–7 (2017).
16. Schiffer, D., Annovazzi, L., Mazzucco, M. & Mellai, M. The origin of circumscribed necroses and perinecrotic niches in glioblastoma multiforme: An additional hypothesis. *Integr. Cancer Sci. Ther.* **2**, 75–78 (2015).
17. Keith, B., Johnson, R. S. & Simon, M. C. HIF1 α and HIF2 α : sibling rivalry in hypoxic tumour growth and progression. *Nat. Rev. Cancer* **12**, 9–22 (2012).
18. Lombardi, M. Y. & Assem, M. Glioblastoma Genomics: A Very Complicated Story. *Glioblastoma* 3–25 (2017) doi:10.15586/codon.glioblastoma.2017.ch1.
19. Loeb, L. A. Human cancers express mutator phenotypes: Origin, consequences and targeting. *Nat. Rev. Cancer* **11**, 450–457 (2011).
20. Cohen, A. L., Holmen, S. L., & Colman, H. IDH1 and IDH2 Mutations in Gliomas Adam. *Curr Neurol Neurosci Rep.* **13**, 345 (2013).
21. Kayabolen, A., Yilmaz, E. & Bagci-Onder, T. IDH mutations in glioma: Double-edged sword in clinical applications? *Biomedicines* **9**, (2021).
22. Nicholas, M. K., Lukas, R. V., Jafri, N. F., Faoro, L. & Salgia, R. Epidermal growth factor receptor-mediated signal transduction in the development and therapy of gliomas. *Clin. Cancer Res.* **12**, 7261–7270 (2006).
23. Sugawa, N., Ekstrand, A. J., James, C. D. & Collins, V. P. Identical splicing of aberrant epidermal growth factor receptor transcripts from amplified rearranged genes in human glioblastomas. *Proc. Natl. Acad. Sci. U. S. A.* **87**, 8602–8606 (1990).
24. Rajasekhar, V. K. *et al.* Oncogenic Ras and Akt signaling contribute to glioblastoma formation by differential recruitment of existing mRNAs to polysomes. *Mol. Cell* **12**, 889–901 (2003).
25. Furnari, F. B. *et al.* Malignant astrocytic glioma: Genetics, biology, and paths to treatment. *Genes Dev.* **21**, 2683–2710 (2007).
26. Knudsen, E. S. & Wang, J. Y. J. Targeting the RB-pathway in cancer therapy. *Clin.*

- Cancer Res.* **16**, 1094–1099 (2010).
27. Sanjeev Shangary and Shaomeng Wang. Small-Molecule Inhibitors of the MDM2-p53 Protein-Protein Interaction to Reactivate p53 Function: A Novel Approach for Cancer Therapy. *Annu Rev Pharmacol Toxicol* **49**, 223–241 (2009).
 28. Gritsch S, Batchelor T.T, G. C. L. N. Diagnostic, therapeutic, and prognostic implications of the 2021 World Health Organization classification of tumors of the central nervous system. *Cancer* **128**, 47–58 (2021).
 29. Brat, D. J. *et al.* cIMPACT-NOW update 3: recommended diagnostic criteria for “Diffuse astrocytic glioma, IDH-wildtype, with molecular features of glioblastoma, WHO grade IV”. *Acta Neuropathol.* **136**, 805–810 (2018).
 30. Liu, X. Y. *et al.* Frequent ATRX mutations and loss of expression in adult diffuse astrocytic tumors carrying IDH1/IDH2 and TP53 mutations. *Acta Neuropathol.* **124**, 615–625 (2012).
 31. Appay, R. *et al.* CDKN2A homozygous deletion is a strong adverse prognosis factor in diffuse malignant IDH-mutant gliomas. *Neuro. Oncol.* **21**, 1519–1528 (2019).
 32. Schwartzbaum, J. A., Fisher, J. L., Aldape, K. D. & Wrensch, M. Epidemiology and molecular pathology of glioma. *Nat. Clin. Pract. Neurol.* **2**, 494–503 (2006).
 33. Wrensch, M., Minn, Y., Chew, T., Bondy, M. & Berger, M. S. Epidemiology of primary brain tumors: Current concepts and review of the literature. *Neuro. Oncol.* **4**, 278–299 (2002).
 34. Manuscript, A. Brain Tumor Susceptibility: the Role of Genetic Factors and Uses of Mouse Models to Unravel Risk Karlyne. *Brain Pathol.* **19**, 121–131 (2010).
 35. Yuile, P., Dent, O., Cook, R., Biggs, M. & Little, N. Survival of glioblastoma patients related to presenting symptoms, brain site and treatment variables. *J. Clin. Neurosci.* **13**, 747–751 (2006).
 36. Gilard, V. *et al.* Diagnosis and management of glioblastoma: A comprehensive perspective. *J. Pers. Med.* **11**, (2021).
 37. Wirsching, H., Galanis, E. & Weller, M. Glioblastoma. **134**, (2016).
 38. Peeken, J. C. *et al.* Combining multimodal imaging and treatment features improves machine learning-based prognostic assessment in patients with glioblastoma multiforme. *Cancer Med.* **8**, 128–136 (2019).
 39. Price, S. J. *et al.* Multimodal MRI can identify perfusion and metabolic changes in the invasive margin of glioblastomas. *J. Magn. Reson. Imaging* **43**, 487–494

- (2016).
40. Yu, W., Zhang, L., Wei, Q. & Shao, A. O6-Methylguanine-DNA Methyltransferase (MGMT): Challenges and New Opportunities in Glioma Chemotherapy. *Front. Oncol.* **9**, 1–11 (2020).
 41. Zagzag, D., Douglas, C. M. & Kricheff, I. I. Glial Neoplasms: Dynamic Contrast-enhanced T2*-weighted MR Imaging. *Neuroradiology* 791–798 (1999).
 42. Bulsara, K. R., Johnson, J. & Villavicencio, A. T. Improvements in brain tumor surgery: the modern history of awake craniotomies. *Neurosurg. Focus* **18**, 3–5 (2005).
 43. Wolbers, J. G. Novel strategies in glioblastoma surgery aim at safe, super-maximum resection in conjunction with local therapies. *Chin. J. Cancer* **33**, 8–15 (2014).
 44. Stummer, W. *et al.* Fluorescence-guided surgery with 5-aminolevulinic acid for resection of malignant glioma: a randomised controlled multicentre phase III trial. *Lancet Oncol.* **7**, 392–401 (2006).
 45. Goryaynov, S. A. *et al.* The role of 5-ALA in low-grade gliomas and the influence of antiepileptic drugs on intraoperative fluorescence. *Front. Oncol.* **9**, 1–7 (2019).
 46. Yoshiura, T., Wu, O. & Sorensen, A. G. Advanced MR techniques. Diffusion MR imaging, perfusion MR imaging, and spectroscopy. *Neuroimaging Clin. N. Am.* **9**, 439–453 (1999).
 47. Gilbert, M. R. *et al.* Dose-dense temozolomide for newly diagnosed glioblastoma: A randomized phase III clinical trial. *J. Clin. Oncol.* **31**, 4085–4091 (2013).
 48. Rapp, M., Baernreuther, J., Turowski, B., Steiger, H. & Kamp, M. A. SC. (2017) doi:10.1016/j.wneu.2017.04.053.This.
 49. Friedman, H. S. *et al.* Bevacizumab alone and in combination with irinotecan in recurrent glioblastoma. *J. Clin. Oncol.* **27**, 4733–4740 (2009).
 50. Minniti, G., Niyazi, M., Alongi, F., Navarria, P. & Belka, C. Current status and recent advances in reirradiation of glioblastoma. *Radiat. Oncol.* **16**, 1–14 (2021).
 51. Briana C. Prager, Qi Xie, Shideng Bao, J. N. R. Cancer Stem Cells: The Architects of the Tumor Ecosystem. *Cell Stem Cell*, **24**, 41–53 (2019).
 52. Persano, L., Rampazzo, E., Basso, G. & Viola, G. Glioblastoma cancer stem cells: Role of the microenvironment and therapeutic targeting. *Biochem. Pharmacol.* **85**, 612–622 (2013).
 53. Clarke, M. F. *et al.* Cancer stem cells - Perspectives on current status and future

- directions: AACR workshop on cancer stem cells. *Cancer Res.* **66**, 9339–9344 (2006).
54. Suvà, M. L. & Tirosh, I. The Glioma Stem Cell Model in the Era of Single-Cell Genomics. *Cancer Cell* **37**, 630–636 (2020).
 55. Dirkse, A. *et al.* Stem cell-associated heterogeneity in Glioblastoma results from intrinsic tumor plasticity shaped by the microenvironment. *Nat. Commun.* **10**, 1–16 (2019).
 56. Khan, I. S. & Ehtesham, M. Targeting glioblastoma cancer stem cells: The next great hope? *Neurosurg. Focus* **37**, (2014).
 57. Ehtesham, M., Mapara, K. Y., Stevenson, C. B. & Thompson, R. C. CXCR4 mediates the proliferation of glioblastoma progenitor cells. *Cancer Lett.* **274**, 305–312 (2009).
 58. Schulz, A., Meyer, F., Dubrovskaya, A. & Borgmann, K. Cancer stem cells and radioresistance: DNA repair and beyond. *Cancers (Basel)*. **11**, 13–15 (2019).
 59. Hambardzumyan D, B. G. Glioblastoma: Defining Tumor Niches. *Trends Cancer* **1**, 252–265 (2015).
 60. Calabrese, C. *et al.* A Perivascular Niche for Brain Tumor Stem Cells. *Cancer Cell* **11**, 69–82 (2007).
 61. Bao, S. *et al.* Stem cell-like glioma cells promote tumor angiogenesis through vascular endothelial growth factor. *Cancer Res.* **66**, 7843–7848 (2006).
 62. Du R, Lu KV, Petritsch C, Liu P, Ganss R, Passegué E, Song H, Vandenberg S, Johnson RS, Werb Z, B. G. HIF1alpha induces the recruitment of bone marrow-derived vascular modulatory cells to regulate tumor angiogenesis and invasion. *Cancer Cell.* **13**, 206–220 (2008).
 63. Bergers, G. & Song, S. The role of pericytes in blood-vessel formation and maintenance. *Neuro. Oncol.* **7**, 452–464 (2005).
 64. Feng, X. *et al.* Loss of CX3CR1 increases accumulation of inflammatory monocytes and promotes gliomagenesis. *Oncotarget* **6**, 15077–15094 (2015).
 65. Liang J, Piao Y, Holmes L, Fuller GN, Henry V, Tiao N, de G. J. Neutrophils promote the malignant glioma phenotype through S100A4. *Clin Cancer Res.* **20**, 187–98 (2014).
 66. Kohanbash, G. & Okada, H. Myeloid-derived Suppressor Cells (MDSCs) in gliomas and glioma-development. *Immunol. Invest.* **41**, 658–679 (2012).
 67. Brat, D. J. *et al.* Pseudopalisades in Glioblastoma Are Hypoxic, Express

- Extracellular Matrix Proteases, and Are Formed by an Actively Migrating Cell Population. *Cancer Res.* **64**, 920–927 (2004).
68. Yancopoulos, G. D. *et al.* Vascular-specific growth factors and blood vessel formation. *Nature* **407**, 242–248 (2000).
 69. Brat, D. J. & Van Meir, E. G. Vaso-occlusive and prothrombotic mechanisms associated with tumor hypoxia, necrosis, and accelerated growth in glioblastoma. *Lab. Investig.* **84**, 397–405 (2004).
 70. Semenza, G. L. Defining the Role of Hypoxia-Inducible Factor 1 in Cancer Biology and Therapeutics. *Oncogene.* **29**, 625–634 (2010).
 71. Seidel, S. *et al.* A hypoxic niche regulates glioblastoma stem cells through hypoxia inducible factor 2 α . *Brain* **133**, 983–995 (2010).
 72. Bar, E. E., Lin, A., Mahairaki, V., Matsui, W. & Eberhart, C. G. Hypoxia increases the expression of stem-cell markers and promotes clonogenicity in glioblastoma neurospheres. *Am. J. Pathol.* **177**, 1491–1502 (2010).
 73. Zagzag, D. *et al.* Hypoxia-inducible factor 1 and VEGF upregulate CXCR4 in glioblastoma: Implications for angiogenesis and glioma cell invasion. *Lab. Investig.* **86**, 1221–1232 (2006).
 74. Cuddapah VA, Robel S, Watkins S, S. H. A neurocentric perspective on glioma invasion. *Nat Rev Neurosci.* **7**, 455–65 (2014).
 75. Zimmermann, D. R. & Dours-Zimmermann, M. T. Extracellular matrix of the central nervous system: From neglect to challenge. *Histochem. Cell Biol.* **130**, 635–653 (2008).
 76. Mentlein, R., Hattermann, K. & Held-Feindt, J. Lost in disruption: Role of proteases in glioma invasion and progression. *Biochim. Biophys. Acta - Rev. Cancer* **1825**, 178–185 (2012).
 77. Mathiisen, T. M., Lehre, K. P., Danbolt, N. C. & Ottersen, O. P. The perivascular astroglial sheath provides a complete covering of the brain microvessels: An electron microscopic 3D reconstruction. *Glia* **58**, 1094–1103 (2010).
 78. Friedmann-Morvinski, D. & Verma, I. M. Dedifferentiation and reprogramming: Origins of cancer stem cells. *EMBO Rep.* **15**, 244–253 (2014).
 79. Bachoo, R. M. *et al.* Epidermal growth factor receptor and Ink4a/Arf: Convergent mechanisms governing terminal differentiation and transformation along the neural stem cell to astrocyte axis. *Cancer Cell* **1**, 269–277 (2002).
 80. Reynolds, B. A. & Weiss, S. Generation of neurons and astrocytes from isolated

- cells of the adult mammalian central nervous system. *Science (80-.)*. **255**, 1707–1710 (1992).
81. Lois, C. & Alvarez-Buylla, A. Proliferating subventricular zone cells in the adult mammalian forebrain can differentiate into neurons and glia. *Proc. Natl. Acad. Sci. U. S. A.* **90**, 2074–2077 (1993).
 82. Human, T., Group, O., Natural, T., Museum, H. & Road, C. R reconstructing recent h u m an evolution. 217–224 (1992).
 83. Sanai, H. *et al.* Unique astrocyte ribbon in adult human brain contains neural stem cells but lacks chain migration. *Nature* **427**, 740–744 (2004).
 84. Quiñones-Hinojosa, A. *et al.* Cellular composition and cytoarchitecture of the adult human subventricular zone: A niche of neural stem cells. *J. Comp. Neurol.* **494**, 415–434 (2006).
 85. Altmann, C., Keller, S. & Schmidt, M. H. H. The role of svz stem cells in glioblastoma. *Cancers (Basel)*. **11**, 1–23 (2019).
 86. Lim, D. A. *et al.* Relationship of glioblastoma multiforme to neural stem cell regions predicts invasive and multifocal tumor phenotype. *Neuro. Oncol.* **9**, 424–429 (2007).
 87. Lois, C. & Alvarez-buylla, A. Long-Distance Neuronal Migration in the Adult Mammalian Brain Author (s): Carlos Lois and Arturo Alvarez-Buylla Published by: American Association for the Advancement of Science Stable URL : <http://www.jstor.org/stable/2885135> Long-Distance Neuronal Mi. **264**, 1145–1148 (1996).
 88. Menn, B. *et al.* Origin of oligodendrocytes in the subventricular zone of the adult brain. *J. Neurosci.* **26**, 7907–7918 (2006).
 89. Verhaak, R. G. W. *et al.* NIH Public Access. **17**, 1–25 (2011).
 90. Parsons, D. W. *et al.* NIH Public Access. **321**, (2010).
 91. Lee, J. H. *et al.* Human glioblastoma arises from subventricular zone cells with low-level driver mutations. *Nature* **560**, 243–247 (2018).
 92. Lombard, A. *et al.* The Subventricular Zone, a Hideout for Adult and Pediatric High-Grade Glioma Stem Cells. *Front. Oncol.* **10**, 1–13 (2021).
 93. Sampetean, O. *et al.* Invasion precedes tumor mass formation in a malignant brain tumor model of genetically modified neural stem cells. *Neoplasia* **13**, 784–791 (2011).
 94. Goffart, N. *et al.* Adult mouse subventricular zones stimulate glioblastoma stem

- cells specific invasion through CXCL12/CXCR4 signaling. *Neuro. Oncol.* **17**, 81–94 (2015).
95. Meyrath, M. *et al.* The atypical chemokine receptor ACKR3/CXCR7 is a broad-spectrum scavenger for opioid peptides. *Nat. Commun.* **11**, (2020).
 96. Yang, L. *et al.* Blocking CXCR4-mediated cyclic AMP suppression inhibits brain tumor growth in vivo. *Cancer Res.* **67**, 651–658 (2007).
 97. Zhu, Y. *et al.* The effect of CXCR4 silencing on epithelial-mesenchymal transition related genes in glioma U87 cells. *Anat. Rec.* **296**, 1850–1856 (2013).
 98. Dedobbeleer, M. *et al.* MKP1 phosphatase is recruited by CXCL12 in glioblastoma cells and plays a role in DNA strand breaks repair. *Carcinogenesis* **41**, 417–429 (2020).
 99. Willems, E. *et al.* Aurora A plays a dual role in migration and survival of human glioblastoma cells according to the CXCL12 concentration. *Oncogene* **38**, 73–87 (2019).
 100. Anup Kumar Singh, Rakesh Kumar Arya, Arun Kumar Trivedi, Sabyasachi Sanyal, Rathindranath Baral, Olivier Dormond, David M. Briscoe, and D. D. Chemokine receptor trio: CXCR3, CXCR4 and CXCR7 crosstalk via CXCL11 and CXCL12. *Cytokine Growth Factor Rev.* **24**, 41–49 (2013).
 101. Bachelier, F. *et al.* New nomenclature for atypical chemokine receptors. *Nat. Immunol.* **15**, 207–208 (2014).
 102. Hamm, H. E. Minireview The Many Faces of G Protein. *Biochemistry* 5–8.
 103. Feng, Y., Broder, C. C., Kennedy, P. E. & Berger, E. A. HIV-1 Entry Cofactor : Functional cDNA Cloning of a Seven-Transmembrane , G Protein- Coupled Receptor Author (s): Yu Feng , Christopher C . Broder , Paul E . Kennedy and Edward A . Berger Published by : American Association for the Advancement of Scienc. *Science (80-.)*. **272**, 872–877 (1996).
 104. Bajetto, A., Bonavia, R., Barbero, S. & Schettini, G. Characterization of chemokines and their receptors in the central nervous system: Physiopathological implications. *J. Neurochem.* **82**, 1311–1329 (2002).
 105. Würth, R., Bajetto, A., Harrison, J. K., Barbieri, F. & Florio, T. CXCL12 modulation of CXCR4 and CXCR7 activity in human glioblastoma stem-like cells and regulation of the tumor microenvironment. *Front. Cell. Neurosci.* **8**, 1–19 (2014).
 106. Domanska, U. M. *et al.* A review on CXCR4/CXCL12 axis in oncology: No place

- to hide. *Eur. J. Cancer* **49**, 219–230 (2013).
107. Nagasawa, T. *et al.* Defects of B-cell lymphopoiesis and bone-marrow myelopoiesis in mice lacking the CXC chemokine PBSF/SDF-1. *Nature* vol. 382 635–638 (1996).
 108. Cheng, Z. J. *et al.* β -Arrestin differentially regulates the chemokine receptor CXCR4-mediated signaling and receptor internalization, and this implicates multiple interaction sites between β -arrestin and CXCR4. *J. Biol. Chem.* **275**, 2479–2485 (2000).
 109. Hall, J. M. & Korach, K. S. Stromal cell-derived factor 1, a novel target of estrogen receptor action, mediates the mitogenic effects of estradiol in ovarian and breast cancer cells. *Mol. Endocrinol.* **17**, 792–803 (2003).
 110. Taichman, R. S. *et al.* Use of the stromal cell-derived factor-1/CXCR4 pathway in prostate cancer metastasis to bone. *Cancer Res.* **62**, 1832–1837 (2002).
 111. Kaifi, J. T. *et al.* Tumor-cell homing to lymph nodes and bone marrow and CXCR4 expression in esophageal cancer. *J. Natl. Cancer Inst.* **97**, 1840–1847 (2005).
 112. Kim, S. Y., Lee, C. H., Midura, B. V., Yeung, C., Mendoza, A., Hong, S. H., Ren, L., Wong, D., Korz, W., Merzouk, A., Salari, H., Zhang, H., Hwang, S. T., Khanna, C., & Helman, L. J. Inhibition of the CXCR4/CXCL12 chemokine pathway reduces the development of murine pulmonary metastases. *Clin. Exp. Metastasis* **25**, 201–211 (2008).
 113. Geminder, H. *et al.* A Possible Role for CXCR4 and Its Ligand, the CXC Chemokine Stromal Cell-Derived Factor-1, in the Development of Bone Marrow Metastases in Neuroblastoma. *J. Immunol.* **167**, 4747–4757 (2001).
 114. Teicher, B. A. & Fricker, S. P. CXCL12 (SDF-1)/CXCR4 pathway in cancer. *Clin. Cancer Res.* **16**, 2927–2931 (2010).
 115. Salmaggi, A. *et al.* CXCL12 expression is predictive of a shorter time to tumor progression in low-grade glioma: A single-institution study in 50 patients. *J. Neurooncol.* **74**, 287–293 (2005).
 116. Hariz, M. I. Psychosurgery, deep brain stimulation, and the re-writing of history. *Neurosurgery* **63**, (2008).
 117. Ehteshami, M., Winston, J. A., Kabos, P. & Thompson, R. C. CXCR4 expression mediates glioma cell invasiveness. *Oncogene* **25**, 2801–2806 (2006).
 118. Liu, C. *et al.* Expression and Functional Heterogeneity of Chemokine Receptors CXCR4 and CXCR7 in Primary Patient-Derived Glioblastoma Cells. *PLoS One* **8**,

- (2013).
119. Goffart, N. *et al.* CXCL12 mediates glioblastoma resistance to radiotherapy in the subventricular zone. *Neuro. Oncol.* **19**, 66–77 (2017).
 120. Piccirillo, S. G. M. *et al.* Contributions to drug resistance in glioblastoma derived from malignant cells in the sub-ependymal zone. *Cancer Res.* **75**, 194–202 (2015).
 121. Fanelli, G. N. *et al.* Decipher the glioblastoma microenvironment: The first milestone for new groundbreaking therapeutic strategies. *Genes (Basel)*. **12**, (2021).
 122. Dapash, M., Hou, D., Castro, B., Lee-Chang, C. & Lesniak, M. S. The interplay between glioblastoma and its microenvironment. *Cells* **10**, 1–14 (2021).
 123. Engler, J. R. *et al.* Increased microglia/macrophage gene expression in a subset of adult and pediatric astrocytomas. *PLoS One* **7**, 1–12 (2012).
 124. Charles, N. A., Holland, E. C., Gilbertson, R., Glass, R. & Kettenmann, H. The brain tumor microenvironment. *Glia* **60**, 502–514 (2012).
 125. Chen, Z. & Hambardzumyan, D. Immune microenvironment in glioblastoma subtypes. *Front. Immunol.* **9**, 1–8 (2018).
 126. Ginhoux, F. *et al.* NIH Public Access. **330**, 841–845 (2013).
 127. Shi C, P. E. Monocyte recruitment during infection and inflammation. *Nat Rev Immunol* **11**, 762–74. (2011).
 128. Dal-Secco, D. *et al.* A dynamic spectrum of monocytes arising from the in situ reprogramming of CCR2+ monocytes at a site of sterile injury. *J. Exp. Med.* **212**, 447–456 (2015).
 129. Chen, Z. *et al.* Cellular and molecular identity of tumor-associated macrophages in glioblastoma. *Cancer Res.* **77**, 2266–2278 (2017).
 130. Hambardzumyan, D., Gutmann, D. H. & Kettenmann, H. The role of microglia and macrophages in glioma maintenance and progression. *Nat. Neurosci.* **19**, 20–27 (2015).
 131. Brüne, B. *et al.* Redox control of inflammation in macrophages. *Antioxidants Redox Signal.* **19**, 595–637 (2013).
 132. Piaszyk-Borychowska, A. *et al.* Signal integration of IFN-I and IFN-II with TLR4 involves sequential recruitment of STAT1-Complexes and NFκB to enhance pro-inflammatory transcription. *Front. Immunol.* **10**, 1–20 (2019).
 133. Platanitis, E. & Decker, T. Regulatory networks involving STATs, IRFs, and NFκB in inflammation. *Front. Immunol.* **9**, 1–16 (2018).

134. Mantovani, A., Biswas, S. K., Galdiero, M. R., Sica, A. & Locati, M. Macrophage plasticity and polarization in tissue repair and remodelling. *J. Pathol.* **229**, 176–185 (2013).
135. Szulzewsky, F. *et al.* Glioma-associated microglia/macrophages display an expression profile different from M1 and M2 polarization and highly express Gpnmb and Spp1. *PLoS One* **10**, 1–27 (2015).
136. Komai, T. *et al.* Transforming growth factor- β and interleukin-10 synergistically regulate humoral immunity via modulating metabolic signals. *Front. Immunol.* **9**, 1–15 (2018).
137. Russell, L. & Peng, K. W. The emerging role of oncolytic virus therapy against cancer. *Chinese Clin. Oncol.* **7**, (2018).
138. Martikainen, M. & Essand, M. Virus-based immunotherapy of glioblastoma. *Cancers (Basel)*. **11**, (2019).
139. Koks, C. A. E., de Vleeschouwer, S., Graf, N. & van Gool, S. W. Immune suppression during oncolytic virotherapy for high-grade glioma; Yes or No? *J. Cancer* **6**, 203–217 (2015).
140. Ooi, Y. C. *et al.* The role of regulatory T-cells in glioma immunology. *Clin. Neurol. Neurosurg.* **119**, 125–132 (2014).
141. Serrano Cardona, L. & Muñoz Mata, E. *Paraninfo Digital. Early Human Development* vol. 83 (2013).
142. Adeegbe, D. O. & Nishikawa, H. Natural and induced T regulatory cells in cancer. *Front. Immunol.* **4**, 1–14 (2013).
143. Jordan, J. T. *et al.* Preferential migration of regulatory T cells mediated by glioma-secreted chemokines can be blocked with chemotherapy. *Cancer Immunol. Immunother.* **57**, 123–131 (2008).
144. Chang, A. L. *et al.* CL2 produced by the glioma microenvironment is essential for the recruitment of regulatory T cells and myeloid-derived suppressor cells. *Physiol. Behav.* **176**, 139–148 (2016).
145. Kmiecik, J. *et al.* Elevated CD3⁺ and CD8⁺ tumor-infiltrating immune cells correlate with prolonged survival in glioblastoma patients despite integrated immunosuppressive mechanisms in the tumor microenvironment and at the systemic level. *J. Neuroimmunol.* **264**, 71–83 (2013).
146. Lohr, J. *et al.* Effector T-cell infiltration positively impacts survival of glioblastoma patients and is impaired by tumor-derived TGF- β . *Clin. Cancer Res.*

- 17, 4296–4308 (2011).
147. Steinman, R. M. & Banchereau, J. Taking dendritic cells into medicine. *Nature* **449**, 419–426 (2007).
 148. Wang J. et al; Nrf2 suppresses the function of dendritic cells to facilitate the immune escape of glioma cells. *Exp. Cell Res.* **360**, 66–73 (2017).
 149. Raychaudhuri, B. *et al.* Myeloid-derived suppressor cell accumulation and function in patients with newly diagnosed glioblastoma. *Neuro. Oncol.* **13**, 591–599 (2011).
 150. Raychaudhuri, B. *et al.* Myeloid derived suppressor cell infiltration of murine and human gliomas is associated with reduction of tumor infiltrating lymphocytes. *J. Neurooncol.* **122**, 293–301 (2015).
 151. Mi, Y. *et al.* The Emerging Role of Myeloid-Derived Suppressor Cells in the Glioma Immune Suppressive Microenvironment. *Front. Immunol.* **11**, 1–11 (2020).
 152. Komotar, R. J., Otten, M. L., Moise, G. & Connolly, E. S. Radiotherapy plus concomitant and adjuvant temozolomide for glioblastoma—A critical review. *Clin. Med. Oncol.* **2**, 421–422 (2008).
 153. Chinot, O. L. *et al.* Bevacizumab plus Radiotherapy–Temozolomide for Newly Diagnosed Glioblastoma. *N. Engl. J. Med.* **370**, 709–722 (2014).
 154. Yu, M. W. & Quail, D. F. Immunotherapy for Glioblastoma: Current Progress and Challenge. *Front. Immunol.* **12**, 1–12 (2021).
 155. Huang, B. *et al.* Current Immunotherapies for Glioblastoma Multiforme. *Front. Immunol.* **11**, 1–12 (2021).
 156. Leach, D. R., Krummel, M. F. & Allison, J. P. Enhancement of antitumor immunity by CTLA-4 blockade. *Science (80-.).* **271**, 1734–1736 (1996).
 157. Ishida, Y., Agata, Y., Shibahara, K. & Honjo, T. Induced expression of PD-1, a novel member of the immunoglobulin gene superfamily, upon programmed cell death. *EMBO J.* **11**, 3887–3895 (1992).
 158. Larkin, J. *et al.* Five-Year Survival with Combined Nivolumab and Ipilimumab in Advanced Melanoma. *N. Engl. J. Med.* **381**, 1535–1546 (2019).
 159. Hellmann, M. D. *et al.* Nivolumab plus Ipilimumab in Advanced Non–Small-Cell Lung Cancer. *N. Engl. J. Med.* **381**, 2020–2031 (2019).
 160. Engels, B. *et al.* Relapse or eradication of cancer is predicted by peptide-major histocompatibility complex affinity. *Cancer Cell* **23**, 516–526 (2013).

161. Pardoll, D. M. The blockade of immune checkpoints in cancer immunotherapy. *Nat. Rev. Cancer* **12**, 252–264 (2012).
162. Buchbinder, E. I. & Desai, A. CTLA-4 and PD-1 pathways similarities, differences, and implications of their inhibition. *Am. J. Clin. Oncol. Cancer Clin. Trials* **39**, 98–106 (2016).
163. Bloch, O. *et al.* Gliomas promote immunosuppression through induction of B7-H1 expression in tumor-associated macrophages. *Clin. Cancer Res.* **19**, 3165–3175 (2013).
164. Fecci, P. E. *et al.* Increased regulatory T-cell fraction amidst a diminished CD4 compartment explains cellular immune defects in patients with malignant glioma. *Cancer Res.* **66**, 3294–3302 (2006).
165. Berghoff, A. S. *et al.* Programmed death ligand 1 expression and tumor-infiltrating lymphocytes in glioblastoma. *Neuro. Oncol.* **17**, 1064–1075 (2015).
166. Nduom, E. K. *et al.* PD-L1 expression and prognostic impact in glioblastoma. *Neuro. Oncol.* **18**, 195–205 (2016).
167. Savoia, P., Astrua, C. & Fava, P. Ipilimumab (Anti-Ctla-4 Mab) in the treatment of metastatic melanoma: Effectiveness and toxicity management. *Hum. Vaccines Immunother.* **12**, 1092–1101 (2016).
168. Fecci, P. E. *et al.* Systemic CTLA-4 blockade ameliorates glioma-induced changes to the CD4 + T cell compartment without affecting regulatory T-cell function. *Clin. Cancer Res.* **13**, 2158–2167 (2007).
169. Park, J. *et al.* Effect of combined anti-PD-1 and temozolomide therapy in glioblastoma. *Oncoimmunology* **8**, (2019).
170. Omuro, A. *et al.* Nivolumab with or without ipilimumab in patients with recurrent glioblastoma: Results from exploratory phase i cohorts of CheckMate 143. *Neuro. Oncol.* **20**, 674–686 (2018).
171. Reardon, D. A. *et al.* Effect of Nivolumab vs Bevacizumab in Patients with Recurrent Glioblastoma: The CheckMate 143 Phase 3 Randomized Clinical Trial. *JAMA Oncol.* **6**, 1003–1010 (2020).
172. Klemm, F. *et al.* Interrogation of the Microenvironmental Landscape in Brain Tumors Reveals Disease-Specific Alterations of Immune Cells. *Cell* **181**, 1643–1660.e17 (2020).
173. Koyama, S. *et al.* Adaptive resistance to therapeutic PD-1 blockade is associated with upregulation of alternative immune checkpoints. *Nat. Commun.* **7**, 1–9

- (2016).
174. Zhou, W. *et al.* Periostin secreted by glioblastoma stem cells recruits M2 tumour-associated macrophages and promotes malignant growth. *Nat. Cell Biol.* **17**, 170–182 (2015).
 175. Wu, A. *et al.* Glioma cancer stem cells induce immunosuppressive macrophages/microglia. *Neuro. Oncol.* **12**, 1113–1125 (2010).
 176. Akins, E. A., Aghi, M. K. & Kumar, S. Incorporating Tumor-Associated Macrophages into Engineered Models of Glioma. *iScience* **23**, 1–18 (2020).
 177. Hussain, S. F. *et al.* The role of human glioma-infiltrating microglia/macrophages in mediating antitumor immune responses. *Neuro. Oncol.* **8**, 261–279 (2006).
 178. Rahma, O. E. & Hodi, F. S. The intersection between tumor angiogenesis and immune suppression. *Clin. Cancer Res.* **25**, 5449–5457 (2019).
 179. Pyonteck, S. M. *et al.* CSF-1R inhibition alters macrophage polarization and blocks glioma progression. *Nat. Med.* **19**, 1264–1272 (2013).
 180. Butowski, N. *et al.* Orally administered colony stimulating factor 1 receptor inhibitor PLX3397 in recurrent glioblastoma: An Ivy Foundation Early Phase Clinical Trials Consortium phase II study. *Neuro. Oncol.* **18**, 557–564 (2016).
 181. Sahin, U. & Türeci, Ö. Personalized vaccines for cancer immunotherapy. *Science (80-.).* **359**, 1355–1360 (2018).
 182. Filley, A. C. & Dey, M. Dendritic cell based vaccination strategy: an evolving paradigm. *J. Neurooncol.* **133**, 223–235 (2017).
 183. Lynes, J., Sanchez, V., Dominah, G., Nwankwo, A. & Nduom, E. Current options and future directions in immune therapy for glioblastoma. *Front. Oncol.* **8**, 1–22 (2018).
 184. Prins, R. M. *et al.* Gene expression profile correlates with T-cell infiltration and relative survival in glioblastoma patients vaccinated with dendritic cell immunotherapy. *Clin. Cancer Res.* **17**, 1603–1615 (2011).
 185. Sottoriva, A. *et al.* Intratumor heterogeneity in human glioblastoma reflects cancer evolutionary dynamics. *Proc. Natl. Acad. Sci. U. S. A.* **110**, 4009–4014 (2013).
 186. Wang, Q. T. *et al.* Tumor-associated antigen-based personalized dendritic cell vaccine in solid tumor patients. *Cancer Immunol. Immunother.* **69**, 1375–1387 (2020).
 187. Platten, M. *et al.* A vaccine targeting mutant IDH1 in newly diagnosed glioma. *Nature* **592**, 463–468 (2021).

188. Rafiq, S., Hackett, C. S. & Brentjens, R. J. therapy. **17**, (2020).
189. Brudno, J. N. & Kochenderfer, J. N. Chimeric antigen receptor T-cell therapies for lymphoma. *Nat. Rev. Clin. Oncol.* **15**, 31–46 (2018).
190. Hucks, G. & Rheingold, S. R. The journey to CAR T cell therapy: the pediatric and young adult experience with relapsed or refractory B-ALL. *Blood Cancer J.* **9**, (2019).
191. Gatt, A. & Vella, K. Teaching an old dog new tricks? *Br. J. Haematol.* **187**, 416–417 (2019).
192. Sahin, A. *et al.* Development of third generation anti-EGFRvIII chimeric T cells and EGFRvIII-expressing artificial antigen presenting cells for adoptive cell therapy for glioma. *PLoS One* **13**, 1–19 (2018).
193. Brown, C. E. *et al.* Bioactivity and safety of IL13R α 2-redirected chimeric antigen receptor CD8⁺ T cells in patients with recurrent glioblastoma. *Clin. Cancer Res.* **21**, 4062–4072 (2015).
194. Brown, C. E. *et al.* Glioma IL13R α 2 is associated with mesenchymal signature gene expression and poor patient prognosis. *PLoS One* **8**, 1–14 (2013).
195. Brown, C. E. *et al.* Regression of Glioblastoma after Chimeric Antigen Receptor T-Cell Therapy. *N. Engl. J. Med.* **375**, 2561–2569 (2016).
196. Ahmed, N. *et al.* HER2-specific T cells target primary glioblastoma stem cells and induce regression of autologous experimental tumors. *Clin. Cancer Res.* **16**, 474–485 (2010).
197. Hegde, M. *et al.* Tandem CAR T cells targeting HER2 and IL13R α 2 mitigate tumor antigen escape. *J. Clin. Invest.* **126**, 3036–3052 (2016).
198. Qiu, H. *et al.* A Prognostic Microenvironment-Related Immune Signature via ESTIMATE (PROMISE Model) Predicts Overall Survival of Patients With Glioma. *Front. Oncol.* **10**, 1–16 (2020).
199. Burger, M. C. *et al.* CAR-Engineered NK Cells for the Treatment of Glioblastoma: Turning Innate Effectors Into Precision Tools for Cancer Immunotherapy. *Front. Immunol.* **10**, 1–16 (2019).
200. Russell SJ, Peng KW, B. J. ONCOLYTIC VIROTHERAPY. *Nat Biotechnol* **10;30**, 658–70 (2012).
201. Atherton, M. J. & Lichty, B. D. Evolution of oncolytic viruses: Novel strategies for cancer treatment. *Immunotherapy* **5**, 1191–1206 (2013).
202. EA Chiocca & SD Rabkin. Oncolytic Viruses and Their Application to Cancer

- Immunotherapy. *Cancer Immunol Res.* **2**, 295–300 (20014).
203. Cattaneo R, Miest T, Shashkova EV, B. M. Reprogrammed viruses as cancer therapeutics: targeted, armed and shielded. *Nat Rev Microbiol.* **6**, 529–40 (2008).
 204. Rahman, M. M. & McFadden, G. Oncolytic viruses: Newest frontier for cancer immunotherapy. *Cancers (Basel).* **13**, (2021).
 205. Alberts, P., Tilgase, A., Rasa, A., Bandere, K. & Venskus, D. The advent of oncolytic virotherapy in oncology: The Rigvir® story. *Eur. J. Pharmacol.* **837**, 117–126 (2018).
 206. Wei, D., Xu, J., Liu, X. Y., Chen, Z. N. & Bian, H. Fighting Cancer with Viruses: Oncolytic Virus Therapy in China. *Hum. Gene Ther.* **29**, 151–159 (2018).
 207. Raman, S. S., Hecht, J. R. & Chan, E. Talimogene laherparepvec: Review of its mechanism of action and clinical efficacy and safety. *Immunotherapy* **11**, 705–723 (2019).
 208. Daiichi Sankyo. Press Release DELYTACT ® Oncolytic Virus G47Δ Approved in Japan for Treatment of Patients with Malignant Glioma. 3–5 (2021).
 209. Frederick F Lang. Oncolytic Adenovirus DNX-2401 in Treating Patients With Recurrent High-Grade Glioma. *ClinicalTrials.gov NCT03896568* (2019).
 210. Targovax Oy. A Pilot Study of Sequential ONCOS-102, an Engineered Oncolytic Adenovirus Expressing GMCSF, and Pembrolizumab in Patients With Advanced or Unresectable Melanoma Progressing After Programmed Cell Death Protein 1 (PD1) Blockade. *ClinicalTrials.gov NCT03003676* (2021).
 211. Steve Bernstein, M. Trial of MG1-E6E7 With Ad-E6E7 and Atezolizumab in Patients With HPV Associated Cancers (Kingfisher). *ClinicalTrials.gov NCT03618953* <https://clinicaltrials.gov/ct2/show/NCT03618953> (2018).
 212. Reinhard Dummer, P. D. T-VEC in Non-melanoma Skin Cancer (20139157 T-VEC). *ClinicalTrials.gov* *NCT03458117* <https://clinicaltrials.gov/ct2/show/NCT03458117?term=T-VEC&draw=2&rank=1>.
 213. John Haanen, P. Neo-adjuvant T-VEC + Nivolumab Combination Therapy for Resectable Early Metastatic (Stage IIIB/C/D-IV M1a) Melanoma With Injectable Disease (NIVEC). *ClinicalTrials.gov* *NCT04330430* <https://clinicaltrials.gov/ct2/show/NCT04330430?term=T-VEC&draw=2&rank=2> (2020).
 214. Gregory Friedman, M. . HSV G207 in Children With Recurrent or Refractory

- Cerebellar Brain Tumors. *ClinicalTrials.gov* NCT03911388 (2019).
215. Geletneky, K. *et al.* Phase I/IIa study of intratumoral/intracerebral or intravenous/intracerebral administration of Parvovirus H-1 (ParvOryx) in patients with progressive primary or recurrent glioblastoma multiforme: ParvOryx01 protocol. *BMC Cancer* **12**, (2012).
 216. Lee's Pharmaceutical Limited. Phase Ib/II Clinical Study of Pexa-Vec (Vaccinia GM CSF / Thymidine Kinase-Deactivated Virus) Combined With Recombinant Whole Human Anti-PD-L1 Monoclonal Antibody (ZKAB001) in Metastatic Melanoma. *ClinicalTrials.gov* NCT04849260
<https://clinicaltrials.gov/ct2/show/NCT04849260> (2021).
 217. Tony Reid, Md, P. A Study of Recombinant Vaccinia Virus to Treat Unresectable Primary Hepatocellular Carcinoma. *ClinicalTrials.gov* NCT00554372
<https://clinicaltrials.gov/ct2/show/NCT00554372> (2015).
 218. Ren, H. *et al.* Erratum: Immunogene therapy of recurrent glioblastoma multiforme with a liposomally encapsulated replication-incompetent Semliki forest virus vector carrying the human interleukin-12 gene - A phase I/II clinical protocol (Journal of Neuro-Oncology (2003) . *J. Neurooncol.* **65**, 191 (2003).
 219. Sabine Mueller, MD, PhD, M. Modified Measles Virus (MV-NIS) for Children and Young Adults With Recurrent Medulloblastoma or Recurrent ATRT. *ClinicalTrials.gov* NCT02962167
<https://www.clinicaltrials.gov/ct2/show/NCT02962167> (2016).
 220. LLC, M. A Study of MEDI5395 in Combination With Durvalumab in Subjects With Select Advanced Solid Tumors. *ClinicalTrials.gov* NCT03889275
<https://www.clinicaltrials.gov/ct2/show/NCT03889275> (2019).
 221. Hardev Pandha. CAVATAK (CVA21) in Non-muscle Invasive Bladder Cancer (VLA-012 CANON) (CANON). *ClinicalTrials.gov* NCT02316171
<https://clinicaltrials.gov/ct2/show/NCT02316171> (2019).
 222. Dina Randazzo, D. PVSRIPO in Recurrent Malignant Glioma. *ClinicalTrials.gov* NCT02986178
<https://clinicaltrials.gov/ct2/show/NCT02986178> (2016).
 223. Rudin Charles, MD, P. Safety Study of Seneca Valley Virus in Patients With Solid Tumors With Neuroendocrine Features. *ClinicalTrials.gov* NCT00314925
<https://clinicaltrials.gov/ct2/show/NCT00314925> (2006).
 224. Vanessa Bernstein. A Study of Reolysin For Patients With Advanced/Metastatic Breast Cancer. *ClinicalTrials.gov* NCT01656538

- <https://clinicaltrials.gov/ct2/show/NCT01656538> (2012).
225. Alex Adjei, MD, P. Ph I/II Trial of Systemic VSV-IFN β -NIS and Pembrolizumab in Refractory NSCLC and NEC. *ClinicalTrials.gov* NCT03647163 <https://www.clinicaltrials.gov/ct2/show/NCT03647163> (2018).
226. Derek Jonker. MG1 Maraba/MAGE-A3, With and Without Adenovirus Vaccine With Transgenic MAGE-A3 Insertion in Incurable MAGE-A3-Expressing Solid Tumours. *ClinicalTrials.gov* NCT02285816 <https://clinicaltrials.gov/ct2/show/NCT02285816> (2014).
227. Roizman, B. THE ORGANIZATION OF THE HERPES SIMPLEX VIRUS GENOMES. *Ann. Rev. Genet.* **13**, 25–57 (1979).
228. Davison AJ, Eberle R, Ehlers B, Hayward GS, McGeoch DJ, Minson AC, Pellett PE, Roizman B, Studdert MJ, T. E. The order Herpesvirales. *Arch Virol* **154**, 171–7 (2009).
229. Denes CE, Everett RD, D. R. Tour de Herpes: Cycling Through the Life and Biology of HSV-1. in *Herpes Simplex Virus (Methods and Protocols)* 1–30 (2020). doi:10.1007/978-1-4939-9814-2_1.
230. Birkmann, A. & Zimmermann, H. HSV antivirals - Current and future treatment options. *Curr. Opin. Virol.* **18**, 9–13 (2016).
231. Jane Flint, Vincent Racaniello, Glenn Rall, Anna Marie Skalka, L. E. *Principles of Virology, 4ed.* (2007).
232. Krishnan, R. & Stuart, P. M. Developments in Vaccination for Herpes Simplex Virus. *Front. Microbiol.* **12**, (2021).
233. Madavaraju, K., Koganti, R., Volety, I., Yadavalli, T. & Shukla, D. Herpes Simplex Virus Cell Entry Mechanisms: An Update. *Front. Cell. Infect. Microbiol.* **10**, 1–18 (2021).
234. Shukla, A. M. A. and D. Cell entry mechanisms of HSV: what we have learned in recent years. *Futur. Virol.* **10**, 1145–1154 (2015).
235. Campadelli-Fiume, G., Cocchi, F., Menotti, L. & Lopez, M. The novel receptors that mediate the entry of herpes simplex viruses and animal alphaherpesviruses into cells. *Rev. Med. Virol.* **10**, 305–319 (2000).
236. Agelidis, A. M. & Shukla, D. Cell entry mechanisms of HSV: What we have learned in recent years. *Future Virol.* **10**, 1145–1154 (2015).
237. Arii J, K. Y. The Role of HSV Glycoproteins in Mediating Cell Entry. in *Human Herpes Virus (Adv Exp Med Biol)*, 2018). doi:doi: 10.1007/978-981-10-7230-7_1.

238. Verzosa, A. L. *et al.* Herpes Simplex Virus 1 Infection of Neuronal and Non-Neuronal Cells Elicits Specific Innate Immune Responses and Immune Evasion Mechanisms. *Front. Immunol.* **12**, 1–17 (2021).
239. Weller, S. K. & Coen, D. M. Herpes simplex viruses: Mechanisms of DNA replication. *Cold Spring Harb. Perspect. Biol.* **4**, (2012).
240. Mettenleiter TC, Klupp BG, G. H. Herpesvirus assembly: An update. *Virus Res.* **143**, 222–234 (2009).
241. Aldrak, N. *et al.* Oncolytic herpes simplex virus-based therapies for cancer. *Cells* **10**, 1–17 (2021).
242. Sankyo, D. *Daiichi Sankyo Launches DELYTACT® Oncolytic Virus G47Δ in Japan.* www.daiichisankyo.com. (2021).
243. Macdonald, S. J., Mostafa, H. H., Morrison, L. A. & Davido, D. J. Genome Sequence of Herpes Simplex Virus 1 Strain KOS. *J. Virol.* **86**, 6371–6372 (2012).
244. Shen, Y. & Nemunaitis, J. Herpes simplex virus 1 (HSV-1) for cancer treatment. *Cancer Gene Ther.* **13**, 975–992 (2006).
245. Rehman, H., Silk, A. W., Kane, M. P. & Kaufman, H. L. Into the clinic: Talimogene laherparepvec (T-VEC), a first-in-class intratumoral oncolytic viral therapy. *J. Immunother. Cancer* **4**, 1–8 (2016).
246. Kaufman, H. L. *et al.* Local and distant immunity induced by intralesional vaccination with an oncolytic herpes virus encoding GM-CSF in patients with stage IIIc and IV melanoma. *Ann. Surg. Oncol.* **17**, 718–730 (2010).
247. Conry, R. M., Westbrook, B., McKee, S. & Norwood, T. G. Talimogene laherparepvec: First in class oncolytic virotherapy. *Hum. Vaccines Immunother.* **14**, 839–846 (2018).
248. Wilcox, D. R. & Longnecker, R. The Herpes Simplex Virus Neurovirulence Factor γ 34.5: Revealing Virus–Host Interactions. *PLoS Pathog.* **12**, 1–7 (2016).
249. Cassady, K. A., Gross, M. & Roizman, B. The Second-Site Mutation in the Herpes Simplex Virus Recombinants Lacking the γ 1 34.5 Genes Precludes Shutoff of Protein Synthesis by Blocking the Phosphorylation of eIF-2 α . *J. Virol.* **72**, 7005–7011 (1998).
250. MacLean, A. R., Ul-Fareed, M., Robertson, L., Harland, J. & Brown, S. M. Herpes simplex virus type 1 deletion variants 1714 and 1716 pinpoint neurovirulence-related sequences in Glasgow strain 17+ between immediate early gene 1 and the ‘a’ sequence. *J. Gen. Virol.* **72**, 631–639 (1991).

251. Toshihiro Mineta, Samuel D. Rabkin, Takahito Yazaki, W. D. H. & R. L. M. Attenuated multi-mutated herpes simplex virus-1 for the treatment of malignant gliomas. *Nature* **2**, 983–989 (1995).
252. Aghi, M., Visted, T., DePinho, R. A. & Chiocca, E. A. Oncolytic herpes virus with defective ICP6 specifically replicates in quiescent cells with homozygous genetic mutations in p16. *Oncogene* **27**, 4249–4254 (2008).
253. Mineta T, Rabkin SD, Yazaki T, Hunter WD, M. R. Attenuated multi-mutated herpes simplex virus-1 for the treatment of malignant gliomas. *Nature* **2**, 938–43 (1995).
254. Peters, C. & Rabkin, S. D. Designing herpes viruses as oncolytics. *Mol. Ther. - Oncolytics* **2**, 15010 (2015).
255. Hill, A., Jugovic, P., York, I. et al. Herpes simplex virus turns off the TAP to evade host immunity. *Nature* **375**, 411–415 (1995).
256. Todo, T., Martuza, R. L., Rabkin, S. D. & Johnson, P. A. Oncolytic herpes simplex virus vector with enhanced MHC class I presentation and tumor cell killing. *Proc. Natl. Acad. Sci. U. S. A.* **98**, 6396–6401 (2001).
257. Interactions, V. et al. Restriction of Replication of Oncolytic Herpes Simplex Virus. *J. Virol.* **92**, 1–17 (2018).
258. Todo, T. Results of phase II clinical trial of oncolytic herpes virus G47 Δ in patients with Glioblastoma. *Neuro. Oncol.* **11**, 3347097 (2019).
259. Friedman, G. K. et al. Enhanced Sensitivity of Patient-Derived Pediatric High-Grade Brain Tumor Xenografts to Oncolytic HSV-1 Virotherapy Correlates with Nectin-1 Expression. *Sci. Rep.* **8**, 1–10 (2018).
260. Campadelli-Fiume, G. et al. Retargeting strategies for oncolytic herpes simplex viruses. *Viruses* **8**, (2016).
261. Campadelli-Fiume, G., Menotti, L., Avitabile, E. & Gianni, T. Viral and cellular contributions to herpes simplex virus entry into the cell. *Curr. Opin. Virol.* **2**, 28–36 (2012).
262. Milne, R. S. B. et al. Function of Herpes Simplex Virus Type 1 gD Mutants with Different Receptor-Binding Affinities in Virus Entry and Fusion. *J. Virol.* **77**, 8962–8972 (2003).
263. Carfi, A. et al. Herpes simplex virus glycoprotein D bound to the human receptor HveA. *Mol. Cell* **8**, 169–179 (2001).
264. Zhang, N. et al. Binding of herpes simplex virus glycoprotein D to nectin-1

- exploits host cell adhesion. *Nat. Commun.* **2**, 1–10 (2011).
265. Krummenacher, C. *et al.* Localization of a Binding Site for Herpes Simplex Virus Glycoprotein D on Herpesvirus Entry Mediator C by Using Antireceptor Monoclonal Antibodies. *J. Virol.* **74**, 10863–10872 (2000).
 266. Navaratnarajah, C. K., Miest, T. S., Carfi, A. & Cattaneo, R. Targeted entry of enveloped viruses: Measles and herpes simplex virus i. *Curr. Opin. Virol.* **2**, 43–49 (2012).
 267. Xu, H. *et al.* Epidermal growth factor receptor in glioblastoma (Review). *Oncol. Lett.* **14**, 512–516 (2017).
 268. Uchida, H. *et al.* Effective treatment of an orthotopic xenograft model of human glioblastoma using an EGFR-retargeted oncolytic herpes simplex virus. *Mol. Ther.* **21**, 561–569 (2013).
 269. Menotti, L., Cerretani, A., Hengel, H. & Campadelli-Fiume, G. Construction of a Fully Retargeted Herpes Simplex Virus 1 Recombinant Capable of Entering Cells Solely via Human Epidermal Growth Factor Receptor 2. *J. Virol.* **82**, 10153–10161 (2008).
 270. Liu, G. *et al.* HER-2, gp100, and MAGE-1 are expressed in human glioblastoma and recognized by cytotoxic T cells. *Cancer Res.* **64**, 4980–4986 (2004).
 271. Gambini, E. *et al.* Replication-competent herpes simplex virus retargeted to HER2 as therapy for high-grade glioma. *Mol. Ther.* **20**, 994–1001 (2012).
 272. Nguyen, H.-M. & Saha, D. The Current State of Oncolytic Herpes Simplex Virus for Glioblastoma Treatment. *Oncolytic Virotherapy* **Volume 10**, 1–27 (2021).
 273. Zhou, Z. *et al.* Multiple strategies to improve the therapeutic efficacy of oncolytic herpes simplex virus in the treatment of glioblastoma (Review). *Oncol. Lett.* **22**, 1–10 (2021).
 274. Totsch, S. K., Schlappi, C., Kang, K. D., Ishizuka, A. S., Lynn, G. M., Fox, B., Beierle, E. A., Whitley, R. J., Markert, J. M., Gillespie, G. Y., Bernstock, J. D., & Friedman, G. K. Oncolytic Herpes Simplex Virus Immunotherapy for Brain Tumors: Current Pitfalls and Emerging Strategies to Overcome Therapeutic Resistance. *Oncogene.* **389**, 6159–6171 (2019).
 275. Nguyen, K. G. *et al.* Localized Interleukin-12 for Cancer Immunotherapy. *Front. Immunol.* **11**, 1–36 (2020).
 276. Cheema, T. A. *et al.* Multifaceted oncolytic virus therapy for glioblastoma in an immunocompetent cancer stem cell model. *Proc. Natl. Acad. Sci. U. S. A.* **110**,

- 12006–12011 (2013).
277. Zachary Barnard, MS, Hiroshi Wakimoto, MD, Cecile Zaupa, PhD, D. Sanjeeva Jeyeretna, MD, Anoop P. Patel, MD, Jacqueline Kle, Robert L Martuza, MD, Samuel D. Rabkin, PhD, and William T. Curry Jr., M. Expression of FMS-like Tyrosine Kinase 3 Ligand by Oncolytic Herpes Simplex Virus Type I Prolongs Survival in Mice Bearing Established Syngeneic Intracranial Malignant Glioma. *Neurosurgery*. **71**, 741–748 (2012).
 278. Tamura, K. *et al.* Multimechanistic tumor targeted oncolytic virus overcomes resistance in brain tumors. *Mol. Ther.* **21**, 68–77 (2013).
 279. Deng, L., Zhai, X., Liang, P. & Cui, H. Overcoming trail resistance for glioblastoma treatment. *Biomolecules* **11**, 1–17 (2021).
 280. Rozanov, D. V. *et al.* Engineering a leucine zipper-TRAIL homotrimer with improved cytotoxicity in tumor cells. *Mol. Cancer Ther.* **8**, 1515–1525 (2009).
 281. Jahan, N. *et al.* Therapeutic targeting of chemoresistant and recurrent glioblastoma stem cells with a proapoptotic variant of oncolytic herpes simplex virus. **141**, 1671–1681 (2017).
 282. Zhang, W. *et al.* Combination of oncolytic herpes simplex Viruses armed with angiostatin and IL-12 enhances antitumor efficacy in human Glioblastoma models. *Neoplasia (United States)* **15**, 591–599 (2013).
 283. Zhang, W. *et al.* Bevacizumab with angiostatin-armed oHSV increases antiangiogenesis and decreases bevacizumab-induced invasion in U87 glioma. *Mol. Ther.* **20**, 37–45 (2012).
 284. Zhang, G. *et al.* Enhanced antitumor efficacy of an oncolytic herpes simplex virus expressing an endostatin-angiostatin fusion gene in human glioblastoma stem cell xenografts. *PLoS One* **9**, 1–9 (2014).
 285. Mustafa Khasraw, David A. Reardon, Michael Weller, J. H. S. PD-1 inhibitors: Do they have a future in the treatment of glioblastoma? *Clin Cancer Res.* **26**, 5287–5296 (2020).
 286. Passaro C, Alayo Q, De Laura I, McNulty J, Grauwet K, Ito H, Bhaskaran V, Mineo M, Lawler SE, Shah K, Speranza MC, Goins W, McLaughlin E, Fernandez S, Reardon DA, Freeman GJ, Chiocca EA, N. H. Arming an Oncolytic Herpes Simplex Virus Type 1 with a Single- chain Fragment Variable Antibody against PD-1 for Experimental Glioblastoma Therapy. *Clin Cancer Res.* **26**, 758 (2019).
 287. Martuza, R. L., Malick, A., Markert, J. M., Ruffner, K. L. & Coen, D. M.

- Experimental therapy of human glioma by means of a genetically engineered virus mutant. *Science (80-.)*. **252**, 854–856 (1991).
288. Mineta, T., Rabkin, S. D. & Martuza, R. L. Treatment of Malignant Gliomas Using Ganciclovir-hypersensitive, Ribonucleotide Reductase-deficient Herpes Simplex Viral Mutant. *Cancer Res.* **54**, 3963–3966 (1994).
289. Kesari S, Randazzo BP, Valyi-Nagy T, Huang QS, Brown SM, MacLean AR, Lee VM, Trojanowski JQ, F. N. Therapy of experimental human brain tumors using a neuroattenuated herpes simplex virus mutant. *Lab Invest.* **73**, 636–48 (1995).
290. Advani, S. J. *et al.* Enhancement of replication of genetically engineered herpes simplex viruses by ionizing radiation: A new paradigm for destruction of therapeutically intractable tumors. *Gene Ther.* **5**, 160–165 (1998).
291. Chiocca, E. A., Nakashima, H., Kasai, K., Fernandez, S. A. & Oglesbee, M. Preclinical Toxicology of rQNestin34.5v.2: An Oncolytic Herpes Virus with Transcriptional Regulation of the ICP34.5 Neurovirulence Gene. *Mol. Ther. - Methods Clin. Dev.* **17**, 871–893 (2020).
292. Shah, A. C. *et al.* Enhanced antiglioma activity of chimeric HCMV/HSV-1 oncolytic viruses. *Gene Ther.* **14**, 1045–1054 (2007).
293. Ryuichi Kanai, Hiroaki Wakimoto, Robert L. Martuza, and S. D. R. A Novel Oncolytic Herpes Simplex Virus that Synergizes with Phosphatidylinositol 3-Kinase/Akt Pathway Inhibitors to Target Glioblastoma Stem Cells. *Clin Cancer* **17**, 3686–3696 (2011).
294. Reisoli, E. *et al.* Efficacy of HER2 retargeted herpes simplex virus as therapy for high-grade glioma in immunocompetent mice. *Cancer Gene Ther.* **19**, 788–795 (2012).
295. Alessandrini, F. *et al.* Eradication of glioblastoma by immuno-virotherapy with a retargeted oncolytic HSV in a preclinical model. *Oncogene* **38**, 4467–4479 (2019).
296. Mazzacurati, L. *et al.* Use of miRNA response sequences to block off-target replication and increase the safety of an unattenuated, glioblastoma-targeted oncolytic HSV. *Mol. Ther.* **23**, 99–107 (2015).
297. Sette, P. *et al.* GBM-Targeted oHSV Armed with Matrix Metalloproteinase 9 Enhances Anti-tumor Activity and Animal Survival. *Mol. Ther. - Oncolytics* **15**, 214–222 (2019).
298. Tomita, Y. *et al.* Oncolytic herpes virus armed with vasculostatin in combination with bevacizumab abrogates glioma invasion via the CCN1 and AKT signaling

- pathways. *Mol. Cancer Ther.* **18**, 1418–1429 (2019).
299. Fujii, K., Kurozumi, K., Ichikawa, T., Onishi, M., Shimazu, Y., Ishida, J., Chiocca, E. A., Kaur, B., & Date, I. The integrin inhibitor cilengitide enhances the anti-glioma efficacy of vasculostatin-expressing oncolytic virus. *Cancer Gene Ther.* **20**, 139–148 (2013).
 300. Ryuichi Kanai, MD, PhD, Hiroaki Wakimoto, MD, PhD Tooba Cheema, PhD, Samuel D Rabkin, P. Oncolytic herpes simplex virus vectors and chemotherapy: are combinatorial strategies more effective for cancer? *Futur. Oncol* **6**, 619–634 (2010).
 301. Aghi, M., Rabkin, S. & Martuza, R. L. Effect of chemotherapy-induced DNA repair on oncolytic herpes simplex viral replication. *J. Natl. Cancer Inst.* **98**, 38–50 (2006).
 302. Hadjipanayis, C. G. & DeLuca, N. A. Inhibition of DNA repair by a herpes simplex virus vector enhances the radiosensitivity of human glioblastoma cells. *Cancer Res.* **65**, 5310–5316 (2005).
 303. Matthias Preusser, Michael Lim, David A. Hafler, David A. Reardon, and J. H. S. Prospects of immune checkpoint modulators in the treatment of glioblastoma. *Nat Rev Neurol.* **11**, 504–514 (2015).
 304. Saha D, Martuza RL, R. S. Macrophage polarization contributes to Glioblastoma eradication by combination immunovirotherapy and immune checkpoint blockade. *Cancer Cell* **32**, 253–267 (2017).
 305. Bommareddy, P. K., Peters, C., Saha, D., Rabkin, S. D. & Kaufman, H. L. Oncolytic Herpes Simplex Viruses as a Paradigm for the Treatment of Cancer. *Annu. Rev. Cancer Biol.* **2**, 155–173 (2018).
 306. Ribas, A. *et al.* Oncolytic Virotherapy Promotes Intratumoral T Cell Infiltration and Improves Anti-PD-1 Immunotherapy. *Cell* **170**, 1109-1119.e10 (2017).
 307. Saha, D., Martuza, R. L. & Rabkin, S. D. Oncolytic herpes simplex virus immunovirotherapy in combination with immune checkpoint blockade to treat glioblastoma. *Immunotherapy* **10**, 779–786 (2018).
 308. Cerullo, V. & Ylo, E. Design and application of oncolytic viruses for cancer immunotherapy – sma – ki and Vincenzo Cerullo. *Curr. Opin. Biotechnol.* (2019).
 309. Bartlett, D. L. *et al.* Oncolytic viruses as therapeutic cancer vaccines. *Mol. Cancer* **12**, 1–16 (2013).
 310. Takasu, A. *et al.* Immunogenic cell death by oncolytic herpes simplex virus type 1

- in squamous cell carcinoma cells. *Cancer Gene Ther.* **23**, 107–113 (2016).
311. Guo, Z. S., Liu, Z. & Bartlett, D. L. Oncolytic immunotherapy: Dying the right way is a key to eliciting potent antitumor immunity. *Front. Oncol.* **4 APR**, 1–11 (2014).
 312. Stefani Spranger, Daisy Dai, Brendan Horton, and T. G. Tumor-residing Batf3 dendritic cells are required for effector T cell trafficking and adoptive T cell therapy. *Cancer Cell.* **31**, 711–723 (2017).
 313. Schmidt, S. V., Nino-Castro, A. C. & Schultze, J. L. Regulatory dendritic cells: There is more than just immune activation. *Front. Immunol.* **3**, 1–17 (2012).
 314. Cai, X., Chiu, Y. H. & Chen, Z. J. The cGAS-cGAMP-STING pathway of cytosolic DNA sensing and signaling. *Mol. Cell* **54**, 289–296 (2014).
 315. Mihret, A., Mamo, G., Tafesse, M., Hailu, A. & Parida, S. Dendritic cells activate and mature after infection with mycobacterium tuberculosis. *BMC Res. Notes* **4**, 1–7 (2011).
 316. Takeuchi, O. & Akira, S. Pattern Recognition Receptors and Inflammation. *Cell* **140**, 805–820 (2010).
 317. Müller, M., Carter, S., Hofer, M. J. & Campbell, I. L. Review: The chemokine receptor CXCR3 and its ligands CXCL9, CXCL10 and CXCL11 in neuroimmunity - A tale of conflict and conundrum. *Neuropathol. Appl. Neurobiol.* **36**, 368–387 (2010).
 318. Bommareddy, P. K., Shettigar, M. & Kaufman, H. L. Integrating oncolytic viruses in combination cancer immunotherapy. *Nat. Rev. Immunol.* **18**, 498–513 (2018).
 319. Goldsmith, K., Chen, W., Johnson, D. C. & Hendricks, R. L. Infected cell protein (ICP)47 enhances herpes simplex virus neurovirulence by blocking the CD8+ T cell response. *J. Exp. Med.* **187**, 341–348 (1998).
 320. Brode, S. & MacAry, P. A. Cross-presentation: Dendritic cells and macrophages bite off more than they can chew! *Immunology* **112**, 345–351 (2004).
 321. Gulley, J. L. *et al.* Role of antigen spread and distinctive characteristics of immunotherapy in cancer treatment. *J. Natl. Cancer Inst.* **109**, 1–9 (2017).
 322. Gujar, S. A. & Lee, P. W. K. Oncolytic virus-mediated reversal of impaired tumor antigen presentation. *Front. Oncol.* **4 APR**, 1–7 (2014).
 323. Koch, M. S., Lawler, S. E. & Antonio Chiocca, E. Hsv-1 oncolytic viruses from bench to bedside: An overview of current clinical trials. *Cancers (Basel)*. **12**, 1–16 (2020).

324. Streby, K. A. *et al.* First-in-Human Intravenous Seprehvir in Young Cancer Patients: A Phase 1 Clinical Trial. *Mol. Ther.* **27**, 1930–1938 (2019).
325. MacKie, R. M., Stewart, B. & Brown, S. M. Intralesional injection of herpes simplex virus 1716 in metastatic melanoma. *Lancet* **357**, 525–526 (2001).
326. Rampling, R. *et al.* Toxicity evaluation of replication-competent herpes simplex virus (ICP 34.5 null mutant 1716) in patients with recurrent malignant glioma. *Gene Ther.* **7**, 859–866 (2000).
327. Papanastassiou, V. *et al.* The potential for efficacy of the modified (ICP 34.5-) herpes simplex virus HSV1716 following intratumoural injection into malignant glioma: A proof of principle study. *Gene Ther.* **9**, 398–406 (2002).
328. Harrow, S. *et al.* HSV1716 injection into the brain adjacent to tumour following surgical resection of high-grade glioma: Safety data and long-term survival. *Gene Ther.* **11**, 1648–1658 (2004).
329. Markert, J. M. *et al.* A phase 1 trial of oncolytic HSV-1, g207, given in combination with radiation for recurrent GBM demonstrates safety and radiographic responses. *Mol. Ther.* **22**, 1048–1055 (2014).
330. Foreman, P. M., Friedman, G. K., Cassady, K. A. & Markert, J. M. Oncolytic Virotherapy for the Treatment of Malignant Glioma. *Neurotherapeutics* **14**, 333–344 (2017).
331. Markert, J. M. *et al.* Conditionally replicating herpes simplex virus mutant G207 for the treatment of malignant glioma: Results of a phase I trial. *Gene Ther.* **7**, 867–874 (2000).
332. Markert, J. M. *et al.* Phase Ib trial of mutant herpes simplex virus G207 inoculated pre-and post-tumor resection for recurrent GBM. *Mol. Ther.* **17**, 199–207 (2009).
333. Taguchi, S., Fukuhara, H. & Todo, T. Oncolytic virus therapy in Japan: Progress in clinical trials and future perspectives. *Jpn. J. Clin. Oncol.* **49**, 201–209 (2019).
334. Hua, L. & Wakimoto, H. Oncolytic herpes simplex virus therapy for malignant glioma: current approaches to successful clinical application. *Expert Opin. Biol. Ther.* **19**, 845–854 (2019).
335. Patel, D. M. *et al.* Design of a Phase i Clinical Trial to Evaluate M032, a Genetically Engineered HSV-1 Expressing IL-12, in Patients with Recurrent/Progressive Glioblastoma Multiforme, Anaplastic Astrocytoma, or Gliosarcoma. *Hum. Gene Ther. Clin. Dev.* **27**, 69–78 (2016).
336. Eissa, I. R. *et al.* Genomic signature of the natural oncolytic herpes simplex virus

- HF10 and its therapeutic role in preclinical and clinical trials. *Front. Oncol.* **7**, 1–12 (2017).
337. Nakao, A. *et al.* A phase I dose-escalation clinical trial of intraoperative direct intratumoral injection of HF10 oncolytic virus in non-resectable patients with advanced pancreatic cancer. *Cancer Gene Ther.* **18**, 167–175 (2011).
338. Kelly, K. J., Wong, J. & Fong, Y. Herpes simplex virus NV1020 as a novel and promising therapy for hepatic malignancy. *Expert Opin. Investig. Drugs* **17**, 1105–1113 (2008).
339. Ebright, M. I. *et al.* Replication-competent herpes virus NV1020 as direct treatment of pleural cancer in a rat model. *J. Thorac. Cardiovasc. Surg.* **124**, 123–129 (2002).
340. Bennett, J. J. *et al.* Comparison of safety, delivery, and efficacy of two oncolytic herpes viruses (G207 and NV1020) for peritoneal cancer. *Cancer Gene Ther.* **9**, 935–945 (2002).
341. Liu, B. L. *et al.* ICP34.5 deleted herpes simplex virus with enhanced oncolytic, immune stimulating, and anti-tumour properties. *Gene Ther.* **10**, 292–303 (2003).
342. Puzanov, I. *et al.* Talimogene laherparepvec in combination with ipilimumab in previously untreated, unresectable stage IIIB-IV melanoma. *J. Clin. Oncol.* **34**, 2619–2626 (2016).
343. Waters, A. M. *et al.* Rationale and Design of a Phase 1 Clinical Trial to Evaluate HSV G207 Alone or with a Single Radiation Dose in Children with Progressive or Recurrent Malignant Supratentorial Brain Tumors. *Hum. Gene Ther. Clin. Dev.* **28**, 7–16 (2017).
344. Bernstock, J. D. *et al.* Design and Rationale for First-in-Human Phase 1 Immunovirotherapy Clinical Trial of Oncolytic HSV G207 to Treat Malignant Pediatric Cerebellar Brain Tumors. *Hum. Gene Ther.* **31**, 1132–1139 (2020).
345. Tischer, B. K., Von Einem, J., Kaufer, B. & Osterrieder, N. Two-step Red-mediated recombination for versatile high-efficiency markerless DNA manipulation in *Escherichia coli*. *Biotechniques* **40**, 191–197 (2006).
346. Todo, T., Martuza, R. L., Rabkin, S. D. & Johnson, P. A. Oncolytic herpes simplex virus vector with enhanced MHC class I presentation and tumor cell killing. *Proc. Natl. Acad. Sci. U. S. A.* **98**, 6396–401 (2001).
347. Shah, K., Tung, C. H., Yang, K., Weissleder, R. & Breakefield, X. O. Inducible Release of TRAIL Fusion Proteins from a Proapoptotic Form for Tumor Therapy.

- Cancer Res.* **64**, 3236–3242 (2004).
348. Uchida, H. *et al.* A Double Mutation in Glycoprotein gB Compensates for Ineffective gD-Dependent Initiation of Herpes Simplex Virus Type 1 Infection. *J. Virol.* **84**, 12200–12209 (2010).
349. WF, G. *et al.* Engineering HSV-1 Vectors for Gene Therapy. *Methods Mol. Biol.* **2060**, (2020).
350. Marconi, P. & Manservigi, R. Herpes simplex virus growth, preparation, and assay. *Methods Mol. Biol.* **1144**, 19–29 (2014).
351. Kroonen, J. *et al.* Human glioblastoma-initiating cells invade specifically the subventricular zones and olfactory bulbs of mice after striatal injection. *Int. J. Cancer* **129**, 574–585 (2011).
352. Wakimoto, H. *et al.* Human glioblastoma-derived cancer stem cells: Establishment of invasive glioma models and treatment with oncolytic herpes simplex virus vectors. *Cancer Res.* **69**, 3472–3481 (2009).
353. US20170362314A1 - Anti-CXCL12 Antibody Molecules and Their Uses - Google Patents.
354. Uchida, H. *et al.* Effective treatment of an orthotopic xenograft model of human glioblastoma using an EGFR-retargeted oncolytic herpes simplex virus. *Mol. Ther.* **21**, 561–9 (2013).
355. Cocchi, F., Menotti, L., Mirandola, P., Lopez, M. & Campadelli-Fiume, G. The Ectodomain of a Novel Member of the Immunoglobulin Subfamily Related to the Poliovirus Receptor Has the Attributes of a Bona Fide Receptor for Herpes Simplex Virus Types 1 and 2 in Human Cells. *J. Virol.* **72**, 9992–10002 (1998).
356. Uchida, H. *et al.* Generation of Herpesvirus Entry Mediator (HVEM)-Restricted Herpes Simplex Virus Type 1 Mutant Viruses: Resistance of HVEM-Expressing Cells and Identification of Mutations That Rescue Nectin-1 Recognition. *J. Virol.* **83**, 2951–2961 (2009).
357. Frampton, A. R. *et al.* Equine Herpesvirus 1 Enters Cells by Two Different Pathways, and Infection Requires the Activation of the Cellular Kinase ROCK1. *J. Virol.* **81**, 10879–10889 (2007).
358. Lathia, J. D., Mack, S. C., Mulkearns-Hubert, E. E., Valentim, C. L. L. & Rich, J. N. Cancer stem cells in glioblastoma. *Genes and Development* vol. 29 1203–1217 (2015).
359. Tang, X. *et al.* Targeting Glioblastoma Stem Cells: A Review on Biomarkers,

- Signal Pathways and Targeted Therapy. *Frontiers in Oncology* vol. 11 (2021).
360. Connolly, S. A., Jardetzky, T. S. & Longnecker, R. The structural basis of herpesvirus entry. *Nature Reviews Microbiology* vol. 19 110–121 (2021).
 361. Zhou, G. & Roizman, B. Construction and properties of a herpes simplex virus 1 designed to enter cells solely via the IL-13 α 2 receptor. *Proc. Natl. Acad. Sci. U. S. A.* **103**, 5508–5513 (2006).
 362. Kamiyama, H., Zhou, G. & Roizman, B. Herpes simplex virus 1 recombinant virions exhibiting the amino terminal fragment of urokinase-type plasminogen activator can enter cells via the cognate receptor. *Gene Ther.* **13**, 621–629 (2006).
 363. Menotti, L. *et al.* Inhibition of human tumor growth in mice by an oncolytic herpes simplex virus designed to target solely HER-2-positive cells. *Proc. Natl. Acad. Sci. U. S. A.* **106**, 9039–44 (2009).
 364. Glorioso, J. C. Identification of mutations in herpes simplex virus envelope glycoproteins that enable or enhance vector retargeting to novel non-HSV receptors. vol. 2 (2013).
 365. Wajant, H. Molecular mode of action of TRAIL receptor agonists—Common principles and their translational exploitation. *Cancers (Basel)*. **11**, (2019).
 366. Ashkenazi, A. & Dixit, V. M. Apoptosis control by death and decoy receptors. *Curr. Opin. Cell Biol.* **11**, 255–260 (1999).
 367. Wu, X., He, Y., Falo, L. D., Hui, K. M. & Huang, L. Regression of human mammary adenocarcinoma by systemic administration of a recombinant gene encoding the hFlex-TRAIL fusion protein. *Mol. Ther.* **3**, 368–374 (2001).
 368. Lynch DH, Andreason A, Maraskovsky E, Whitmore J, Miller RE, S. J. Flt3 ligand induces tumor regression and anti-tumor immune responses in vivo. *Nat Med* **3**, 625–31 (1997).
 369. Wu, X. & Hui, K. M. Induction of potent TRAIL-mediated tumoricidal activity by hFlex/furin/TRAIL recombinant DNA construct]. *Mol. Ther.* **9**, 674–681 (2004).
 370. Jahan, N., Lee, J. M., Shah, K. & Wakimoto, H. Therapeutic targeting of chemoresistant and recurrent glioblastoma stem cells with a proapoptotic variant of oncolytic herpes simplex virus. *Int. J. cancer* **141**, 1671–1681 (2017).
 371. Tamura, K. *et al.* Multimechanistic tumor targeted oncolytic virus overcomes resistance in brain tumors. *Mol. Ther.* **21**, 68–77 (2013).
 372. Tang, X. *et al.* Targeting Glioblastoma Stem Cells: A Review on Biomarkers, Signal Pathways and Targeted Therapy. *Front. Oncol.* **11**, 1–17 (2021).

373. Kambara, H., Okano, H., Chiocca, E. A. & Saeki, Y. An oncolytic HSV-1 mutant expressing ICP34.5 under control of a nestin promoter increases survival of animals even when symptomatic from a brain tumor. *Cancer Res.* **65**, 2832–2839 (2005).
374. Tang, C. & Guo, W. Implantation of a mini-osmotic pump plus stereotactical injection of retrovirus to study newborn neuron development in adult mouse hippocampus. *STAR Protoc.* **2**, 100374 (2021).
375. Jahan, N. *et al.* Therapeutic targeting of chemoresistant and recurrent glioblastoma stem cells with a proapoptotic variant of oncolytic herpes simplex virus. **141**, 1671–1681 (2018).
376. Meisen WH, Wohleb ES, Jaime-Ramirez AC, Bolyard C, Yoo JY, Russell L, Hardcastle J, Dubin S, Muili K, Yu J, Caligiuri M, Godbout J, K. B. The impact of macrophage and microglia secreted TNF α on oncolytic HSV-1 therapy in the glioblastoma tumor microenvironment. *Clin Cancer Res.* **21**, 3274–85 (2015).
377. Hutzen, B. *et al.* TGF- β Inhibition Improves Oncolytic Herpes Viroimmunotherapy in Murine Models of Rhabdomyosarcoma. *Mol. Ther. - Oncolytics* **7**, 17–26 (2017).
378. Lee TJ, Nair M, Banasavadi-Siddegowda Y, Liu J, Nallanagulagari T, Jaime-Ramirez AC, Guo JY, Quadri H, Zhang J, Bockhorst KH, Aghi MK, Carbonell WS, Kaur B, Y. J. Enhancing Therapeutic Efficacy of Oncolytic Herpes Simplex Virus-1 with Integrin β 1 Blocking Antibody OS2966. *Mol Cancer Ther* **18**, 1127–1136 (2019).
379. Tasaki, T. *et al.* MET expressed in glioma stem cells is a potent therapeutic target for glioblastoma multiforme. *Anticancer Res.* **36**, 3571–3577 (2016).
380. Alves, A. L. V. *et al.* Role of glioblastoma stem cells in cancer therapeutic resistance: a perspective on antineoplastic agents from natural sources and chemical derivatives. *Stem Cell Res. Ther.* **12**, 1–22 (2021).
381. Jacob F, Salinas RD, Zhang DY, Nguyen PTT, Schnoll JG, Wong SZH, Thokala R, Sheikh S, Saxena D, Prokop S, Liu DA, Qian X, Petrov D, Lucas T, Chen HI, Dorsey JF, Christian KM, Binder ZA, Nasrallah M, Brem S, O'Rourke DM, Ming GL, S. H. A Patient-Derived Glioblastoma Organoid Model and Biobank Recapitulates Inter- and Intra-tumoral Heterogeneity. *Cell* **180**, 188–204 (2020).
382. Lee, J. *et al.* Tumor stem cells derived from glioblastomas cultured in bFGF and EGF more closely mirror the phenotype and genotype of primary tumors than do

- serum-cultured cell lines. *Cancer Cell* **9**, 391–403 (2006).
383. Nguyen, M. L., Kraft, R. M. & Blaho, J. A. Susceptibility of cancer cells to herpes simplex virus-dependent apoptosis. *J. Gen. Virol.* **88**, 1866–1875 (2007).
384. Nguyen, M. L. *et al.* p53 and hTERT Determine Sensitivity to Viral Apoptosis. *J. Virol.* **81**, 12985–12995 (2007).
385. Maruzuru, Y. *et al.* p53 Is a Host Cell Regulator during Herpes Simplex Encephalitis. *J. Virol.* **90**, 6738–6745 (2016).
386. LeBlanc, H. N. & Ashkenazi, A. Apo2L/TRAIL and its death and decoy receptors. *Cell Death Differ.* **10**, 66–75 (2003).
387. Bellail, A. C. *et al.* DR5-mediated DISC controls caspase-8 cleavage and initiation of apoptosis in human glioblastomas. *J. Cell. Mol. Med.* **14**, 1303–1317 (2010).
388. Ding L, Yuan C, Wei F, Wang G, Zhang J, Bellail AC, Zhang Z, Olson JJ, H. C. Cisplatin Restores TRAIL apoptotic pathway in Glioblastoma- Derived Stem Cells through Up-regulation of DR5 and Down- regulation of c-FLIP. *Cancer Invest.* **29**, 551–520 (2011).
389. Yan, W., Xiao, D. & Yao, K. Combined bioluminescence and fluorescence imaging visualizing orthotopic lung adenocarcinoma xenograft in vivo. *Acta Biochim. Biophys. Sin. (Shanghai)*. **43**, 595–600 (2011).
390. Alvarez-Breckenridge, C. A. *et al.* NK cells impede glioblastoma virotherapy through NKp30 and NKp46 natural cytotoxicity receptors. *Nat. Med.* **18**, 1827–34 (2012).
391. Fulci, G. *et al.* Depletion of Peripheral Macrophages and Brain Microglia Increases Brain Tumor Titers of Oncolytic Viruses. **67**, 9398–9406 (2007).
392. Meisen, W. H., Wohleb, E. S., Jaime-Ramirez, A. C., Bolyard, C., Yoo, J. Y., Russell, L., Hardcastle, J., Dubin, S., Muili, K., Yu, J., Caligiuri, M., Godbout, J., & Kaur, B. The impact of macrophage and microglia secreted TNF α on oncolytic HSV-1 therapy in the glioblastoma tumor microenvironment. *Clin Cancer Res.* **2015** **21**, 3274–3285 (2015).
393. Buonfiglioli, A. & Hambarzumyan, D. Macrophages and microglia: the cerberus of glioblastoma. *Acta Neuropathol. Commun.* **9**, 1–21 (2021).
394. Kaminska, B. Characteristics of Phenotype and Pro-Tumorigenic Roles of Glioma Infiltrating Microglia/Macrophages. *J. Neurol. Neurophysiol.* **s5**, 1–8 (2011).
395. Blitz, S. E. *et al.* Tumor-Associated Macrophages/Microglia in Glioblastoma Oncolytic Virotherapy: A Double-Edged Sword. *Int. J. Mol. Sci.* **23**, (2022).

396. Uche, I. K., Kousoulas, K. G. & Rider, P. J. F. The Effect of Herpes Simplex Virus-Type-1 (HSV-1) Oncolytic Immunotherapy on the Tumor Microenvironment. **1**, 1–16 (2021).
397. Isci, D. *et al.* Patient-oriented perspective on chemokine receptor expression and function in glioma. *Cancers (Basel)*. **14**, 1–17 (2022).
398. Lee, E. Q. *et al.* Phase I and biomarker study of plerixafor and bevacizumab in recurrent high-grade glioma. *Clin. Cancer Res.* **24**, 4643–4649 (2018).
399. Hattermann, K. *et al.* Chemokine expression profile of freshly isolated human glioblastoma-associated macrophages/microglia. *Oncol. Rep.* **32**, 270–276 (2014).
400. Feng, Y., Broder, C. C., Kennedy, P. E. & Berger, E. A. HIV-1 entry cofactor: Functional cDNA cloning of a seven-transmembrane, G protein-coupled receptor. *Science (80-.)*. **272**, 872–877 (1996).
401. Alimohammadi, M., Rahimi, A., Faramarzi, F., Alizadeh-Navaei, R. & Rafiei, A. Overexpression of chemokine receptor CXCR4 predicts lymph node metastatic risk in patients with melanoma: A systematic review and meta-analysis. *Cytokine* **148**, 155691 (2021).
402. Salmaggi, A. *et al.* CXCL12 expression is predictive of a shorter time to tumor progression in low-grade glioma: A single-institution study in 50 patients. *J. Neurooncol.* **74**, 287–293 (2005).
403. Katsumoto, K. & Kume, S. The role of CXCL12-CXCR4 signaling pathway in pancreatic development. *Theranostics* vol. 3 11–17 (2013).
404. Gagliardi, F. *et al.* The role of CXCR4 in highly malignant human gliomas biology: Current knowledge and future directions. *Glia* **62**, 1015–1023 (2014).
405. Santagata, S. *et al.* CXCR4 and CXCR7 Signaling Pathways: A Focus on the Cross-Talk Between Cancer Cells and Tumor Microenvironment. *Frontiers in Oncology* vol. 11:591386. (2021).
406. Gagner, J. P. *et al.* Multifaceted C-X-C Chemokine Receptor 4 (CXCR4) Inhibition Interferes with Anti-Vascular Endothelial Growth Factor Therapy-Induced Glioma Dissemination. *Am. J. Pathol.* **187**, 2080–2094 (2017).
407. Gatti, M. *et al.* Inhibition of CXCL12/CXCR4 autocrine/paracrine loop reduces viability of human glioblastoma stem-like cells affecting self-renewal activity. *Toxicology* **314**, 209–220 (2013).
408. Mercurio, L. *et al.* Targeting CXCR4 by a selective peptide antagonist modulates tumor microenvironment and microglia reactivity in a human glioblastoma model.

- J. Exp. Clin. Cancer Res.* **35**, 1–15 (2016).
409. Gil, M., Seshadri, M., Komorowski, M. P., Abrams, S. I. & Kozbor, D. Targeting CXCL12/CXCR4 signaling with oncolytic virotherapy disrupts tumor vasculature and inhibits breast cancer metastases. *Proc. Natl. Acad. Sci. U. S. A.* **110**, E1291–300 (2013).
 410. Scala, S. Molecular pathways: Targeting the CXCR4-CXCL12 Axis-Untapped potential in the tumor microenvironment. *Clin. Cancer Res.* **21**, 4278–4285 (2015).
 411. Kioi, M. *et al.* Inhibition of vasculogenesis, but not angiogenesis, prevents the recurrence of glioblastoma after irradiation in mice. *J. Clin. Invest.* **120**, 694–705 (2010).
 412. Lee, C. C. *et al.* Disrupting the CXCL12/CXCR4 axis disturbs the characteristics of glioblastoma stem-like cells of rat RG2 glioblastoma. *Cancer Cell Int.* **13**, (2013).
 413. Ostrom, Q. T. *et al.* CBTRUS statistical report: Primary brain and other central nervous system tumors diagnosed in the United States in 2011-2015. *Neuro-Oncology* vol. 20 iv1–iv86 (2018).
 414. Stupp, R. *et al.* Effect of Tumor-Treating Fields Plus Maintenance Temozolomide vs Maintenance Temozolomide Alone on Survival in Patients With Glioblastoma: A Randomized Clinical Trial. *JAMA* **318**, 2306–2316 (2017).
 415. Lara-Velazquez, M. *et al.* Advances in brain tumor surgery for glioblastoma in adults. *Brain Sciences* vol. 7 166 (2017).
 416. Singh, S. K. *et al.* Identification of human brain tumour initiating cells. *Nature* **432**, 396–401 (2004).
 417. Galli, R. *et al.* Isolation and characterization of tumorigenic, stem-like neural precursors from human glioblastoma. *Cancer Res.* **64**, 7011–7021 (2004).
 418. Chen, R. *et al.* A Hierarchy of Self-Renewing Tumor-Initiating Cell Types in Glioblastoma. *Cancer Cell* **17**, 362–375 (2010).
 419. Singh, S. K. *et al.* Identification of a cancer stem cell in human brain tumors. *Cancer Res.* **63**, 5821–5828 (2003).
 420. Goffart, N. *et al.* Adult mouse subventricular zones stimulate glioblastoma stem cells specific invasion through CXCL12/CXCR4 signaling. *Neuro. Oncol.* **17**, 81–94 (2015).
 421. Goffart, N. *et al.* CXCL12 mediates glioblastoma resistance to radiotherapy in the subventricular zone. *Neuro. Oncol.* **19**, 66–77 (2017).

422. Dedobbeleer, M. *et al.* MKP1 phosphatase is recruited by CXCL12 in glioblastoma cells and plays a role in DNA strand breaks repair. *Carcinogenesis* **41**, 417–429 (2020).
423. Cheray, M. *et al.* Cancer Stem-Like Cells in Glioblastoma. in *Glioblastoma* 59–71 (Codon Publications, 2017). doi:10.15586/codon.glioblastoma.2017.ch4.
424. Lombard, A. *et al.* The Subventricular Zone, a Hideout for Adult and Pediatric High-Grade Glioma Stem Cells. *Frontiers in Oncology* vol. 10 (2021).
425. Fountzilias, C., Patel, S. & Mahalingam, D. Review: Oncolytic virotherapy, updates and future directions. *Oncotarget* **8**, 102617–102639 (2017).
426. Miyauchi, J. T. & Tsirka, S. E. Advances in immunotherapeutic research for glioma therapy. *J. Neurol.* **265**, 741–756 (2018).
427. Friedman, G. K. *et al.* Engineered herpes simplex viruses efficiently infect and kill CD133+ human glioma xenograft cells that express CD111. *J. Neurooncol* **95**, 199–209 (2009).
428. Rueger, M. A. *et al.* Variability in infectivity of primary cell cultures of human brain tumors with HSV-1 amplicon vectors. *Gene Ther.* **12**, 588–596 (2005).
429. Grandi, P. *et al.* Targeting HSV-1 virions for specific binding to epidermal growth factor receptor-vIII-bearing tumor cells. *Cancer Gene Ther.* **17**, 655–63 (2010).
430. Shibata, T. *et al.* Development of an oncolytic HSV vector fully retargeted specifically to cellular EpCAM for virus entry and cell-to-cell spread. *Gene Ther.* **23**, 479–488 (2016).
431. Alessandrini, F. *et al.* Eradication of glioblastoma by immuno-virotherapy with a retargeted oncolytic HSV in a preclinical model. *Oncogene* (2019) doi:10.1038/s41388-019-0737-2.
432. Kim, M.-H., Billiar, T. R. & Seol, D.-W. The secretable form of trimeric TRAIL, a potent inducer of apoptosis. *Biochem. Biophys. Res. Commun.* **321**, 930–935 (2004).
433. Kock, N., Kasmieh, R., Weissledery, R. & Shah, K. Tumor therapy mediated by lentiviral expression of shBcl-2 and S-TRAIL1. *Neoplasia* **9**, 435–442 (2007).
434. US20170362314A1 - Anti-CXCL12 Antibody Molecules and Their Uses - Google Patents.
435. Uchida, H. *et al.* Effective treatment of an orthotopic xenograft model of human glioblastoma using an EGFR-retargeted oncolytic herpes simplex virus. *Mol. Ther.* **21**, 561–9 (2013).

436. Bian, X. *et al.* Preferential expression of chemokine receptor CXCR4 by highly malignant human gliomas and its association with poor patient survival. *Neurosurgery* **61**, 570–579 (2007).
437. Van Den Bossche, W. B. L. *et al.* Oncolytic virotherapy in glioblastoma patients induces a tumor macrophage phenotypic shift leading to an altered glioblastoma microenvironment. *Neuro. Oncol.* **20**, 1494–1504 (2018).
438. Isci, D. *et al.* Patient-oriented perspective on chemokine receptor expression and function in glioma. *Cancers* vol. 14 (2022).
439. Tischer, B. K. *et al.* A self-excisable infectious bacterial artificial chromosome clone of varicella-zoster virus allows analysis of the essential tegument protein encoded by ORF9. *J. Virol.* **81**, 13200–8 (2007).

VIII. APPENDICES

Part of this data has been submitted in a manuscript entitled:

“Nanobody-based retargeting of an oncolytic herpesvirus for eliminating CXCR4⁺ GBM cells: a proof-of-principle”

1 Nanobody-based retargeting of an oncolytic herpesvirus for eliminating CXCR4⁺ GBM
2 cells: a proof-of-principle

3

4 Judit Sanchez Gil¹, Maxime Dubois¹, Virginie Neirinckx², Arnaud Lombard^{2,3}, Natacha
5 Coppieters², Paolo D'Arrigo¹, Damla Isci², Therese Aldenhoff², Benoit Brouwers²,
6 Cédric Lassence¹, Bernard Rogister^{2,4}, Marielle Lebrun¹ and Catherine Sadzot-
7 Delvaux¹.

8

9 ¹ Laboratory of Virology, GIGA Infection, Inflammation and Immunity (GIGA I3),
10 University of Liège, Liège, Belgium

11 ² Laboratory of Nervous system Disorders and Therapy, GIGA-Neurosciences,
12 University of Liège, Belgium

13 ³ Department of Neurosurgery, CHU of Liège, Liège, Belgium

14 ⁴ Department of Neurology, CHU of Liège, Liège, Belgium

15

16 Correspondence should be addressed to C.S-D, (csadzot@uliege.be), Laboratory of
17 Virology and Immunology, GIGA I3, University of Liège, 11 Avenue de l'Hôpital, 4000
18 LIEGE, Belgium. Tel: +32 366 24 45

19

20 **SHORT TITLE:**

21 CXCR4⁺ GBM cell killing with a Nb-retargeted oHSV: a proof-of-principle

22

23

24

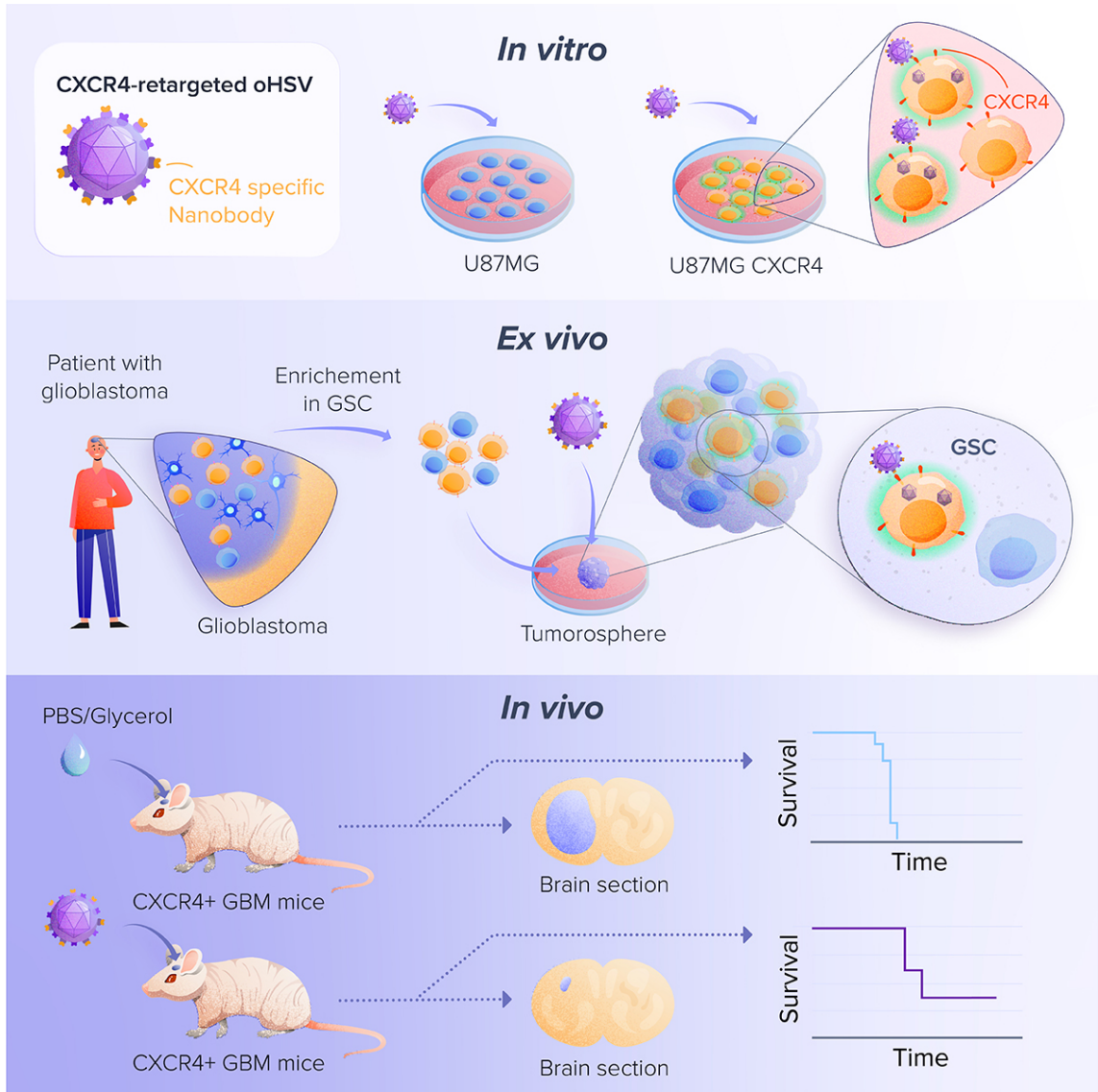
25

26

27 **ABSTRACT**

28 Glioblastoma (GBM) is the most aggressive primary brain tumor in adults, which
29 remains difficult to cure. The very high recurrence rate has been partly attributed to the
30 presence of glioblastoma stem-like cells (GSCs) within the tumors, which have been
31 associated with elevated CXCR4 expression. CXCR4 is frequently overexpressed in
32 cancer tissues, including GBM, and usually correlates with a poor prognosis. We have
33 created a CXCR4-retargeted oncolytic herpesvirus (oHSV) by insertion of an anti-
34 human CXCR4 nanobody in glycoprotein D of an attenuated HSV-1 (Δ ICP34.5; Δ ICP6;
35 Δ ICP47), thereby describing a proof-of-principle for the use of nanobodies to target
36 oHSVs towards specific cellular entities. Moreover, this virus has been armed with a
37 transgene expressing a soluble form of TRAIL to trigger apoptosis. *In vitro*, this oHSV
38 infects U87MG CXCR4⁺ and patient-derived GBM stem-like cells (GSCs) on a CXCR4-
39 dependent manner and, when armed, triggers apoptosis. In a U87MG CXCR4⁺
40 orthotopic xenograft mouse model, this oHSV slows down tumor growth and
41 significantly improves mice survival. Customizing oHSVs with diverse nanobodies for
42 targeting multiple proteins appears as an interesting approach for tackling the
43 heterogeneity of GBM, especially GSCs. Altogether, our study must be considered as
44 a proof-of-principle and a first step towards personalized GBM virotherapies to
45 complement current treatments.

GRAPHICAL ABSTRACT



50 INTRODUCTION

51 The chemokine receptor 4 (CXCR4), first described for its role in leukocyte
52 trafficking or HIV infection ⁴⁰⁰, is a largely studied G-protein-coupled receptor
53 which activates various signaling pathways upon binding of its unique ligand
54 CXCL12, also known as stromal cell-derived factor 1. CXCR4 overexpression
55 has been reported in a wide range of tumors, including glioblastoma multiforme
56 (GBM) ^{401–404} and increasing evidence has suggested its central role in cancer
57 progression ⁴⁰⁵. Multiple preclinical or clinical studies have demonstrated that the
58 disruption of CXCR4 downstream signaling via several approaches (CXCR4
59 shRNA, CXCL12 mimetic peptide, anti-CXCR4 antibodies or nanobodies)
60 diminishes tumor growth and synergizes with chemo- or radiotherapy ^{406–412}.

61 GBM is the most frequent primary malignant brain tumor, classified by the World
62 Health Organization as a grade 4 glioma ⁴¹³. Despite standard therapies that
63 associate surgical resection with radio- or chemotherapy, the prognosis remains
64 dramatically poor, with a median survival of 16 months from diagnosis ⁴¹⁴. GBM
65 is indeed highly diffuse and tumor cells infiltrate healthy brain tissue, making the
66 total resection of the tumor rather difficult or even impossible. GBM recurrences
67 frequently develop within the margin of the resection cavity or at distant sites ⁴¹⁵.

68 In addition, GBM is characterized by a high degree of heterogeneity at the
69 genetic, epigenetic and transcriptomic levels. Many studies reported the
70 presence of self-renewing, multipotent subsets of GBM cells endowed with high
71 tumorigenic capacity, considered as GBM stem-like cells (GSCs)^{416–418}. GSCs
72 have been associated with the expression of specific markers, form
73 tumorspheres *in vitro* upon limiting dilution, and are able to initiate a tumor when

74 serially-transplanted in mice brain. GSCs have long been considered as key
75 actors in GBM relapse, and the mechanisms underlying GSC development,
76 maintenance and phenotypic plasticity yet remain intensively investigated ⁴¹⁹. We
77 previously have shown that upon GBM xenotransplantation, CXCR4⁺ GSCs
78 escape the tumor core and reach the subventricular zones (SVZ) based on a
79 CXCR4/CXCL12-dependent signaling ^{420,421}. GSCs hosted in the SVZ display an
80 improved DNA double-strand break repair, and hence are resistant to
81 radiotherapy ^{421,422}. These observations have been confirmed in GBM patients,
82 in which GSCs can be found both in the tumor core where the hypoxic
83 environment constitutes an appropriate niche and in the SVZ, reinforcing the role
84 of these CXCR4⁺ cells in GBM recurrence ^{423,424}. Importantly, a high expression
85 of CXCR4 positively correlates with tumor size, tumor progression, recurrence
86 and ultimately with patient survival ^{402,404}. Targeting GSCs and particularly
87 CXCR4⁺ cells therefore provides an opportunity to reach tumor cells that escape
88 current treatments ³⁵⁹.

89 Over the last decade, virotherapy has emerged as a promising approach for
90 cancer treatment ⁴²⁵. Oncolytic viruses (OV) are currently at different stages of
91 preclinical investigations and numerous clinical trials are ongoing. In the context
92 of GBM, virotherapy and oncolytic herpesviruses (oHSV) in particular are
93 currently being evaluated as an alternative or complementary therapeutic
94 approach for patients resistant to traditional therapies ⁴²⁶. oHSV efficacy depends
95 on the capacity of the virus to specifically infect cancer cells. However, it is
96 estimated that about 20% of the GBM cells are not efficiently infected by oHSV
97 partly due to a low expression of CD111 (Nectin 1, one of the HSV-1 natural
98 receptors) ^{427,428}. A virus able to target cancer cells and, GSCs in particular,

99 through its interaction with a membrane protein specifically expressed by these
100 cells, would thus allow to reach cells that have escaped standard therapeutic
101 approaches. One strategy for oHSV retargeting is to replace the domain
102 responsible for glycoprotein D (gD) interaction with its natural cellular receptors
103 by a ligand able to interact with a protein of interest expressed by the target cells.
104 Single chain Immunoglobulin (scFv) or ligands such as cytokines or peptides
105 have been successfully introduced in gD to target cancer cells ^{361–363,429–431}.
106 Nanobodies are single heavy variable domain of camelid antibodies and
107 constitute an interesting alternative to retarget an oHSV. They can be selected
108 from a synthetic or immune library with a huge diversity and can recognize cryptic
109 antigens with a high affinity. These nanobodies therefore open the possibility to
110 develop a panel of tailored oHSVs for personalized therapy.

111 In this context, we have developed, as a proof-of-principle, an oncolytic HSV-1
112 specifically targeting CXCR4, thanks to the insertion in gD of an anti-human
113 CXCR4 nanobody previously described for its capacity to efficiently recognize
114 CXCR4 (WO 2016/156570 A1). This virus (oHSV/Nb-gD) has been further armed
115 with a transgene expressing the soluble form of TRAIL (oHSV/Nb-gD:sTRAIL),
116 whose efficacy to trigger the extrinsic apoptosis pathway has been previously
117 documented ^{370,371,432,433}. We demonstrated that the engineered virus infects
118 U87MG CXCR4⁺ and patient-derived GSCs in a CXCR4-dependent manner, can
119 replicate efficiently in these cells and lead to sTRAIL expression, thereby
120 triggering apoptosis. When used in an *in vivo* orthotopic xenograft GBM model,
121 oHSV/Nb-gD armed or not with sTRAIL had a clear impact on tumor progression
122 and significantly improved mice survival. These results confirm nanobodies as
123 appropriate tools for retargeting oHSVs towards specific cell subsets and

124 constitute a proof-of-principle of an oHSV design strategy that could be
125 considered for personalized treatment.

126 RESULTS

127 1. Construction of a nanobody-retargeted and armed oncolytic herpesvirus

128 To specifically target GBM cells expressing CXCR4, we engineered an oHSV that
129 was first detargeted from its natural receptors HVEM and nectin-1, prior to being
130 retargeted to CXCR4 (Figure 1). These modifications were introduced within
131 fQuick-1 (kind gift from Prof. EA. Chiocca), a BAC containing the HSV-1 genome
132 (Strain F; Δ ICP34.5/ Δ ICP6/EGFP⁺). This backbone was further deleted from
133 US12 coding for ICP47, this deletion being important to partly overcome the
134 attenuation resulting from γ 34.5 deletion ³⁵². The detargeting/retargeting was
135 achieved by replacing the residues 2-24 of gD, within the HVEM-binding domain
136 by an anti-human CXCR4 nanobody ⁴³⁴. In addition, the residue 38 of gD was
137 mutated (Y38C) to impair gD interaction with nectin-1, another natural receptor
138 ⁴³⁵. Moreover, two mutations (D285N and A549T) shown to improve the fusion
139 capacity of glycoprotein B (gB) were introduced in UL27 ³⁴⁸. Finally, the virus was
140 armed with a transgene expressing a soluble form of TRAIL (sTRAIL) ³⁴⁷ under
141 the control of a nestin promoter. After transfection of these constructs into VERO
142 cells previously transduced with the human CXCR4, oHSVs were produced in
143 the supernatant, and further purified and titrated. In this publication, they are
144 referred to as oHSV/gD (non-retargeted; non-armed), oHSV/Nb-gD (CXCR4-
145 retargeted; non-armed), oHSV/Nb-gD:sTRAIL (CXCR4-retargeted and sTRAIL-
146 armed).

147 2. Efficacy of the CXCR4-retargeting.

148 To verify the detargeting efficacy, J1.1-2, hamster cells resistant to HSV due to
149 the lack of HVEM or nectin-1 expression at the cell surface ³⁵⁵, as well as their
150 modified version J/A and J/C expressing respectively human HVEM ³⁵⁶ or nectin-

151 1³⁵⁷ (kind gift from Pr. G. Campadelli Fiume), were infected with oHSV/gD or
152 oHSV/Nb-gD (MOI: 0.01; 0.1 and 1). Contrary to oHSV/gD which led to numerous
153 infectious foci in J/A and J/C, no foci were detected upon oHSV/Nb-gD infection,
154 demonstrating that oHSV/Nb-gD was properly detargeted (Figure 2A). To
155 evaluate the capacity of oHSV/Nb-gD to specifically infect CXCR4⁺ cells,
156 glioblastoma U87MG cells which express CXCR4 at a very low level (Figures
157 S1A and B) were transduced with a lentivirus expressing the human CXCR4. The
158 ectopic expression of CXCR4 was confirmed by flow cytometry (Figures S1A and
159 B). U87MG and U87MG CXCR4⁺ were infected with oHSV/gD or oHSV/Nb-gD
160 (MOI: 0.1) and the level of infection was evaluated by real-time GFP imaging and
161 quantification with Incucyte® S3 (Figure 2B, C and S2). As expected, oHSV/gD
162 efficiently replicated in both cell lines independently of CXCR4 expression. On
163 the contrary, oHSV/Nb-gD infection remained very low in U87MG cells with only
164 very few cells infected as reflected by a very weak eGFP expression and no
165 statistical difference with the non-infected cells. This clearly contrasted with
166 numerous foci and overtime increasing eGFP signal in oHSV/Nb-gD-infected
167 U87MG CXCR4⁺ cells, confirming that oHSV/Nb-gD infection relies on the
168 expression of CXCR4. Importantly, the efficacy of infection of oHSV/gD and
169 oHSV/Nb-gD in U87MG CXCR4⁺ cells was similar. This was further confirmed by
170 This was further confirmed by a growing curve of both oHSVs in U87MG-CXCR4⁺
171 cells. No statistical difference was observed (Figure S3).

172 **3. CXCR4-dependent infection of patient-derived GSCs by oHSV/Nb-gD.**

173 The efficacy of oHSV/gD and oHSV/Nb-gD was further evaluated on four different
174 GBM stem-like cells cultures (T08, T013, T018 and T033) directly established
175 from residual GBM tissue obtained from surgical resection (Department of

176 Neurosurgery, CHU Liège, Belgium) and maintained as tumorspheres. In
177 opposition to U87MG cells, GSCs express high levels of *SOX2*, *POU3F2* and
178 *SALL2* (Figure S4). The percentage of CXCR4⁺ cells among the four different
179 GSC cultures analyzed by flow cytometry was highly variable (Figures 3A and B).
180 While less than 3% of T08 cells were positive for CXCR4, around 75% of T033
181 expressed this chemokine receptor, T013 and T018 being intermediate. As
182 expected, the endogenous expression of CXCR4 was much lower than the
183 ectopic expression by U87MG CXCR4⁺ cells (Figures 3 A and B). To evaluate
184 the efficacy of the retargeted oHSV and to compare it with the non-retargeted
185 virus efficacy, primary GSCs were cultured as tumorspheres and infected with
186 oHSV/gD or oHSV/Nb-gD (10⁶ PFU/ml). Forty-eight hours post-infection, cells
187 were dissociated and the percentage of eGFP positive cells was analyzed by flow
188 cytometry.

189 Interestingly, the percentage of oHSV/Nb-gD infected cells clearly reflected the
190 level of CXCR4 expression (Figure 3C). T033 which express CXCR4 at a high
191 level were the most infected (34.8% of eGFP cells on an average, 48hpi) while
192 less than 2% of T08 cells which do not express CXCR4 or express it at a very
193 low level, were positive for eGFP. As expected, in most primary cells, oHSV/gD
194 led to a higher percentage of infected cells compared to oHSV/Nb-gD (Figures
195 3C and S5). However, an Incucyte ® S5 overtime analysis of T033 cells infected
196 with a high titer (10⁷/ml) indicated that both the dynamics and the eGFP
197 fluorescence were similar for both viruses (Figure S6). Finally, it is worth
198 mentioning that although all primary cell lines were infected by the non-retargeted
199 virus, its efficacy greatly varied with T013 being significantly less infected than
200 the other cell lines.

201 In parallel, tumorspheres were infected with oHSV/Nb-gD (10^6 PFU/ml) for
202 immunostainings. Forty-eight hours post-infection, epifluorescence observation
203 of oHSV infected tumorspheres revealed that eGFP intensity was very low in
204 T08 and much brighter in T033, confirming that the level of infection reflects the
205 level of CXCR4 expression (Figure 3D, left panels). Tumorspheres were then
206 fixed for immunostainings. Confocal microscopy of oHSV/Nb-gD infected
207 tumorspheres sections confirmed that only very few T08 cells were eGFP⁺ while
208 more infected cells were observed in T013, T018 and T033 tumorspheres
209 (Figure 3D). Although no clear co-localization between GFP and CXCR4 was
210 observed at the cellular level, infected cells were usually observed in the CXCR4⁺
211 area.

212 **4. *In vitro* evaluation of the efficacy of the sTRAIL-arming.**

213 oHSV/Nb-gD, shown to be efficiently retargeted and to specifically infect CXCR4⁺
214 cells was further armed with the gene coding for the soluble form of TRAIL under
215 the control of the nestin promoter to trigger apoptosis upon viral infection. First,
216 we showed that the armed- and non-armed oHSVs replicated with the same
217 efficacy in VERO CXCR4⁺ (data not shown) or U87MG CXCR4⁺ cells (Figure 4A),
218 demonstrating that the arming does not impair oHSV replication. The efficacy of
219 sTRAIL to trigger the apoptosis pathway was analyzed either by western blotting
220 or using an annexin V/DAPI assay, while the viability was evaluated by measuring
221 the cellular metabolism with resazurin. The expression of sTRAIL upon infection
222 of U87MG CXCR4⁺ by oHSV/Nb-gD:sTRAIL led to the cleavage of PARP and
223 caspase 3, while no cleavage was observed upon oHSV/Nb-gD infection (Figure
224 4B). The annexin V/DAPI assay further confirmed apoptosis in oHSV infected
225 U87MG CXCR4⁺ cells. sTRAIL-induced apoptosis was detectable at 48hpi and

226 reached significance only at 72hpi with an average of 36% of apoptotic cells upon
227 oHSV/Nb-gD:sTRAIL infection compared to 12% upon oHSV/Nb-gD infection
228 (Figure 4C). At 72hpi, the percentage of apoptotic cells upon oHSV/Nb-
229 gD:sTRAIL infection increased according to the MOI which was not the case with
230 the non-armed oHSV (Figure S7). Interestingly, the viability of the cells infected
231 by oHSV/Nb-gD or oHDSV/Nb-gD:sTRAIL measured 24, 48h or 72hpi was not
232 statistically different (Figure 4C).

233 When used to infect patient-derived GSCs tumorspheres, oHSV/Nb-gD:sTRAIL
234 led to the expression of gD and sTRAIL as measured by RT-qPCR and this
235 expression was significantly higher in T033 tumorspheres (Figures 4D and E).

236 **5. Evaluation of the therapeutic efficacy of oHSV/Nb-gD and oHSV/Nb- 237 gD:sTRAIL using an orthotopic xenograft GBM model**

238 The capacity of oHSV/Nb-gD and oHSV/Nb-gD:sTRAIL to impact tumor growth
239 was evaluated *in vivo*, using an orthotopic xenograft GBM mouse model. A first
240 experiment was set up with engraftment of 5×10^4 U87MG CXCR4⁺Luc⁺ into the
241 right striatum under stereotactic control (Figure S8A). PBS or oHSVs (1.4×10^6
242 PFU in 2 μ l) were injected within the tumor on day 16. Weekly bioluminescence
243 analysis revealed a very rapid tumor growth in all groups even beyond oHSV
244 intratumoral injection, although tumor growth appeared slightly reduced in
245 oHSV/Nb-gD or oHSV/Nb-gD:sTRAIL treated mice compared to PBS-treated
246 mice (Figure S8B). From day 19 on, PBS-treated mice health status rapidly
247 evolved towards a critical point that justified sacrifice on day 24 (Figure S8C).
248 Although not conclusive, these results paved the way for the design of another
249 experiment, in which PBS or oHSVs (1.4×10^6 PFU in 2 μ l) were injected on day
250 7 after engraftment of 5×10^4 U87MG CXCR4⁺Luc⁺ GBM cells (Figure 5A). Body

251 weight was monitored every second day, and bioluminescence recording was
252 performed weekly to evaluate the tumor size evolution. On day 22, mice were
253 anesthetized and either perfused with saline solution only (for RNA extraction
254 from brain tissue) or followed by paraformaldehyde to allow immunostaining
255 analyses. Contrary to oHSV-treated mice which, temporary lost weight just after
256 virus infection but showed a continuous weight gain until the end of the
257 experiment, PBS-treated mice displayed a clear weight loss from day 20 on
258 (Figure 5B). On day 6, the tumor size appeared homogeneous among groups,
259 with no significant difference in the bioluminescent signal (Figures 5C and S9A).
260 On day 13, bioluminescence in PBS-treated mice dramatically increased up to
261 day 20, whereas the signal in oHSV-treated mice remained similar to day 6 or
262 even decreased, becoming even undetectable in some mice (Figure 5C). All mice
263 were sacrificed on day 22 and brains were harvested for either anti-human
264 vimentin immunohistochemical staining and tumor size measurement (5
265 mice/group) or RNA extraction and RT-qPCR analyses (4 mice/group). The size
266 of the tumor, calculated by measuring the area positive for human vimentin on
267 serial sections and 3D volume reconstruction, clearly showed a significant impact
268 of both oHSV/Nb-gD and oHSV/Nb-gD:sTRAIL treatment, even if no significant
269 difference was observed between the two viruses (Figures 5D and E). For RNA
270 extraction, right hemispheres, in which the cells were engrafted, were divided into
271 three parts (frontal, middle, and occipital). Human CXCR4 expression, reflecting
272 the presence of implanted human CXCR4⁺ GBM cells, was evaluated in each
273 block individually and expressed as the relative expression to the level of
274 expression in the middle part of PBS-treated mice brains (Figure 5F). Overall,
275 human CXCR4 expression was significantly decreased in oHSV-treated mice

276 compared to PBS-treated mice. In both oHSV-treated groups, differences in the
277 level of expression of hCXCR4 were observed between the 3 blocks, with a
278 higher abundance of human transcripts detected in samples corresponding to the
279 frontal and middle samples, covering the initial site of engraftment. These results
280 were confirmed by RT-qPCR for human nestin and TBP (data not shown) and
281 corroborated bioluminescence analyses that showed some signal, although quite
282 low in oHSV-treated mice (Figure S9A). At the end of the experiment (15 days
283 after virus injection), we were unable to detect gD or sTRAIL neither by
284 immunohistochemistry nor by RT-qPCR (data not shown).

285 To verify whether, *in vivo*, oHSVs effectively replicate in tumor cells and sTRAIL
286 is expressed, this experiment was repeated with the same settings, but mice were
287 sacrificed two days after virus injection. Right hemispheres were divided into
288 three parts (frontal, middle, and occipital) and total RNA was extracted from the
289 brain tissue. gD and sTRAIL relative expression measured by RT-qPCR
290 demonstrated the presence of gD transcripts in brains injected with oHSV/Nb-gD
291 and oHSV/Nb-gD:sTRAIL while sTRAIL transcripts were detected only in the
292 oHSV/Nb-gD:sTRAIL group (Figures S9B and C). Finally, a survival assay was
293 set up with similar experimental settings (Figure 6A). U87MG CXCR4⁺Luc⁺ cells
294 were injected under stereotactic control. All mice developed tumors (Figure
295 S10B) and viral suspension, or PBS was injected within the tumor on day 7. Body
296 weight was monitored every second day and mice were sacrificed when showing
297 a significant weight loss or severe clinical signs. From day 19, all PBS-treated
298 mice continuously lost weight, while oHSV-treated mice started to lose weight
299 only on day 29, with the mice still alive 35 days after infection continuing to gain
300 weight (Figure S10A). Again, tumor size appeared similar in all groups just before

301 (day 5) virus injection (Figures 6B and S10B). However, one week after the
302 intratumoral injection (day 13), bioluminescence signal in oHSV-treated mice was
303 significantly reduced compared to the PBS group. In these oHSV-injected tumors,
304 bioluminescence was very low and even undetectable in 4/6 and 3/5 mice in
305 oHSV/Nb-gD and oHSV/Nb-gD:sTRAIL, respectively (Figures 6B and S10B).
306 However, no significant difference was observed between oHSV/Nb-gD and
307 oHSV/Nb-gD:sTRAIL-treated mice (Figure 6B). Importantly, while all PBS-treated
308 mice died between day 21 and 27, the oHSV-treated mice death was significantly
309 delayed with the first deaths observed on day 31 (Figure 6C). At day 61, 1/6
310 oHSV/Nb-gD and 2/5 oHSV/Nb-gD:sTRAIL treated mice were still alive. Taken
311 together, all these results show that oHSV/Nb-gD and oHSV/Nb-gD:sTRAIL are
312 suited for intratumoral injection in GBM orthotopic models and exert a potent
313 oncolytic activity *in vivo*.

314

315 **DISCUSSION**

316 Glioblastoma (GBM) remains the most aggressive form of adult brain cancer,
317 associated to a dismal prognosis. Therapeutic failure and high recurrence rate
318 endorse the need for novel, alternative, or add-on approaches to improve the
319 standard-of-care therapy. GBM exhibits a wide cellular diversity, with malignant
320 cells being highly heterogeneous in terms of molecular profile, phenotype,
321 tumorigenic potential and resistance to treatment. Such heterogeneity is largely
322 accountable for tumor recurrence.

323 A subset of GBM cells considered as stem-like cells (GSCs) display stemness
324 features, appear more resistant to radio- and chemotherapies and are endowed
325 with increased tumorigenicity³⁵⁸. Targeting GSCs thus appears as an opportunity
326 for new therapeutic approaches. A wide variety of therapeutic strategies aiming

327 to target GSCs have been evaluated in preclinical models and are being clinically
328 translated ³⁵⁹. However, considering the biological complexity and phenotypic
329 plasticity of those cells, the main hurdle is to target GSCs without impairing
330 normal tissue. In the perspective of eradicating peculiar GBM cell entities such
331 as GSCs, highly specific and targeted strategies should be considered.

332 Oncolytic virotherapy has been proposed as a promising avenue for GBM
333 therapy, and herpesviruses offer numerous opportunities for tailored design and
334 targeting strategies. oHSVs are the first viruses approved by the FDA for
335 virotherapy. Their mechanism of cell entry is well documented ³⁶⁰, and can be
336 modified to restrict oHSV entry into cells that specifically express a receptor of
337 interest at their surface. oHSV retargeting requires the replacement of the viral
338 glycoprotein domain important for their interaction with either the heparan sulfate
339 or the natural receptors, by a ligand specific for a protein of interest. Single-chain
340 antibodies (scFv), cytokines or specific ligands have been described for their
341 efficacy to retarget oHSV ^{361–363,429,430}. In our study, we describe oHSV
342 retargeting using a nanobody. Nanobodies correspond to the single heavy
343 variable domain of camelid antibodies. They can be quite easily obtained by
344 screening either immune or artificial libraries characterized by a huge sequence
345 diversity, and thereby constitute an interesting tool for oHSV customization and
346 specific targeting.

347 In this study, GBM has been chosen as a model to evaluate the nanobody-based
348 oHSV retargeting. As a proof-of-principle, we considered to genetically engineer
349 an oHSV whose gD is modified by the insertion of a nanobody able to recognize
350 hCXCR4, a chemokine receptor expressed on several GBM cell subtypes,
351 including glioblastoma stem-like cells (GSCs). CXCR4 has been associated with

352 cancer cell proliferation, tumorigenesis, migration and its expression correlates
353 with a poor prognosis⁴³⁶. Additionally, we have previously shown CXCR4⁺ cells
354 as able to move away from the tumor core and specifically invade the
355 subventricular zones ⁴²⁰, and targeting of CXCR4 therefore appears as an
356 encouraging approach. The CXCR4-retargeted oHSV described in this paper
357 (namely oHSV/Nb-gD) has been engineered from an attenuated backbone
358 (Δ ICP34.5, Δ ICP6 and Δ ICP47) whose safety in GBM treatment has been largely
359 documented ³⁵². Other oHSVs retargeted to the Epidermal Growth Factor
360 Receptor (EGFR), the human receptor tyrosine-protein kinase erbB-2 (hHER2),
361 the interleukin 13 receptor, the epithelial cell adhesion molecule (EpCAM), or the
362 urokinase Plasminogen Activator Receptor, all described to be overexpressed in
363 cancer tissues have been constructed and characterized^{361–363,429–431}. Contrarily
364 to the oHSVs described in this paper, all these retargeted viruses were
365 engineered in a non-attenuated HSV background, inducing a higher level of viral
366 replication. However, their safety only relies on the tight control of their entry into
367 cancer cells and consequently requires an absence or a very low expression of
368 the target of interest on healthy cells. Similarly, the CXCR4-retargeted oHSVs
369 entry depends on the capacity of the virus to specifically interact with a receptor
370 but its attenuated character limits its replication in non-cancer cells, improving its
371 safety. We show that the CXCR4-retargeted virus (oHSV/Nb-gD) can specifically
372 infect on a CXCR4-dependent manner, not only U87MG CXCR4⁺ but also
373 patient-derived GSCs, despite a much lower CXCR4 endogenous expression. *In*
374 *vitro*, when armed with a secreted form of TRAIL (oHSV/Nb-gD:sTRAIL), this
375 virus is able to trigger apoptosis. The replication of these oncolytic viruses in cells
376 transduced with CXCR4 is not impaired nor by the retargeting or the arming.

377 Importantly, when inoculated at high titers (10^7 PFU/ml) on primary GBM cells
378 expressing a high level of endogenous CXCR4 (T033), both the retargeted and
379 the non-retargeted virus show the same kinetics and the same efficacy of
380 infection.

381 When used *in vivo* in an orthotopic xenograft model of GBM in which U87MG
382 CXCR4⁺ cells were engrafted, both sTRAIL-armed and non-armed oHSVs were
383 able to limit the tumor progression and to significantly improve mice survival.
384 Even though sTRAIL triggers apoptosis *in vitro*, its impact in the xenograft model
385 seems to be limited. Contrarily to the sTRAIL-armed oHSV previously described
386 in the literature and whose expression is driven by the HSV immediate early
387 promoter IE4/5^{370,371}, sTRAIL expression in oHSV/Nb-gD:sTRAIL is driven by
388 the nestin promoter. Although nestin is overexpressed in most GBM tumors³⁵⁹,
389 it might not be activated at the same level in all GBM cells and hence be too
390 restrictive for an optimal expression of sTRAIL. Moreover, *in vitro*, the percentage
391 of apoptotic cells as measured by flow cytometry, does not reflect the strong
392 impact of oHSV infection on U87MG viability (Figure 4C). The oncolysis mediated
393 by the virus itself may hide the sTRAIL-induced apoptosis when high MOI are
394 used^{370,371}. The efficacy of the arming should be further evaluated *in vivo* in the
395 xenograft model after engraftment of patient-derived GSCs. If needed, a stronger
396 promoter should be considered to drive sTRAIL expression. U87MG CXCR4⁺
397 cells engrafted in the xenograft model have a very rapid growth kinetics. Such a
398 rapid growth can hamper the total elimination of the tumor after a single virus
399 injection and could explain the regrowth observed in some mice. In this context,
400 it would be worth evaluating the impact of repeated injections or of continuous
401 delivery of the virus thanks to a mini-osmotic pump system³⁷⁴. In addition, the

402 role of the tumor microenvironment and especially of the innate immune response
403 should not be underestimated. oHSV virotherapy has been shown to rapidly
404 activate natural killer (NK) cells which diminish the virotherapy efficacy³⁹⁰ while
405 adenovirus virotherapy has been shown to induce a phenotypic shift of
406 macrophages from pro-tumoral M2-like toward the anti-tumoral and pro-
407 inflammatory M1-like phenotype⁴³⁷. A deeper characterization of the tumor
408 microenvironment upon virotherapy will provide important information that might
409 help to improve the treatment.

410 An important issue that must be carefully studied when targeting tumor cells is
411 the fact that healthy cells might express the target of interest and thus be infected
412 by the oncolytic virus. Although in our study oHSVs are attenuated, this issue
413 must be taken into consideration. CXCR4 is mainly expressed in the bone marrow
414 or lymphoid tissues and poorly expressed in the brain
415 (<https://www.proteinatlas.org/ENSG00000121966-CXCR4>). Taking into
416 consideration that the oHSV is injected within the tumor, CXCR4 expression on
417 non-tumoral cells in the vicinity of the tumor must however be considered. We
418 recently analyzed chemokine receptors (among which CXCR4) expression in
419 GBM based on publicly available patient-derived transcriptomic data, which
420 shows that CXCR4 is expressed in malignant cells, in endothelial cells within the
421 tumor as well as on TAMs (tumor associated macrophages) and TIL (Tumor
422 infiltrating lymphocytes)⁴³⁸. The capacity of the CXCR4-retargeted virus to infect
423 and potentially destroy these cells, especially endothelial cells and M2-like
424 macrophages, would certainly be of interest, still the benefit/risk balance has to
425 be assessed very carefully. Unfortunately, the anti-hCXCR4 nanobody used in
426 this study does not recognize the murine CXCR4 which limits the questions that

427 could be addressed in the human GBM xenograft model. We are currently
428 screening a nanobody library to identify nanobodies that recognize both the
429 human and murine CXCR4 receptor. Such nanobodies would allow not only to
430 address important issues such as the undesired targeting of healthy cells but also
431 to evaluate the importance of the immune response and particularly of the
432 adaptive immune response, this latest requiring a syngeneic GBM murine model.

433

434 Altogether, the results described in this proof-of-principle study show that the
435 retargeting of oHSVs by the insertion of a nanobody appears highly encouraging
436 and constitutes an interesting approach for the targeting of GBM cell subsets,
437 e.g. GSCs, expressing specific proteins of interest. Our data support the idea that
438 a set of nanobodies specific for diverse GSCs markers may be used to customize
439 oHSVs that could be exploited as an add-on to complement the current standard-
440 of-care therapeutic approaches.

441 **MATERIAL and METHODS**

442 **Cell lines**

443 VERO cells (ATCC, #CCL-81) and human glioblastoma U87MG (ATCC # HTB-
444 14) cells were maintained in Dulbecco's modified Eagle minimal essential
445 medium (DMEM, Lonza, Verviers, Belgium) supplemented with 10% fetal bovine
446 serum (FBS). J1.1-2 cells are HSV-1 resistant baby hamster kidney cells lacking
447 both HVEM and nectin-1, two natural HSV-1 receptors. J/A and J/C cells are J1.1
448 transduced with HVEM and nectin-1 respectively (kind gift of Pr. G. Campadelli-
449 Fiume (University of Bologna, Italy). They were cultured with DMEM
450 supplemented with 5% of FBS. J/A and J/C cells were treated with 400 µg/ml of
451 G418 (Invivogen, Belgium). VERO CXCR4⁺ and U87MG CXCR4⁺ obtained by
452 transduction of a lentivirus (Viral Vector platform, University of Liege) were
453 treated with 20 ng/ml and 10 ng/ml of blasticidin, respectively. Primary GBM
454 primary cultures (T08, T013, T018 and T033) were established from freshly
455 resected human glioblastoma tissue obtained from GBM patients. They were
456 cultured as tumorspheres in stem cell medium (DMEM/F-12 with GlutaMAX
457 (Gibco) supplemented with B27 (1/50) without vitamin A (Gibco), 1% Penicillin-
458 streptomycin (Lonza, Verviers, Belgium), 1 µg/ml of heparin (n 7692.1, Carl Roth,
459 Belgium), human EGF (20 ng/ml) and βFGF (20 ng/ml) (Peprotech).

460 **Construction of recombinant oHSVs.**

461 Recombinant viruses were engineered in fHsvQuik-1 Bacterial artificial
462 chromosome (BAC) containing an attenuated strain F HSV-1 ($\Delta\gamma$ 34.5, Δ UL39,
463 GFP⁺; kind gift from A. Chiocca from the University of Pittsburg, USA).
464 Recombinants were obtained by the two-step Red recombination technique "en

465 passant”⁴³⁹. ICP47 deletion was done as described by Todo T *et al.*, 2001³⁴⁶.
466 The detargeting of gD from its natural receptors was performed according to
467 Uchida *et al.*, 2012⁴³⁵. For retargeting, we inserted a patented sequence coding
468 for a nanobody against human CXCR4 receptor (CXCR4-NB; WO 2016/156570
469 AI) in the gD coding sequence. The “arming” sequence containing a soluble form
470 of TRAIL (sTRAIL)³⁴⁷ under the nestin promoter was inserted before the ICP6
471 promoter as shown in Figure 1. A double mutation (D285N and A549T) was
472 inserted within gB to compensate the loss of infectivity generally observed upon
473 gD retargeting³⁴⁸. CXCR4⁺ Vero cells were plated in 6 well-plate at 40%
474 confluence and transfected with 3 µg of BAC using JETPEI (Polyplus, Illkirch –
475 FRANCE). Viral replication was detected 48h after transfection by the
476 visualization of fluorescent foci. Virus stocks were produced and concentrated as
477 previously described³⁴⁹. Briefly, cells were infected at low MOI (0.005) and
478 cultured for four to five days at 33°C. The day before the experiment, cells were
479 treated with 0,45 M of NaCl and 100 µg/ml of dextran sulfate. Supernatant was
480 collected and centrifuged at 2200 g for 10 min at 4°C, then filtered with 0.8 µm
481 filter to discard cell debris. Then, viral particles were ultracentrifuged at 47.850g
482 at 4°C using Beckman SW27 rotor. Centrifuged virus was resuspended in PBS
483 with 10% glycerol, aliquoted and stored at -80°C. Plaque assay in VERO
484 CXCR4⁺ was used to titrate the virus and determine the amount of PFU/ml³⁵⁰.

485 **Viral growth assay**

486 U87MG CXCR4⁺ or VERO CXCR4⁺ cells were seeded in a 12-well plate and
487 infected with oHSV/gD, oHSV/Nb-gD or oHSV/Nb-gD:sTRAIL at a MOI of 1 for
488 24, 48 or 72h. Supernatant was then harvested and titer (PFU/ml) was

489 determined by plaque assay as previously described³⁵⁰. The number of foci was
490 calculated based on Incucyte® S3 imaging.

491 **Entry assay**

492 J1.1-2, J/A and J/C cells were seeded in a 24 well-plate the day before infection.
493 Cells were infected with a MOI of 1, 0.1 and 0.01. After 48h, cells were fixed with
494 4% paraformaldehyde and washed with PBS. Images were collected with the
495 Incucyte® S3 (Sartorius).

496 **RT-qPCR**

497 Total RNA was isolated using the RNA isolation Nucleospin® kit (Macherey-
498 Nagel) according to the manufacturer's protocol. 500 ng of RNA were reverse
499 transcribed using RevertAid H Minus First Strand cDNA Synthesis Kit (Thermo
500 Scientific) with Random primers (for gD or sTRAIL transcripts detection) or oligo-
501 dT primers (for stemness markers transcripts detection). TBP or 18S were used
502 as controls. RT-qPCR reaction samples were prepared as follows: 4 µl of the
503 diluted cDNA (2.5 ng in total for gD and sTRAIL or 10ng in total for stemness
504 markers) were mixed with 5 µl of SYBR green (TAKYON, Eurogentec, Liege,
505 Belgium) and 100 µM of primers in a final volume of 10 µl. Primers used for
506 transcripts detection are described in Table 1. Quantitative realtime PCR was
507 done using the Roche LightCycler 480 (3 min. at 95°C of activation; 45 cycles:
508 Denaturation 95°C, 3 sec, Hybridization and Elongation 60°C 25 sec).

509 **Flow cytometry**

510 For CXCR4 detection by Flow Cytometry, cells were plated in 6 well-plate two
511 days before analysis or cultured as tumorspheres. Tumorspheres and cells
512 cultured as monolayers were washed with PBS and dissociated by incubating the

513 cells for 10 min at 37°C with Accutase (Biowest, Nuaille, France). Dissociated
514 cells were centrifugated at 350g for 5 min at 4°C and washed with Flow Buffer
515 (PBS with BSA 1%, EDTA 1mM and Azide 0,1 %). 5 µl of APC-conjugated anti-
516 CXCR4 antibody (Biolegend, Amsterdam, The Nertherlands) were added to
517 1x10⁵ cells in 100µl of Flow buffer (dilution 1/20) and kept at 4°C for 1 hour in the
518 dark. Cells were washed by adding 1 ml of Flow Buffer and centrifugated at 400g
519 for 4 min at 4°C. After a second wash, cells were resuspended in 200 µl of Flow
520 buffer and directly analyzed with the FACS CANTO II (BD biosciences). Data
521 were analyzed with FlowJo software.

522 **Annexin/DAPI assay**

523 For Annexin V/DAPI apoptosis assay, 92.000 cells were seeded in a 12-well plate
524 and infected with a MOI of 1, 5 or 10 for 72 hours. Cells were collected and
525 resuspended in 140 µl of 1X Binding Buffer (Ref. 556454, BD Pharmingen,). Ten
526 µl of DAPI (Invitrogen, 1:100) and 5µl of Annexin V-PE (Ref. AB 2869071, BD
527 Biosciences,) were added and cells were incubated for 15 min at RT in the dark.
528 Finally, 200 µl of 1X Binding buffer was added and samples were directly
529 analyzed with the FACS FORTESSA™ (BD biosciences). Data were analyzed
530 with FlowJo software.

531 **Viability assay**

532 U87MG and U87MG CXCR4⁺ cells were plated in a 12-well plate and infected
533 with the different viruses at a MOI of 5. Measure of viability was done at 24, 48
534 and 72h post infection by evaluating the metabolic activity using a Resazurin
535 assay. At each time point, media was removed and replaced by 500 µL of
536 resazurin (20% (v/v) in DMEM-10% FBS) and cells were further incubated for 4h

537 at 37°C. Metabolized media was transferred into a 96-well flat-bottom black plate
538 and read (λ ex= 535 nm; λ em=595 nm) using the multi-mode microplate reader
539 (FilterMax F5). Results are expressed as a percentage of the control.

540 **Real time measure of the GFP fluorescence.**

541 U87MG and U87MG CXCR4+ cells were plated in 24 flat bottom plate (46.000
542 cells/well). After 24 hours of monolayer culture, cells were infected with oHSV/gD or
543 oHSV/Nb-gD (MOI: 0.1) and incubated in the Incucyte®S3 for real-time analyses of
544 the mean eGFP fluorescence intensity with the whole well module (Magnification
545 4X).

546 Patient-derived GSCs cells were seeded in 96 round bottom plate (10.0000
547 cells/well) in stem cell medium. Twenty-four hours after seeding, tumorspheres
548 were infected with oHSV/gD or oHSV/Nb-gD (10^4 PFU/well) and incubated in the
549 Incucyte® S5 for a real-time analysis of the mean eGFP fluorescence intensity with
550 the organoid module (Magnification 4X).

551 **Immunofluorescence staining on tumorspheres**

552 Tumorspheres were infected with 10^6 PFU/ml. Forty-eight hours post-infection
553 (hpi), cells were washed and fixed with 4% paraformaldehyde for 20 minutes
554 (min) and incubated overnight with 20% PBS-sucrose before being embedded
555 with colored OCT (Neg-50™). Spheroids were cut into 5 μ m-thick cryosections
556 (Microm HM 560, ThermoScientific) and placed onto SuperFrost slides (Thermo
557 Scientific). Sections were permeabilized with 0.3% Triton X-100 PBS solution for
558 10 min and unspecific binding sites were blocked with 5% BSA for 30 min.
559 Tumorspheres sections were incubated overnight at 4°C with primary antibodies
560 diluted in 5% BSA (rabbit anti-CXCR4 (Ref. AB124824, Abcam, 1:200); mouse

561 anti-nestin (Ref. sc-23927, Santa Cruz, 1:250). After two washes, slides were
562 incubated for 1h at RT in the dark with secondary antibodies (goat anti-mouse
563 Alexa fluor 633 and goat anti-rabbit Alexa fluor 568, 1:500). Nuclei were stained
564 by incubation with Hoechst for 10 min at 1:50000. Finally, Mowiol (Sigma) was
565 added, and sections were covered by a coverslip. Staining was analyzed with
566 Nikon A1R confocal microscope. Figures were composed and examined with
567 ImageJ software.

568 **Western-Blot assay**

569 Cells were lysed with RIPA modified buffer (50mM of Tris-HCl, 150mM of NaCl,
570 1mM of EDTA, 1% NP40 and 0,25% of DOC). 80 µg of proteins were loaded on
571 a 6 (for PARP and gD detection) or 12% (for caspase 3 and a-tubulin detection)
572 SDS-acrylamide gel. After electrophoresis, proteins were transferred on a PVDF
573 membrane (GE Healthcare) according to standard protocols. Mouse anti-gD was
574 used to determine viral infection level (Ref. sc-21719, Santa Cruz, 1:1000), rabbit
575 anti-PARP (Ref. 9532, Cell Signaling, 1:1000) and mouse anti-caspase 3 (CC3)
576 (Ref. ALX-804-305, Enzo, Life Sciences, Brussels, Belgium, 1:1000,) were used
577 to detect the activation of the apoptotic pathway. Mouse anti-alpha-tubulin (Ref.
578 T6199, Sigma, 1:2000) was used as loading control. HRP-conjugated-anti-rabbit-
579 IgG (Ref. 7074, Cell Signaling) and HRP-conjugated anti-mouse-IgG (Ref. 7076,
580 Cell Signaling) were used as secondary antibodies. Signals were revealed using
581 ECL and imaged with LAS4000 CCD camera (GE Healthcare).

582 ***In vivo* experiments**

583 Adult 6 weeks female immunodeficient Crl:NU-Foxn1nu mice (Charles River
584 Laboratories, Brussels, Belgium) were used for xenograft experiments. The

585 athymic nude mice were housed in sterilized, filter-topped cages the Animal
586 Facility at the University of Liège and all experiments were performed as
587 previously approved by the Animal Ethical Committee of the University of Liège,
588 in accordance with the Declaration of Helsinki and following the guidelines of the
589 Belgium Ministry of Agriculture in agreement with European Commission
590 Laboratory Animal Care and Use Regulation. Intrastratial grafts were performed
591 following the previously described procedures ³⁵¹. Briefly, 50.000 U87MG
592 CXCR4⁺Luc⁺ cells resuspended in 2 µl of PBS were injected into the right striatum
593 of mice previously anesthetized with an intraperitoneal injection of a Rompun
594 (Sedativum 2%, Bayer, Brussels, Belgium) and Ketalar (Ketamin 50 mg/mL,
595 Pfizer, Brussels, Belgium) solution (V/V) prepared just before injection. Injection
596 was performed according to stereotactic coordinates (0.5 mm anterior and 2.5
597 mm lateral from the bregma and at a depth of 3 mm), allowing a precise and
598 reproducible injection site. Later, oncolytic viruses resuspended in 2 µl of PBS
599 were injected, under similar anesthesia, within the tumor using the same
600 stereotactic coordinates. Mice health status was evaluated daily, and mice were
601 weighed regularly.

602 **Bioluminescence activity**

603 Immunodeficient nude mice bearing intracranial U87MG CXCR4⁺Luc⁺ xenografts
604 were injected intraperitoneally with Beetle Luciferin Potassium salt (Ref. E1605,
605 Promega) (150 mg/kg). Under anesthesia using 2.5% isoflurane, mice were
606 imaged with camera-based bioluminescence imaging system (Xenogen IVIS 50®;
607 exposure time 1 min, 15 min after intraperitoneal injection). Regions of interest
608 were defined manually, and images were processed using Living Image and

609 IgorPro Software (Version 2.60.1). Raw data were expressed as total counts/sec
610 or total counts/min.

611 **Brain tissue processing and tumor volume measurement**

612 Mice were euthanized with i.p. injection of Euthazol Vet (140 mg/kg) and
613 intracardiac perfusion of ice-cold saline solution, followed by paraformaldehyde
614 4% in PBS (for histology). Brains were extracted, placed in sucrose 30% for tissue
615 cryopreservation, and sectioned into 14 μ m-thick serial sections using a cryostat.
616 Tumor volume analysis was performed by immunohistochemistry for human
617 vimentin detection (Mouse anti-human vimentin, MAB3400, Merck, 1:200) with
618 Polyview®Plus HRP-DAB kit (Enzo Life Sciences, Brussels, Belgium). Tumor
619 was delineated based on anti-vimentin positivity. 10 to 12 serial brain sections
620 were analyzed using the Mercator software (ExploraNova, La Rochelle, France).
621 3D reconstitution and extrapolation of tumor volume were performed using
622 Map3D software.

623 **Statistical analysis**

624 All statistical analyses were performed using GraphPad Prism 9. Data are
625 displayed as Mean \pm SEM. Depending on the experiments, paired *t*-Test, Krustall-
626 Wallis or two-way ANOVAs were performed as indicated in the figure legends.
627 Statistical significance of survival assay was analyzed by log-ranked (Mantel-
628 Cox) test.

629
630

631

632 **Acknowledgments**

633 This work was supported by grants from the National Fund for Scientific
634 Research (FNRS, Télévie), the Special Funds of the University of Liège, the
635 Leon Frédéricq Foundation, Liège, Belgium and the Neurological Foundation of
636 New Zealand.

637 The authors would like to thank all the members of the GIGA Viral Vector,
638 Imaging and Flow cytometry, Genomics platforms and animal facilities for
639 valuable technical support.

640

641

642 **Author contributions**

643 Conception of the project: C.S-D.; Funding acquisition B.R. and C.S-D.; Design
644 of the experiments: J.S-G., V.N., A.L., N.C., M.L, C.S-D; Experiments: J.S-G.,
645 D.I., M.D., P.D.; Technical assistance: C.L., T.A., B.B., Writing: C.S-D. and J.S-
646 G.; Reviewing: P.D., V.N., B.R., A.L., M.L., N.C.

647

648 **REFERENCES**

- 649 1. Louis, D. N. *et al.* The 2021 WHO classification of tumors of the central
650 nervous system: A summary. *Neuro. Oncol.* **23**, 1231–1251 (2021).
- 651 2. Patel, A. P. *et al.* Single-cell RNA-seq highlights intratumoral
652 heterogeneity in primary glioblastoma. *Science (80-.)*. **344**, 1396–1401
653 (2014).
- 654 3. Neftel C, Laffy J, Filbin MG, Hara T, Shore ME, Rahme GJ, Richman AR,
655 Silverbush D, Shaw ML, Hebert CM, Dewitt J, Gritsch S, Perez EM,
656 Gonzalez Castro LN, Lan X, Druck N, Rodman C, Dionne D, Kaplan A,
657 Bertalan MS, Small J, Pelton K, Becker S, Bonal D, Ngu, S. M. An
658 integrative model of cellular states, plasticity and genetics for
659 glioblastoma. *Cell*. **178**, 835–849 (2019).
- 660 4. Ostrom, Q. T. *et al.* CBTRUS statistical report: Primary brain and central
661 nervous system tumors diagnosed in the United States in 2006-2010.
662 *Neuro. Oncol.* **15**, (2013).
- 663 5. Hanif, F., Muzaffar, K., Perveen, K., Malhi, S. M. & Simjee, S. U.
664 Glioblastoma multiforme: A review of its epidemiology and pathogenesis
665 through clinical presentation and treatment. *Asian Pacific J. Cancer Prev.*
666 **18**, 3–9 (2017).
- 667 6. Thakkar, J. P. *et al.* Epidemiologic and molecular prognostic review of
668 glioblastoma. *Cancer Epidemiol. Biomarkers Prev.* **23**, 1985–1996 (2014).
- 669 7. TAMIMI, A. F. & JUWEID, M. Epidemiology and Outcome of
670 Glioblastoma. *Glioblastoma* 143–153 (2017)
671 doi:10.15586/codon.glioblastoma.2017.ch8.
- 672 8. Urbanska, K., Sokolowska, J., Szmidt, M. & Sysa, P. Glioblastoma

- 673 multiforme - An overview. *Wspolczesna Onkol.* **18**, 307–312 (2014).
- 674 9. Schultz, S. *et al.* Fine needle aspiration diagnosis of extracranial
675 glioblastoma multiforme: Case report and review of the literature.
676 *Cytojournal* **2**, 1–6 (2005).
- 677 10. Rickert, C. H. *et al.* Glioblastoma with adipocyte-like tumor cell
678 differentiation - Histological and molecular features of a rare differentiation
679 pattern. *Brain Pathol.* **19**, 431–438 (2009).
- 680 11. D’Alessio, A., Proietti, G., Sica, G. & Scicchitano, B. M. Pathological and
681 molecular features of glioblastoma and its peritumoral tissue. *Cancers*
682 *(Basel)*. **11**, (2019).
- 683 12. Rojiani, A. M. & Dorovini-Zis, K. Glomeruloid vascular structures in
684 glioblastoma multiforme: An immunohistochemical and ultrastructural
685 study. *J. Neurosurg.* **85**, 1078–1084 (1996).
- 686 13. Coomberl, B. L., Stewart, P. A., Hayakawa, K., Farrell, C. L. & Del
687 Maestros, R. F. Quantitative morphology of human glioblastoma
688 multiforme microvessels: structural basis of blood-brain barrier defect. *J.*
689 *Neurooncol.* **5**, 299–307 (1987).
- 690 14. La, M. Palisades and Pseudopalisades. *Ajnr. Am. J. Neuroradiol.* 2037–
691 2041 (2006).
- 692 15. Liu, S. *et al.* Relationship between necrotic patterns in glioblastoma and
693 patient survival: Fractal dimension and lacunarity analyses using
694 magnetic resonance imaging. *Sci. Rep.* **7**, 1–7 (2017).
- 695 16. Schiffer, D., Annovazzi, L., Mazzucco, M. & Mellai, M. The origin of
696 circumscribed necroses and perinecrotic niches in glioblastoma
697 multiforme: An additional hypothesis. *Integr. Cancer Sci. Ther.* **2**, 75–78

- 698 (2015).
- 699 17. Keith, B., Johnson, R. S. & Simon, M. C. HIF1 α and HIF2 α : sibling
700 rivalry in hypoxic tumour growth and progression. *Nat. Rev. Cancer* **12**,
701 9–22 (2012).
- 702 18. Lombardi, M. Y. & Assem, M. Glioblastoma Genomics: A Very
703 Complicated Story. *Glioblastoma* 3–25 (2017)
704 doi:10.15586/codon.glioblastoma.2017.ch1.
- 705 19. Loeb, L. A. Human cancers express mutator phenotypes: Origin,
706 consequences and targeting. *Nat. Rev. Cancer* **11**, 450–457 (2011).
- 707 20. Cohen, A. L., Holmen, S. L., & Colman, H. IDH1 and IDH2 Mutations in
708 Gliomas Adam. *Curr Neurol Neurosci Rep.* **13**, 345 (2013).
- 709 21. Kayabolen, A., Yilmaz, E. & Bagci-Onder, T. IDH mutations in glioma:
710 Double-edged sword in clinical applications? *Biomedicines* **9**, (2021).
- 711 22. Nicholas, M. K., Lukas, R. V., Jafri, N. F., Faoro, L. & Salgia, R.
712 Epidermal growth factor receptor-mediated signal transduction in the
713 development and therapy of gliomas. *Clin. Cancer Res.* **12**, 7261–7270
714 (2006).
- 715 23. Sugawa, N., Ekstrand, A. J., James, C. D. & Collins, V. P. Identical
716 splicing of aberrant epidermal growth factor receptor transcripts from
717 amplified rearranged genes in human glioblastomas. *Proc. Natl. Acad.*
718 *Sci. U. S. A.* **87**, 8602–8606 (1990).
- 719 24. Rajasekhar, V. K. *et al.* Oncogenic Ras and Akt signaling contribute to
720 glioblastoma formation by differential recruitment of existing mRNAs to
721 polysomes. *Mol. Cell* **12**, 889–901 (2003).
- 722 25. Furnari, F. B. *et al.* Malignant astrocytic glioma: Genetics, biology, and

- 723 paths to treatment. *Genes Dev.* **21**, 2683–2710 (2007).
- 724 26. Knudsen, E. S. & Wang, J. Y. J. Targeting the RB-pathway in cancer
725 therapy. *Clin. Cancer Res.* **16**, 1094–1099 (2010).
- 726 27. Sanjeev Shangary and Shaomeng Wang. Small-Molecule Inhibitors of the
727 MDM2-p53 Protein-Protein Interaction to Reactivate p53 Function: A
728 Novel Approach for Cancer Therapy. *Annu Rev Pharmacol Toxicol* **49**,
729 223–241 (2009).
- 730 28. Gritsch S, Batchelor T.T, G. C. L. N. Diagnostic, therapeutic, and
731 prognostic implications of the 2021 World Health Organization
732 classification of tumors of the central nervous system. *Cancer* **128**, 47–58
733 (2021).
- 734 29. Brat, D. J. *et al.* cIMPACT-NOW update 3: recommended diagnostic
735 criteria for “Diffuse astrocytic glioma, IDH-wildtype, with molecular
736 features of glioblastoma, WHO grade IV”. *Acta Neuropathol.* **136**, 805–
737 810 (2018).
- 738 30. Liu, X. Y. *et al.* Frequent ATRX mutations and loss of expression in adult
739 diffuse astrocytic tumors carrying IDH1/IDH2 and TP53 mutations. *Acta*
740 *Neuropathol.* **124**, 615–625 (2012).
- 741 31. Appay, R. *et al.* CDKN2A homozygous deletion is a strong adverse
742 prognosis factor in diffuse malignant IDH-mutant gliomas. *Neuro. Oncol.*
743 **21**, 1519–1528 (2019).
- 744 32. Schwartzbaum, J. A., Fisher, J. L., Aldape, K. D. & Wrensch, M.
745 Epidemiology and molecular pathology of glioma. *Nat. Clin. Pract. Neurol.*
746 **2**, 494–503 (2006).
- 747 33. Wrensch, M., Minn, Y., Chew, T., Bondy, M. & Berger, M. S.

- 748 Epidemiology of primary brain tumors: Current concepts and review of the
749 literature. *Neuro. Oncol.* **4**, 278–299 (2002).
- 750 34. Manuscript, A. Brain Tumor Susceptibility: the Role of Genetic Factors
751 and Uses of Mouse Models to Unravel Risk Karlyne. *Brain Pathol.* **19**,
752 121–131 (2010).
- 753 35. Yuile, P., Dent, O., Cook, R., Biggs, M. & Little, N. Survival of
754 glioblastoma patients related to presenting symptoms, brain site and
755 treatment variables. *J. Clin. Neurosci.* **13**, 747–751 (2006).
- 756 36. Gilard, V. *et al.* Diagnosis and management of glioblastoma: A
757 comprehensive perspective. *J. Pers. Med.* **11**, (2021).
- 758 37. Wirsching, H., Galanis, E. & Weller, M. Glioblastoma. **134**, (2016).
- 759 38. Peeken, J. C. *et al.* Combining multimodal imaging and treatment features
760 improves machine learning-based prognostic assessment in patients with
761 glioblastoma multiforme. *Cancer Med.* **8**, 128–136 (2019).
- 762 39. Price, S. J. *et al.* Multimodal MRI can identify perfusion and metabolic
763 changes in the invasive margin of glioblastomas. *J. Magn. Reson.*
764 *Imaging* **43**, 487–494 (2016).
- 765 40. Yu, W., Zhang, L., Wei, Q. & Shao, A. O6-Methylguanine-DNA
766 Methyltransferase (MGMT): Challenges and New Opportunities in Glioma
767 Chemotherapy. *Front. Oncol.* **9**, 1–11 (2020).
- 768 41. Zagzag, D., Douglas, C. M. & Kricheff, I. I. Glial Neoplasms: Dynamic
769 Contrast-enhanced T2*-weighted MR Imaging. *Neuroradiology* 791–798
770 (1999).
- 771 42. Bulsara, K. R., Johnson, J. & Villavicencio, A. T. Improvements in brain
772 tumor surgery: the modern history of awake craniotomies. *Neurosurg.*

- 773 *Focus* **18**, 3–5 (2005).
- 774 43. Wolbers, J. G. Novel strategies in glioblastoma surgery aim at safe,
775 super-maximum resection in conjunction with local therapies. *Chin. J.*
776 *Cancer* **33**, 8–15 (2014).
- 777 44. Stummer, W. *et al.* Fluorescence-guided surgery with 5-aminolevulinic
778 acid for resection of malignant glioma: a randomised controlled
779 multicentre phase III trial. *Lancet Oncol.* **7**, 392–401 (2006).
- 780 45. Goryaynov, S. A. *et al.* The role of 5-ALA in low-grade gliomas and the
781 influence of antiepileptic drugs on intraoperative fluorescence. *Front.*
782 *Oncol.* **9**, 1–7 (2019).
- 783 46. Yoshiura, T., Wu, O. & Sorensen, A. G. Advanced MR techniques.
784 Diffusion MR imaging, perfusion MR imaging, and spectroscopy.
785 *Neuroimaging Clin. N. Am.* **9**, 439–453 (1999).
- 786 47. Gilbert, M. R. *et al.* Dose-dense temozolomide for newly diagnosed
787 glioblastoma: A randomized phase III clinical trial. *J. Clin. Oncol.* **31**,
788 4085–4091 (2013).
- 789 48. Rapp, M., Baernreuther, J., Turowski, B., Steiger, H. & Kamp, M. A. SC.
790 (2017) doi:10.1016/j.wneu.2017.04.053.This.
- 791 49. Friedman, H. S. *et al.* Bevacizumab alone and in combination with
792 irinotecan in recurrent glioblastoma. *J. Clin. Oncol.* **27**, 4733–4740 (2009).
- 793 50. Minniti, G., Niyazi, M., Alongi, F., Navarria, P. & Belka, C. Current status
794 and recent advances in reirradiation of glioblastoma. *Radiat. Oncol.* **16**,
795 1–14 (2021).
- 796 51. Briana C. Prager, Qi Xie, Shideng Bao, J. N. R. Cancer Stem Cells: The
797 Architects of the Tumor Ecosystem. *Cell Stem Cell*, **24**, 41–53 (2019).

- 798 52. Persano, L., Rampazzo, E., Basso, G. & Viola, G. Glioblastoma cancer
799 stem cells: Role of the microenvironment and therapeutic targeting.
800 *Biochem. Pharmacol.* **85**, 612–622 (2013).
- 801 53. Clarke, M. F. *et al.* Cancer stem cells - Perspectives on current status and
802 future directions: AACR workshop on cancer stem cells. *Cancer Res.* **66**,
803 9339–9344 (2006).
- 804 54. Suvà, M. L. & Tirosh, I. The Glioma Stem Cell Model in the Era of Single-
805 Cell Genomics. *Cancer Cell* **37**, 630–636 (2020).
- 806 55. Dirkse, A. *et al.* Stem cell-associated heterogeneity in Glioblastoma
807 results from intrinsic tumor plasticity shaped by the microenvironment.
808 *Nat. Commun.* **10**, 1–16 (2019).
- 809 56. Khan, I. S. & Ehtesham, M. Targeting glioblastoma cancer stem cells: The
810 next great hope? *Neurosurg. Focus* **37**, (2014).
- 811 57. Ehtesham, M., Mapara, K. Y., Stevenson, C. B. & Thompson, R. C.
812 CXCR4 mediates the proliferation of glioblastoma progenitor cells. *Cancer*
813 *Lett.* **274**, 305–312 (2009).
- 814 58. Schulz, A., Meyer, F., Dubrovskaja, A. & Borgmann, K. Cancer stem cells
815 and radioresistance: DNA repair and beyond. *Cancers (Basel)*. **11**, 13–15
816 (2019).
- 817 59. Hambardzumyan D, B. G. Glioblastoma: Defining Tumor Niches. *Trends*
818 *Cancer* **1**, 252–265 (2015).
- 819 60. Calabrese, C. *et al.* A Perivascular Niche for Brain Tumor Stem Cells.
820 *Cancer Cell* **11**, 69–82 (2007).
- 821 61. Bao, S. *et al.* Stem cell-like glioma cells promote tumor angiogenesis
822 through vascular endothelial growth factor. *Cancer Res.* **66**, 7843–7848

- 823 (2006).
- 824 62. Du R, Lu KV, Petritsch C, Liu P, Ganss R, Passegué E, Song H,
825 Vandenberg S, Johnson RS, Werb Z, B. G. HIF1alpha induces the
826 recruitment of bone marrow-derived vascular modulatory cells to regulate
827 tumor angiogenesis and invasion. *Cancer Cell*. **13**, 206–220 (2008).
- 828 63. Bergers, G. & Song, S. The role of pericytes in blood-vessel formation
829 and maintenance. *Neuro. Oncol*. **7**, 452–464 (2005).
- 830 64. Feng, X. *et al.* Loss of CX3CR1 increases accumulation of inflammatory
831 monocytes and promotes gliomagenesis. *Oncotarget* **6**, 15077–15094
832 (2015).
- 833 65. Liang J, Piao Y, Holmes L, Fuller GN, Henry V, Tiao N, de G. J.
834 Neutrophils promote the malignant glioma phenotype through S100A4.
835 *Clin Cancer Res*. **20**, 187–98 (2014).
- 836 66. Kohanbash, G. & Okada, H. Myeloid-derived Suppressor Cells (MDSCs)
837 in gliomas and glioma-development. *Immunol. Invest*. **41**, 658–679
838 (2012).
- 839 67. Brat, D. J. *et al.* Pseudopalisades in Glioblastoma Are Hypoxic, Express
840 Extracellular Matrix Proteases, and Are Formed by an Actively Migrating
841 Cell Population. *Cancer Res*. **64**, 920–927 (2004).
- 842 68. Yancopoulos, G. D. *et al.* Vascular-specific growth factors and blood
843 vessel formation. *Nature* **407**, 242–248 (2000).
- 844 69. Brat, D. J. & Van Meir, E. G. Vaso-occlusive and prothrombotic
845 mechanisms associated with tumor hypoxia, necrosis, and accelerated
846 growth in glioblastoma. *Lab. Investig*. **84**, 397–405 (2004).
- 847 70. Semenza, G. L. Defining the Role of Hypoxia-Inducible Factor 1 in Cancer

- 848 Biology and Therapeutics. *Oncogene*. **29**, 625–634 (2010).
- 849 71. Seidel, S. *et al.* A hypoxic niche regulates glioblastoma stem cells through
850 hypoxia inducible factor 2 α . *Brain* **133**, 983–995 (2010).
- 851 72. Bar, E. E., Lin, A., Mahairaki, V., Matsui, W. & Eberhart, C. G. Hypoxia
852 increases the expression of stem-cell markers and promotes
853 clonogenicity in glioblastoma neurospheres. *Am. J. Pathol.* **177**, 1491–
854 1502 (2010).
- 855 73. Zagzag, D. *et al.* Hypoxia-inducible factor 1 and VEGF upregulate CXCR4
856 in glioblastoma: Implications for angiogenesis and glioma cell invasion.
857 *Lab. Investig.* **86**, 1221–1232 (2006).
- 858 74. Cuddapah VA, Robel S, Watkins S, S. H. A neurocentric perspective on
859 glioma invasion. *Nat Rev Neurosci.* **7**, 455–65 (2014).
- 860 75. Zimmermann, D. R. & Dours-Zimmermann, M. T. Extracellular matrix of
861 the central nervous system: From neglect to challenge. *Histochem. Cell*
862 *Biol.* **130**, 635–653 (2008).
- 863 76. Mentlein, R., Hattermann, K. & Held-Feindt, J. Lost in disruption: Role of
864 proteases in glioma invasion and progression. *Biochim. Biophys. Acta -*
865 *Rev. Cancer* **1825**, 178–185 (2012).
- 866 77. Mathiisen, T. M., Lehre, K. P., Danbolt, N. C. & Ottersen, O. P. The
867 perivascular astroglial sheath provides a complete covering of the brain
868 microvessels: An electron microscopic 3D reconstruction. *Glia* **58**, 1094–
869 1103 (2010).
- 870 78. Friedmann-Morvinski, D. & Verma, I. M. Dedifferentiation and
871 reprogramming: Origins of cancer stem cells. *EMBO Rep.* **15**, 244–253
872 (2014).

- 873 79. Bachoo, R. M. *et al.* Epidermal growth factor receptor and Ink4a/Arf:
874 Convergent mechanisms governing terminal differentiation and
875 transformation along the neural stem cell to astrocyte axis. *Cancer Cell* **1**,
876 269–277 (2002).
- 877 80. Reynolds, B. A. & Weiss, S. Generation of neurons and astrocytes from
878 isolated cells of the adult mammalian central nervous system. *Science*
879 (80-). **255**, 1707–1710 (1992).
- 880 81. Lois, C. & Alvarez-Buylla, A. Proliferating subventricular zone cells in the
881 adult mammalian forebrain can differentiate into neurons and glia. *Proc.*
882 *Natl. Acad. Sci. U. S. A.* **90**, 2074–2077 (1993).
- 883 82. Human, T., Group, O., Natural, T., Museum, H. & Road, C. R
884 econstructing recent h u m an evolution. 217–224 (1992).
- 885 83. Sanai, H. *et al.* Unique astrocyte ribbon in adult human brain contains
886 neural stem cells but lacks chain migration. *Nature* **427**, 740–744 (2004).
- 887 84. Quiñones-Hinojosa, A. *et al.* Cellular composition and cytoarchitecture of
888 the adult human subventricular zone: A niche of neural stem cells. *J.*
889 *Comp. Neurol.* **494**, 415–434 (2006).
- 890 85. Altmann, C., Keller, S. & Schmidt, M. H. H. The role of svz stem cells in
891 glioblastoma. *Cancers (Basel)*. **11**, 1–23 (2019).
- 892 86. Lim, D. A. *et al.* Relationship of glioblastoma multiforme to neural stem
893 cell regions predicts invasive and multifocal tumor phenotype. *Neuro.*
894 *Oncol.* **9**, 424–429 (2007).
- 895 87. Lois, C. & Alvarez-buylla, A. Long-Distance Neuronal Migration in the
896 Adult Mammalian Brain Author (s): Carlos Lois and Arturo Alvarez-Buylla
897 Published by : American Association for the Advancement of Science

- 898 Stable URL : <http://www.jstor.org/stable/2885135> Long-Distance Neuronal
899 Mi. **264**, 1145–1148 (1996).
- 900 88. Menn, B. *et al.* Origin of oligodendrocytes in the subventricular zone of
901 the adult brain. *J. Neurosci.* **26**, 7907–7918 (2006).
- 902 89. Verhaak, R. G. W. *et al.* NIH Public Access. **17**, 1–25 (2011).
- 903 90. Parsons, D. W. *et al.* NIH Public Access. **321**, (2010).
- 904 91. Lee, J. H. *et al.* Human glioblastoma arises from subventricular zone cells
905 with low-level driver mutations. *Nature* **560**, 243–247 (2018).
- 906 92. Lombard, A. *et al.* The Subventricular Zone, a Hideout for Adult and
907 Pediatric High-Grade Glioma Stem Cells. *Front. Oncol.* **10**, 1–13 (2021).
- 908 93. Sampetean, O. *et al.* Invasion precedes tumor mass formation in a
909 malignant brain tumor model of genetically modified neural stem cells.
910 *Neoplasia* **13**, 784–791 (2011).
- 911 94. Goffart, N. *et al.* Adult mouse subventricular zones stimulate glioblastoma
912 stem cells specific invasion through CXCL12/CXCR4 signaling. *Neuro.*
913 *Oncol.* **17**, 81–94 (2015).
- 914 95. Meyrath, M. *et al.* The atypical chemokine receptor ACKR3/CXCR7 is a
915 broad-spectrum scavenger for opioid peptides. *Nat. Commun.* **11**, (2020).
- 916 96. Yang, L. *et al.* Blocking CXCR4-mediated cyclic AMP suppression inhibits
917 brain tumor growth in vivo. *Cancer Res.* **67**, 651–658 (2007).
- 918 97. Zhu, Y. *et al.* The effect of CXCR4 silencing on epithelial-mesenchymal
919 transition related genes in glioma U87 cells. *Anat. Rec.* **296**, 1850–1856
920 (2013).
- 921 98. Dedobbeleer, M. *et al.* MKP1 phosphatase is recruited by CXCL12 in
922 glioblastoma cells and plays a role in DNA strand breaks repair.

- 923 *Carcinogenesis* **41**, 417–429 (2020).
- 924 99. Willems, E. *et al.* Aurora A plays a dual role in migration and survival of
925 human glioblastoma cells according to the CXCL12 concentration.
926 *Oncogene* **38**, 73–87 (2019).
- 927 100. Anup Kumar Singh, Rakesh Kumar Arya, Arun Kumar Trivedi,
928 Sabyasachi Sanyal, Rathindranath Baral, Olivier Dormond, David M.
929 Briscoe, and D. D. Chemokine receptor trio: CXCR3, CXCR4 and
930 CXCR7 crosstalk via CXCL11 and CXCL12. *Cytokine Growth Factor Rev.*
931 **24**, 41–49 (2013).
- 932 101. Bachelerie, F. *et al.* New nomenclature for atypical chemokine receptors.
933 *Nat. Immunol.* **15**, 207–208 (2014).
- 934 102. Hamm, H. E. Minireview The Many Faces of G Protein. *Biochemistry* 5–8.
- 935 103. Feng, Y., Broder, C. C., Kennedy, P. E. & Berger, E. A. HIV-1 Entry
936 Cofactor : Functional cDNA Cloning of a Seven-Transmembrane , G
937 Protein- Coupled Receptor Author (s): Yu Feng , Christopher C . Broder
938 , Paul E . Kennedy and Edward A . Berger Published by : American
939 Association for the Advancement of Scienc. *Science (80-)*. **272**, 872–877
940 (1996).
- 941 104. Bajetto, A., Bonavia, R., Barbero, S. & Schettini, G. Characterization of
942 chemokines and their receptors in the central nervous system:
943 Physiopathological implications. *J. Neurochem.* **82**, 1311–1329 (2002).
- 944 105. Würth, R., Bajetto, A., Harrison, J. K., Barbieri, F. & Florio, T. CXCL12
945 modulation of CXCR4 and CXCR7 activity in human glioblastoma stem-
946 like cells and regulation of the tumor microenvironment. *Front. Cell.*
947 *Neurosci.* **8**, 1–19 (2014).

- 948 106. Domanska, U. M. *et al.* A review on CXCR4/CXCL12 axis in oncology: No
949 place to hide. *Eur. J. Cancer* **49**, 219–230 (2013).
- 950 107. Nagasawa, T. *et al.* Defects of B-cell lymphopoiesis and bone-marrow
951 myelopoiesis in mice lacking the CXC chemokine PBSF/SDF-1. *Nature*
952 vol. 382 635–638 (1996).
- 953 108. Cheng, Z. J. *et al.* β -Arrestin differentially regulates the chemokine
954 receptor CXCR4- mediated signaling and receptor internalization, and this
955 implicates multiple interaction sites between β -arrestin and CXCR4. *J.*
956 *Biol. Chem.* **275**, 2479–2485 (2000).
- 957 109. Hall, J. M. & Korach, K. S. Stromal cell-derived factor 1, a novel target of
958 estrogen receptor action, mediates the mitogenic effects of estradiol in
959 ovarian and breast cancer cells. *Mol. Endocrinol.* **17**, 792–803 (2003).
- 960 110. Taichman, R. S. *et al.* Use of the stromal cell-derived factor-1/CXCR4
961 pathway in prostate cancer metastasis to bone. *Cancer Res.* **62**, 1832–
962 1837 (2002).
- 963 111. Kaifi, J. T. *et al.* Tumor-cell homing to lymph nodes and bone marrow and
964 CXCR4 expression in esophageal cancer. *J. Natl. Cancer Inst.* **97**, 1840–
965 1847 (2005).
- 966 112. Kim, S. Y., Lee, C. H., Midura, B. V., Yeung, C., Mendoza, A., Hong, S.
967 H., Ren, L., Wong, D., Korz, W., Merzouk, A., Salari, H., Zhang, H.,
968 Hwang, S. T., Khanna, C., & Helman, L. J. Inhibition of the
969 CXCR4/CXCL12 chemokine pathway reduces the development of murine
970 pulmonary metastases. *Clin. Exp. Metastasis* **25**, 201–211 (2008).
- 971 113. Geminder, H. *et al.* A Possible Role for CXCR4 and Its Ligand, the CXC
972 Chemokine Stromal Cell-Derived Factor-1, in the Development of Bone

- 973 Marrow Metastases in Neuroblastoma. *J. Immunol.* **167**, 4747–4757
974 (2001).
- 975 114. Teicher, B. A. & Fricker, S. P. CXCL12 (SDF-1)/CXCR4 pathway in
976 cancer. *Clin. Cancer Res.* **16**, 2927–2931 (2010).
- 977 115. Salmaggi, A. *et al.* CXCL12 expression is predictive of a shorter time to
978 tumor progression in low-grade glioma: A single-institution study in 50
979 patients. *J. Neurooncol.* **74**, 287–293 (2005).
- 980 116. Hariz, M. I. Psychosurgery, deep brain stimulation, and the re-writing of
981 history. *Neurosurgery* **63**, (2008).
- 982 117. Ehtesham, M., Winston, J. A., Kabos, P. & Thompson, R. C. CXCR4
983 expression mediates glioma cell invasiveness. *Oncogene* **25**, 2801–2806
984 (2006).
- 985 118. Liu, C. *et al.* Expression and Functional Heterogeneity of Chemokine
986 Receptors CXCR4 and CXCR7 in Primary Patient-Derived Glioblastoma
987 Cells. *PLoS One* **8**, (2013).
- 988 119. Goffart, N. *et al.* CXCL12 mediates glioblastoma resistance to
989 radiotherapy in the subventricular zone. *Neuro. Oncol.* **19**, 66–77 (2017).
- 990 120. Piccirillo, S. G. M. *et al.* Contributions to drug resistance in glioblastoma
991 derived from malignant cells in the sub-ependymal zone. *Cancer Res.* **75**,
992 194–202 (2015).
- 993 121. Fanelli, G. N. *et al.* Decipher the glioblastoma microenvironment: The first
994 milestone for new groundbreaking therapeutic strategies. *Genes (Basel)*.
995 **12**, (2021).
- 996 122. Dapash, M., Hou, D., Castro, B., Lee-Chang, C. & Lesniak, M. S. The
997 interplay between glioblastoma and its microenvironment. *Cells* **10**, 1–14

- 998 (2021).
- 999 123. Engler, J. R. *et al.* Increased microglia/macrophage gene expression in a
1000 subset of adult and pediatric astrocytomas. *PLoS One* **7**, 1–12 (2012).
- 1001 124. Charles, N. A., Holland, E. C., Gilbertson, R., Glass, R. & Kettenmann, H.
1002 The brain tumor microenvironment. *Glia* **60**, 502–514 (2012).
- 1003 125. Chen, Z. & Hambardzumyan, D. Immune microenvironment in
1004 glioblastoma subtypes. *Front. Immunol.* **9**, 1–8 (2018).
- 1005 126. Ginhoux, F. *et al.* NIH Public Access. **330**, 841–845 (2013).
- 1006 127. Shi C, P. E. Monocyte recruitment during infection and inflammation. *Nat*
1007 *Rev Immunol* **11**, 762–74. (2011).
- 1008 128. Dal-Secco, D. *et al.* A dynamic spectrum of monocytes arising from the in
1009 situ reprogramming of CCR2+ monocytes at a site of sterile injury. *J. Exp.*
1010 *Med.* **212**, 447–456 (2015).
- 1011 129. Chen, Z. *et al.* Cellular and molecular identity of tumor-associated
1012 macrophages in glioblastoma. *Cancer Res.* **77**, 2266–2278 (2017).
- 1013 130. Hambardzumyan, D., Gutmann, D. H. & Kettenmann, H. The role of
1014 microglia and macrophages in glioma maintenance and progression. *Nat.*
1015 *Neurosci.* **19**, 20–27 (2015).
- 1016 131. Brüne, B. *et al.* Redox control of inflammation in macrophages.
1017 *Antioxidants Redox Signal.* **19**, 595–637 (2013).
- 1018 132. Piaszyk-Borychowska, A. *et al.* Signal integration of IFN-I and IFN-II with
1019 TLR4 involves sequential recruitment of STAT1-Complexes and NFκB to
1020 enhance pro-inflammatory transcription. *Front. Immunol.* **10**, 1–20 (2019).
- 1021 133. Platanitis, E. & Decker, T. Regulatory networks involving STATs, IRFs,
1022 and NFκB in inflammation. *Front. Immunol.* **9**, 1–16 (2018).

- 1023 134. Mantovani, A., Biswas, S. K., Galdiero, M. R., Sica, A. & Locati, M.
1024 Macrophage plasticity and polarization in tissue repair and remodelling. *J.*
1025 *Pathol.* **229**, 176–185 (2013).
- 1026 135. Szulzewsky, F. *et al.* Glioma-associated microglia/macrophages display
1027 an expression profile different from M1 and M2 polarization and highly
1028 express Gpnmb and Spp1. *PLoS One* **10**, 1–27 (2015).
- 1029 136. Komai, T. *et al.* Transforming growth factor- β and interleukin-10
1030 synergistically regulate humoral immunity via modulating metabolic
1031 signals. *Front. Immunol.* **9**, 1–15 (2018).
- 1032 137. Russell, L. & Peng, K. W. The emerging role of oncolytic virus therapy
1033 against cancer. *Chinese Clin. Oncol.* **7**, (2018).
- 1034 138. Martikainen, M. & Essand, M. Virus-based immunotherapy of
1035 glioblastoma. *Cancers (Basel)*. **11**, (2019).
- 1036 139. Koks, C. A. E., de Vleeschouwer, S., Graf, N. & van Gool, S. W. Immune
1037 suppression during oncolytic virotherapy for high-grade glioma; Yes or
1038 No? *J. Cancer* **6**, 203–217 (2015).
- 1039 140. Ooi, Y. C. *et al.* The role of regulatory T-cells in glioma immunology. *Clin.*
1040 *Neurol. Neurosurg.* **119**, 125–132 (2014).
- 1041 141. Serrano Cardona, L. & Muñoz Mata, E. *Paraninfo Digital. Early Human*
1042 *Development* vol. 83 (2013).
- 1043 142. Adeegbe, D. O. & Nishikawa, H. Natural and induced T regulatory cells in
1044 cancer. *Front. Immunol.* **4**, 1–14 (2013).
- 1045 143. Jordan, J. T. *et al.* Preferential migration of regulatory T cells mediated by
1046 glioma-secreted chemokines can be blocked with chemotherapy. *Cancer*
1047 *Immunol. Immunother.* **57**, 123–131 (2008).

- 1048 144. Chang, A. L. et al. CL2 produced by the glioma microenvironment is
1049 essential for the recruitment of regulatory T cells and myeloid-derived
1050 suppressor cells. *Physiol. Behav.* **176**, 139–148 (2016).
- 1051 145. Kmiecik, J. et al. Elevated CD3+ and CD8+ tumor-infiltrating immune cells
1052 correlate with prolonged survival in glioblastoma patients despite
1053 integrated immunosuppressive mechanisms in the tumor
1054 microenvironment and at the systemic level. *J. Neuroimmunol.* **264**, 71–
1055 83 (2013).
- 1056 146. Lohr, J. et al. Effector T-cell infiltration positively impacts survival of
1057 glioblastoma patients and is impaired by tumor-derived TGF- β . *Clin.*
1058 *Cancer Res.* **17**, 4296–4308 (2011).
- 1059 147. Steinman, R. M. & Banchereau, J. Taking dendritic cells into medicine.
1060 *Nature* **449**, 419–426 (2007).
- 1061 148. Wang J. et al; Nrf2 suppresses the function of dendritic cells to facilitate
1062 the immune escape of glioma cells. *Exp. Cell Res.* **360**, 66–73 (2017).
- 1063 149. Raychaudhuri, B. et al. Myeloid-derived suppressor cell accumulation and
1064 function in patients with newly diagnosed glioblastoma. *Neuro. Oncol.* **13**,
1065 591–599 (2011).
- 1066 150. Raychaudhuri, B. et al. Myeloid derived suppressor cell infiltration of
1067 murine and human gliomas is associated with reduction of tumor
1068 infiltrating lymphocytes. *J. Neurooncol.* **122**, 293–301 (2015).
- 1069 151. Mi, Y. et al. The Emerging Role of Myeloid-Derived Suppressor Cells in
1070 the Glioma Immune Suppressive Microenvironment. *Front. Immunol.* **11**,
1071 1–11 (2020).
- 1072 152. Komotar, R. J., Otten, M. L., Moise, G. & Connolly, E. S. Radiotherapy

- 1073 plus concomitant and adjuvant temozolomide for glioblastoma—A critical
1074 review. *Clin. Med. Oncol.* **2**, 421–422 (2008).
- 1075 153. Chinot, O. L. *et al.* Bevacizumab plus Radiotherapy–Temozolomide for
1076 Newly Diagnosed Glioblastoma. *N. Engl. J. Med.* **370**, 709–722 (2014).
- 1077 154. Yu, M. W. & Quail, D. F. Immunotherapy for Glioblastoma: Current
1078 Progress and Challenge. *Front. Immunol.* **12**, 1–12 (2021).
- 1079 155. Huang, B. *et al.* Current Immunotherapies for Glioblastoma Multiforme.
1080 *Front. Immunol.* **11**, 1–12 (2021).
- 1081 156. Leach, D. R., Krummel, M. F. & Allison, J. P. Enhancement of antitumor
1082 immunity by CTLA-4 blockade. *Science (80-.)*. **271**, 1734–1736 (1996).
- 1083 157. Ishida, Y., Agata, Y., Shibahara, K. & Honjo, T. Induced expression of
1084 PD-1, a novel member of the immunoglobulin gene superfamily, upon
1085 programmed cell death. *EMBO J.* **11**, 3887–3895 (1992).
- 1086 158. Larkin, J. *et al.* Five-Year Survival with Combined Nivolumab and
1087 Ipilimumab in Advanced Melanoma. *N. Engl. J. Med.* **381**, 1535–1546
1088 (2019).
- 1089 159. Hellmann, M. D. *et al.* Nivolumab plus Ipilimumab in Advanced Non–
1090 Small-Cell Lung Cancer. *N. Engl. J. Med.* **381**, 2020–2031 (2019).
- 1091 160. Engels, B. *et al.* Relapse or eradication of cancer is predicted by peptide-
1092 major histocompatibility complex affinity. *Cancer Cell* **23**, 516–526 (2013).
- 1093 161. Pardoll, D. M. The blockade of immune checkpoints in cancer
1094 immunotherapy. *Nat. Rev. Cancer* **12**, 252–264 (2012).
- 1095 162. Buchbinder, E. I. & Desai, A. CTLA-4 and PD-1 pathways similarities,
1096 differences, and implications of their inhibition. *Am. J. Clin. Oncol. Cancer*
1097 *Clin. Trials* **39**, 98–106 (2016).

- 1098 163. Bloch, O. *et al.* Gliomas promote immunosuppression through induction of
1099 B7-H1 expression in tumor-associated macrophages. *Clin. Cancer Res.*
1100 **19**, 3165–3175 (2013).
- 1101 164. Fecci, P. E. *et al.* Increased regulatory T-cell fraction amidst a diminished
1102 CD4 compartment explains cellular immune defects in patients with
1103 malignant glioma. *Cancer Res.* **66**, 3294–3302 (2006).
- 1104 165. Berghoff, A. S. *et al.* Programmed death ligand 1 expression and tumor-
1105 infiltrating lymphocytes in glioblastoma. *Neuro. Oncol.* **17**, 1064–1075
1106 (2015).
- 1107 166. Nduom, E. K. *et al.* PD-L1 expression and prognostic impact in
1108 glioblastoma. *Neuro. Oncol.* **18**, 195–205 (2016).
- 1109 167. Savoia, P., Astrua, C. & Fava, P. Ipilimumab (Anti-Ctla-4 Mab) in the
1110 treatment of metastatic melanoma: Effectiveness and toxicity
1111 management. *Hum. Vaccines Immunother.* **12**, 1092–1101 (2016).
- 1112 168. Fecci, P. E. *et al.* Systemic CTLA-4 blockade ameliorates glioma-induced
1113 changes to the CD4 + T cell compartment without affecting regulatory T-
1114 cell function. *Clin. Cancer Res.* **13**, 2158–2167 (2007).
- 1115 169. Park, J. *et al.* Effect of combined anti-PD-1 and temozolomide therapy in
1116 glioblastoma. *Oncoimmunology* **8**, (2019).
- 1117 170. Omuro, A. *et al.* Nivolumab with or without ipilimumab in patients with
1118 recurrent glioblastoma: Results from exploratory phase i cohorts of
1119 CheckMate 143. *Neuro. Oncol.* **20**, 674–686 (2018).
- 1120 171. Reardon, D. A. *et al.* Effect of Nivolumab vs Bevacizumab in Patients with
1121 Recurrent Glioblastoma: The CheckMate 143 Phase 3 Randomized
1122 Clinical Trial. *JAMA Oncol.* **6**, 1003–1010 (2020).

- 1123 172. Klemm, F. *et al.* Interrogation of the Microenvironmental Landscape in
1124 Brain Tumors Reveals Disease-Specific Alterations of Immune Cells. *Cell*
1125 **181**, 1643-1660.e17 (2020).
- 1126 173. Koyama, S. *et al.* Adaptive resistance to therapeutic PD-1 blockade is
1127 associated with upregulation of alternative immune checkpoints. *Nat.*
1128 *Commun.* **7**, 1–9 (2016).
- 1129 174. Zhou, W. *et al.* Periostin secreted by glioblastoma stem cells recruits M2
1130 tumour-associated macrophages and promotes malignant growth. *Nat.*
1131 *Cell Biol.* **17**, 170–182 (2015).
- 1132 175. Wu, A. *et al.* Glioma cancer stem cells induce immunosuppressive
1133 macrophages/microglia. *Neuro. Oncol.* **12**, 1113–1125 (2010).
- 1134 176. Akins, E. A., Aghi, M. K. & Kumar, S. Incorporating Tumor-Associated
1135 Macrophages into Engineered Models of Glioma. *iScience* **23**, 1–18
1136 (2020).
- 1137 177. Hussain, S. F. *et al.* The role of human glioma-infiltrating
1138 microglia/macrophages in mediating antitumor immune responses. *Neuro.*
1139 *Oncol.* **8**, 261–279 (2006).
- 1140 178. Rahma, O. E. & Hodi, F. S. The intersection between tumor angiogenesis
1141 and immune suppression. *Clin. Cancer Res.* **25**, 5449–5457 (2019).
- 1142 179. Pyonteck, S. M. *et al.* CSF-1R inhibition alters macrophage polarization
1143 and blocks glioma progression. *Nat. Med.* **19**, 1264–1272 (2013).
- 1144 180. Butowski, N. *et al.* Orally administered colony stimulating factor 1 receptor
1145 inhibitor PLX3397 in recurrent glioblastoma: An Ivy Foundation Early
1146 Phase Clinical Trials Consortium phase II study. *Neuro. Oncol.* **18**, 557–
1147 564 (2016).

- 1148 181. Sahin, U. & Türeci, Ö. Personalized vaccines for cancer immunotherapy.
1149 *Science* (80-.). **359**, 1355–1360 (2018).
- 1150 182. Filley, A. C. & Dey, M. Dendritic cell based vaccination strategy: an
1151 evolving paradigm. *J. Neurooncol.* **133**, 223–235 (2017).
- 1152 183. Lynes, J., Sanchez, V., Dominah, G., Nwankwo, A. & Nduom, E. Current
1153 options and future directions in immune therapy for glioblastoma. *Front.*
1154 *Oncol.* **8**, 1–22 (2018).
- 1155 184. Prins, R. M. *et al.* Gene expression profile correlates with T-cell infiltration
1156 and relative survival in glioblastoma patients vaccinated with dendritic cell
1157 immunotherapy. *Clin. Cancer Res.* **17**, 1603–1615 (2011).
- 1158 185. Sottoriva, A. *et al.* Intratumor heterogeneity in human glioblastoma
1159 reflects cancer evolutionary dynamics. *Proc. Natl. Acad. Sci. U. S. A.* **110**,
1160 4009–4014 (2013).
- 1161 186. Wang, Q. T. *et al.* Tumor-associated antigen-based personalized dendritic
1162 cell vaccine in solid tumor patients. *Cancer Immunol. Immunother.* **69**,
1163 1375–1387 (2020).
- 1164 187. Platten, M. *et al.* A vaccine targeting mutant IDH1 in newly diagnosed
1165 glioma. *Nature* **592**, 463–468 (2021).
- 1166 188. Rafiq, S., Hackett, C. S. & Brentjens, R. J. therapy. **17**, (2020).
- 1167 189. Brudno, J. N. & Kochenderfer, J. N. Chimeric antigen receptor T-cell
1168 therapies for lymphoma. *Nat. Rev. Clin. Oncol.* **15**, 31–46 (2018).
- 1169 190. Hucks, G. & Rheingold, S. R. The journey to CAR T cell therapy: the
1170 pediatric and young adult experience with relapsed or refractory B-ALL.
1171 *Blood Cancer J.* **9**, (2019).
- 1172 191. Gatt, A. & Vella, K. Teaching an old dog new tricks? *Br. J. Haematol.* **187**,

- 1173 416–417 (2019).
- 1174 192. Sahin, A. *et al.* Development of third generation anti-EGFRvIII chimeric T
1175 cells and EGFRvIII-expressing artificial antigen presenting cells for
1176 adoptive cell therapy for glioma. *PLoS One* **13**, 1–19 (2018).
- 1177 193. Brown, C. E. *et al.* Bioactivity and safety of IL13R α 2-redirected chimeric
1178 antigen receptor CD8⁺ T cells in patients with recurrent glioblastoma.
1179 *Clin. Cancer Res.* **21**, 4062–4072 (2015).
- 1180 194. Brown, C. E. *et al.* Glioma IL13R α 2 is associated with mesenchymal
1181 signature gene expression and poor patient prognosis. *PLoS One* **8**, 1–14
1182 (2013).
- 1183 195. Brown, C. E. *et al.* Regression of Glioblastoma after Chimeric Antigen
1184 Receptor T-Cell Therapy. *N. Engl. J. Med.* **375**, 2561–2569 (2016).
- 1185 196. Ahmed, N. *et al.* HER2-specific T cells target primary glioblastoma stem
1186 cells and induce regression of autologous experimental tumors. *Clin.*
1187 *Cancer Res.* **16**, 474–485 (2010).
- 1188 197. Hegde, M. *et al.* Tandem CAR T cells targeting HER2 and IL13R α 2
1189 mitigate tumor antigen escape. *J. Clin. Invest.* **126**, 3036–3052 (2016).
- 1190 198. Qiu, H. *et al.* A Prognostic Microenvironment-Related Immune Signature
1191 via ESTIMATE (PROMISE Model) Predicts Overall Survival of Patients
1192 With Glioma. *Front. Oncol.* **10**, 1–16 (2020).
- 1193 199. Burger, M. C. *et al.* CAR-Engineered NK Cells for the Treatment of
1194 Glioblastoma: Turning Innate Effectors Into Precision Tools for Cancer
1195 Immunotherapy. *Front. Immunol.* **10**, 1–16 (2019).
- 1196 200. Russell SJ, Peng KW, B. J. ONCOLYTIC VIROTHERAPY. *Nat Biotechnol*
1197 **10;30**, 658–70 (2012).

- 1198 201. Atherton, M. J. & Lichty, B. D. Evolution of oncolytic viruses: Novel
1199 strategies for cancer treatment. *Immunotherapy* **5**, 1191–1206 (2013).
- 1200 202. EA Chiocca & SD Rabkin. Oncolytic Viruses and Their Application to
1201 Cancer Immunotherapy. *Cancer Immunol Res.* **2**, 295–300 (2014).
- 1202 203. Cattaneo R, Miest T, Shashkova EV, B. M. Reprogrammed viruses as
1203 cancer therapeutics: targeted, armed and shielded. *Nat Rev Microbiol.* **6**,
1204 529–40 (2008).
- 1205 204. Rahman, M. M. & McFadden, G. Oncolytic viruses: Newest frontier for
1206 cancer immunotherapy. *Cancers (Basel).* **13**, (2021).
- 1207 205. Alberts, P., Tilgase, A., Rasa, A., Bandere, K. & Venskus, D. The advent
1208 of oncolytic virotherapy in oncology: The Rigvir® story. *Eur. J. Pharmacol.*
1209 **837**, 117–126 (2018).
- 1210 206. Wei, D., Xu, J., Liu, X. Y., Chen, Z. N. & Bian, H. Fighting Cancer with
1211 Viruses: Oncolytic Virus Therapy in China. *Hum. Gene Ther.* **29**, 151–159
1212 (2018).
- 1213 207. Raman, S. S., Hecht, J. R. & Chan, E. Talimogene laherparepvec:
1214 Review of its mechanism of action and clinical efficacy and safety.
1215 *Immunotherapy* **11**, 705–723 (2019).
- 1216 208. Daiichi Sankyo. Press Release DELYTACT® Oncolytic Virus G47Δ
1217 Approved in Japan for Treatment of Patients with Malignant Glioma. 3–5
1218 (2021).
- 1219 209. Frederick F Lang. Oncolytic Adenovirus DNX-2401 in Treating Patients
1220 With Recurrent High-Grade Glioma. *ClinicalTrials.gov NCT03896568*
1221 (2019).
- 1222 210. Targovax Oy. A Pilot Study of Sequential ONCOS-102, an Engineered

- 1223 Oncolytic Adenovirus Expressing GMCSF, and Pembrolizumab in
1224 Patients With Advanced or Unresectable Melanoma Progressing After
1225 Programmed Cell Death Protein 1 (PD1) Blockade. *ClinicalTrials.gov*
1226 *NCT03003676* (2021).
- 1227 211. Steve Bernstein, M. Trial of MG1-E6E7 With Ad-E6E7 and Atezolizumab
1228 in Patients With HPV Associated Cancers (Kingfisher). *ClinicalTrials.gov*
1229 *NCT03618953* <https://clinicaltrials.gov/ct2/show/NCT03618953> (2018).
- 1230 212. Reinhard Dummer, P. D. T-VEC in Non-melanoma Skin Cancer
1231 (20139157 T-VEC). *ClinicalTrials.gov* *NCT03458117*
1232 [https://clinicaltrials.gov/ct2/show/NCT03458117?term=T-](https://clinicaltrials.gov/ct2/show/NCT03458117?term=T-VEC&draw=2&rank=1)
1233 [VEC&draw=2&rank=1](https://clinicaltrials.gov/ct2/show/NCT03458117?term=T-VEC&draw=2&rank=1).
- 1234 213. John Haanen, P. Neo-adjuvant T-VEC + Nivolumab Combination Therapy
1235 for Resectable Early Metastatic (Stage IIIB/C/D-IV M1a) Melanoma With
1236 Injectable Disease (NIVVEC). *ClinicalTrials.gov* *NCT04330430*
1237 [https://clinicaltrials.gov/ct2/show/NCT04330430?term=T-](https://clinicaltrials.gov/ct2/show/NCT04330430?term=T-VEC&draw=2&rank=2)
1238 [VEC&draw=2&rank=2](https://clinicaltrials.gov/ct2/show/NCT04330430?term=T-VEC&draw=2&rank=2) (2020).
- 1239 214. Gregory Friedman, M. . HSV G207 in Children With Recurrent or
1240 Refractory Cerebellar Brain Tumors. *ClinicalTrials.gov* *NCT03911388*
1241 (2019).
- 1242 215. Geletneky, K. *et al.* Phase I/IIa study of intratumoral/intracerebral or
1243 intravenous/intracerebral administration of Parvovirus H-1 (ParvOryx) in
1244 patients with progressive primary or recurrent glioblastoma multiforme:
1245 ParvOryx01 protocol. *BMC Cancer* **12**, (2012).
- 1246 216. Lee's Pharmaceutical Limited. Phase Ib/II Clinical Study of Pexa-Vec
1247 (Vaccinia GM CSF / Thymidine Kinase-Deactivated Virus) Combined With

- 1248 Recombinant Whole Human Anti-PD-L1 Monoclonal Antibody (ZKAB001)
1249 in Metastatic Melanoma. *ClinicalTrials.gov* NCT04849260
1250 <https://clinicaltrials.gov/ct2/show/NCT04849260> (2021).
- 1251 217. Tony Reid, Md, P. A Study of Recombinant Vaccinia Virus to Treat
1252 Unresectable Primary Hepatocellular Carcinoma. *ClinicalTrials.gov*
1253 NCT00554372 <https://clinicaltrials.gov/ct2/show/NCT00554372> (2015).
- 1254 218. Ren, H. *et al.* Erratum: Immunogene therapy of recurrent glioblastoma
1255 multiforme with a liposomally encapsulated replication-incompetent
1256 Semliki forest virus vector carrying the human interleukin-12 gene - A
1257 phase I/II clinical protocol (Journal of Neuro-Oncology (2003) . *J.*
1258 *Neurooncol.* **65**, 191 (2003).
- 1259 219. Sabine Mueller, MD, PhD, M. Modified Measles Virus (MV-NIS) for
1260 Children and Young Adults With Recurrent Medulloblastoma or Recurrent
1261 ATRT. *ClinicalTrials.gov* NCT02962167
1262 <https://www.clinicaltrials.gov/ct2/show/NCT02962167> (2016).
- 1263 220. LLC, M. A Study of MEDI5395 in Combination With Durvalumab in
1264 Subjects With Select Advanced Solid Tumors. *ClinicalTrials.gov*
1265 NCT03889275 <https://www.clinicaltrials.gov/ct2/show/NCT03889275>
1266 (2019).
- 1267 221. Hardev Pandha. CAVATAK (CVA21) in Non-muscle Invasive Bladder
1268 Cancer (VLA-012 CANON) (CANON). *ClinicalTrials.gov* NCT02316171
1269 <https://clinicaltrials.gov/ct2/show/NCT02316171> (2019).
- 1270 222. Dina Randazzo, D. PVSRIPO in Recurrent Malignant Glioma.
1271 *ClinicalTrials.gov* NCT02986178
1272 <https://clinicaltrials.gov/ct2/show/NCT02986178> (2016).

- 1273 223. Rudin Charles, MD, P. Safety Study of Seneca Valley Virus in Patients
1274 With Solid Tumors With Neuroendocrine Features. *ClinicalTrials.gov*
1275 *NCT00314925* <https://clinicaltrials.gov/ct2/show/NCT00314925> (2006).
- 1276 224. Vanessa Bernstein. A Study of Reolysin For Patients With
1277 Advanced/Metastatic Breast Cancer. *ClinicalTrials.gov* *NCT01656538*
1278 <https://clinicaltrials.gov/ct2/show/NCT01656538> (2012).
- 1279 225. Alex Adjei, MD, P. Ph I/II Trial of Systemic VSV-IFN β -NIS and
1280 Pembrolizumab in Refractory NSCLC and NEC. *ClinicalTrials.gov*
1281 *NCT03647163* <https://www.clinicaltrials.gov/ct2/show/NCT03647163>
1282 (2018).
- 1283 226. Derek Jonker. MG1 Maraba/MAGE-A3, With and Without Adenovirus
1284 Vaccine With Transgenic MAGE-A3 Insertion in Incurable MAGE-A3-
1285 Expressing Solid Tumours. *ClinicalTrials.gov* *NCT02285816*
1286 <https://clinicaltrials.gov/ct2/show/NCT02285816> (2014).
- 1287 227. Roizman, B. THE ORGANIZATION OF THE HERPES SIMPLEX VIRUS
1288 GENOMES. *Ann. Rev. Genet.* **13**, 25–57 (1979).
- 1289 228. Davison AJ, Eberle R, Ehlers B, Hayward GS, McGeoch DJ, Minson AC,
1290 Pellett PE, Roizman B, Studdert MJ, T. E. The order Herpesvirales. *Arch*
1291 *Viro* **154**, 171–7 (2009).
- 1292 229. Denes CE, Everett RD, D. R. Tour de Herpes: Cycling Through the Life
1293 and Biology of HSV-1. in *Herpes Simplex Virus (Methods and Protocols)*
1294 1–30 (2020). doi:10.1007/978-1-4939-9814-2_1.
- 1295 230. Birkmann, A. & Zimmermann, H. HSV antivirals - Current and future
1296 treatment options. *Curr. Opin. Virol.* **18**, 9–13 (2016).
- 1297 231. Jane Flint, Vincent Racaniello, Glenn Rall, Anna Marie Skalka, L. E.

- 1298 *Principles of Virology, 4ed.* (2007).
- 1299 232. Krishnan, R. & Stuart, P. M. Developments in Vaccination for Herpes
1300 Simplex Virus. *Front. Microbiol.* **12**, (2021).
- 1301 233. Madavaraju, K., Koganti, R., Volety, I., Yadavalli, T. & Shukla, D. Herpes
1302 Simplex Virus Cell Entry Mechanisms: An Update. *Front. Cell. Infect.*
1303 *Microbiol.* **10**, 1–18 (2021).
- 1304 234. Shukla, A. M. A. and D. Cell entry mechanisms of HSV: what we have
1305 learned in recent years. *Futur. Virol.* **10**, 1145–1154 (2015).
- 1306 235. Campadelli-Fiume, G., Cocchi, F., Menotti, L. & Lopez, M. The novel
1307 receptors that mediate the entry of herpes simplex viruses and animal
1308 alphaherpesviruses into cells. *Rev. Med. Virol.* **10**, 305–319 (2000).
- 1309 236. Agelidis, A. M. & Shukla, D. Cell entry mechanisms of HSV: What we
1310 have learned in recent years. *Future Virol.* **10**, 1145–1154 (2015).
- 1311 237. Ariei J, K. Y. The Role of HSV Glycoproteins in Mediating Cell Entry. in
1312 *Human Herpes Virus* (Adv Exp Med Biol, 2018). doi:doi: 10.1007/978-
1313 981-10-7230-7_1.
- 1314 238. Verzosa, A. L. *et al.* Herpes Simplex Virus 1 Infection of Neuronal and
1315 Non-Neuronal Cells Elicits Specific Innate Immune Responses and
1316 Immune Evasion Mechanisms. *Front. Immunol.* **12**, 1–17 (2021).
- 1317 239. Weller, S. K. & Coen, D. M. Herpes simplex viruses: Mechanisms of DNA
1318 replication. *Cold Spring Harb. Perspect. Biol.* **4**, (2012).
- 1319 240. Mettenleiter TC, Klupp BG, G. H. Herpesvirus assembly: An update. *Virus*
1320 *Res.* **143**, 222–234 (2009).
- 1321 241. Aldrak, N. *et al.* Oncolytic herpes simplex virus-based therapies for
1322 cancer. *Cells* **10**, 1–17 (2021).

- 1323 242. Sankyo, D. *Daiichi Sankyo Launches DELYTACT® Oncolytic Virus G47Δ*
1324 *in Japan*. www.daiichisankyo.com. (2021).
- 1325 243. Macdonald, S. J., Mostafa, H. H., Morrison, L. A. & Davido, D. J. Genome
1326 Sequence of Herpes Simplex Virus 1 Strain KOS. *J. Virol.* **86**, 6371–6372
1327 (2012).
- 1328 244. Shen, Y. & Nemunaitis, J. Herpes simplex virus 1 (HSV-1) for cancer
1329 treatment. *Cancer Gene Ther.* **13**, 975–992 (2006).
- 1330 245. Rehman, H., Silk, A. W., Kane, M. P. & Kaufman, H. L. Into the clinic:
1331 Talimogene laherparepvec (T-VEC), a first-in-class intratumoral oncolytic
1332 viral therapy. *J. Immunother. Cancer* **4**, 1–8 (2016).
- 1333 246. Kaufman, H. L. *et al.* Local and distant immunity induced by intralesional
1334 vaccination with an oncolytic herpes virus encoding GM-CSF in patients
1335 with stage IIIc and IV melanoma. *Ann. Surg. Oncol.* **17**, 718–730 (2010).
- 1336 247. Conry, R. M., Westbrook, B., McKee, S. & Norwood, T. G. Talimogene
1337 laherparepvec: First in class oncolytic virotherapy. *Hum. Vaccines*
1338 *Immunother.* **14**, 839–846 (2018).
- 1339 248. Wilcox, D. R. & Longnecker, R. The Herpes Simplex Virus Neurovirulence
1340 Factor γ 34.5: Revealing Virus–Host Interactions. *PLoS Pathog.* **12**, 1–7
1341 (2016).
- 1342 249. Cassady, K. A., Gross, M. & Roizman, B. The Second-Site Mutation in
1343 the Herpes Simplex Virus Recombinants Lacking the γ 1 34.5 Genes
1344 Precludes Shutoff of Protein Synthesis by Blocking the Phosphorylation of
1345 eIF-2 α . *J. Virol.* **72**, 7005–7011 (1998).
- 1346 250. MacLean, A. R., Ul-Fareed, M., Robertson, L., Harland, J. & Brown, S. M.
1347 Herpes simplex virus type 1 deletion variants 1714 and 1716 pinpoint

- 1348 neurovirulence-related sequences in Glasgow strain 17+ between
1349 immediate early gene 1 and the 'a' sequence. *J. Gen. Virol.* **72**, 631–639
1350 (1991).
- 1351 251. Toshihiro Mineta, Samuel D. Rabkin, Takahito Yazaki, W. D. H. & R. L. M.
1352 Attenuated multi-mutated herpes simplex virus-1 for the treatment of
1353 malignant gliomas. *Nature* **2**, 983–989 (1995).
- 1354 252. Aghi, M., Visted, T., DePinho, R. A. & Chiocca, E. A. Oncolytic herpes
1355 virus with defective ICP6 specifically replicates in quiescent cells with
1356 homozygous genetic mutations in p16. *Oncogene* **27**, 4249–4254 (2008).
- 1357 253. Mineta T, Rabkin SD, Yazaki T, Hunter WD, M. R. Attenuated multi-
1358 mutated herpes simplex virus–1 for the treatment of malignant gliomas.
1359 *Nature* **2**, 938–43 (1995).
- 1360 254. Peters, C. & Rabkin, S. D. Designing herpes viruses as oncolytics. *Mol.*
1361 *Ther. - Oncolytics* **2**, 15010 (2015).
- 1362 255. Hill, A., Jugovic, P., York, I. et al. Herpes simplex virus turns off the TAP
1363 to evade host immunity. *Nature* **375**, 411–415 (1995).
- 1364 256. Todo, T., Martuza, R. L., Rabkin, S. D. & Johnson, P. A. Oncolytic herpes
1365 simplex virus vector with enhanced MHC class I presentation and tumor
1366 cell killing. *Proc. Natl. Acad. Sci. U. S. A.* **98**, 6396–6401 (2001).
- 1367 257. Interactions, V. et al. Restriction of Replication of Oncolytic Herpes
1368 Simplex Virus. *J. Virol.* **92**, 1–17 (2018).
- 1369 258. Todo, T. Results of phase II clinical trial of oncolytic herpes virus G47Δ in
1370 patients with Glioblastoma. *Neuro. Oncol.* **11**, 3347097 (2019).
- 1371 259. Friedman, G. K. et al. Enhanced Sensitivity of Patient-Derived Pediatric
1372 High-Grade Brain Tumor Xenografts to Oncolytic HSV-1 Virotherapy

- 1373 Correlates with Nectin-1 Expression. *Sci. Rep.* **8**, 1–10 (2018).
- 1374 260. Campadelli-Fiume, G. *et al.* Retargeting strategies for oncolytic herpes
1375 simplex viruses. *Viruses* **8**, (2016).
- 1376 261. Campadelli-Fiume, G., Menotti, L., Avitabile, E. & Gianni, T. Viral and
1377 cellular contributions to herpes simplex virus entry into the cell. *Curr.*
1378 *Opin. Virol.* **2**, 28–36 (2012).
- 1379 262. Milne, R. S. B. *et al.* Function of Herpes Simplex Virus Type 1 gD Mutants
1380 with Different Receptor-Binding Affinities in Virus Entry and Fusion. *J.*
1381 *Viol.* **77**, 8962–8972 (2003).
- 1382 263. Carfi, A. *et al.* Herpes simplex virus glycoprotein D bound to the human
1383 receptor HveA. *Mol. Cell* **8**, 169–179 (2001).
- 1384 264. Zhang, N. *et al.* Binding of herpes simplex virus glycoprotein D to nectin-1
1385 exploits host cell adhesion. *Nat. Commun.* **2**, 1–10 (2011).
- 1386 265. Krummenacher, C. *et al.* Localization of a Binding Site for Herpes Simplex
1387 Virus Glycoprotein D on Herpesvirus Entry Mediator C by Using
1388 Antireceptor Monoclonal Antibodies. *J. Virol.* **74**, 10863–10872 (2000).
- 1389 266. Navaratnarajah, C. K., Miest, T. S., Carfi, A. & Cattaneo, R. Targeted
1390 entry of enveloped viruses: Measles and herpes simplex virus i. *Curr.*
1391 *Opin. Virol.* **2**, 43–49 (2012).
- 1392 267. Xu, H. *et al.* Epidermal growth factor receptor in glioblastoma (Review).
1393 *Oncol. Lett.* **14**, 512–516 (2017).
- 1394 268. Uchida, H. *et al.* Effective treatment of an orthotopic xenograft model of
1395 human glioblastoma using an EGFR-retargeted oncolytic herpes simplex
1396 virus. *Mol. Ther.* **21**, 561–569 (2013).
- 1397 269. Menotti, L., Cerretani, A., Hengel, H. & Campadelli-Fiume, G.

- 1398 Construction of a Fully Retargeted Herpes Simplex Virus 1 Recombinant
1399 Capable of Entering Cells Solely via Human Epidermal Growth Factor
1400 Receptor 2. *J. Virol.* **82**, 10153–10161 (2008).
- 1401 270. Liu, G. *et al.* HER-2, gp100, and MAGE-1 are expressed in human
1402 glioblastoma and recognized by cytotoxic T cells. *Cancer Res.* **64**, 4980–
1403 4986 (2004).
- 1404 271. Gambini, E. *et al.* Replication-competent herpes simplex virus retargeted
1405 to HER2 as therapy for high-grade glioma. *Mol. Ther.* **20**, 994–1001
1406 (2012).
- 1407 272. Nguyen, H.-M. & Saha, D. The Current State of Oncolytic Herpes Simplex
1408 Virus for Glioblastoma Treatment. *Oncolytic Virotherapy* **Volume 10**, 1–
1409 27 (2021).
- 1410 273. Zhou, Z. *et al.* Multiple strategies to improve the therapeutic efficacy of
1411 oncolytic herpes simplex virus in the treatment of glioblastoma (Review).
1412 *Oncol. Lett.* **22**, 1–10 (2021).
- 1413 274. Totsch, S. K., Schlappi, C., Kang, K. D., Ishizuka, A. S., Lynn, G. M., Fox,
1414 B., Beierle, E. A., Whitley, R. J., Markert, J. M., Gillespie, G. Y.,
1415 Bernstock, J. D., & Friedman, G. K. Oncolytic Herpes Simplex Virus
1416 Immunotherapy for Brain Tumors: Current Pitfalls and Emerging
1417 Strategies to Overcome Therapeutic Resistance. *Oncogene.* **389**, 6159–
1418 6171 (2019).
- 1419 275. Nguyen, K. G. *et al.* Localized Interleukin-12 for Cancer Immunotherapy.
1420 *Front. Immunol.* **11**, 1–36 (2020).
- 1421 276. Cheema, T. A. *et al.* Multifaceted oncolytic virus therapy for glioblastoma
1422 in an immunocompetent cancer stem cell model. *Proc. Natl. Acad. Sci. U.*

- 1423 S. A. **110**, 12006–12011 (2013).
- 1424 277. Zachary Barnard, MS, Hiroshi Wakimoto, MD, Cecile Zaupa, PhD, D.
1425 Sanjeeva Jeyeretna, MD, Anoop P. Patel, MD, Jacqueline Kle, Robert L
1426 Martuza, MD, Samuel D. Rabkin, PhD, and William T. Curry Jr., M.
1427 Expression of FMS-like Tyrosine Kinase 3 Ligand by Oncolytic Herpes
1428 Simplex Virus Type I Prolongs Survival in Mice Bearing Established
1429 Syngeneic Intracranial Malignant Glioma. *Neurosurgery*. **71**, 741–748
1430 (2012).
- 1431 278. Tamura, K. *et al.* Multimechanistic tumor targeted oncolytic virus
1432 overcomes resistance in brain tumors. *Mol. Ther.* **21**, 68–77 (2013).
- 1433 279. Deng, L., Zhai, X., Liang, P. & Cui, H. Overcoming trail resistance for
1434 glioblastoma treatment. *Biomolecules* **11**, 1–17 (2021).
- 1435 280. Rozanov, D. V. *et al.* Engineering a leucine zipper-TRAIL homotrimer with
1436 improved cytotoxicity in tumor cells. *Mol. Cancer Ther.* **8**, 1515–1525
1437 (2009).
- 1438 281. Jahan, N. *et al.* Therapeutic targeting of chemoresistant and recurrent
1439 glioblastoma stem cells with a proapoptotic variant of oncolytic herpes
1440 simplex virus. **141**, 1671–1681 (2017).
- 1441 282. Zhang, W. *et al.* Combination of oncolytic herpes simplex Viruses armed
1442 with angiostatin and IL-12 enhances antitumor efficacy in human
1443 Glioblastoma models. *Neoplasia (United States)* **15**, 591–599 (2013).
- 1444 283. Zhang, W. *et al.* Bevacizumab with angiostatin-armed oHSV increases
1445 antiangiogenesis and decreases bevacizumab-induced invasion in U87
1446 glioma. *Mol. Ther.* **20**, 37–45 (2012).
- 1447 284. Zhang, G. *et al.* Enhanced antitumor efficacy of an oncolytic herpes

- 1448 simplex virus expressing an endostatin-angiostatin fusion gene in human
1449 glioblastoma stem cell xenografts. *PLoS One* **9**, 1–9 (2014).
- 1450 285. Mustafa Khasraw, David A. Reardon, Michael Weller, J. H. S. PD-1
1451 inhibitors: Do they have a future in the treatment of glioblastoma? *Clin*
1452 *Cancer Res.* **26**, 5287–5296 (2020).
- 1453 286. Passaro C, Alayo Q, De Laura I, McNulty J, Grauwet K, Ito H, Bhaskaran
1454 V, Mineo M, Lawler SE, Shah K, Speranza MC, Goins W, McLaughlin E,
1455 Fernandez S, Reardon DA, Freeman GJ, Chiocca EA, N. H. Arming an
1456 Oncolytic Herpes Simplex Virus Type 1 with a Single- chain Fragment
1457 Variable Antibody against PD-1 for Experimental Glioblastoma Therapy.
1458 *Clin Cancer Res.* **26**, 758 (2019).
- 1459 287. Martuza, R. L., Malick, A., Markert, J. M., Ruffner, K. L. & Coen, D. M.
1460 Experimental therapy of human glioma by means of a genetically
1461 engineered virus mutant. *Science (80-)*. **252**, 854–856 (1991).
- 1462 288. Mineta, T., Rabkin, S. D. & Martuza, R. L. Treatment of Malignant
1463 Gliomas Using Ganciclovir-hypersensitive, Ribonucleotide Reductase-
1464 deficient Herpes Simplex Viral Mutant. *Cancer Res.* **54**, 3963–3966
1465 (1994).
- 1466 289. Kesari S, Randazzo BP, Valyi-Nagy T, Huang QS, Brown SM, MacLean
1467 AR, Lee VM, Trojanowski JQ, F. N. Therapy of experimental human brain
1468 tumors using a neuroattenuated herpes simplex virus mutant. *Lab Invest.*
1469 **73**, 636–48 (1995).
- 1470 290. Advani, S. J. *et al.* Enhancement of replication of genetically engineered
1471 herpes simplex viruses by ionizing radiation: A new paradigm for
1472 destruction of therapeutically intractable tumors. *Gene Ther.* **5**, 160–165

- 1473 (1998).
- 1474 291. Chiocca, E. A., Nakashima, H., Kasai, K., Fernandez, S. A. & Oglesbee,
1475 M. Preclinical Toxicology of rQNestin34.5v.2: An Oncolytic Herpes Virus
1476 with Transcriptional Regulation of the ICP34.5 Neurovirulence Gene. *Mol.*
1477 *Ther. - Methods Clin. Dev.* **17**, 871–893 (2020).
- 1478 292. Shah, A. C. *et al.* Enhanced antiglioma activity of chimeric HCMV/HSV-1
1479 oncolytic viruses. *Gene Ther.* **14**, 1045–1054 (2007).
- 1480 293. Ryuichi Kanai, Hiroaki Wakimoto, Robert L. Martuza, and S. D. R. A
1481 Novel Oncolytic Herpes Simplex Virus that Synergizes with
1482 Phosphatidylinositol 3-Kinase/Akt Pathway Inhibitors to Target
1483 Glioblastoma Stem Cells. *Clin Cancer* **17**, 3686–3696 (2011).
- 1484 294. Reisoli, E. *et al.* Efficacy of HER2 retargeted herpes simplex virus as
1485 therapy for high-grade glioma in immunocompetent mice. *Cancer Gene*
1486 *Ther.* **19**, 788–795 (2012).
- 1487 295. Alessandrini, F. *et al.* Eradication of glioblastoma by immuno-virotherapy
1488 with a retargeted oncolytic HSV in a preclinical model. *Oncogene* **38**,
1489 4467–4479 (2019).
- 1490 296. Mazzacurati, L. *et al.* Use of miRNA response sequences to block off-
1491 target replication and increase the safety of an unattenuated,
1492 glioblastoma-targeted oncolytic HSV. *Mol. Ther.* **23**, 99–107 (2015).
- 1493 297. Sette, P. *et al.* GBM-Targeted oHSV Armed with Matrix Metalloproteinase
1494 9 Enhances Anti-tumor Activity and Animal Survival. *Mol. Ther. -*
1495 *Oncolytics* **15**, 214–222 (2019).
- 1496 298. Tomita, Y. *et al.* Oncolytic herpes virus armed with vasculostatin in
1497 combination with bevacizumab abrogates glioma invasion via the CCN1

- 1498 and AKT signaling pathways. *Mol. Cancer Ther.* **18**, 1418–1429 (2019).
- 1499 299. Fujii, K., Kurozumi, K., Ichikawa, T., Onishi, M., Shimazu, Y., Ishida, J.,
1500 Chiocca, E. A., Kaur, B., & Date, I. The integrin inhibitor cilengitide
1501 enhances the anti-glioma efficacy of vasculostatin-expressing oncolytic
1502 virus. *Cancer Gene Ther.* **20**, 139–148 (2013).
- 1503 300. Ryuichi Kanai, MD, PhD, Hiroaki Wakimoto, MD, PhD Tooba Cheema,
1504 PhD, Samuel D Rabkin, P. Oncolytic herpes simplex virus vectors and
1505 chemotherapy: are combinatorial strategies more effective for cancer?
1506 *Futur. Oncol* **6**, 619–634 (2010).
- 1507 301. Aghi, M., Rabkin, S. & Martuza, R. L. Effect of chemotherapy-induced
1508 DNA repair on oncolytic herpes simplex viral replication. *J. Natl. Cancer*
1509 *Inst.* **98**, 38–50 (2006).
- 1510 302. Hadjipanayis, C. G. & DeLuca, N. A. Inhibition of DNA repair by a herpes
1511 simplex virus vector enhances the radiosensitivity of human glioblastoma
1512 cells. *Cancer Res.* **65**, 5310–5316 (2005).
- 1513 303. Matthias Preusser, Michael Lim, David A. Hafler, David A. Reardon, and
1514 J. H. S. Prospects of immune checkpoint modulators in the treatment of
1515 glioblastoma. *Nat Rev Neurol.* **11**, 504–514 (2015).
- 1516 304. Saha D, Martuza RL, R. S. Macrophage polarization contributes to
1517 Glioblastoma eradication by combination immunovirotherapy and immune
1518 checkpoint blockade. *Cancer Cell* **32**, 253–267 (2017).
- 1519 305. Bommareddy, P. K., Peters, C., Saha, D., Rabkin, S. D. & Kaufman, H. L.
1520 Oncolytic Herpes Simplex Viruses as a Paradigm for the Treatment of
1521 Cancer. *Annu. Rev. Cancer Biol.* **2**, 155–173 (2018).
- 1522 306. Ribas, A. *et al.* Oncolytic Virotherapy Promotes Intratumoral T Cell

- 1523 Infiltration and Improves Anti-PD-1 Immunotherapy. *Cell* **170**, 1109-
1524 1119.e10 (2017).
- 1525 307. Saha, D., Martuza, R. L. & Rabkin, S. D. Oncolytic herpes simplex virus
1526 immunovirotherapy in combination with immune checkpoint blockade to
1527 treat glioblastoma. *Immunotherapy* **10**, 779–786 (2018).
- 1528 308. Cerullo, V. & Ylo, E. Design and application of oncolytic viruses for cancer
1529 immunotherapy – sma – ki and Vincenzo Cerullo. *Curr. Opin. Biotechnol.*
1530 (2019).
- 1531 309. Bartlett, D. L. *et al.* Oncolytic viruses as therapeutic cancer vaccines. *Mol.*
1532 *Cancer* **12**, 1–16 (2013).
- 1533 310. Takasu, A. *et al.* Immunogenic cell death by oncolytic herpes simplex
1534 virus type 1 in squamous cell carcinoma cells. *Cancer Gene Ther.* **23**,
1535 107–113 (2016).
- 1536 311. Guo, Z. S., Liu, Z. & Bartlett, D. L. Oncolytic immunotherapy: Dying the
1537 right way is a key to eliciting potent antitumor immunity. *Front. Oncol.* **4**
1538 **APR**, 1–11 (2014).
- 1539 312. Stefani Spranger, Daisy Dai, Brendan Horton, and T. G. Tumor-residing
1540 Batf3 dendritic cells are required for effector T cell trafficking and adoptive
1541 T cell therapy. *Cancer Cell.* **31**, 711–723 (2017).
- 1542 313. Schmidt, S. V., Nino-Castro, A. C. & Schultze, J. L. Regulatory dendritic
1543 cells: There is more than just immune activation. *Front. Immunol.* **3**, 1–17
1544 (2012).
- 1545 314. Cai, X., Chiu, Y. H. & Chen, Z. J. The cGAS-cGAMP-STING pathway of
1546 cytosolic DNA sensing and signaling. *Mol. Cell* **54**, 289–296 (2014).
- 1547 315. Mihret, A., Mamo, G., Tafesse, M., Hailu, A. & Parida, S. Dendritic cells

- 1548 activate and mature after infection with mycobacterium tuberculosis. *BMC*
1549 *Res. Notes* **4**, 1–7 (2011).
- 1550 316. Takeuchi, O. & Akira, S. Pattern Recognition Receptors and
1551 Inflammation. *Cell* **140**, 805–820 (2010).
- 1552 317. Müller, M., Carter, S., Hofer, M. J. & Campbell, I. L. Review: The
1553 chemokine receptor CXCR3 and its ligands CXCL9, CXCL10 and
1554 CXCL11 in neuroimmunity - A tale of conflict and conundrum.
1555 *Neuropathol. Appl. Neurobiol.* **36**, 368–387 (2010).
- 1556 318. Bommareddy, P. K., Shettigar, M. & Kaufman, H. L. Integrating oncolytic
1557 viruses in combination cancer immunotherapy. *Nat. Rev. Immunol.* **18**,
1558 498–513 (2018).
- 1559 319. Goldsmith, K., Chen, W., Johnson, D. C. & Hendricks, R. L. Infected cell
1560 protein (ICP)47 enhances herpes simplex virus neurovirulence by
1561 blocking the CD8+ T cell response. *J. Exp. Med.* **187**, 341–348 (1998).
- 1562 320. Brode, S. & MacAry, P. A. Cross-presentation: Dendritic cells and
1563 macrophages bite off more than they can chew! *Immunology* **112**, 345–
1564 351 (2004).
- 1565 321. Gulley, J. L. *et al.* Role of antigen spread and distinctive characteristics of
1566 immunotherapy in cancer treatment. *J. Natl. Cancer Inst.* **109**, 1–9 (2017).
- 1567 322. Gujar, S. A. & Lee, P. W. K. Oncolytic virus-mediated reversal of impaired
1568 tumor antigen presentation. *Front. Oncol.* **4 APR**, 1–7 (2014).
- 1569 323. Koch, M. S., Lawler, S. E. & Antonio Chiocca, E. Hsv-1 oncolytic viruses
1570 from bench to bedside: An overview of current clinical trials. *Cancers*
1571 *(Basel)*. **12**, 1–16 (2020).
- 1572 324. Streby, K. A. *et al.* First-in-Human Intravenous Seprehvir in Young Cancer

- 1573 Patients: A Phase 1 Clinical Trial. *Mol. Ther.* **27**, 1930–1938 (2019).
- 1574 325. MacKie, R. M., Stewart, B. & Brown, S. M. Intralesional injection of herpes
1575 simplex virus 1716 in metastatic melanoma. *Lancet* **357**, 525–526 (2001).
- 1576 326. Rampling, R. *et al.* Toxicity evaluation of replication-competent herpes
1577 simplex virus (ICP 34.5 null mutant 1716) in patients with recurrent
1578 malignant glioma. *Gene Ther.* **7**, 859–866 (2000).
- 1579 327. Papanastassiou, V. *et al.* The potential for efficacy of the modified (ICP
1580 34.5-) herpes simplex virus HSV1716 following intratumoural injection into
1581 malignant glioma: A proof of principle study. *Gene Ther.* **9**, 398–406
1582 (2002).
- 1583 328. Harrow, S. *et al.* HSV1716 injection into the brain adjacent to tumour
1584 following surgical resection of high-grade glioma: Safety data and long-
1585 term survival. *Gene Ther.* **11**, 1648–1658 (2004).
- 1586 329. Markert, J. M. *et al.* A phase 1 trial of oncolytic HSV-1, g207, given in
1587 combination with radiation for recurrent GBM demonstrates safety and
1588 radiographic responses. *Mol. Ther.* **22**, 1048–1055 (2014).
- 1589 330. Foreman, P. M., Friedman, G. K., Cassady, K. A. & Markert, J. M.
1590 Oncolytic Virotherapy for the Treatment of Malignant Glioma.
1591 *Neurotherapeutics* **14**, 333–344 (2017).
- 1592 331. Markert, J. M. *et al.* Conditionally replicating herpes simplex virus mutant
1593 G207 for the treatment of malignant glioma: Results of a phase I trial.
1594 *Gene Ther.* **7**, 867–874 (2000).
- 1595 332. Markert, J. M. *et al.* Phase Ib trial of mutant herpes simplex virus G207
1596 inoculated pre-and post-tumor resection for recurrent GBM. *Mol. Ther.* **17**,
1597 199–207 (2009).

- 1598 333. Taguchi, S., Fukuhara, H. & Todo, T. Oncolytic virus therapy in Japan:
1599 Progress in clinical trials and future perspectives. *Jpn. J. Clin. Oncol.* **49**,
1600 201–209 (2019).
- 1601 334. Hua, L. & Wakimoto, H. Oncolytic herpes simplex virus therapy for
1602 malignant glioma: current approaches to successful clinical application.
1603 *Expert Opin. Biol. Ther.* **19**, 845–854 (2019).
- 1604 335. Patel, D. M. *et al.* Design of a Phase i Clinical Trial to Evaluate M032, a
1605 Genetically Engineered HSV-1 Expressing IL-12, in Patients with
1606 Recurrent/Progressive Glioblastoma Multiforme, Anaplastic Astrocytoma,
1607 or Gliosarcoma. *Hum. Gene Ther. Clin. Dev.* **27**, 69–78 (2016).
- 1608 336. Eissa, I. R. *et al.* Genomic signature of the natural oncolytic herpes
1609 simplex virus HF10 and its therapeutic role in preclinical and clinical trials.
1610 *Front. Oncol.* **7**, 1–12 (2017).
- 1611 337. Nakao, A. *et al.* A phase i dose-escalation clinical trial of intraoperative
1612 direct intratumoral injection of HF10 oncolytic virus in non-resectable
1613 patients with advanced pancreatic cancer. *Cancer Gene Ther.* **18**, 167–
1614 175 (2011).
- 1615 338. Kelly, K. J., Wong, J. & Fong, Y. Herpes simplex virus NV1020 as a novel
1616 and promising therapy for hepatic malignancy. *Expert Opin. Investig.*
1617 *Drugs* **17**, 1105–1113 (2008).
- 1618 339. Ebright, M. I. *et al.* Replication-competent herpes virus NV1020 as direct
1619 treatment of pleural cancer in a rat model. *J. Thorac. Cardiovasc. Surg.*
1620 **124**, 123–129 (2002).
- 1621 340. Bennett, J. J. *et al.* Comparison of safety, delivery, and efficacy of two
1622 oncolytic herpes viruses (G207 and NV1020) for peritoneal cancer.

- 1623 *Cancer Gene Ther.* **9**, 935–945 (2002).
- 1624 341. Liu, B. L. *et al.* ICP34.5 deleted herpes simplex virus with enhanced
1625 oncolytic, immune stimulating, and anti-tumour properties. *Gene Ther.* **10**,
1626 292–303 (2003).
- 1627 342. Puzanov, I. *et al.* Talimogene laherparepvec in combination with
1628 ipilimumab in previously untreated, unresectable stage IIIB-IV melanoma.
1629 *J. Clin. Oncol.* **34**, 2619–2626 (2016).
- 1630 343. Waters, A. M. *et al.* Rationale and Design of a Phase 1 Clinical Trial to
1631 Evaluate HSV G207 Alone or with a Single Radiation Dose in Children
1632 with Progressive or Recurrent Malignant Supratentorial Brain Tumors.
1633 *Hum. Gene Ther. Clin. Dev.* **28**, 7–16 (2017).
- 1634 344. Bernstock, J. D. *et al.* Design and Rationale for First-in-Human Phase 1
1635 Immunovirotherapy Clinical Trial of Oncolytic HSV G207 to Treat
1636 Malignant Pediatric Cerebellar Brain Tumors. *Hum. Gene Ther.* **31**, 1132–
1637 1139 (2020).
- 1638 345. Tischer, B. K., Von Einem, J., Kaufer, B. & Osterrieder, N. Two-step Red-
1639 mediated recombination for versatile high-efficiency markerless DNA
1640 manipulation in *Escherichia coli*. *Biotechniques* **40**, 191–197 (2006).
- 1641 346. Todo, T., Martuza, R. L., Rabkin, S. D. & Johnson, P. A. Oncolytic herpes
1642 simplex virus vector with enhanced MHC class I presentation and tumor
1643 cell killing. *Proc. Natl. Acad. Sci. U. S. A.* **98**, 6396–401 (2001).
- 1644 347. Shah, K., Tung, C. H., Yang, K., Weissleder, R. & Breakefield, X. O.
1645 Inducible Release of TRAIL Fusion Proteins from a Proapoptotic Form for
1646 Tumor Therapy. *Cancer Res.* **64**, 3236–3242 (2004).
- 1647 348. Uchida, H. *et al.* A Double Mutation in Glycoprotein gB Compensates for

- 1648 Ineffective gD-Dependent Initiation of Herpes Simplex Virus Type 1
1649 Infection. *J. Virol.* **84**, 12200–12209 (2010).
- 1650 349. WF, G. *et al.* Engineering HSV-1 Vectors for Gene Therapy. *Methods*
1651 *Mol. Biol.* **2060**, (2020).
- 1652 350. Marconi, P. & Manservigi, R. Herpes simplex virus growth, preparation,
1653 and assay. *Methods Mol. Biol.* **1144**, 19–29 (2014).
- 1654 351. Kroonen, J. *et al.* Human glioblastoma-initiating cells invade specifically
1655 the subventricular zones and olfactory bulbs of mice after striatal injection.
1656 *Int. J. Cancer* **129**, 574–585 (2011).
- 1657 352. Wakimoto, H. *et al.* Human glioblastoma-derived cancer stem cells:
1658 Establishment of invasive glioma models and treatment with oncolytic
1659 herpes simplex virus vectors. *Cancer Res.* **69**, 3472–3481 (2009).
- 1660 353. US20170362314A1 - Anti-CXCL12 Antibody Molecules and Their Uses -
1661 Google Patents.
- 1662 354. Uchida, H. *et al.* Effective treatment of an orthotopic xenograft model of
1663 human glioblastoma using an EGFR-retargeted oncolytic herpes simplex
1664 virus. *Mol. Ther.* **21**, 561–9 (2013).
- 1665 355. Cocchi, F., Menotti, L., Mirandola, P., Lopez, M. & Campadelli-Fiume, G.
1666 The Ectodomain of a Novel Member of the Immunoglobulin Subfamily
1667 Related to the Poliovirus Receptor Has the Attributes of a Bona Fide
1668 Receptor for Herpes Simplex Virus Types 1 and 2 in Human Cells. *J.*
1669 *Virol.* **72**, 9992–10002 (1998).
- 1670 356. Uchida, H. *et al.* Generation of Herpesvirus Entry Mediator (HVEM)-
1671 Restricted Herpes Simplex Virus Type 1 Mutant Viruses: Resistance of
1672 HVEM-Expressing Cells and Identification of Mutations That Rescue

- 1673 Nectin-1 Recognition. *J. Virol.* **83**, 2951–2961 (2009).
- 1674 357. Frampton, A. R. *et al.* Equine Herpesvirus 1 Enters Cells by Two Different
1675 Pathways, and Infection Requires the Activation of the Cellular Kinase
1676 ROCK1. *J. Virol.* **81**, 10879–10889 (2007).
- 1677 358. Lathia, J. D., Mack, S. C., Mulkearns-Hubert, E. E., Valentim, C. L. L. &
1678 Rich, J. N. Cancer stem cells in glioblastoma. *Genes and Development*
1679 vol. 29 1203–1217 (2015).
- 1680 359. Tang, X. *et al.* Targeting Glioblastoma Stem Cells: A Review on
1681 Biomarkers, Signal Pathways and Targeted Therapy. *Frontiers in*
1682 *Oncology* vol. 11 (2021).
- 1683 360. Connolly, S. A., Jardetzky, T. S. & Longnecker, R. The structural basis of
1684 herpesvirus entry. *Nature Reviews Microbiology* vol. 19 110–121 (2021).
- 1685 361. Zhou, G. & Roizman, B. Construction and properties of a herpes simplex
1686 virus 1 designed to enter cells solely via the IL-13 α 2 receptor. *Proc. Natl.*
1687 *Acad. Sci. U. S. A.* **103**, 5508–5513 (2006).
- 1688 362. Kamiyama, H., Zhou, G. & Roizman, B. Herpes simplex virus 1
1689 recombinant virions exhibiting the amino terminal fragment of urokinase-
1690 type plasminogen activator can enter cells via the cognate receptor. *Gene*
1691 *Ther.* **13**, 621–629 (2006).
- 1692 363. Menotti, L. *et al.* Inhibition of human tumor growth in mice by an oncolytic
1693 herpes simplex virus designed to target solely HER-2-positive cells. *Proc.*
1694 *Natl. Acad. Sci. U. S. A.* **106**, 9039–44 (2009).
- 1695 364. Glorioso, J. C. Identification of mutations in herpes simplex virus envelope
1696 glycoproteins that enable or enhance vector retargeting to novel non-HSV
1697 receptors. vol. 2 (2013).

- 1698 365. Wajant, H. Molecular mode of action of TRAIL receptor agonists—
1699 Common principles and their translational exploitation. *Cancers (Basel)*.
1700 **11**, (2019).
- 1701 366. Ashkenazi, A. & Dixit, V. M. Apoptosis control by death and decoy
1702 receptors. *Curr. Opin. Cell Biol.* **11**, 255–260 (1999).
- 1703 367. Wu, X., He, Y., Falo, L. D., Hui, K. M. & Huang, L. Regression of human
1704 mammary adenocarcinoma by systemic administration of a recombinant
1705 gene encoding the hFlex-TRAIL fusion protein. *Mol. Ther.* **3**, 368–374
1706 (2001).
- 1707 368. Lynch DH, Andreason A, Maraskovsky E, Whitmore J, Miller RE, S. J.
1708 Flt3 ligand induces tumor regression and anti-tumor immune responses in
1709 vivo. *Nat Med* **3**, 625–31 (1997).
- 1710 369. Wu, X. & Hui, K. M. Induction of potent TRAIL-mediated tumoricidal
1711 activity by hFlex/furin/TRAIL recombinant DNA construct]. *Mol. Ther.* **9**,
1712 674–681 (2004).
- 1713 370. Jahan, N., Lee, J. M., Shah, K. & Wakimoto, H. Therapeutic targeting of
1714 chemoresistant and recurrent glioblastoma stem cells with a proapoptotic
1715 variant of oncolytic herpes simplex virus. *Int. J. cancer* **141**, 1671–1681
1716 (2017).
- 1717 371. Tamura, K. *et al.* Multimechanistic tumor targeted oncolytic virus
1718 overcomes resistance in brain tumors. *Mol. Ther.* **21**, 68–77 (2013).
- 1719 372. Tang, X. *et al.* Targeting Glioblastoma Stem Cells: A Review on
1720 Biomarkers, Signal Pathways and Targeted Therapy. *Front. Oncol.* **11**, 1–
1721 17 (2021).
- 1722 373. Kambara, H., Okano, H., Chiocca, E. A. & Saeki, Y. An oncolytic HSV-1

1723 mutant expressing ICP34.5 under control of a nestin promoter increases
1724 survival of animals even when symptomatic from a brain tumor. *Cancer*
1725 *Res.* **65**, 2832–2839 (2005).

1726 374. Tang, C. & Guo, W. Implantation of a mini-osmotic pump plus
1727 stereotactical injection of retrovirus to study newborn neuron development
1728 in adult mouse hippocampus. *STAR Protoc.* **2**, 100374 (2021).

1729 375. Jahan, N. *et al.* Therapeutic targeting of chemoresistant and recurrent
1730 glioblastoma stem cells with a proapoptotic variant of oncolytic herpes
1731 simplex virus. **141**, 1671–1681 (2018).

1732 376. Meisen WH, Wohleb ES, Jaime-Ramirez AC, Bolyard C, Yoo JY, Russell
1733 L, Hardcastle J, Dubin S, Muili K, Yu J, Caligiuri M, Godbout J, K. B. The
1734 impact of macrophage and microglia secreted TNF α on oncolytic HSV-1
1735 therapy in the glioblastoma tumor microenvironment. *Clin Cancer Res.*
1736 **21**, 3274–85 (2015).

1737 377. Hutzen, B. *et al.* TGF- β Inhibition Improves Oncolytic Herpes
1738 Viroimmunotherapy in Murine Models of Rhabdomyosarcoma. *Mol. Ther.*
1739 *- Oncolytics* **7**, 17–26 (2017).

1740 378. Lee TJ, Nair M, Banasavadi-Siddegowda Y, Liu J, Nallanagulagari T,
1741 Jaime-Ramirez AC, Guo JY, Quadri H, Zhang J, Bockhorst KH, Aghi MK,
1742 Carbonell WS, Kaur B, Y. J. Enhancing Therapeutic Efficacy of Oncolytic
1743 Herpes Simplex Virus-1 with Integrin β 1 Blocking Antibody OS2966. *Mol*
1744 *Cancer Ther* **18**, 1127–1136 (2019).

1745 379. Tasaki, T. *et al.* MET expressed in glioma stem cells is a potent
1746 therapeutic target for glioblastoma multiforme. *Anticancer Res.* **36**, 3571–
1747 3577 (2016).

- 1748 380. Alves, A. L. V. *et al.* Role of glioblastoma stem cells in cancer therapeutic
1749 resistance: a perspective on antineoplastic agents from natural sources
1750 and chemical derivatives. *Stem Cell Res. Ther.* **12**, 1–22 (2021).
- 1751 381. Jacob F, Salinas RD, Zhang DY, Nguyen PTT, Schnoll JG, Wong SZH,
1752 Thokala R, Sheikh S, Saxena D, Prokop S, Liu DA, Qian X, Petrov D,
1753 Lucas T, Chen HI, Dorsey JF, Christian KM, Binder ZA, Nasrallah M,
1754 Brem S, O'Rourke DM, Ming GL, S. H. A Patient-Derived Glioblastoma
1755 Organoid Model and Biobank Recapitulates Inter- and Intra-tumoral
1756 Heterogeneity. *Cell* **180**, 188–204 (2020).
- 1757 382. Lee, J. *et al.* Tumor stem cells derived from glioblastomas cultured in
1758 bFGF and EGF more closely mirror the phenotype and genotype of
1759 primary tumors than do serum-cultured cell lines. *Cancer Cell* **9**, 391–403
1760 (2006).
- 1761 383. Nguyen, M. L., Kraft, R. M. & Blaho, J. A. Susceptibility of cancer cells to
1762 herpes simplex virus-dependent apoptosis. *J. Gen. Virol.* **88**, 1866–1875
1763 (2007).
- 1764 384. Nguyen, M. L. *et al.* p53 and hTERT Determine Sensitivity to Viral
1765 Apoptosis. *J. Virol.* **81**, 12985–12995 (2007).
- 1766 385. Maruzuru, Y. *et al.* p53 Is a Host Cell Regulator during Herpes Simplex
1767 Encephalitis. *J. Virol.* **90**, 6738–6745 (2016).
- 1768 386. LeBlanc, H. N. & Ashkenazi, A. Apo2L/TRAIL and its death and decoy
1769 receptors. *Cell Death Differ.* **10**, 66–75 (2003).
- 1770 387. Bellail, A. C. *et al.* DR5-mediated DISC controls caspase-8 cleavage and
1771 initiation of apoptosis in human glioblastomas. *J. Cell. Mol. Med.* **14**,
1772 1303–1317 (2010).

- 1773 388. Ding L, Yuan C, Wei F, Wang G, Zhang J, Bellail AC, Zhang Z, Olson JJ,
1774 H. C. Cisplatin Restores TRAIL apoptotic pathway in Glioblastoma-
1775 Derived Stem Cells through Up-regulation of DR5 and Down- regulation
1776 of c-FLIP. *Cancer Invest.* **29**, 551–520 (2011).
- 1777 389. Yan, W., Xiao, D. & Yao, K. Combined bioluminescence and fluorescence
1778 imaging visualizing orthotopic lung adenocarcinoma xenograft in vivo.
1779 *Acta Biochim. Biophys. Sin. (Shanghai)*. **43**, 595–600 (2011).
- 1780 390. Alvarez-Breckenridge, C. A. *et al.* NK cells impede glioblastoma
1781 virotherapy through NKp30 and NKp46 natural cytotoxicity receptors. *Nat.*
1782 *Med.* **18**, 1827–34 (2012).
- 1783 391. Fulci, G. *et al.* Depletion of Peripheral Macrophages and Brain Microglia
1784 Increases Brain Tumor Titers of Oncolytic Viruses. **67**, 9398–9406 (2007).
- 1785 392. Meisen, W. H., Wohleb, E. S., Jaime-Ramirez, A. C., Bolyard, C., Yoo, J.
1786 Y., Russell, L., Hardcastle, J., Dubin, S., Muili, K., Yu, J., Caligiuri, M.,
1787 Godbout, J., & Kaur, B. The impact of macrophage and microglia
1788 secreted TNF α on oncolytic HSV-1 therapy in the glioblastoma tumor
1789 microenvironment. *Clin Cancer Res.* 2015 **21**, 3274–3285 (2015).
- 1790 393. Buonfiglioli, A. & Hambarzumyan, D. Macrophages and microglia: the
1791 cerberus of glioblastoma. *Acta Neuropathol. Commun.* **9**, 1–21 (2021).
- 1792 394. Kaminska, B. Characteristics of Phenotype and Pro-Tumorigenic Roles of
1793 Glioma Infiltrating Microglia/Macrophages. *J. Neurol. Neurophysiol.* **s5**, 1–
1794 8 (2011).
- 1795 395. Blitz, S. E. *et al.* Tumor-Associated Macrophages/Microglia in
1796 Glioblastoma Oncolytic Virotherapy: A Double-Edged Sword. *Int. J. Mol.*
1797 *Sci.* **23**, (2022).

- 1798 396. Uche, I. K., Kousoulas, K. G. & Rider, P. J. F. The Effect of Herpes
1799 Simplex Virus-Type-1 (HSV-1) Oncolytic Immunotherapy on the Tumor
1800 Microenvironment. **1**, 1–16 (2021).
- 1801 397. Isci, D. *et al.* Patient-oriented perspective on chemokine receptor
1802 expression and function in glioma. *Cancers (Basel)*. **14**, 1–17 (2022).
- 1803 398. Lee, E. Q. *et al.* Phase I and biomarker study of plerixafor and
1804 bevacizumab in recurrent high-grade glioma. *Clin. Cancer Res.* **24**, 4643–
1805 4649 (2018).
- 1806 399. Hattermann, K. *et al.* Chemokine expression profile of freshly isolated
1807 human glioblastoma- associated macrophages/microglia. *Oncol. Rep.* **32**,
1808 270–276 (2014).
- 1809 400. Feng, Y., Broder, C. C., Kennedy, P. E. & Berger, E. A. HIV-1 entry
1810 cofactor: Functional cDNA cloning of a seven-transmembrane, G protein-
1811 coupled receptor. *Science (80-.)*. **272**, 872–877 (1996).
- 1812 401. Alimohammadi, M., Rahimi, A., Faramarzi, F., Alizadeh-Navaei, R. &
1813 Rafiei, A. Overexpression of chemokine receptor CXCR4 predicts lymph
1814 node metastatic risk in patients with melanoma: A systematic review and
1815 meta-analysis. *Cytokine* **148**, 155691 (2021).
- 1816 402. Salmaggi, A. *et al.* CXCL12 expression is predictive of a shorter time to
1817 tumor progression in low-grade glioma: A single-institution study in 50
1818 patients. *J. Neurooncol.* **74**, 287–293 (2005).
- 1819 403. Katsumoto, K. & Kume, S. The role of CXCL12-CXCR4 signaling pathway
1820 in pancreatic development. *Theranostics* vol. 3 11–17 (2013).
- 1821 404. Gagliardi, F. *et al.* The role of CXCR4 in highly malignant human gliomas
1822 biology: Current knowledge and future directions. *Glia* **62**, 1015–1023

- 1823 (2014).
- 1824 405. Santagata, S. *et al.* CXCR4 and CXCR7 Signaling Pathways: A Focus on
1825 the Cross-Talk Between Cancer Cells and Tumor Microenvironment.
1826 *Frontiers in Oncology* vol. 11:591386. (2021).
- 1827 406. Gagner, J. P. *et al.* Multifaceted C-X-C Chemokine Receptor 4 (CXCR4)
1828 Inhibition Interferes with Anti-Vascular Endothelial Growth Factor
1829 Therapy-Induced Glioma Dissemination. *Am. J. Pathol.* **187**, 2080–2094
1830 (2017).
- 1831 407. Gatti, M. *et al.* Inhibition of CXCL12/CXCR4 autocrine/paracrine loop
1832 reduces viability of human glioblastoma stem-like cells affecting self-
1833 renewal activity. *Toxicology* **314**, 209–220 (2013).
- 1834 408. Mercurio, L. *et al.* Targeting CXCR4 by a selective peptide antagonist
1835 modulates tumor microenvironment and microglia reactivity in a human
1836 glioblastoma model. *J. Exp. Clin. Cancer Res.* **35**, 1–15 (2016).
- 1837 409. Gil, M., Seshadri, M., Komorowski, M. P., Abrams, S. I. & Kozbor, D.
1838 Targeting CXCL12/CXCR4 signaling with oncolytic virotherapy disrupts
1839 tumor vasculature and inhibits breast cancer metastases. *Proc. Natl.*
1840 *Acad. Sci. U. S. A.* **110**, E1291-300 (2013).
- 1841 410. Scala, S. Molecular pathways: Targeting the CXCR4-CXCL12 Axis-
1842 Untapped potential in the tumor microenvironment. *Clin. Cancer Res.* **21**,
1843 4278–4285 (2015).
- 1844 411. Kioi, M. *et al.* Inhibition of vasculogenesis, but not angiogenesis, prevents
1845 the recurrence of glioblastoma after irradiation in mice. *J. Clin. Invest.*
1846 **120**, 694–705 (2010).
- 1847 412. Lee, C. C. *et al.* Disrupting the CXCL12/CXCR4 axis disturbs the

- 1848 characteristics of glioblastoma stem-like cells of rat RG2 glioblastoma.
1849 *Cancer Cell Int.* **13**, (2013).
- 1850 413. Ostrom, Q. T. *et al.* CBTRUS statistical report: Primary brain and other
1851 central nervous system tumors diagnosed in the United States in 2011-
1852 2015. *Neuro-Oncology* vol. 20 iv1–iv86 (2018).
- 1853 414. Stupp, R. *et al.* Effect of Tumor-Treating Fields Plus Maintenance
1854 Temozolomide vs Maintenance Temozolomide Alone on Survival in
1855 Patients With Glioblastoma: A Randomized Clinical Trial. *JAMA* **318**,
1856 2306–2316 (2017).
- 1857 415. Lara-Velazquez, M. *et al.* Advances in brain tumor surgery for
1858 glioblastoma in adults. *Brain Sciences* vol. 7 166 (2017).
- 1859 416. Singh, S. K. *et al.* Identification of human brain tumour initiating cells.
1860 *Nature* **432**, 396–401 (2004).
- 1861 417. Galli, R. *et al.* Isolation and characterization of tumorigenic, stem-like
1862 neural precursors from human glioblastoma. *Cancer Res.* **64**, 7011–7021
1863 (2004).
- 1864 418. Chen, R. *et al.* A Hierarchy of Self-Renewing Tumor-Initiating Cell Types
1865 in Glioblastoma. *Cancer Cell* **17**, 362–375 (2010).
- 1866 419. Singh, S. K. *et al.* Identification of a cancer stem cell in human brain
1867 tumors. *Cancer Res.* **63**, 5821–5828 (2003).
- 1868 420. Goffart, N. *et al.* Adult mouse subventricular zones stimulate glioblastoma
1869 stem cells specific invasion through CXCL12/CXCR4 signaling. *Neuro.*
1870 *Oncol.* **17**, 81–94 (2015).
- 1871 421. Goffart, N. *et al.* CXCL12 mediates glioblastoma resistance to
1872 radiotherapy in the subventricular zone. *Neuro. Oncol.* **19**, 66–77 (2017).

- 1873 422. Dedobbeleer, M. *et al.* MKP1 phosphatase is recruited by CXCL12 in
1874 glioblastoma cells and plays a role in DNA strand breaks repair.
1875 *Carcinogenesis* **41**, 417–429 (2020).
- 1876 423. Cheray, M. *et al.* Cancer Stem-Like Cells in Glioblastoma. in *Glioblastoma*
1877 59–71 (Codon Publications, 2017).
1878 doi:10.15586/codon.glioblastoma.2017.ch4.
- 1879 424. Lombard, A. *et al.* The Subventricular Zone, a Hideout for Adult and
1880 Pediatric High-Grade Glioma Stem Cells. *Frontiers in Oncology* vol. 10
1881 (2021).
- 1882 425. Fountzilias, C., Patel, S. & Mahalingam, D. Review: Oncolytic virotherapy,
1883 updates and future directions. *Oncotarget* **8**, 102617–102639 (2017).
- 1884 426. Miyauchi, J. T. & Tsirka, S. E. Advances in immunotherapeutic research
1885 for glioma therapy. *J. Neurol.* **265**, 741–756 (2018).
- 1886 427. Friedman, G. K. *et al.* Engineered herpes simplex viruses efficiently infect
1887 and kill CD133+ human glioma xenograft cells that express CD111. *J.*
1888 *Neurooncol* **95**, 199–209 (2009).
- 1889 428. Rueger, M. A. *et al.* Variability in infectivity of primary cell cultures of
1890 human brain tumors with HSV-1 amplicon vectors. *Gene Ther.* **12**, 588–
1891 596 (2005).
- 1892 429. Grandi, P. *et al.* Targeting HSV-1 virions for specific binding to epidermal
1893 growth factor receptor-vIII-bearing tumor cells. *Cancer Gene Ther.* **17**,
1894 655–63 (2010).
- 1895 430. Shibata, T. *et al.* Development of an oncolytic HSV vector fully retargeted
1896 specifically to cellular EpCAM for virus entry and cell-to-cell spread. *Gene*
1897 *Ther.* **23**, 479–488 (2016).

- 1898 431. Alessandrini, F. *et al.* Eradication of glioblastoma by immuno-virotherapy
1899 with a retargeted oncolytic HSV in a preclinical model. *Oncogene* (2019)
1900 doi:10.1038/s41388-019-0737-2.
- 1901 432. Kim, M.-H., Billiar, T. R. & Seol, D.-W. The secretable form of trimeric
1902 TRAIL, a potent inducer of apoptosis. *Biochem. Biophys. Res. Commun.*
1903 **321**, 930–935 (2004).
- 1904 433. Kock, N., Kasmieh, R., Weissledery, R. & Shah, K. Tumor therapy
1905 mediated by lentiviral expression of shBcl-2 and S-TRAIL1. *Neoplasia* **9**,
1906 435–442 (2007).
- 1907 434. US20170362314A1 - Anti-CXCL12 Antibody Molecules and Their Uses -
1908 Google Patents.
- 1909 435. Uchida, H. *et al.* Effective treatment of an orthotopic xenograft model of
1910 human glioblastoma using an EGFR-retargeted oncolytic herpes simplex
1911 virus. *Mol. Ther.* **21**, 561–9 (2013).
- 1912 436. Bian, X. *et al.* Preferential expression of chemokine receptor CXCR4 by
1913 highly malignant human gliomas and its association with poor patient
1914 survival. *Neurosurgery* **61**, 570–579 (2007).
- 1915 437. Van Den Bossche, W. B. L. *et al.* Oncolytic virotherapy in glioblastoma
1916 patients induces a tumor macrophage phenotypic shift leading to an
1917 altered glioblastoma microenvironment. *Neuro. Oncol.* **20**, 1494–1504
1918 (2018).
- 1919 438. Isci, D. *et al.* Patient-oriented perspective on chemokine receptor
1920 expression and function in glioma. *Cancers* vol. 14 (2022).
- 1921 439. Tischer, B. K. *et al.* A self-excisable infectious bacterial artificial
1922 chromosome clone of varicella-zoster virus allows analysis of the

1923 essential tegument protein encoded by ORF9. *J. Virol.* **81**, 13200–8
1924 (2007).
1925

1926 Table 1: Primers used for RT-qPCR

	Forward	Reverse
HSV-1 gD	GCCCCGCTGGA ACTACTATG	TTATCTTCACGAGCCGC-AGG
sTRAIL	CATCGAGAACGAGATCGCCC	TGTGTTGCTTCTTCCTCTGGT
SOX2	AGTCTCCAAGCGACGAAAAA	TTTCACGTTTGCAACTGTCC
POU3F2	CTGACGATCTCCACGCAGTA	GGCAGAAAGCTGTCCAAGTC
SALL2	ACTCCTCTGGGGTGACCTTT	GGAGTGGTAGTGGAGGTGGA
HSV-1 gD	GCCCCGCTGGA ACTACTATG	TTATCTTCACGAGCCGC-AGG
sTRAIL	CATCGAGAACGAGATCGCCC	TGTGTTGCTTCTTCCTCTGGT
18S	AACTTTGATGGTATCGCCG	CCTTGGATGTGGTAGCCGTTT
hTBP	ACAGCCTGCCACCTTACG	TGCCATAAGGCATCATTGGACTA

1927

1928 **FIGURE LEGENDS**

1929

1930 Figure 1:

1931 **Schematic representation of oHSV/Nb-gD and oHSV/Nb-gD:sTRAIL genomes.**

1932

1933 Figure 2:

1934 **Efficacy of the oHSV de-targeting and re-targeting.**

1935 **(A)** De-targeting was evaluated by infection of J1.1-2, J/A (J1.1 HVEM⁺) and J/C
1936 (J1.1 Nectin⁺) cells were infected for 72 hours at different MOI with the recombinant
1937 oHSV expressing either WT gD (oHSV/gD) or gD modified by the insertion of an
1938 anti-hCXCR4 nanobody (oHSV/Nb-gD). Both viruses express eGFP under the
1939 control of pICP6, allowing the visualization of infected cells by epifluorescence
1940 microscopy.

1941 **(B)** Re-targeting was evaluated on U87MG and U87MG CXCR4⁺ cells. Cells were
1942 plated in 96 well plates, infected with oHSV/gD or oHSV/Nb-gD (MOI 0.1) and
1943 incubated in Incucyte® S3 for real-time analyses during 72hpi. GFP expression and
1944 cell confluency were quantified every 6 hours. Bars represent the Green area/phase
1945 area expressed as the mean \pm SEM of four wells. Statistical significance was
1946 determined by ordinary two-way ANOVA with Bonferroni multiple comparisons of
1947 means with a single pooled variance. (ns: non-significant, **** p<0,0001). Images
1948 were taken every 6 hours and representative images taken at 72hpi are shown.
1949 Additional representative whole-well images taken at 24, 48 and 72 hours are shown
1950 in Figure S2. See also growing curve of oHSV/gD and oHSV/Nb-gD in U87MG
1951 CXCR4⁺ cells in Figure S3.

1952

1953 Figure 3

1954 **Efficacy of the oHSV retargeting in patient-derived GSCs.**

1955 **(A)** Patient-derived GSC cells (T08, T013, T018 and T033), U87MG or U87MG
1956 CXCR4⁺ cells were cultured as tumorspheres and further dissociated for flow
1957 cytometry quantification of the percentage of cells expressing CXCR4 (APC⁺) at
1958 the cell membrane. Bars represent the means \pm SEM of four independent
1959 experiments. Statistical significance was determined by Kruskal-Wallis (Primary
1960 cells, **p < 0.001) or Mann-Whitney (U87MG cells, *p < 0.05) test. **(B)** Overlaid
1961 histograms of a representative analysis allowing the comparison between
1962 endogenous and ectopic CXCR4 expression.

1963 Stemness features (expression of SOX2, POUF3 and SALL2) analyzed by RT-
1964 qPCR are depicted in Figure S4.

1965 **(C)** Tumorspheres cultured in 24-well plates were infected with oHSV/gD or
1966 oHSV/Nb-gD (10⁶PFU/ml). Forty-eight hours post infection, cells were
1967 dissociated and the eGFP fluorescence was analyzed by flow cytometry. Bars
1968 represent the means \pm SEM of three independent experiments. Statistical
1969 significance was determined by ordinary 2-way ANOVA with Bonferroni's multiple
1970 comparisons of means (**p < 0.001). Raw data (overlaid histograms) representative
1971 of one experiment are shown in Figure S5.

1972 **(D)** Tumorspheres cultures in 24-well plates and infected for 48h by oHSV/Nb-
1973 gD (10⁶ PFU/ml) were either analyzed by epifluorescence for eGFP detection (left
1974 panels) or fixed for immunostaining of nestin (white) or CXCR4 (Red) and GFP
1975 detection (green). Nuclei were labeled with DAPI (Blue). Images were recorded with
1976 a NIKON A1R confocal microscope. Magnification: 40x

1977 See also Figure S6 for real-time eGFP quantification and images of T033
1978 tumorspheres infected with oHSV/gD or oHSV/Nb-gD at a higher titer (10^7 PFU/ml)
1979

1980 Figure 4

1981 **Efficacy of the oHSV arming.**

1982 **(A)** The replication efficacy of the non-armed (oHSV/Nb-gD) and sTRAIL-armed
1983 (oHSV/Nb-gD:sTRAIL) oncolytic viruses was evaluated with a growing curve assay.
1984 U87MG CXCR4⁺ cells were infected at a MOI of 1 and supernatant was harvested
1985 at 24, 48 and 72 hours post infection and used for titration as previously described
1986 ³⁵⁰. The number of foci was calculated based on Incucyte®S3 imaging. Bars
1987 represent mean \pm SEM (PFU/ml) of three independent experiments. The lack of
1988 statistical difference is confirmed by unpaired *t*-test analysis.

1989 **(B)** PARP and caspase 3 cleavage was evaluated by Western blot analysis on total
1990 cell extracts from U87MG CXCR4⁺ cells infected for 18h by oHSV/Nb-gD or
1991 oHSV/Nb-gD:sTRAIL (MOI: 0.5 or 1). gD and alpha-tubulin detection were used as
1992 infection or loading control, respectively.

1993 **(C)** Apoptosis was measured at different time points by flow cytometry using annexin
1994 V/DAPI labeling of U87MG CXCR4⁺ cells infected by oHSV/Nb-gD or oHSV/Nb-
1995 gD:sTRAIL (MOI: 5-. The percentage of apoptotic cells corresponds to early
1996 (Annexin V⁺/DAPI⁻) and late apoptotic (Annexin V⁺/DAPI⁺) cells. Percentages of
1997 apoptotic cells upon infection at other MOI (1, 5 and 10) are shown in Figure S7. In
1998 parallel, cells were incubated with resazurin to evaluate the viability upon oHSV
1999 infection. Bars and dots represent the means \pm SEM of three independent
2000 experiments. Statistical significance was determined by ordinary 2-way ANOVA with
2001 Bonferroni's multiple comparisons of means ($***p < 0.001$).

2002 **(D and E)** Patient-derived GSCs (T08, T013, T018 and T033) were cultured as
2003 tumorspheres in 24-well plates and infected with oHSV/Nb-gD or oHSV/Nb-
2004 gD:sTRAIL (10^6 PFU/ml). gD and sTRAIL relative expression was analyzed 48hpi
2005 by RT-qPCR as illustrated by a representative experiment. gD **(D)** and sTRAIL
2006 **(E)** mRNA level in oHSV/Nb-gD:sTRAIL-infected T08 is considered as the base
2007 line. (ND: not detected).

2008

2009 Figure 5

2010 ***In vivo* efficacy of oHSV/Nb-gD and oHSV/Nb-gD:sTRAIL.**

2011 **(A)** Schematic representation of the experimental settings. Nude mice were
2012 engrafted with U87MG CXCR4⁺Luc⁺ cells and virus or PBS was injected in the tumor
2013 on day 7. Mice were sacrificed on day 22 (n= 9 in each group). **(B)** Mice were
2014 regularly weighed, and for each mouse, the weight change is expressed as a
2015 percentage to the weight on day 0, considered as equal to 100%. **(C)**
2016 Bioluminescence activity was recorded with Xenogen IVIS 50[®] on day 6, 13 and 20
2017 after engraftment. See also Figure S9 for Bioluminescence imaging. **(B)** and **(C)**
2018 represent the means \pm SEM (n=9 in each group). Statistical significance was
2019 determined by 2-way ANOVA with Tukey's multiple comparisons of means. (*
2020 $p < 0.05$; ** $p < 0.01$; *** $p < 0.001$).

2021 **(D to F)** On day 22, brain from five mice were sectioned for immunostaining of
2022 human vimentin and the measurement of the tumor volume by 3D reconstruction
2023 **(D)**. Representative pictures of serial sections of 2 mice/group as well as the
2024 estimated volume of the corresponding tumor are shown in **(E)**. Data represent the
2025 means \pm SEM. Statistical significance was determined by Krustall-Wallis test (* $p <$
2026 0.05).

2027 In parallel, brain from the 4 other mice were divided into 3 parts (frontal, middle and
2028 occipital) which were frozen and treated independently for RNA extraction and RT-
2029 qPCR analysis of hCXCR4 expression **(F)**. For each sample, PBS-treated mice
2030 (middle sample) is considered as the base line. Bars represent the means \pm SEM.
2031 Statistical significance was determined by two-way ANOVA with Tukey's multiple
2032 comparisons of means with a single pooled variance (* $p < 0.05$, ** $p < 0.01$).

2033 Figure 6.

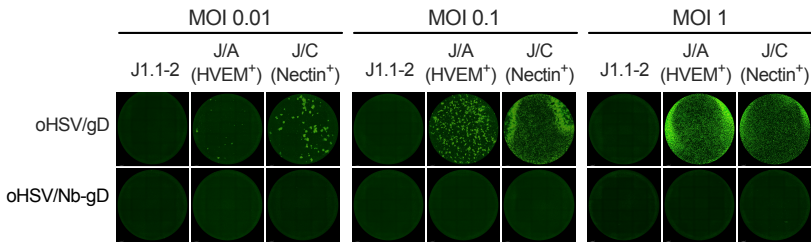
2034 **Survival assay upon oHSV/Nb-gD or oHSV/Nb-gD:sTRAIL treatment.**

2035 **(A)** Schematic representation of the survival assay experimental settings. **(B)**
2036 Bioluminescence activity of nude mice engrafted with 5×10^4 U87MG CXCR4 Luc⁺
2037 cells were recorded with Xenogen IVIS 50[®] on day 5 (two days before treatment)
2038 and 13 (6 days after treatment). Bars represent the means \pm SEM. Statistical
2039 significance was determined by two-way ANOVA with Tukey's multiple comparisons
2040 of means. (** $p < 0.01$). See also Figure S10B for Bioluminescence imaging **(C)**
2041 Probability of survival of mice treated with PBS (n=7), oHSV/Nb-gD (n=6) or
2042 oHSV/Nb-gD:sTRAIL (n=5). The red arrow indicates the day of treatment (Day 7).
2043 Statistical significance was determined by log-ranked (Mantel-Cox) test (****
2044 $p < 0.0001$). See also Figure S10A for weight follow-up.

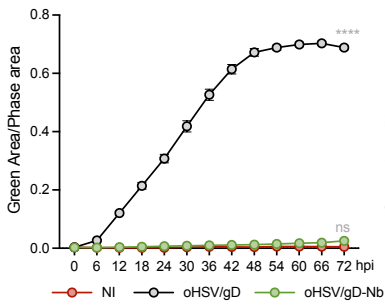
2045

Figure 2

A



B



C

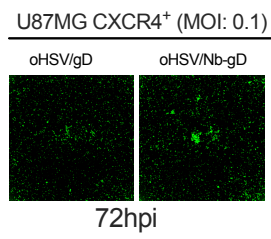
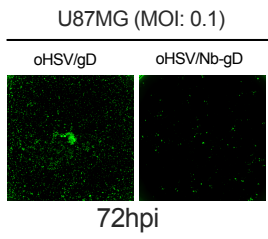
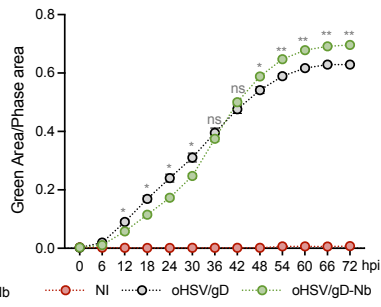
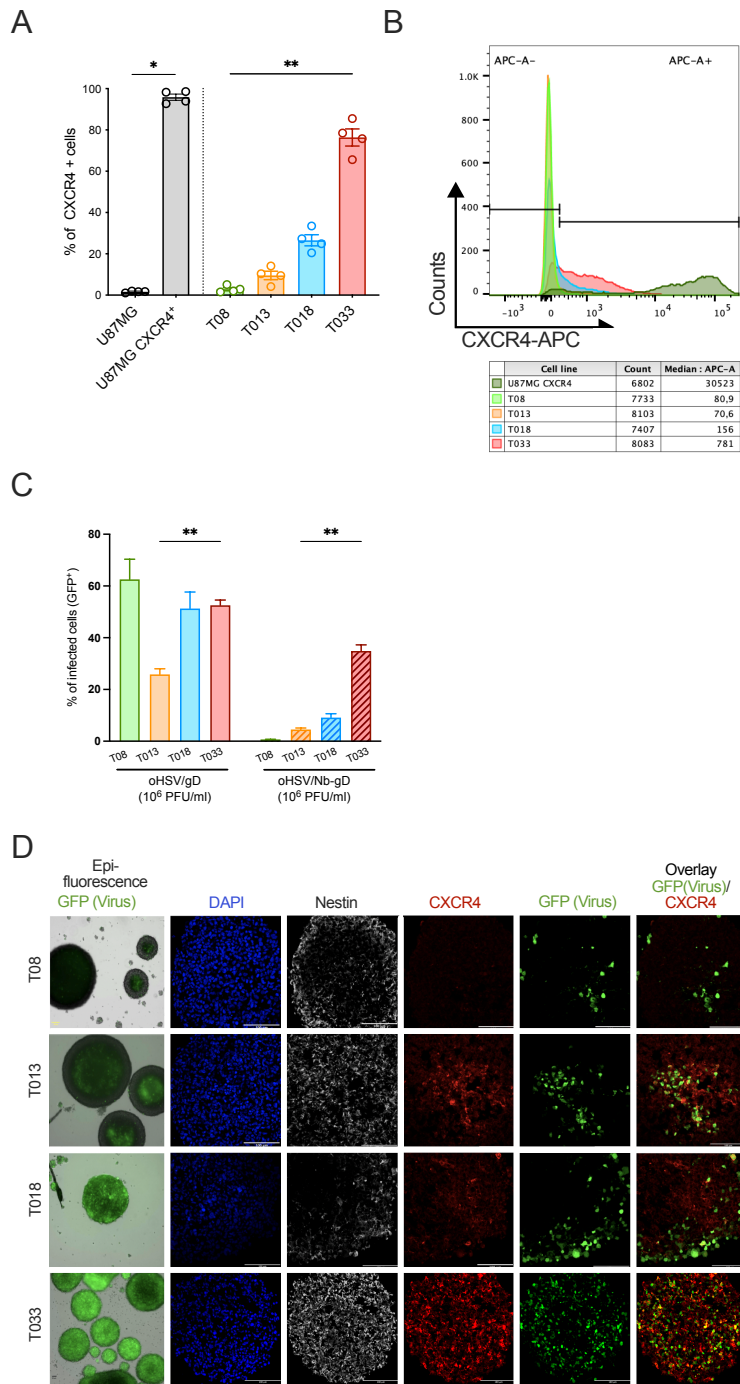


Figure 3



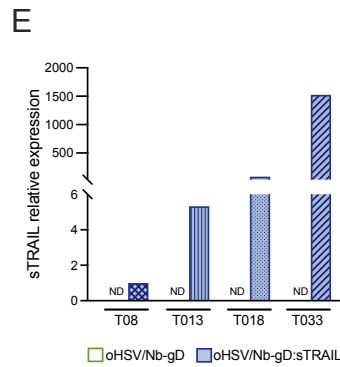
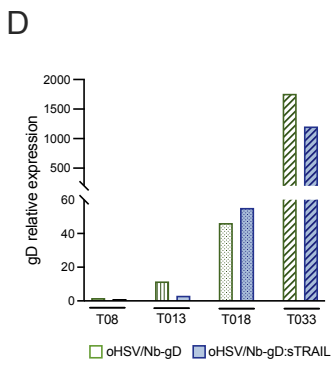
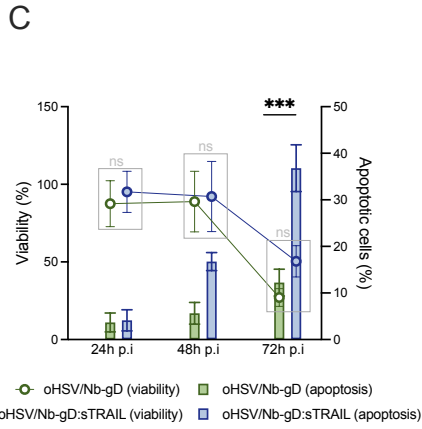
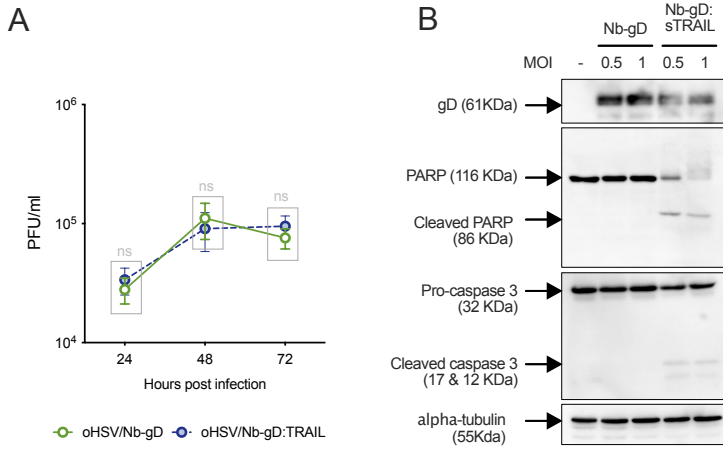
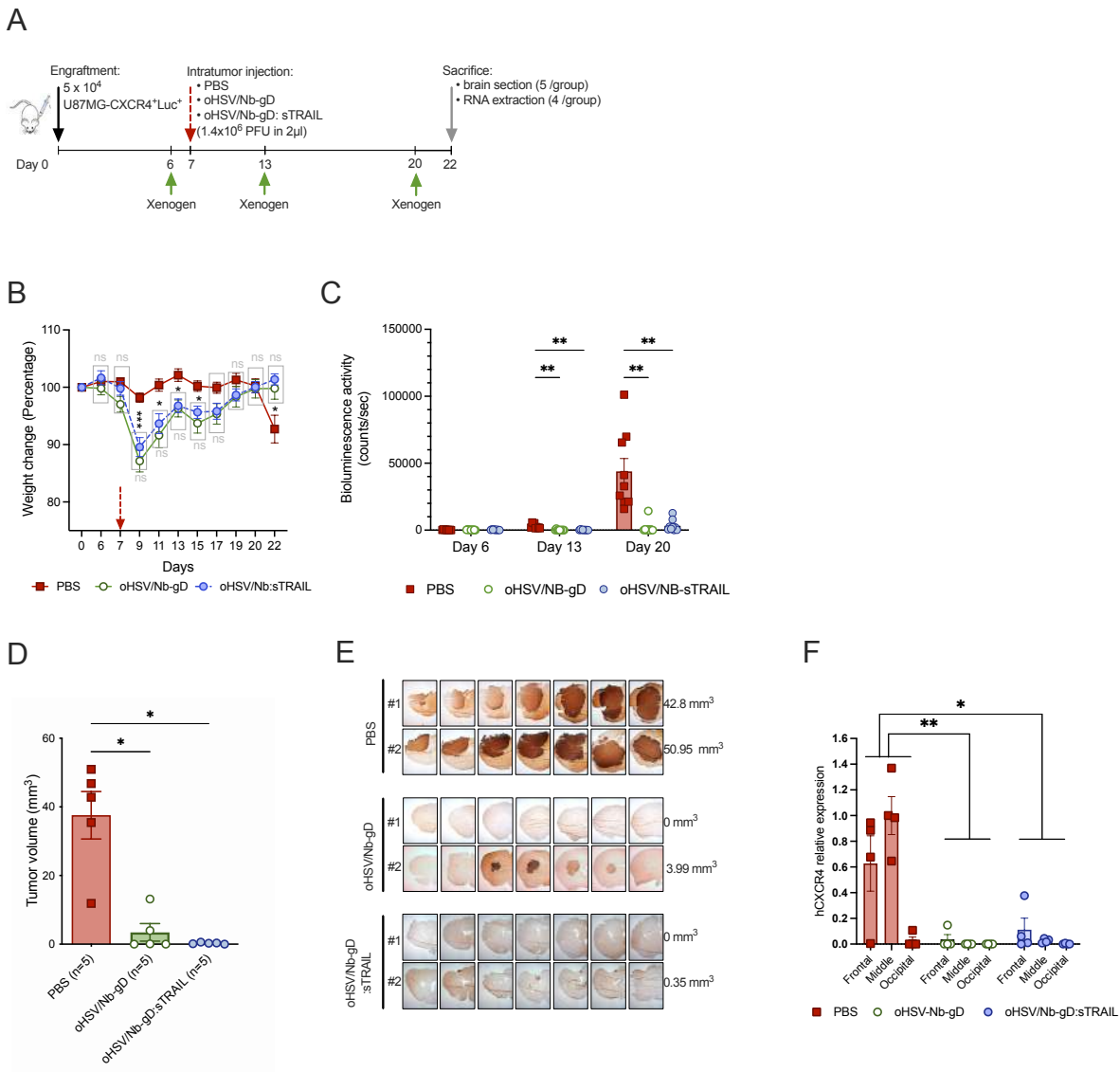
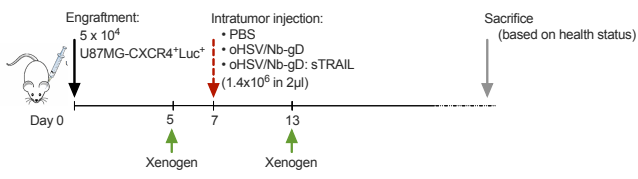


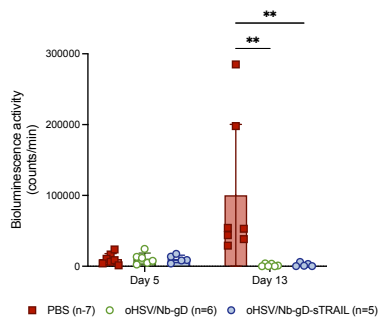
Figure 5



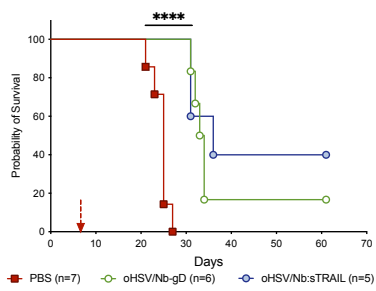
A



B



C



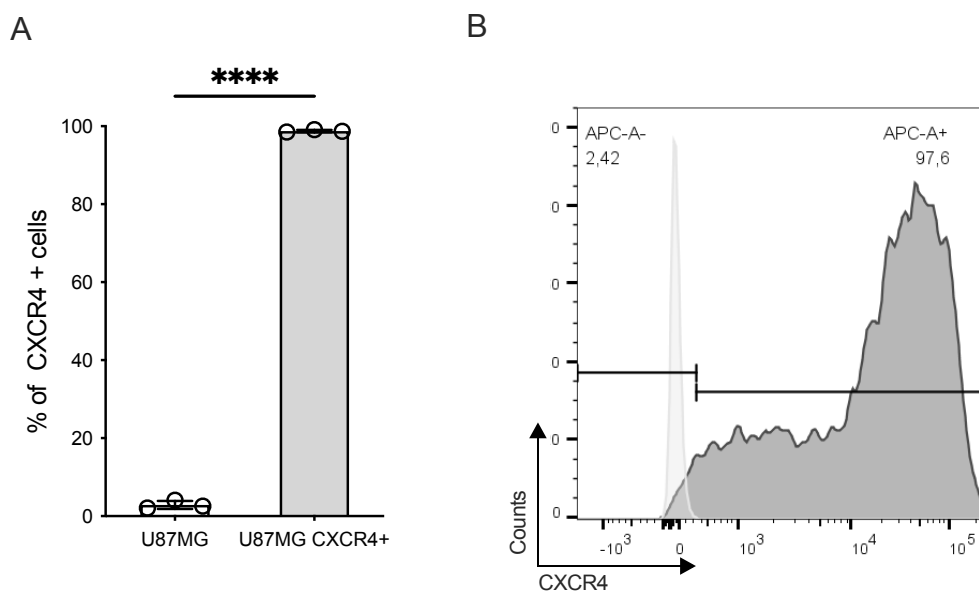


Figure S1

Flow cytometry expression of CXCR4⁺ expression on U87MG transduced or not with human CXCR4.

(A) Percentage of CXCR4⁺ cells. Bars represent the mean \pm SEM of 3 independent measures. Statistical significance was determined by unpaired t-test (**** $p < 0.0001$).

(B) Representative histogram of flow cytometry acquisition

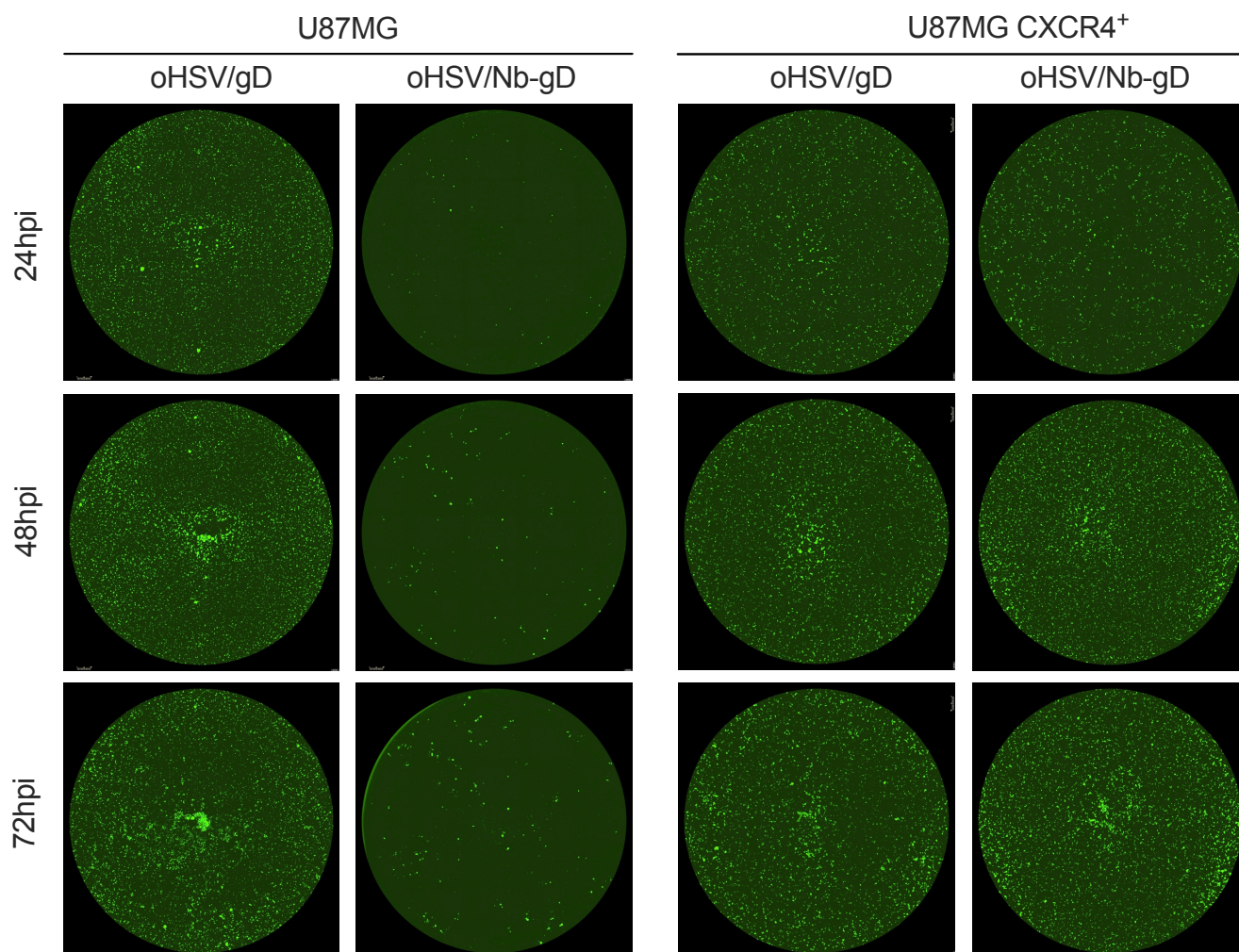


Figure S2

Efficacy of oHSV re-targeting.

U87MG and U87MG CXCR4⁺ cells were infected with oHSV/gD or oHSV/Nb-gD (MOI: 0.1). Both viruses express GFP under the control of pICP6, allowing real-time analyses with Incucyte® S3. Representative pictures show the infection at 24, 48 and 72hpi while fluorescence quantification is shown in Figure 2.

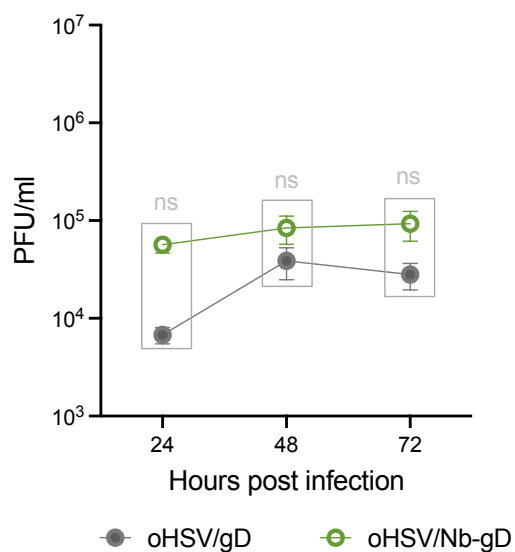


Figure S3

Growing curve of oHSV/gD and oHSV/Nb-gD in U87MG CXCR4⁺

The replication efficacy of the retargeted (oHSV/Nb-gD) and non-retargeted (oHSV/gD) oHSV was evaluated with a growing curve assay. U87MG CXCR4⁺ cells were infected at a MOI of 1 and supernatant was harvested at 24, 48 and 72 hours post infection and used for titration. The number of foci was calculated on images acquired with Incucyte®S3. Bars represent mean \pm SEM (PFU/ml) of three independent experiments. The lack of statistical difference is confirmed by unpaired *t*-test analysis.

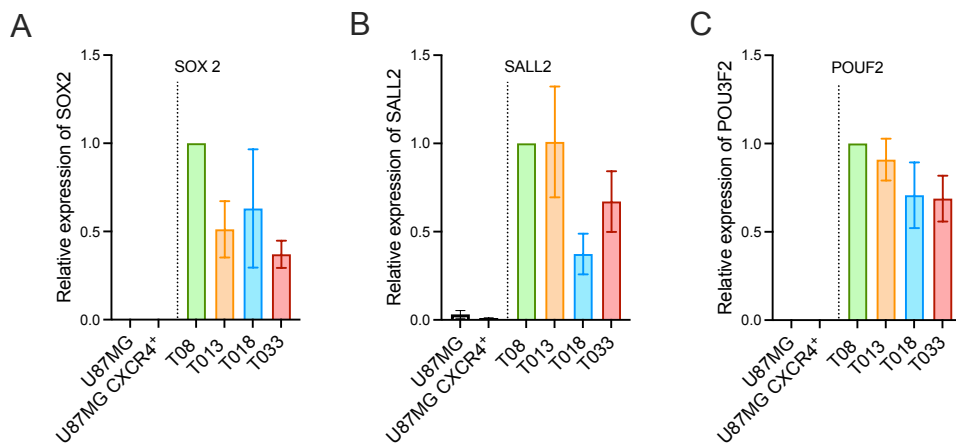
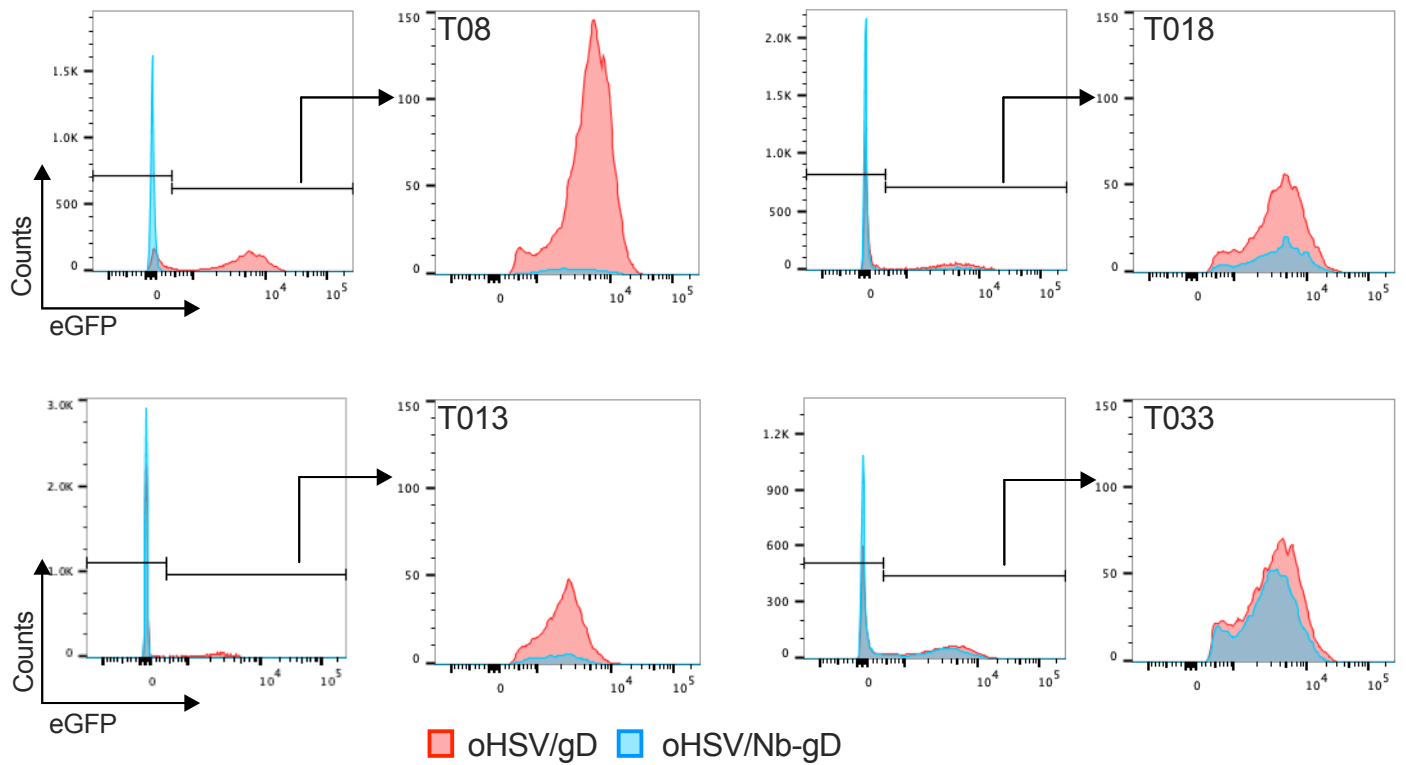


Figure S4

Stemness features of patient-derived GBM cells.

Patient-derived GBM primary cells (T08, T013, T018 and T033) or U87MG and U87MG CXCR4⁺ cells were cultured as tumorspheres and the level of expression of stemness markers (SOX2 **(A)**, SALL2 **(B)** and POU3F2 **(C)**) was evaluated by RT-qPCR and expressed relative to the level of expression in T08 cells considered as 1. Bars represent the mean \pm SEM of three independent analyses.

A



B

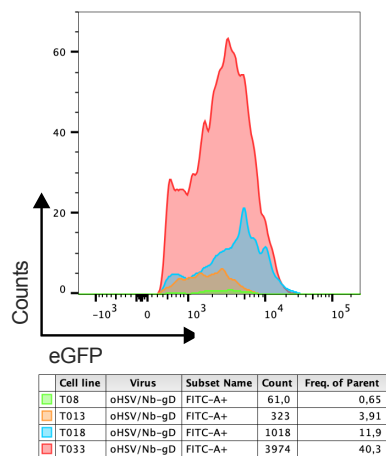


Figure S5

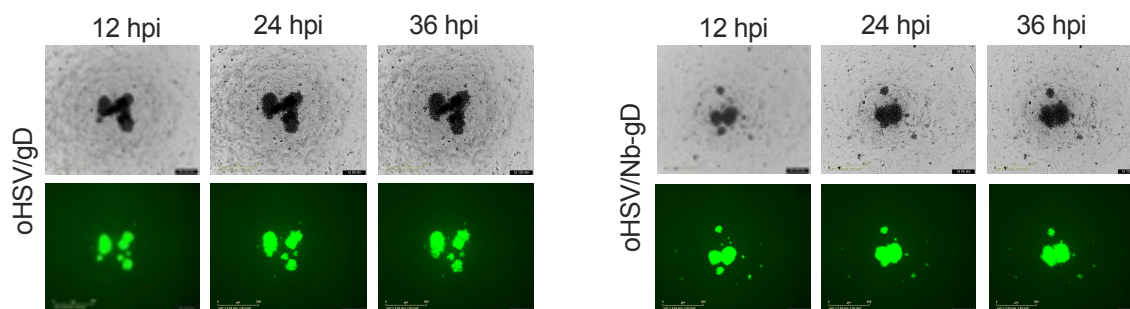
Flow cytometry analysis of patient-derived GSCs infected with oHSV/gD or oHSV/Nb-gD.

Patient-derived GBM cells cultured as tumorspheres in 12 well plates were infected for 48h with oHSV/gD or oHSV/Nb-gD (10^6 PFU/well). Forty-eight hours after infection, cells were dissociated and the level of eGFP expression was analyzed by flow cytometry.

(A): Overlaid histograms of a representative analysis of eGFP⁺ cells for each patient-derived cell line infected by oHSV/gD (red) or oHSV/Nb-gD (blue).

(B): Overlaid representative histograms of a representative analysis of eGFP⁺ cells upon oHSV/Nb-gD infection.

A



B

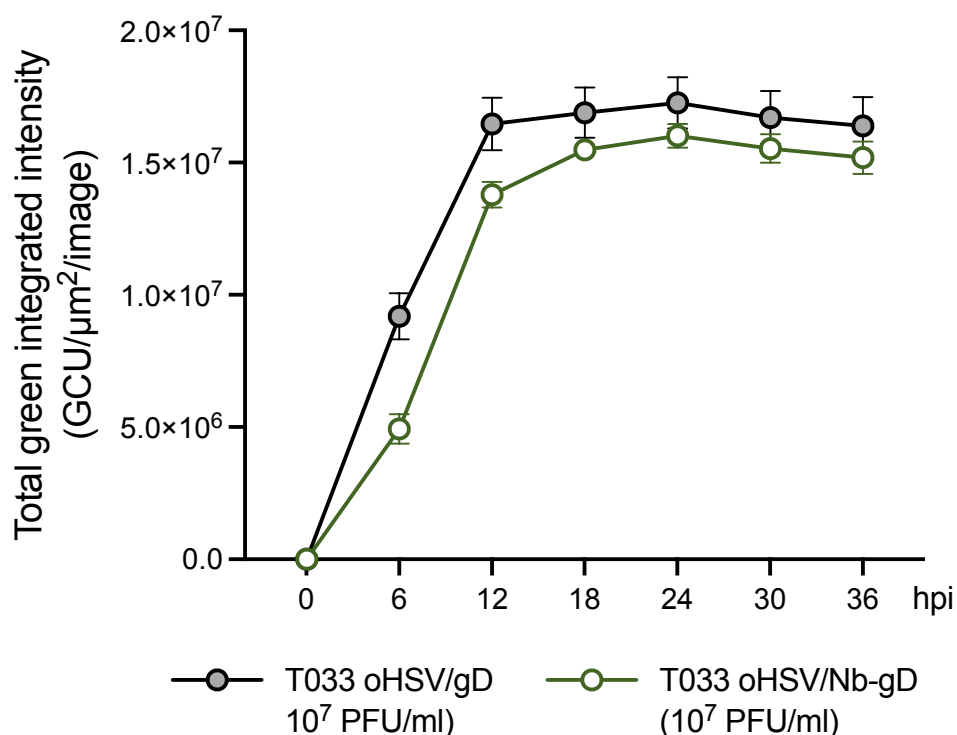


Figure S6

Comparison of oHSV/gD and oHSV/Nb-gD efficacy in T033 patient-derived GBM cells. Patient-derived GBM cells highly positive for CXCR4 (T033) were cultured as neurospheres in 96 well plates and infected with oHSV/gD or oHSV/Nb-gD (10^7 PFU/ml). Both viruses express GFP under the control of pICP6, allowing the real-time analysis with Incucyte S5. **(B)** Representative pictures show either the tumorspheres aspect (phase imaging) or the eGFP expression at indicated time points. Fluorescence quantification expressed as total green integrated intensity (GCU/ $\mu\text{m}^2/\text{image}$) is shown in **(B)**. Dots represent the mean \pm SEM of 5 independent wells.

The lack of statistical difference is confirmed by Mann-Whitney analysis.

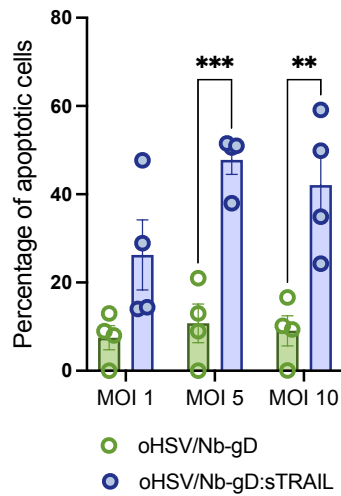


Figure S7

Percentage of apoptotic cells upon infection with increase dose of oHSV.

U87MG CXCR4⁺ cells were infected for 72h by oHSV/Nb-gD or oHSV/Nb-gD:sTRAIL at indicated MOI and apoptosis level was analyzed by quantification of annexin V and DAPI positive cells by flow cytometry. The percentage of apoptotic cells corresponds to early (Annexin V⁺/DAPI⁻) and late apoptotic (Annexin V⁺/DAPI⁺) cells. Bars represent the means \pm SEM of four independent experiments. Statistical significance was determined by ordinary 2-way ANOVA with Bonferroni's multiple comparisons of means (* $p < 0.05$, ** $p < 0.001$).

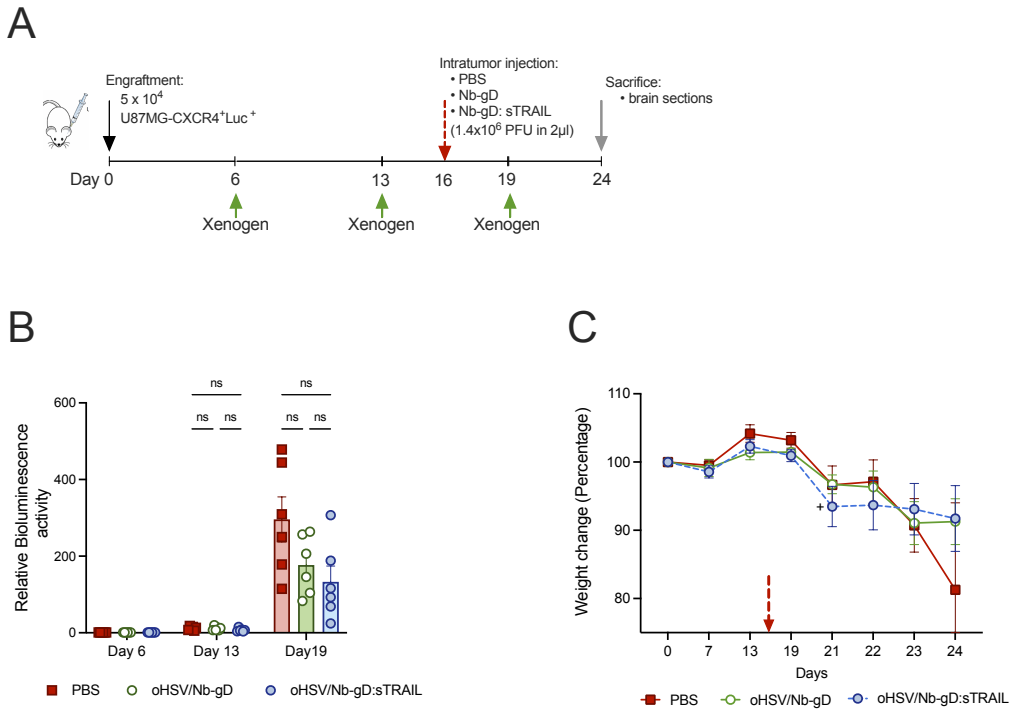


Figure S8

***In vivo* efficacy of oHSV/Nb-gD and oHSV/Nb-gD:sTRAIL (Exp 1).**

(A) Schematic representation of the experimental settings of the first *in vivo* experiment. U87MG CXCR4⁺Luc⁺ cells (5 x 10⁴ cells in 3μl) were injected on day 0 into the right hemisphere of the brain under stereotactic coordinates. Viral suspension (1.4 x 10⁶ PFU in 2μl) or PBS was injected within the tumor on day 16 as indicated by the red arrow. Mice were sacrificed on day 24. **(B)** Bioluminescence activity of mice was recorded with Xenogen IVIS 50[®] on day 6, 13 and 19. For each mouse, evolution of the bioluminescence is calculated regarding the bioluminescence on day 6 considered as equal 1. Bars represent the means ± SEM. Statistical significance was determined by two-way ANOVA with Tukey's multiple comparisons of means. **(C)** Mice were weighed every two days and weight change is expressed as a percentage with the weight on day 0, considered as equal to 100%. Graph represents the mean ± SEM. Statistical significance was determined by mixed-effects analysis with Bonferroni's multiple comparisons of means (PBS, n=7; oHSV/Nb-gD, n= 6; oHSV/Nb-gD:sTRAIL, n=6). There was no statistical difference between groups neither for the weight nor for the relative bioluminescence activity.

(+: One mice from the oHSV/Nb-gD:sTRAIL died on day 21).

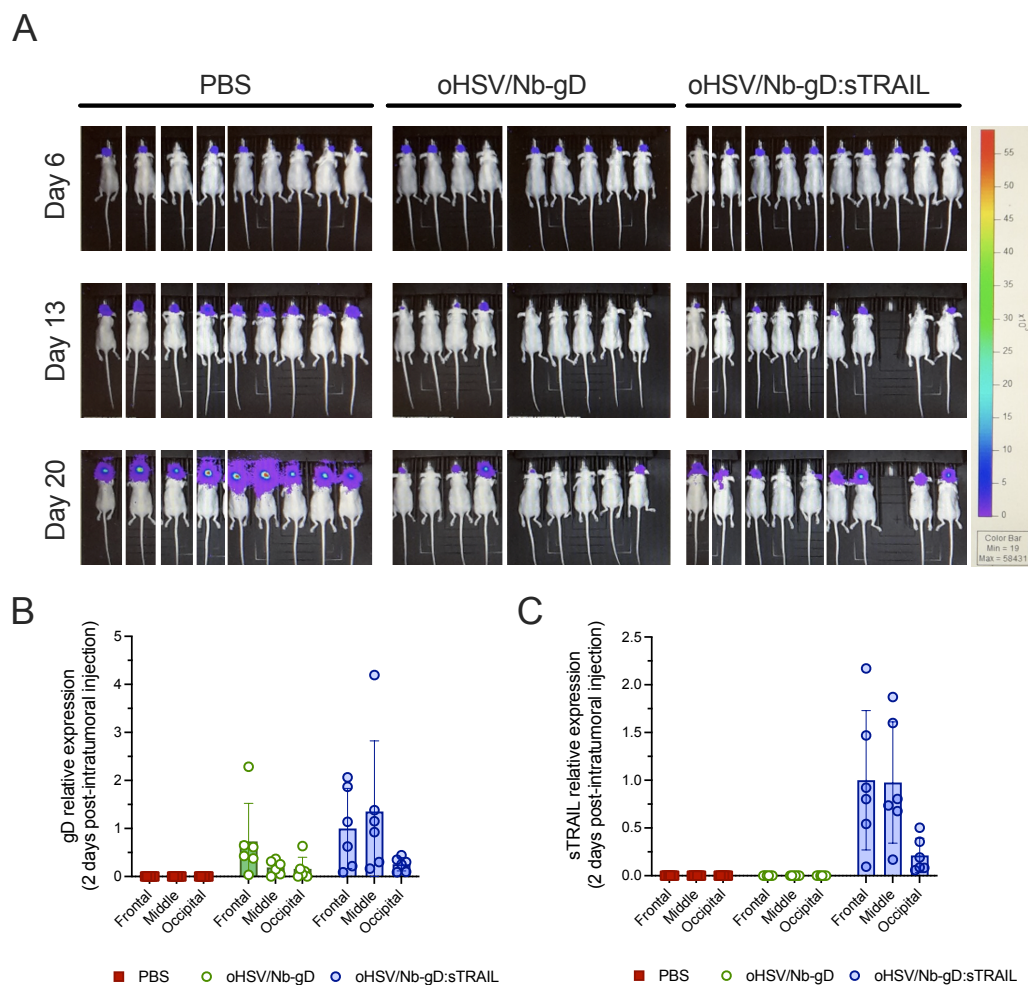


Figure S9

***In vivo* efficacy of oHSV/Nb-gD and oHSV/Nb-gD:sTRAIL (Exp 2).**

(A) Mice were submitted to the settings described in Figure 5A. U87MG CXCR4⁺Luc⁺ cells (5×10^4 cells in $3\mu\text{l}$) were injected on day 0 into the right hemisphere of the brain under stereotactic coordinates. Viral suspension (1.4×10^6 PFU in $2\mu\text{l}$) or PBS was injected within the tumor on day 7. Mice were sacrificed on day 22. Bioluminescence activity was measured on day 6, 13 and 20 by Xenogen IVIS[®] imaging. Mice from each group were not systematically in the same cage. Pictures have thus been edited to regroup mice from each group based on their identification tattoo. See also Figure 5C for bioluminescence activity quantification.

(B and C). This *in vivo* experiment was repeated (same settings for engraftment and virus injection) but mice (6 in each group) were sacrificed two days post injection. Brains were divided into 3 parts (frontal, middle and occipital) which were frozen and treated independently for RNA extraction and RT-qPCR analysis of gD **(B)** or sTRAIL **(C)** expression. For each sample, relative expression is expressed with oHSV/Nb-gD:sTRAIL in the frontal sample considered as the base line. Bars represent the means \pm SEM of 6 mice.

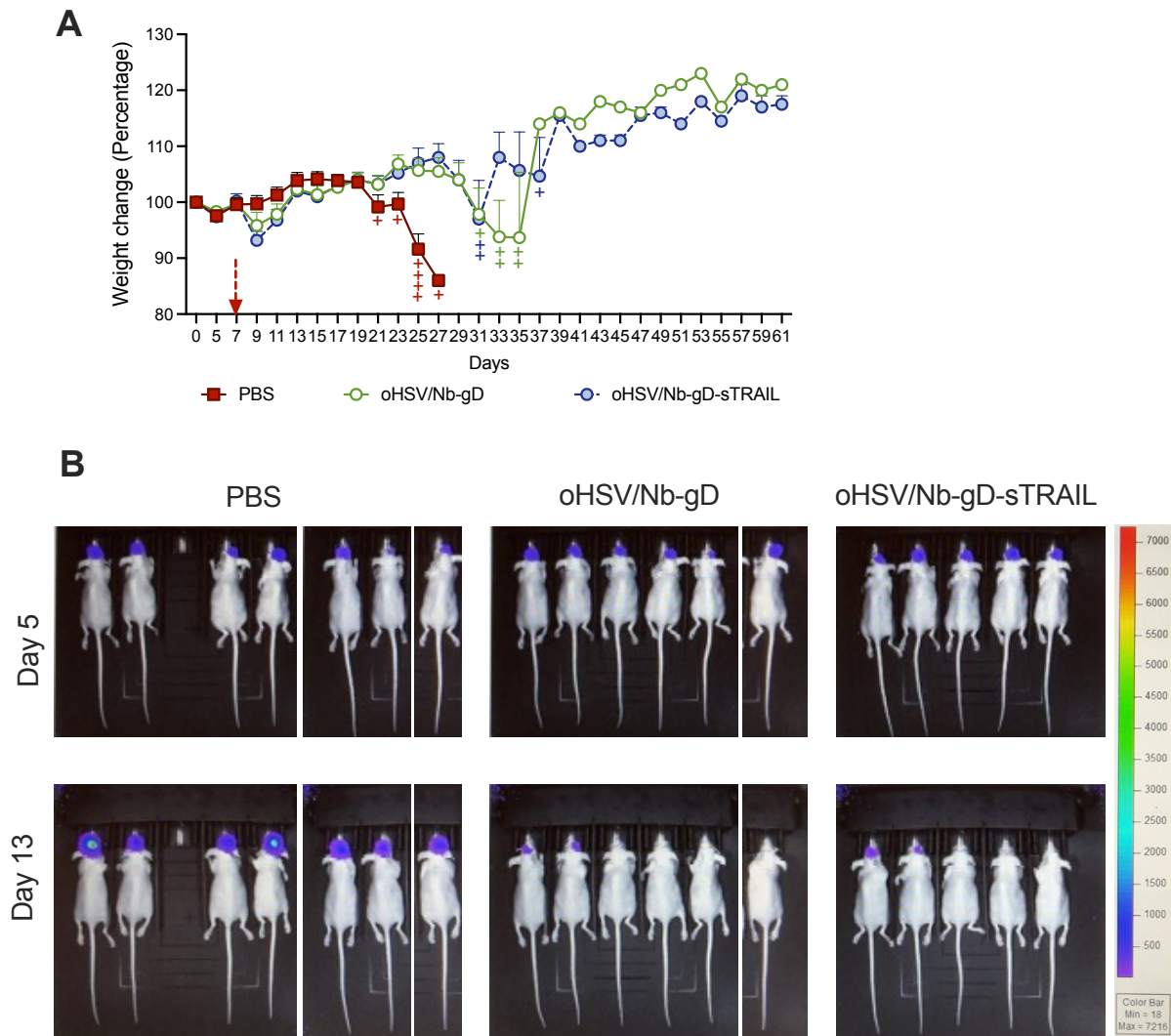
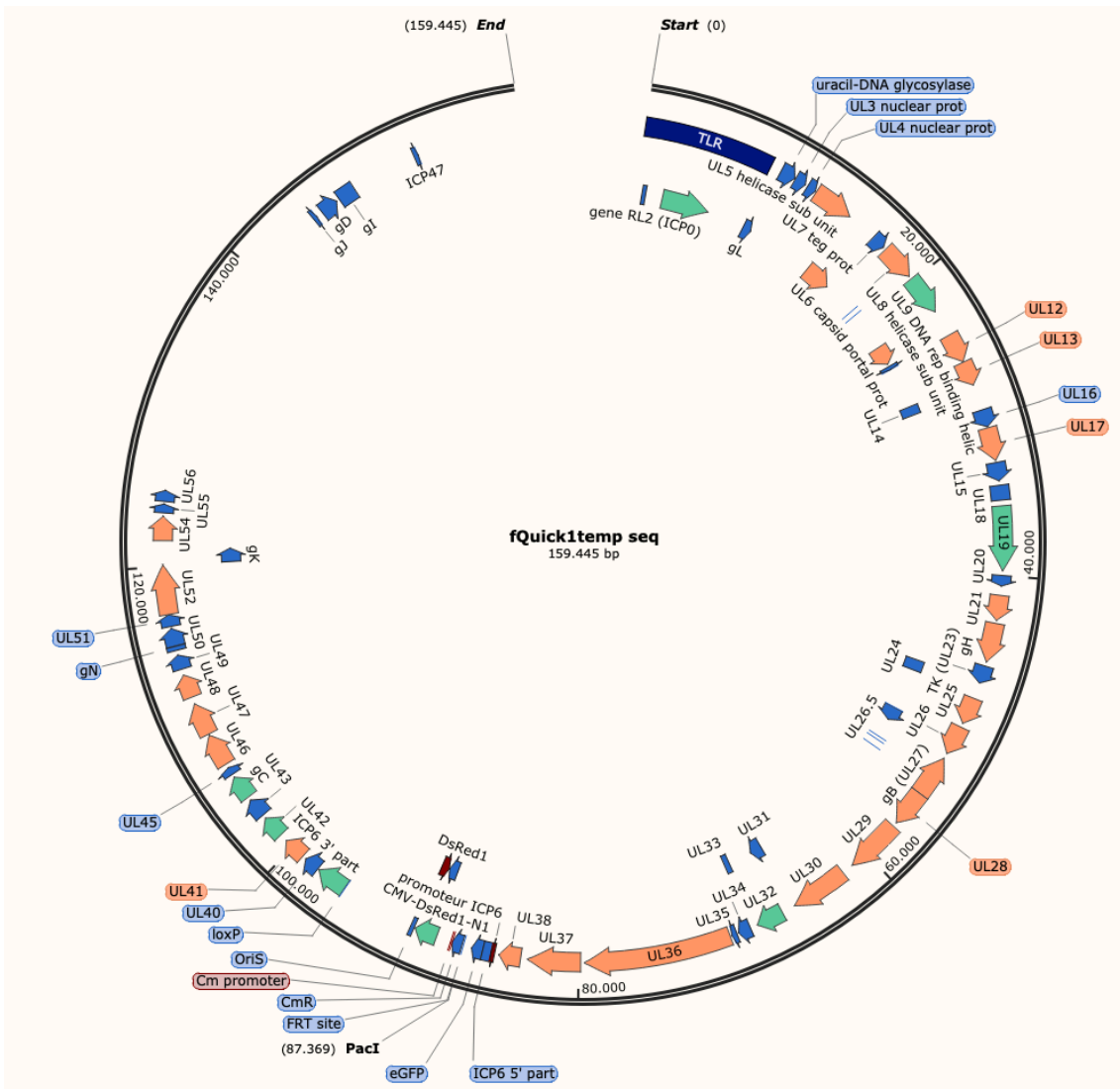


Figure S10

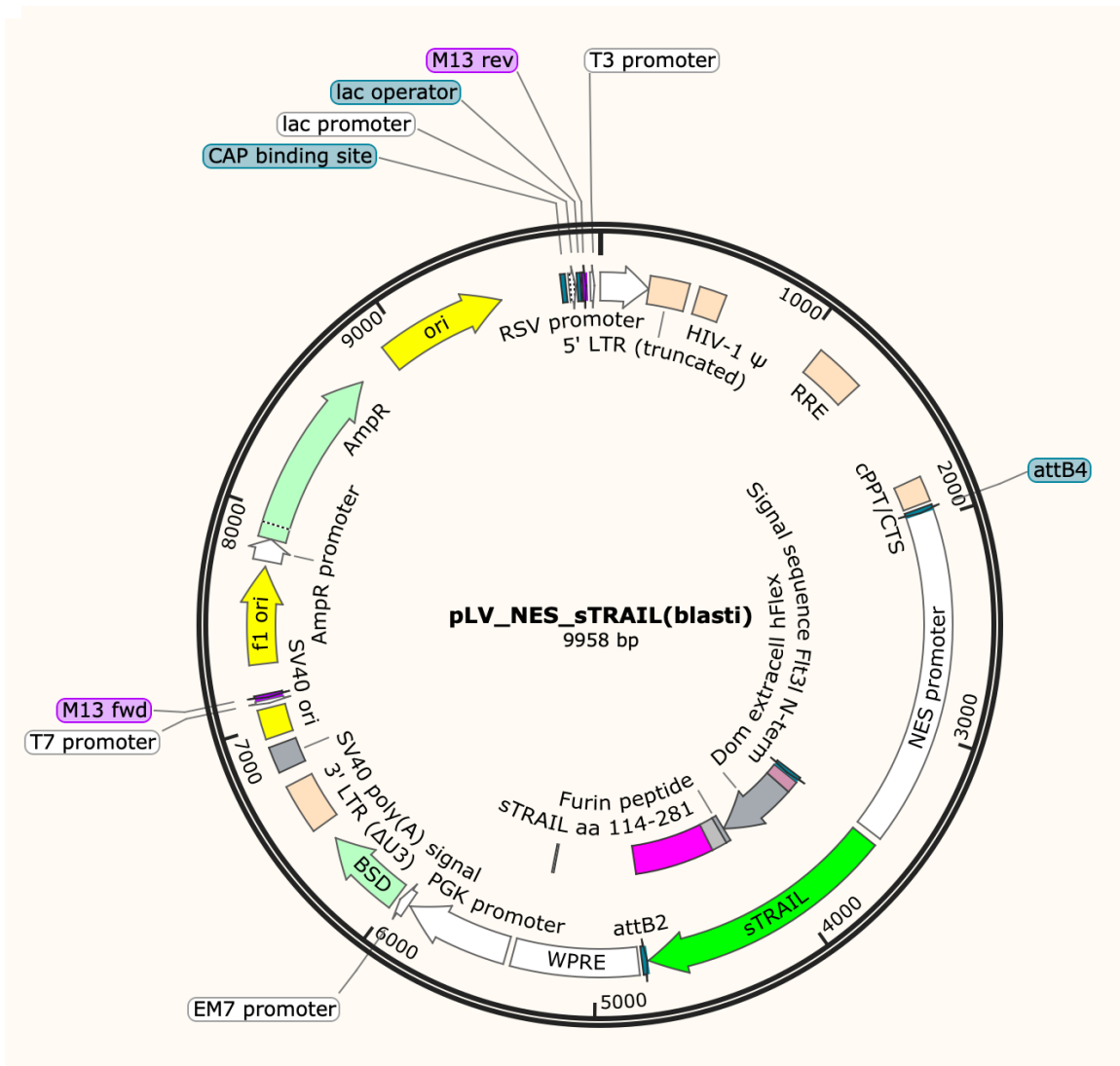
Survival assay upon oHSB/Nb-gD or oHSV/Nb-gD:sTRAIL treatment (EXP 3).

Mice were submitted to the settings described in Figure 6A. U87MG CXCR4⁺Luc⁺ cells (5×10^4 cells in $3\mu\text{l}$) were injected on day 0 into the right hemisphere of the brain under stereotactic coordinates. Viral suspension (1.4×10^6 PFU in $2\mu\text{l}$) or PBS was injected within the tumor on day 7. Mice were sacrificed at different time point depending on their health status. **(A)** Mice were regularly weighed, and the weight change is expressed as a percentage with the weight on day 0 considered as equal to 100%. Graph represents the mean \pm SEM (at the beginning of the experiment PBS n=7, oHSV/Nb-gD n=6, oHSV/Nb-gD:sTRAIL n=5). **(B)** Bioluminescence imaging of mice was recorded with Xenogen IVIS[®] on day 5 (two days before treatment) and day 13 (6 days after treatment). Mice from each group were not systematically in the same cage. Pictures have thus been edited to regroup the mice from each group based on their identification tattoo.

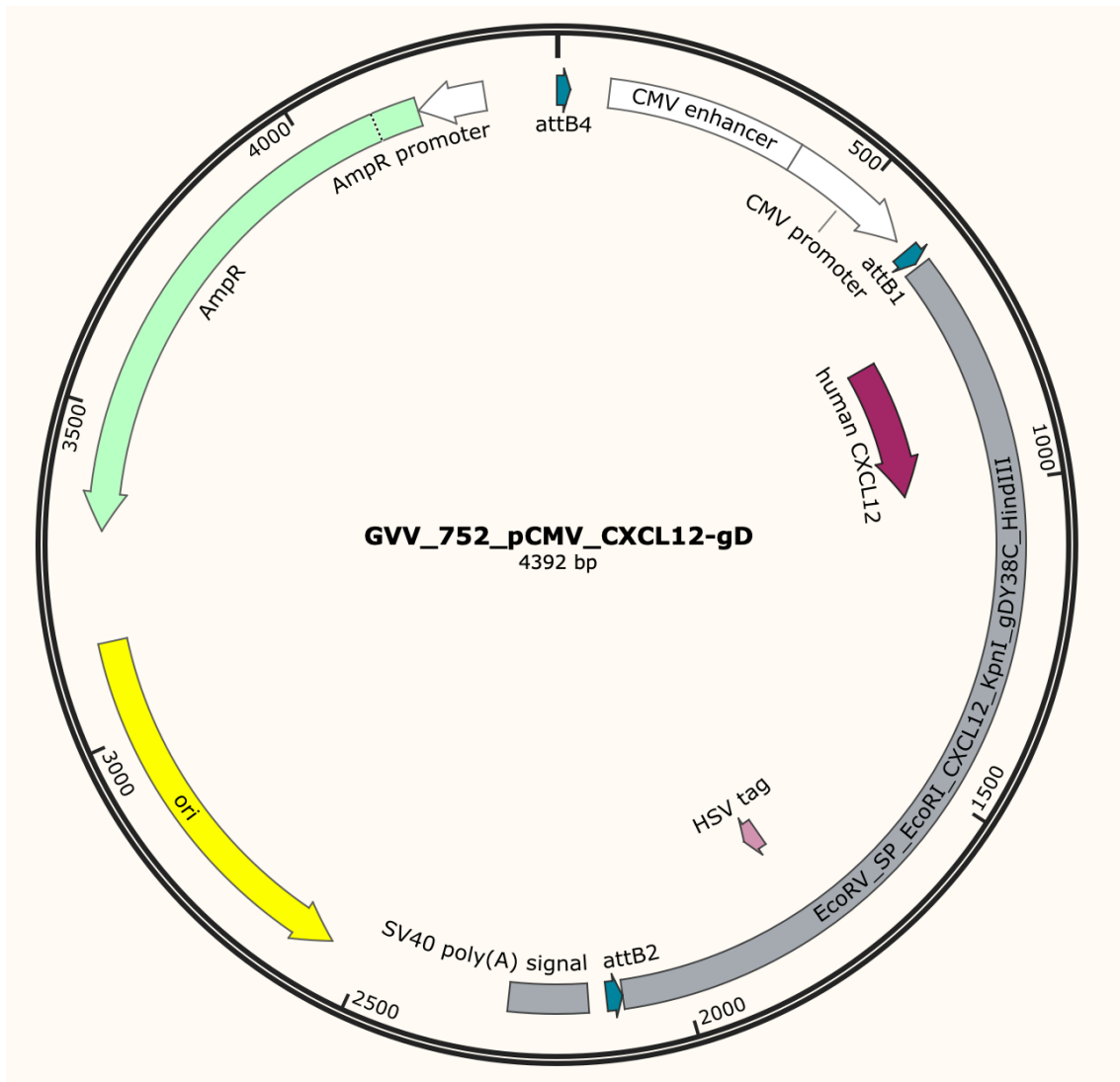
- BAC AND PLASMIDS MAPS



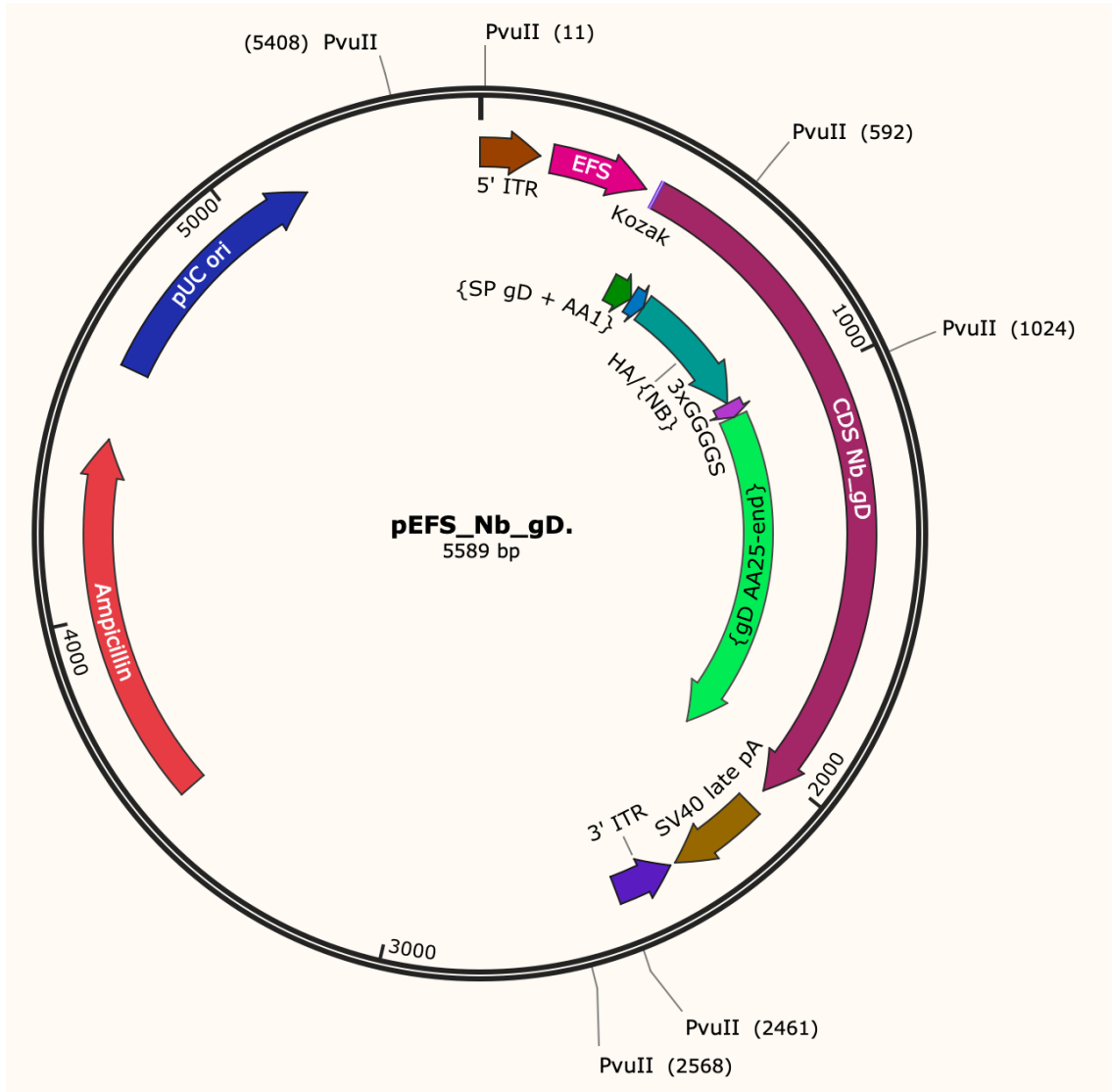
Supplemental Figure 1: Schematic representation of *fQuick-1* BAC with its major features.



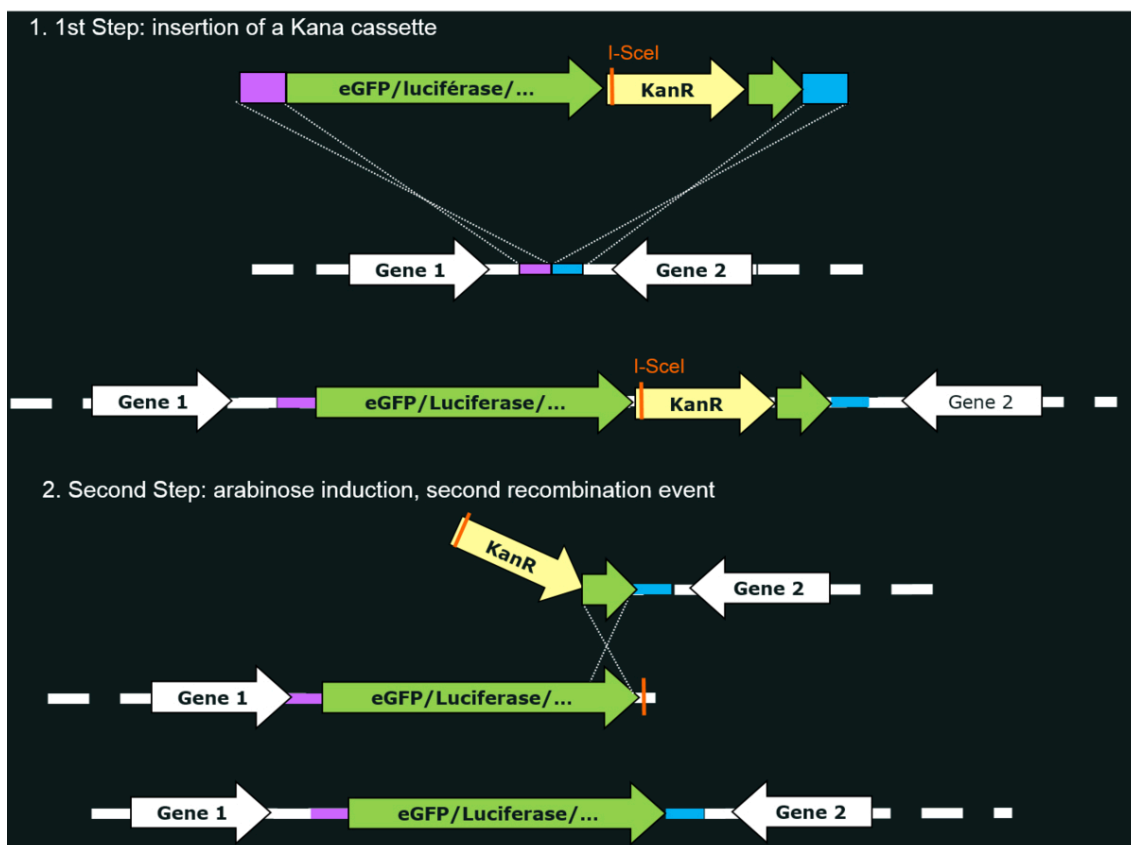
Supplemental Figure 2: Schematic representation of the plasmid used for oHSV pnestin-sTRAIL arming cloning strategy.



Supplemental Figure 3: Schematic representation of the plasmid used in oHSV/CXCL12-gD retargeting cloning.



Supplemental Figure 4: Schematic representation of the plasmid used for oHSV/Nb-gD retargeting cloning.



Supplemental Figure 5: Schematic representation of a long sequence insertion by the Two-step red recombination technique. The transgene is amplified by PCR and integrated into the target region with a first Red recombination. Cleavage of I-SceI site leads to the subsequent second red recombination. This second recombination results in the removal of the positive selection marker (KanaR) leaving the sequence of interest integrated in the right location. Illustration done by Marielle Lebrun.

- PRIMERS SEQUENCES FOR CLONING

Primer name	Sequence
PCR 1	
Fwd BAC-CXCL12	5'CCGTGATTTTGTGGTTCATAGTGGGCCTCCATGGGTCC GCGGCAAAAACGCCAAAGTGGTGGTGGT '3
Rev kana-gD	5'GTTGAATAAATCGATTACCCTGTTATCCCTACTTATCGTCG TCATCCTGTCGTTTATCTTCACGAGCCGCAG '3
PCR 2	
Rev kana	5'AGGATGACGACGATAAGTAGGGATAACAGGG '3
Rev gD-kana	5'AGTTGCCTCCCATCCGAAACCAAGCGATGGTCAGGTTGTA GGGTTGTTTCGCCAGTGTACAAACCAATTAACCAATTCTG'3
PCR screening	
Fwd US5	5'CAAACCTCCCGACACCACCAG '3
Rev seq KanR	5'GTTCAACAGGCCAGCCATTACG '3
Fwd Seq KanF	5'GCATGGTTACTCACCCTGCG '3
Rev gD	5'CCTCCCATCCGAAACCAAG '3

Table A1: Primers sequences for cloning oHSV/CXCL12-gD retargeting.

Primer name	Sequence
PCR 1	
Fwd BAC-Nb	5'CCCCGATCATCAGTTATCCTTAAGGTCTCTTTTGTGTGGTG CGTTCCGGTAAAGCAGGCTGCCACCATGGGC '3
Rev kana-gD	5'GTTGAATAAATCGATTACCCTGTTATCCCTACTTATCGTCG TCATCCTGTCGTTTATCTTCACGAGCCGCAG '3
PCR 2	
Fwd I-SceI Kana	5'AGGATGACGACGATAAGTAGGGATAACAGGG '3
Rev gD-kana	5'AGTTGCCTCCCATCCGAAACCAAGCGATGGTCAGGTTGTA GGGTTGTTTCGCCAGTGTACAAACCAATTAACCAATTCTG'3
PCR screening	
Fwd US5	5'CAAACCTCCCGACACCACCAG '3
Rev seq KanR	5'GTTCAACAGGCCAGCCATTACG '3
Fwd Seq KanF	5'GCATGGTTACTCACCCTGCG '3
Rev gD	5'CCTCCCATCCGAAACCAAG '3

Table A2: Primers sequences for cloning oHSV/Nb-gD retargeting.

Primer name	Sequence
PCR D285N punctual mutation	
Fwd D285N	5'ACATGTACACAAAGTCGCCAGTCGCCAGCACAAACTCGTTGTACGGGTACACCGAGCGCGAGGATGACGACGATAAGTAGGG '3
Rev D285N	5'ATCGTCGAGGAGGTGGACGCGCGCTCGGTGTACCCGTACAACGAGTTTGTGCTGGCGACTCAACCAATTAACCAATTCTGATTAG '3
PCR screening	
Fwd seq D285N	5' GGCCTCGGAGGAGAATCGG '3
Rev seq D285N	5' GCAACAACCTGGAGACCACCG '3
PCR A549T punctual mutation	
Fwd A549T	5'GCGCGCTCACCCGCCGCCACGGTGGCCGAGGCGATGGTGTTGGGGTTCAGCTTTCGGGAGGATGACGACGATAAGTAGG'3
Rev A549T	5'TGACCCTGTGGAACGAGGCCCGCAAGCTGAACCCCAACACATCGCCTCGGCCACCGTGCAACCAATTAACCAATTCTGATTAG '3
PCR screening	
Fwd A549T	5' GCTGACGGTGGTGTGATGTCGG '3
Rev A549T	5' CCTTCTCAGCAACACGCTCGC '3

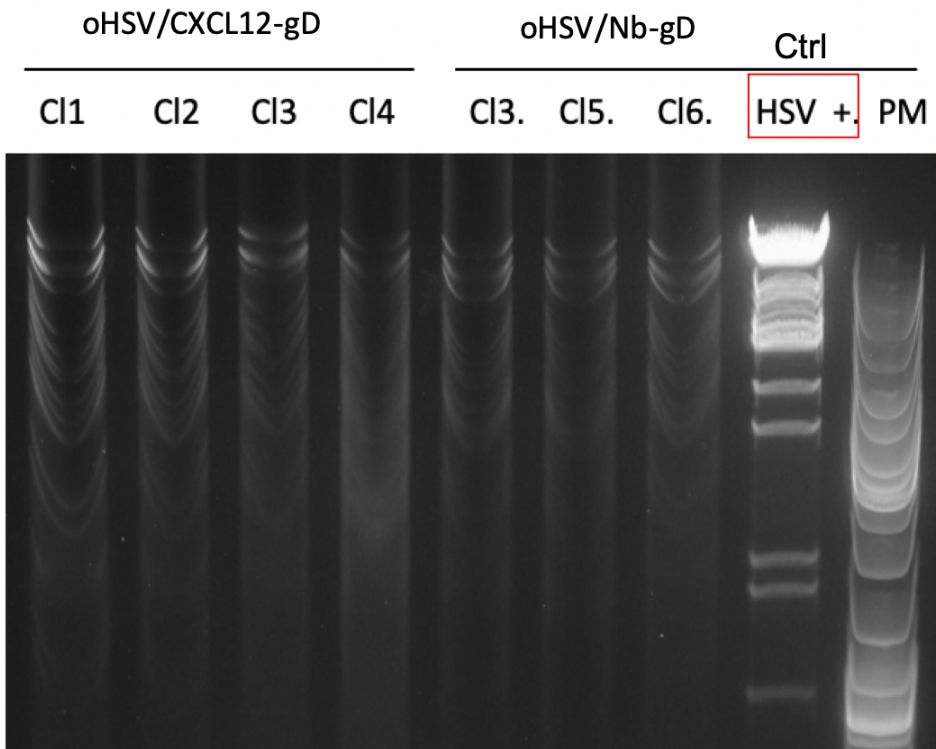
Table A3: Primers sequences for gB double punctual mutations D285N and A549T.

Primer name	Sequence
PCR Δ ICP47 deletion	
Fwd d47/IE_US11	5'ACATGTACACAAAGTCGCCAGTCGCCAGCACAAACTCGTTGTACGGGTACACCGAGCGCGAGGATGACGACGATAAGTAGGG '3
Rev d47/IE_US11	5'GGGGCTCACCCGCGTTCGTGCCTTCCCGCAGGAGGAACGTCGTTGAGTCCCGGGTACGACCAACCAATTAACCAATTCTGATTAG '3
PCR screening	
Fwd US11	5' GACGGCTTCAGATGGCTTCGA '3
Rev US13	5' CCTTTGTGCACGGGTAAGCAC '3

Table A4: Primers sequence for ICP47 deletion in oHSV backbone.

Primer name	Sequence
PCR 1 Arming	
Fwd BAC-pNES	5'ATAAAGCCACTGAAACCCGAAACGCGAGTGTTGTAACGTC CTTTGGGCGGCCCTGAAGAGTTTGTGATCC '3
Rev sTRAIL-Kan	5'TTACCCTGTTATCCCTACTTATCGTCGTCATCCTTTTATTAT CCAGAGGTTGATTATCGG '3
PCR 2 Arming	
Fwd I-SceI Kana	5'AGGATGACGACGATAAGTAGGGATAACAGGG '3
Rev Kan-sTRAIL- BAC	5'ACGGGGGTGTGTTCCCTTCCATGTATCCATTTGCATTTTGT GGCTTCCTCTTTATTATCCAGAGGTTGATTATCGGAATTCGA TTATCACCACCTTTGTACGCCAGTGTTACAACCAATTAACC '3
PCR 3 Arming	
Fwd_3 UL38	5' ATAAAGCCACTGAAACCCGA '3
Rev_3 pICP6	5' ACGGGGGTGTGTTCCCTTCCA '3
PCR screening	
Fwd_seq1 UL38	5' CGTTGTTATTCTGGAAGGCGTG '3
Rev_seq1 pNES- sTRAIL	5' CTGCCTCTGACCTCATGGAC '3
Fwd_seq2 pNES- sTRAIL	5' GGGTACCGAGCTCCAGGAAC '3
Rev_seq2 pNES- sTRAIL	5' GCTCTGCTTCTGGAAGGCTG '3
Fwd_seq3 pNES- sTRAIL	5' CAGCCTTCCCCAGAGCATCC '3
Rev3_s-TRAIL	5' TTCCCTCTCGCCAATGAG '3
seq_sTRAIL_Fw4	5' TGAGGAAATCCTGTCCAAGATTT '3
promICPRev4	5' CGCCTATCTTCTTTGGCTGTCG '3

Table A5: Primers sequences for sTRAIL arming in oHSV backbone.



Supplemental Figure 6: Photo of the restriction fragment length polymorphism (RFLP) pattern. The selected clones of oHSV/CXCL12-gD and oHSV/Nb-gD construction were digested with *EcoRV* restriction enzyme for 1h30 at 37°C and migrated for 3h in a 0,8% agarose gel.

